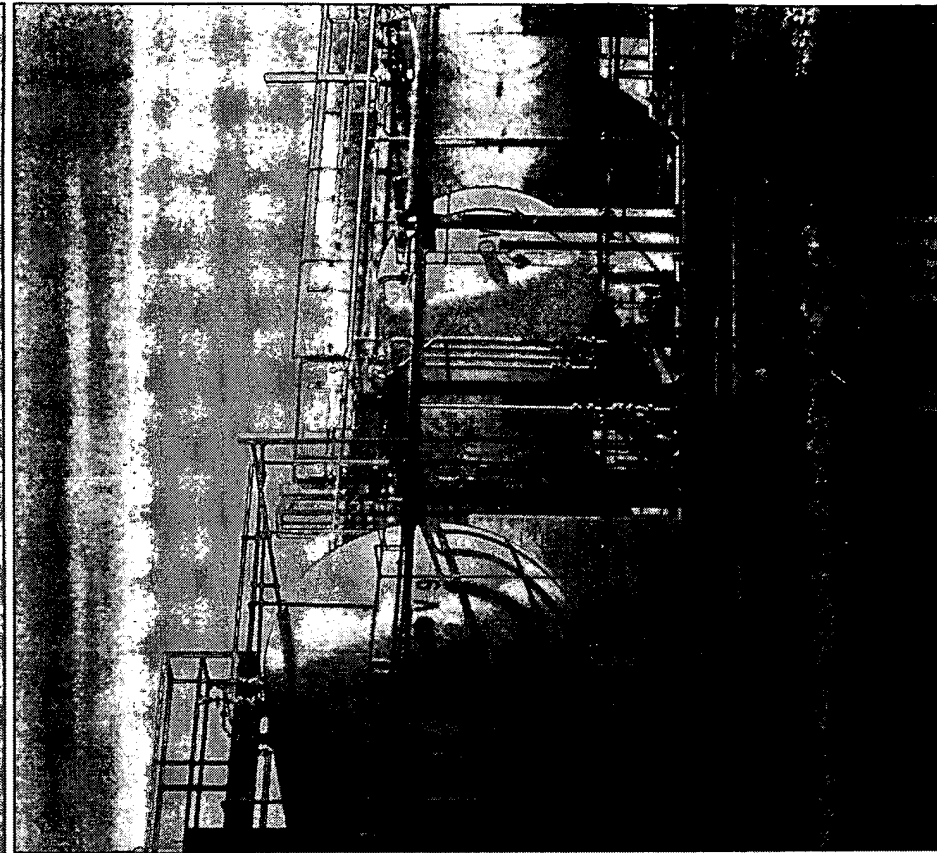


APPENDIX

SIXTH
EDITION

COULSON & RICHARDSON'S CHEMICAL ENGINEERING

J.M. Coulson & J.F. Richardson
with J.R. Backhurst and J.H. Harker



VOLUME 1

Richardson's Chemical Engineering

Engineering, Volume 1, Sixth edition
Transfer and Mass Transfer
J. F. Richardson
and J. H. Harker

Engineering, Volume 2, Fourth edition
Distillation and Separation Processes
J. F. Richardson
and J. H. Harker

Engineering, Volume 3, Third edition
Chemical Reactors & Process Control
J. F. Richardson and D. G. Peacock

Engineering, Volume 4, Second edition
Problems in Volume 1
J. H. Harker

Engineering, Volume 5, Second edition
Problems in Volumes 2 and 3
J. H. Harker

Engineering, Volume 6, Third edition
Plant Design

Coulson & Richardson's

CHEMICAL ENGINEERING

VOLUME 1

SIXTH EDITION

Fluid Flow, Heat Transfer and Mass Transfer

J. M. COULSON

*Late Emeritus Professor of Chemical Engineering
University of Newcastle-upon-Tyne*

and

J. F. RICHARDSON

*Department of Chemical Engineering
University of Wales, Swansea*

WITH

J. R. BACKHURST and J. H. HARKER

*Department of Chemical and Process Engineering
University of Newcastle-upon-Tyne*

BUTTERWORTH
HEINEMANN

Butterworth-Heinemann
Linacre House, Jordan Hill, Oxford OX2 8DP
225 Wildwood Avenue, Woburn, MA 01801-2041
A division of Reed Educational and Professional Publishing Ltd

© A member of the Reed Elsevier plc group

First published by Pergamon Press 1954
Second edition 1964
Third edition 1977
Fourth edition 1990
Fifth edition 1996
Fifth edition (revised) 1997, 1999
Sixth edition 1999

© J. M. Coulson, J. F. Richardson,
J. H.arker and J. R. Backhurst 1990, 1996, 1999

All rights reserved. No part of this publication may be reproduced in any material form (including photocopying or storing in any medium by electronic means and whether or not transiently or incidentally to some other use of this publication) without the written permission of the copyright holder except in accordance with the provisions of the Copyright, Designs and Patents Act 1988 or under the terms of a licence issued by the Copyright Licensing Agency Ltd, 90 Tottenham Court Road, London, England W1P 9HE. Applications for the copyright holder's written permission to reproduce any part of this publication should be addressed to the publishers.

British Library Cataloguing in Publication Data

A catalogue record for this book is available from the British Library

Library of Congress Cataloguing in Publication Data

A catalogue record for this book is available from the Library of Congress

ISBN 0 7506 4414 3

Typeset by Laser Words, Madras, India
Printed in Great Britain by The Bath Press, Bath

Contents

<i>Professor J. M. Coulson</i>	xiii
<i>Preface to Sixth Edition</i>	xv
<i>Preface to Fifth Edition</i>	xvii
<i>Preface to Fourth Edition</i>	xix
<i>Preface to Third Edition</i>	xxi
<i>Preface to Second Edition</i>	xxiii
<i>Preface to First Edition</i>	xxv
<i>Acknowledgements</i>	xxvii
1. Units and Dimensions	1
1.1 Introduction	1
1.2 Systems of units	2
1.2.1 The centimetre–gram–second (cgs) system	2
1.2.2 The metre–kilogram–second (mks) system and the Système International d'Unités (SI)	4
1.2.3 The foot–pound–second (fps) system	5
1.2.4 The British engineering system	5
1.2.5 Non-coherent system employing pound mass and pound force simultaneously	6
1.2.6 Derived units	6
1.2.7 Thermal (heat) units	7
1.2.8 Molar units	8
1.2.9 Electrical units	8
1.3 Conversion of units	9
1.4 Dimensional analysis	12
1.5 Buckingham's Π theorem	15
1.6 Redefinition of the length and mass dimensions	20
1.6.1 Vector and scalar quantities	20
1.6.2 Quantity mass and inertia mass	21
1.7 Further reading	22
1.8 References	22
1.9 Nomenclature	22
Part I Fluid Flow	25
2. Flow of Fluids—Energy and Momentum Relationships	27
2.1 Introduction	27
2.2 Internal energy	27

CONTENTS		
vi		vii
2.3	Types of fluid	154
2.3.1	The incompressible fluid (liquid)	154
2.3.2	The ideal gas	156
2.3.3	The non-ideal gas	158
2.4	The fluid in motion	158
2.4.1	Continuity	159
2.4.2	Momentum changes in a fluid	160
2.4.3	Energy of a fluid in motion	169
2.4.4	Pressure and fluid head	170
2.4.5	Constant flow per unit area	174
2.4.6	Separation	174
2.5	Pressure-volume relationships	178
2.5.1	Incompressible fluids	179
2.5.2	Compressible fluids	179
2.6	Rotational or vortex motion in a fluid	179
2.6.1	The forced vortex	181
2.6.2	The free vortex	181
2.7	Further reading	182
2.8	References	182
2.9	Nomenclature	183
3. Flow of Liquids in Pipes and Open Channels		186
3.1	Introduction	187
3.2	The nature of fluid flow	194
3.2.1	Flow over a surface	195
3.2.2	Flow in a pipe	195
3.3	Newtonian fluids	196
3.3.1	Shearing characteristics of a Newtonian fluid	198
3.3.2	Pressure drop for flow of Newtonian liquids through a pipe	210
3.3.3	Reynolds number and shear stress	213
3.3.4	Velocity distributions and volumetric flowrates for streamline flow	213
3.3.5	The transition from laminar to turbulent flow in a pipe	214
3.3.6	Velocity distributions and volumetric flowrates for turbulent flow	223
3.3.7	Flow through curved pipes	224
3.3.8	Miscellaneous friction losses	226
3.3.9	Flow over banks of tubes	227
3.3.10	Flow with a free surface	229
3.4	Non-Newtonian Fluids	232
3.4.1	Steady-state shear-dependent behaviour	232
3.4.2	Time-dependent behaviour	233
3.4.3	Viscoelastic behaviour	233
3.4.4	Characterisation of non-Newtonian fluids	234
3.4.5	Dimensionless characterisation of viscoelastic flows	237
3.4.6	Relation between rheology and structure of material	240
3.4.7	Streamline flow in pipes and channels of regular geometry	242
3.4.8	Turbulent flow	243
3.4.9	The transition from laminar to turbulent flow	244
3.5	Further reading	245
3.6	References	248
3.7	Nomenclature	254
4. Flow of Compressible Fluids		255
4.1	Introduction	257
4.2	Flow of gas through a nozzle or orifice	261
4.2.1	Isothermal flow	264
4.2.2	Non-isothermal flow	272
4.3	Velocity of propagation of a pressure wave	272
CONTENTS		
vii		viii
4.4	Converging-diverging nozzles for gas flow	154
4.4.1	Maximum flow and critical pressure ratio	154
4.4.2	The pressure and area for flow	156
4.4.3	Effect of back-pressure on flow in nozzle	158
4.5	Flow in a pipe	158
4.5.1	Energy balance for flow of ideal gas	159
4.5.2	Isothermal flow of an ideal gas in a horizontal pipe	160
4.5.3	Non-isothermal flow of an ideal gas in a horizontal pipe	169
4.5.4	Adiabatic flow of an ideal gas in a horizontal pipe	170
4.5.5	Flow of non-ideal gases	174
4.6	Shock waves	174
4.7	Further reading	178
4.8	References	179
4.9	Nomenclature	179
5. Flow of Multiphase Mixtures		181
5.1	Introduction	181
5.2	Two-phase gas (vapour)-liquid flow	182
5.2.1	Introduction	182
5.2.2	Flow regimes and flow patterns	183
5.2.3	Hold-up	186
5.2.4	Pressure, momentum, and energy relations	187
5.2.5	Erosion	194
5.3	Flow of solids-liquid mixtures	195
5.3.1	Introduction	195
5.3.2	Homogeneous non-settling suspensions	196
5.3.3	Coarse solids	198
5.3.4	Coarse solids in horizontal flow	210
5.3.5	Coarse solids in vertical flow	213
5.4	Flow of gas-solids mixtures	213
5.4.1	General considerations	213
5.4.2	Horizontal transport	214
5.4.3	Vertical transport	223
5.4.4	Practical applications	224
5.5	Further reading	226
5.6	References	227
5.7	Nomenclature	229
6. Flow and Pressure Measurement		232
6.1	Introduction	232
6.2	Fluid pressure	233
6.2.1	Static pressure	233
6.2.2	Pressure measuring devices	234
6.2.3	Pressure signal transmission — the differential pressure cell	237
6.2.4	Intelligent pressure transmitters	240
6.2.5	Impact pressure	242
6.3	Measurement of fluid flow	243
6.3.1	The pitot tube	244
6.3.2	Measurement by flow through a constriction	245
6.3.3	The orifice meter	248
6.3.4	The nozzle	254
6.3.5	The venturi meter	255
6.3.6	Pressure recovery in orifice-type meters	256
6.3.7	Variable area meters — rotameters	257
6.3.8	The notch or weir	261
6.3.9	Other methods of measuring flowrates	272
6.4	Further reading	272
6.5	References	272
6.6	Nomenclature	272

CONTENTS

9.3	Heat transfer by conduction	387
9.3.1	Conduction through a plane wall	387
9.3.2	Thermal resistances in series	390
9.3.3	Conduction through a thick-walled tube	392
9.3.4	Conduction through a spherical shell and to a particle	392
9.3.5	Unsteady state conduction	394
9.3.6	Conduction with internal heat source	412
9.4	Heat transfer by convection	414
9.4.1	Natural and forced convection	414
9.4.2	Application of dimensional analysis to convection	415
9.4.3	Forced convection in tubes	417
9.4.4	Forced convection outside tubes	426
9.4.5	Flow in non-circular sections	433
9.4.6	Convection to spherical particles	434
9.4.7	Natural convection	435
9.5	Heat transfer by radiation	438
9.5.1	Introduction	438
9.5.2	Radiation from a black body	439
9.5.3	Radiation from real surfaces	441
9.5.4	Radiation transfer between black surfaces	447
9.5.5	Radiation transfer between grey surfaces	458
9.5.6	Radiation from gases	465
9.6	Heat transfer in the condensation of vapours	471
9.6.1	Film coefficients for vertical and inclined surfaces	471
9.6.2	Condensation on vertical and horizontal tubes	474
9.6.3	Dropletwise condensation	476
9.6.4	Condensation of mixed vapours	482
9.7	Boiling liquids	482
9.7.1	Conditions for boiling	484
9.7.2	Types of boiling	486
9.7.3	Heat transfer coefficients and heat flux	490
9.7.4	Analysis based on bubble characteristics	492
9.7.5	Sub-cooled boiling	496
9.7.6	Design considerations	499
9.8	Heat transfer in reaction vessels	501
9.8.1	Helical cooling coils	503
9.8.2	Jacketed vessels	506
9.8.3	Time required for heating or cooling	510
9.9	Shell and tube heat exchangers	517
9.9.1	General description	517
9.9.2	Basic components	523
9.9.3	Mean temperature difference in multipass exchangers	526
9.9.4	Film coefficients	534
9.9.5	Pressure drop in heat exchangers	535
9.9.6	Heat exchanger design	540
9.9.7	Heat exchanger performance	540
9.9.8	Transfer units	548
9.10	Other forms of equipment	550
9.10.1	Finned-tube units	553
9.10.2	Plate-type exchangers	555
9.10.3	Spiral heat exchangers	557
9.10.4	Compact heat exchangers	561
9.10.5	Scraped-surface heat exchangers	562
9.11	Thermal insulation	566
9.11.1	Heat losses through lagging	
9.11.2	Economic thickness of lagging	
9.11.3	Critical thickness of lagging	
9.12	Further reading	
9.13	References	
9.14	Nomenclature	

CONTENTS

7.	Liquid Mixing	274
7.1	Introduction—types of mixing	274
7.1.1	Single-phase liquid mixing	274
7.1.2	Mixing of immiscible liquids	274
7.1.3	Gas-liquid mixing	275
7.1.4	Liquid-solids mixing	275
7.1.5	Gas-liquid-solids mixing	275
7.1.6	Solids-solids mixing	276
7.1.7	Miscellaneous mixing applications	277
7.2	Mixing mechanisms	277
7.2.1	Laminar mixing	279
7.2.2	Turbulent mixing	280
7.3	Scale-up of stirred vessels	282
7.4	Power consumption in stirred vessels	282
7.4.1	Low viscosity systems	288
7.4.2	High viscosity systems	294
7.5	Flow patterns in stirred tanks	298
7.6	Rate and time for mixing	301
7.7	Mixing equipment	301
7.7.1	Mechanical agitation	306
7.7.2	Portable mixers	307
7.7.3	Extruders	310
7.7.4	Static mixers	310
7.7.5	Other types of mixer	311
7.8	Mixing in continuous systems	311
7.9	Further reading	312
7.10	References	
7.11	Nomenclature	
8.	Pumping of Fluids	314
8.1	Introduction	314
8.2	Pumping equipment for liquids	315
8.2.1	Reciprocating pump	316
8.2.2	Positive-displacement rotary pumps	321
8.2.3	The centrifugal pump	329
8.3	Pumping equipment for gases	344
8.3.1	Fans and rotary compressors	346
8.3.2	Centrifugal and turbocompressors	347
8.3.3	The reciprocating piston compressor	347
8.3.4	Power required for the compression of gases	358
8.4	The use of compressed air for pumping	358
8.4.1	The air-lift pump	364
8.5	Vacuum pumps	367
8.6	Power requirements for pumping through pipelines	368
8.6.1	Liquids	374
8.6.2	Gases	376
8.7	Further reading	376
8.8	References	377
8.9	Nomenclature	
Part 2	Heat Transfer	379
9.	Heat Transfer	381
9.1	Introduction	381
9.2	Basic considerations	381
9.2.1	Individual and overall coefficients of heat transfer	381
9.2.2	Mean temperature difference	384

	CONTENTS	
x		xi
Part 3 Mass Transfer		
10. Mass Transfer		
10.1 Introduction	571	11.6 The boundary layer for heat transfer
10.2 Diffusion in binary gas mixtures	573	11.6.1 Introduction
10.2.1 Properties of binary mixtures	575	11.6.2 The heat balance
10.2.2 Equimolecular counterdiffusion	576	Heat transfer for streamline flow over a plane surface — constant surface temperature
10.2.3 Mass transfer through a stationary second component	577	11.6.4 Heat transfer for streamline flow over a plane surface — constant surface heat flux
10.2.4 Diffusivities of gases and vapours	581	11.7 The boundary layer for mass transfer
10.2.5 Mass transfer velocities	586	11.8 Further reading
10.2.6 General case for gas-phase mass transfer	587	11.9 References
10.2.7 Diffusion as a mass flux	588	11.10 Nomenclature
10.2.8 Thermal diffusion	589	
10.2.9 Unsteady-state mass transfer	590	12. Momentum, Heat, and Mass Transfer
10.3 Multicomponent gas-phase systems	593	12.1 Introduction
10.3.1 Molar flux in terms of effective diffusivity	593	12.2 Transfer by molecular diffusion
10.3.2 Maxwell's law of diffusion	594	12.2.1 Momentum transfer
10.4 Diffusion in liquids	596	12.2.2 Heat transfer
10.4.1 Liquid phase diffusivities	597	12.2.3 Mass transfer
10.5 Mass transfer across a phase boundary	599	12.2.4 Viscosity
10.5.1 The two-film theory	600	12.2.5 Thermal conductivity
10.5.2 The penetration theory	602	12.2.6 Diffusivity
10.5.3 The film-penetration theory	614	12.3 Eddy transfer
10.5.4 Mass transfer to a sphere in a homogeneous fluid	617	12.3.1 The nature of turbulent flow
10.5.5 Other theories of mass transfer	618	12.3.2 Mixing length and eddy kinematic viscosity
10.5.6 Interfacial turbulence	619	12.4 Universal velocity profile
10.5.7 Mass transfer coefficients	621	12.4.1 The turbulent core
10.5.8 Countercurrent mass transfer and transfer units	626	12.4.2 The laminar sub-layer
10.6 Mass transfer and chemical reaction	626	12.4.3 The buffer layer
10.6.1 Steady-state process	631	12.4.4 Velocity profile for all regions
10.6.2 Unsteady-state process	634	12.4.5 Velocity gradients
10.7 Mass transfer and chemical reaction in a catalyst pellet	636	12.4.6 Laminar sub-layer and buffer layer thicknesses
10.7.1 Flat pellets	638	12.4.7 Variation of eddy kinematic viscosity
10.7.2 Spherical pellets	642	12.4.8 Approximate form of velocity profile in turbulent region
10.7.3 Other particle shapes	644	12.4.9 Effect of curvature of pipe wall on shear stress
10.7.4 Mass transfer and chemical reaction with a mass transfer resistance external to the pellet	646	12.5 Friction factor for a smooth pipe
10.8 Practical studies of mass transfer	646	12.6 Effect of surface roughness on shear stress
10.8.1 The j -factor of Chilton and Colburn for flow in tubes	649	12.7 Simultaneous momentum, heat and mass transfer
10.8.2 Mass transfer at plane surfaces	651	Reynolds analogy
10.8.3 Effect of surface roughness and form drag	651	12.8.1 Simple form of analogy between momentum, heat and mass transfer
10.8.4 Mass transfer from a fluid to the surface of particles	654	12.8.2 Mass transfer with bulk flow
10.9 Further reading	655	12.8.3 Taylor-Prandtl modification of Reynolds analogy for heat transfer and mass transfer
10.10 References	661	12.8.4 Use of universal velocity profile in Reynolds analogy
10.11 Nomenclature	663	12.8.5 Flow over a plane surface
		12.8.6 Flow in a pipe
		12.9 Further reading
		12.10 References
		12.11 Nomenclature
Part 4 Momentum, Heat and Mass Transfer		
11. The Boundary Layer		
11.1 Introduction	663	13. Humidification and Water Cooling
11.2 The momentum equation	668	13.1 Introduction
11.3 The streamline portion of the boundary layer	670	Humidification terms
11.4 The turbulent boundary layer	675	13.2 Definitions
11.4.1 The turbulent portion	675	13.2.1 Wet-bulb temperature
11.4.2 The laminar sub-layer	677	13.2.2 Adiabatic saturation temperature
11.5 Boundary layer theory applied to pipe flow	681	Humidity data for the air-water system
11.5.1 Entry conditions	681	13.3.1 Temperature-humidity chart
11.5.2 Application of the boundary-layer theory	682	13.3.2 Enthalpy-humidity chart
		738
		738
		739
		742
		743
		746
		749
		751

13.4	Determination of humidity	756
13.5	Humidification and dehumidification	759
13.5.1	Methods of increasing humidity	759
13.5.2	Dehumidification	761
13.6	Water cooling	762
13.6.1	Cooling towers	762
13.6.2	Design of natural-draught towers	765
13.6.3	Height of packing for both natural and mechanical draught towers	767
13.6.4	Change in air condition	772
13.6.5	Temperature and humidity gradients in a water cooling tower	773
13.6.6	Evaluation of heat and mass transfer coefficients	774
13.6.7	Humidifying towers	778
13.7	Systems other than air-water	779
13.8	Further reading	785
13.9	References	786
13.10	Nomenclature	787
	Appendix	789
A1.	Tables of physical properties	790
A2.	Steam tables	806
A3.	Mathematical tables	815
	Fold-out charts	
	Problems	825
	Index	869

Professor J. M. Coulson

JOHN COULSON, who died on 6 January 1990 at the age of 79, came from a family with close involvement with education. Both he and his twin brother Charles (renowned physicist and mathematician), who predeceased him, became professors. John did his undergraduate studies at Cambridge and then moved to Imperial College where he took the postgraduate course in chemical engineering—the normal way to qualify at that time—and then carried out research on the flow of fluids through packed beds. He then became an Assistant Lecturer at Imperial College and, after war-time service in the Royal Ordnance Factories, returned as Lecturer and was subsequently promoted to a Readership. At Imperial College he initially had to run the final year of the undergraduate course almost single-handed, a very demanding assignment. During this period he collaborated with Sir Frederick (Ned) Warner to write a model design exercise for the I. Chem. E. Home Paper on "The Manufacture of Nitrotoluene". He published research papers on heat transfer and evaporation, on distillation, and on liquid extraction, and co-authored this textbook of Chemical Engineering. He did valiant work for the Institution of Chemical Engineers which awarded him its Davis medal in 1973, and was also a member of the Advisory Board for what was then a new Pergamon journal, *Chemical Engineering Science*.

In 1954 he was appointed to the newly established Chair at Newcastle-upon-Tyne, where Chemical Engineering became a separate Department and independent of Mechanical Engineering of which it was formerly part, and remained there until his retirement in 1975. He took a period of secondment to Heriot Watt University where, following the splitting of the joint Department of Chemical Engineering with Edinburgh, he acted as adviser and *de facto* Head of Department. The Scottish university awarded him an Honorary D.Sc. in 1973.

John's first wife Dora sadly died in 1961; they had two sons, Anthony and Simon. He remarried in 1965 and is survived by Christine.

JFR

Heat Transfer

9.1. INTRODUCTION

In the majority of chemical processes heat is either given out or absorbed, and fluids must often be either heated or cooled in a wide range of plant, such as furnaces, evaporators, distillation units, dryers, and reaction vessels where one of the major problems is that of transferring heat at the desired rate. In addition, it may be necessary to prevent the loss of heat from a hot vessel or pipe system. The control of the flow of heat at the desired rate forms one of the most important areas of chemical engineering. Provided that a temperature difference exists between two parts of a system, heat transfer will take place in one or more of three different ways.

Conduction. In a solid, the flow of heat by conduction is the result of the transfer of vibrational energy from one molecule to another, and in fluids it occurs in addition as a result of the transfer of kinetic energy. Heat transfer by conduction may also arise from the movement of free electrons, a process which is particularly important with metals and accounts for their high thermal conductivities.

Convection. Heat transfer by convection arises from the mixing of elements of fluid. If this mixing occurs as a result of density differences as, for example, when a pool of liquid is heated from below, the process is known as *natural convection*. If the mixing results from eddy movement in the fluid, for example when a fluid flows through a pipe heated on the outside, it is called *forced convection*. It is important to note that convection requires mixing of fluid elements, and is not governed by temperature difference alone as is the case in conduction and radiation.

Radiation. All materials radiate thermal energy in the form of electromagnetic waves. When this radiation falls on a second body it may be partially reflected, transmitted, or absorbed. It is only the fraction that is absorbed that appears as heat in the body.

9.2. BASIC CONSIDERATIONS

9.2.1. Individual and overall coefficients of heat transfer

In many of the applications of heat transfer in process plants, one or more of the mechanisms of heat transfer may be involved. In the majority of heat exchangers heat passes through a series of different intervening layers before reaching the second fluid (Figure 9.1). These layers may be of different thicknesses and of different thermal conductivities. The problem of transferring heat to crude oil in the primary furnace before it enters the first distillation column may be considered as an example. The heat from the flames passes by radiation and convection to the pipes in the furnace, by conduction through the

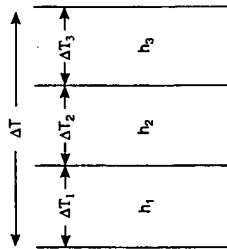


Figure 9.1. Heat transfer through a composite wall

pipe walls, and by forced convection from the inside of the pipe to the oil. Here all three modes of transfer are involved. After prolonged usage, solid deposits may form on both the inner and outer walls of the pipes, and these will then contribute additional resistance to the transfer of heat. The simplest form of equation which represents this heat transfer operation may be written as:

$$Q = U A \Delta T \quad (9.1)$$

where Q is the heat transferred per unit time, A the area available for the flow of heat, ΔT the difference in temperature between the flame and the boiling oil, and U is known as the overall heat transfer coefficient ($\text{W/m}^2 \text{ K}$ in SI units).

At first sight, equation 9.1 implies that the relationship between Q and ΔT is linear. Whereas this is approximately so over limited ranges of temperature difference for which U is nearly constant, in practice U may well be influenced both by the temperature difference and by the absolute value of the temperatures.

If it is required to know the area needed for the transfer of heat at a specified rate, the temperature difference ΔT , and the value of the overall heat-transfer coefficient must be known. Thus the calculation of the value of U is a key requirement in any design problem in which heating or cooling is involved. A large part of the study of heat transfer is therefore devoted to the evaluation of this coefficient.

The value of the coefficient will depend on the mechanism by which heat is transferred, on the fluid dynamics of both the heated and the cooled fluids, on the properties of the materials through which the heat must pass, and on the geometry of the fluid paths. In solids, heat is normally transferred by conduction; some materials such as metals have a high thermal conductivity, whilst others such as ceramics have a low conductivity. Transparent solids like glass also transmit radiant energy particularly in the visible part of the spectrum.

Liquids also transmit heat readily by conduction, though circulating currents are frequently set up and the resulting convective transfer may be considerably greater than the transfer by conduction. Many liquids also transmit radiant energy. Gases are poor conductors of heat and circulating currents are difficult to suppress; convection is therefore much more important than conduction in a gas. Radiant energy is transmitted with only limited absorption in gases and, of course, without any absorption *in vacuo*. Radiation is the only mode of heat transfer which does not require the presence of an intervening medium.

If the heat is being transmitted through a number of media in series, the overall heat transfer coefficient may be broken down into individual coefficients h each relating to a single medium. This is as shown in Figure 9.1. It is assumed that there is good contact between each pair of elements so that the temperature is the same on the two sides of each junction.

If heat is being transferred through three media, each of area A , and individual coefficients for each of the media are h_1 , h_2 , and h_3 , and the corresponding temperature changes are ΔT_1 , ΔT_2 , and ΔT_3 then, provided that there is no accumulation of heat in the media, the heat transfer rate Q will be the same through each. Three equations, analogous to equation 9.1 can therefore be written:

$$\left. \begin{aligned} Q &= h_1 A \Delta T_1 \\ Q &= h_2 A \Delta T_2 \\ Q &= h_3 A \Delta T_3 \end{aligned} \right\} \quad (9.2)$$

Rearranging:

$$\begin{aligned} \Delta T_1 &= \frac{Q}{A} \frac{1}{h_1} \\ \Delta T_2 &= \frac{Q}{A} \frac{1}{h_2} \\ \Delta T_3 &= \frac{Q}{A} \frac{1}{h_3} \end{aligned}$$

$$\text{Adding:} \quad \Delta T_1 + \Delta T_2 + \Delta T_3 = \frac{Q}{A} \left(\frac{1}{h_1} + \frac{1}{h_2} + \frac{1}{h_3} \right) \quad (9.3)$$

Noting that $(\Delta T_1 + \Delta T_2 + \Delta T_3) = \text{total temperature difference } \Delta T$:

$$\text{then:} \quad \Delta T = \frac{Q}{A} \left(\frac{1}{h_1} + \frac{1}{h_2} + \frac{1}{h_3} \right) \quad (9.4)$$

$$\text{From equation 9.1:} \quad \Delta T = \frac{Q}{A} U \quad (9.5)$$

Comparing equations 9.4 and 9.5:

$$\frac{1}{U} = \frac{1}{h_1} + \frac{1}{h_2} + \frac{1}{h_3} \quad (9.6)$$

The reciprocals of the heat transfer coefficients are resistances, and equation 9.6 therefore illustrates that the resistances are additive.

In some cases, particularly for the radial flow of heat through a thick pipe wall or cylinder, the area for heat transfer is a function of position. Thus the area for transfer applicable to each of the three media could differ and may be A_1 , A_2 and A_3 . Equation 9.3 then becomes:

$$\Delta T_1 + \Delta T_2 + \Delta T_3 = Q \left(\frac{1}{h_1 A_1} + \frac{1}{h_2 A_2} + \frac{1}{h_3 A_3} \right) \quad (9.7)$$

Equation 9.7 must then be written in terms of one of the area terms A_1 , A_2 , and A_3 , or sometimes in terms of a mean area. Since Q and ΔT must be independent of the particular

area considered, the value of U will vary according to which area is used as the basis. Thus equation 9.7 may be written, for example:

$$Q = U_1 A_1 \Delta T \quad \text{or} \quad \Delta T = \frac{Q}{U_1 A_1} \quad (9.8)$$

This will then give U_1 as:

$$\frac{1}{U_1} = \frac{1}{h_1} + \frac{A_1}{A_2} \left(\frac{1}{h_2} \right) + \frac{A_1}{A_3} \left(\frac{1}{h_3} \right) \quad (9.8)$$

In this analysis it is assumed that the heat flowing per unit time through each of the media is the same.

Now that the overall coefficient U has been broken down into its component parts, each of the individual coefficients h_1 , h_2 , and h_3 must be evaluated. This can be done from a knowledge of the nature of the heat transfer process in each of the media. A study will therefore be made of how these individual coefficients can be calculated for conduction, convection, and radiation.

9.2.2. Mean temperature difference

Where heat is being transferred from one fluid to a second fluid through the wall of a vessel and the temperature is the same throughout the bulk of each of the fluids, there is no difficulty in specifying the overall temperature difference ΔT . Frequently, however, each fluid is flowing through a heat exchanger such as a pipe or a series of pipes in parallel, and its temperature changes as it flows, and consequently the temperature difference is continuously changing. If the two fluids are flowing in the same direction (*co-current flow*), the temperatures of the two streams progressively approach one another as shown in Figure 9.2. In these circumstances the outlet temperature of the heating fluid must always be higher than that of the cooling fluid. If the fluids are flowing in opposite directions (*countercurrent flow*), the temperature difference will show less variation throughout the heat exchanger as shown in Figure 9.3. In this case it is possible for the cooling liquid to leave at a higher temperature than the heating liquid, and one of the great advantages of

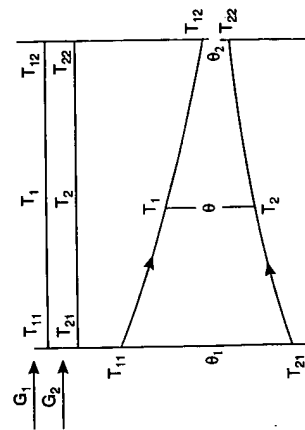


Figure 9.2. Mean temperature difference for co-current flow

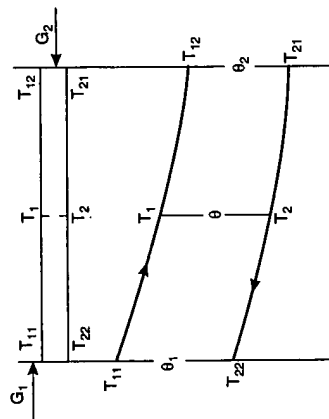


Figure 9.3. Mean temperature difference for countercurrent flow

countercurrent flow is that it is possible to extract a higher proportion of the heat content of the heating fluid. The calculation of the appropriate value of the temperature difference for co-current and for countercurrent flow is now considered. It is assumed that the overall heat transfer coefficient U remains constant throughout the heat exchanger.

It is necessary to find the average value of the temperature difference θ_m to be used in the general equation:

$$Q = UA\theta_m \quad (\text{equation 9.1})$$

Figure 9.3 shows the temperature conditions for the fluids flowing in opposite directions, a condition known as countercurrent flow.

The outside stream specific heat C_{p1} and mass flow rate G_1 falls in temperature from T_{11} to T_{12} .

The inside stream specific heat C_{p2} and mass flow rate G_2 rises in temperature from T_{21} to T_{22} .

Over a small element of area dA where the temperatures of the streams are T_1 and T_2 . The temperature difference:

$$\theta = T_1 - T_2$$

$$d\theta = dT_1 - dT_2$$

$$\text{Heat given out by the hot stream} = dQ = -G_1 C_{p1} dT_1$$

$$\text{Heat taken up by the cold stream} = dQ = G_2 C_{p2} dT_2$$

$$\therefore d\theta = -\frac{dQ}{G_1 C_{p1}} - \frac{dQ}{G_2 C_{p2}} = -dQ \left(\frac{G_1 C_{p1} + G_2 C_{p2}}{G_1 C_{p1} \times G_2 C_{p2}} \right) = -\psi dQ \quad (\text{say})$$

$$\theta_1 - \theta_2 = \psi Q$$

$$U dA \theta = dQ$$

$$U dA \theta = -\frac{d\theta}{\psi}$$

If U may be taken as constant:

$$-\psi U \int_0^A dA = \int_{\theta_1}^{\theta_2} \frac{d\theta}{\theta}$$

$$-\psi UA = -\ln \frac{\theta_1}{\theta_2}$$

From the definition of θ_m , $Q = UA\theta_m$.

$$\theta_1 - \theta_2 = \psi Q = \psi UA\theta_m = \ln \frac{\theta_1(\theta_m)}{\theta_2}$$

and:

$$\theta_m = \frac{\theta_1 - \theta_2}{\ln(\theta_1/\theta_2)} \quad (9.9)$$

where θ_m is known as the *logarithmic mean temperature difference*.

UNDERWOOD⁽¹⁾ proposed the following approximation for the logarithmic mean temperature difference:

$$(\theta_m)^{1/3} = \frac{1}{2}(\theta_1^{1/3} + \theta_2^{1/3}) \quad (9.10)$$

and, for example, when $\theta_1 = 1$ K and $\theta_2 = 100$ K, θ_m is 22.4 K compared with a logarithmic mean of 21.5 K. When $\theta_1 = 10$ K and $\theta_2 = 100$ K, both the approximation and the logarithmic mean values coincide at 39 K.

If the two fluids flow in the same direction on each side of a tube, co-current flow is taking place and the general shape of the temperature profile along the tube is as shown in Figure 9.2. A similar analysis will show that this gives the same expression for θ_m , the logarithmic mean temperature difference. For the same terminal temperatures it is important to note that the value of θ_m for countercurrent flow is appreciably greater than the value for co-current flow. This is seen from the temperature profiles, where with co-current flow the cold fluid cannot be heated to a higher temperature than the exit temperature of the hot fluid as illustrated in Example 9.1.

Example 9.1

A heat exchanger is required to cool 20 kg/s of water from 360 K to 340 K by means of 25 kg/s water entering at 300 K. If the overall coefficient of heat transfer is constant at 2 kW/m²K, calculate the surface area required in (a) a countercurrent concentric tube exchanger, and (b) a co-current flow concentric tube exchanger.

Solution

Heat load: $Q = 20 \times 4.18(360 - 340) = 1672$ kW

The cooling water outlet temperature is given by:

$$1672 = 25 \times 4.18(\theta_2 - 300) \quad \text{or} \quad \theta_2 = 316 \text{ K}$$

(a) *Counterflow*

In equation 9.9:

$$\theta_m = \frac{44 - 40}{\ln(44/40)} = 41.9 \text{ K}$$

Heat transfer area:

$$A = \frac{Q}{U\theta_m}$$

(b) *Co-current flow*

In equation 9.9:

$$\theta_m = \frac{60 - 24}{\ln(60/24)} = 39.3 \text{ K}$$

Heat transfer area:

$$A = \frac{1672}{2 \times 39.3} = 21.27 \text{ m}^2$$

It may be noted that using Underwood's approximation (equation 9.10), the calculated values for the mean temperature driving forces are 41.9 K and 39.3 K for counter- and co-current flow respectively, which agree exactly with the logarithmic mean values.

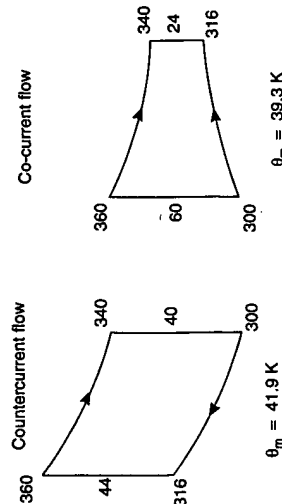


Figure 9.4. Data for Example 9.1

9.3. HEAT TRANSFER BY CONDUCTION

9.3.1. Conduction through a plane wall

This important mechanism of heat transfer is now considered in more detail for the flow of heat through a plane wall of thickness x as shown in Figure 9.5.

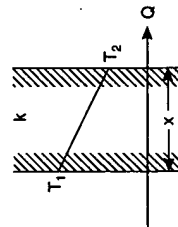


Figure 9.5. Conduction of heat through a plane wall

The rate of heat flow Q over the area A and a small distance dx may be written as:

$$\bar{Q} = -kA \left(\frac{dT}{dx} \right) \quad (9.11)$$

which is often known as *Fourier's equation*, where the negative sign indicates that the temperature gradient is in the opposite direction to the flow of heat and k is the thermal conductivity of the material. Integrating for a wall of thickness x with boundary temperatures T_1 and T_2 , as shown in Figure 9.5:

$$\bar{Q} = \frac{kA(T_1 - T_2)}{x} \quad (9.12)$$

Thermal conductivity is a function of temperature and experimental data may often be expressed by a linear relationship of the form:

$$k = k_0(1 + k'T) \quad (9.13)$$

where k is the thermal conductivity at the temperature T and k_0 and k' are constants. Combining equations 9.11 and 9.13:

$$-k \, dT = -k_0(1 + k'T) \, dT = \frac{Q \, dx}{A}$$

Integrating between the temperature limits T_1 and T_2 ,

$$-\int_{T_1}^{T_2} k dT = (T_1 - T_2)k_0 \left\{ 1 + k' \left(\frac{T_1 + T_2}{2} \right) \right\} = Q \int_{x_1}^{x_2} \frac{dx}{A} \quad (9.14)$$

Where k is a linear function of T , the following equation may therefore be used:

$$k_a(T_1 - T_2) = Q \int_{x_1}^{x_2} \frac{dx}{A} \quad (9.15)$$

where k_a is the arithmetic mean of k_1 and k_2 at T_1 and T_2 respectively or the thermal conductivity at the arithmetic mean of T_1 and T_2 .

Where k is a non-linear function of T , some mean value, k_m will apply, where:

$$k_m = \frac{1}{T_2 - T_1} \int_{T_1}^{T_2} k dT \quad (9.16)$$

From Table 9.1 it will be seen that metals have very high thermal conductivities, non-metallic solids lower values, non-metallic liquids low values, and gases very low values. It is important to note that amongst metals, stainless steel has a low value, that water has a very high value for liquids (due to partial ionisation), and that hydrogen has a high value for gases (due to the high mobility of the molecules). With gases, k decreases with increase in molecular mass and increases with the temperature. In addition, for gases the dimensionless *Prandtl group* $C_p \mu / k$, which is approximately constant (where C_p is the specific heat at constant pressure and μ is the viscosity), can be used to evaluate k at high temperatures where it is difficult to determine a value experimentally because of the formation of convection currents. k does not vary significantly with pressure, except where this is reduced to a value so low that the mean free path of the molecules becomes

Table 9.1. Thermal conductivities of selected materials

Temp (K)	(Btu/h ft ² °F/ft)	(W/mK)
573	133	230
291	54	94
373	218	377
291	35	61
326	27.6	48
373	19	33
373	33	57
373	238	412
291	26	45
291	32	55
303	65	113
109	109	189
9.2	9.2	16
0.096	0.17	0.17
0.09	0.16	0.16
0.11	0.19	0.19
0.12	0.21	0.21
0.18	0.31	0.31
0.63	1.09	1.09
0.029	0.050	0.050
0.25	0.43	0.43
0.087	0.15	0.15
0.03	0.032	0.032
0.025	0.043	0.043
0.024	0.041	0.041
0.04	0.070	0.070
151		
573	133	230
291	54	94
373	218	377
291	35	61
326	27.6	48
373	19	33
373	33	57
373	238	412
291	26	45
291	32	55
303	65	113
109	109	189
9.2	9.2	16
0.096	0.17	0.17
0.09	0.16	0.16
0.11	0.19	0.19
0.12	0.21	0.21
0.18	0.31	0.31
0.63	1.09	1.09
0.029	0.050	0.050
0.25	0.43	0.43
0.087	0.15	0.15
0.03	0.032	0.032
0.025	0.043	0.043
0.024	0.041	0.041
0.04	0.070	0.070
151		
573	133	230
291	54	94
373	218	377
291	35	61
326	27.6	48
373	19	33
373	33	57
373	238	412
291	26	45
291	32	55
303	65	113
109	109	189
9.2	9.2	16
0.096	0.17	0.17
0.09	0.16	0.16
0.11	0.19	0.19
0.12	0.21	0.21
0.18	0.31	0.31
0.63	1.09	1.09
0.029	0.050	0.050
0.25	0.43	0.43
0.087	0.15	0.15
0.03	0.032	0.032
0.025	0.043	0.043
0.024	0.041	0.041
0.04	0.070	0.070
151		
573	133	230
291	54	94
373	218	377
291	35	61
326	27.6	48
373	19	33
373	33	57
373	238	412
291	26	45
291	32	55
303	65	113
109	109	189
9.2	9.2	16
0.096	0.17	0.17
0.09	0.16	0.16
0.11	0.19	0.19
0.12	0.21	0.21
0.18	0.31	0.31
0.63	1.09	1.09
0.029	0.050	0.050
0.25	0.43	0.43
0.087	0.15	0.15
0.03	0.032	0.032
0.025	0.043	0.043
0.024	0.041	0.041
0.04	0.070	0.070
151		
573	133	230
291	54	94
373	218	377
291	35	61
326	27.6	48
373	19	33
373	33	57
373	238	412
291	26	45
291	32	55
303	65	113
109	109	189
9.2	9.2	16
0.096	0.17	0.17
0.09	0.16	0.16
0.11	0.19	0.19
0.12	0.21	0.21
0.18	0.31	0.31
0.63	1.09	1.09
0.029	0.050	0.050
0.25	0.43	0.43
0.087	0.15	

comparable with the dimensions of the vessel; further reduction of pressure then causes k to decrease.

Typical values for Prandtl numbers are as follows:

Air	0.71	<i>n</i> -Butanol	50
Oxygen	0.63	Light oil	600
Ammonia (gas)	1.38	Glycerol	1000
Water	5–10	Polymer melts	10,000
		Mercury	0.02

The low conductivity of heat insulating materials, such as cork, glass wool, and so on, is largely accounted for by their high proportion of air space. The flow of heat through such materials is governed mainly by the resistance of the air spaces, which should be sufficiently small for convection currents to be suppressed.

It is convenient to rearrange equation 9.12 to give:

$$Q = \frac{(T_1 - T_2)A}{(x/k)} \quad (9.17)$$

where x/k is known as the *thermal resistance* and k/x is the *transfer coefficient*.

Example 9.2.

Estimate the heat loss per square metre of surface through a brick wall 0.5 m thick when the inner surface is at 400 K and the outside surface is at 300 K. The thermal conductivity of the brick may be taken as 0.7 W/mK.

Solution

From equation 9.12:

$$Q = \frac{0.7 \times 1 \times (400 - 300)}{0.5} = 140 \text{ W/m}^2$$

$$\frac{\text{W}}{\text{m}^2 \cdot \text{K}} \cdot \frac{\text{K}}{\text{m}} = \frac{\text{W}}{\text{m}^2}$$

9.3.2. Thermal resistances in series

It has been noted earlier that thermal resistances may be added together for the case of heat transfer through a complete section formed from different media in series.

Figure 9.6 shows a composite wall made up of three materials with thermal conductivities k_1 , k_2 , and k_3 , with thicknesses as shown and with the temperatures T_1 , T_2 , T_3 , and T_4 at the faces. Applying equation 9.12 to each section in turn, and noting that the same quantity of heat Q must pass through each area A :

$$T_1 - T_2 = \frac{x_1}{k_1} Q, \quad T_2 - T_3 = \frac{x_2}{k_2} Q, \quad \text{and} \quad T_3 - T_4 = \frac{x_3}{k_3} Q$$

On addition:

$$(T_1 - T_4) = \left(\frac{x_1}{k_1 A} + \frac{x_2}{k_2 A} + \frac{x_3}{k_3 A} \right) Q \quad (9.18)$$

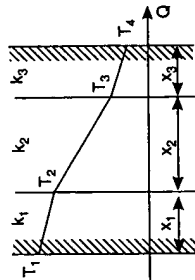


Figure 9.6. Conduction of heat through a composite wall

$$\text{or:} \quad Q = \frac{T_1 - T_4}{\Sigma(x_i/k_i A)}$$

$$= \frac{\text{Total driving force}}{\text{Total (thermal resistance/area)}} \quad (9.19)$$

Example 9.3

A furnace is constructed with 0.20 m of firebrick, 0.10 m of insulating brick, and 0.20 m of building brick. The inside temperature is 1200 K and the outside temperature is 330 K. If the thermal conductivities are as shown in Figure 9.7, estimate the heat loss per unit area and the temperature at the junction of the firebrick and the insulating brick.

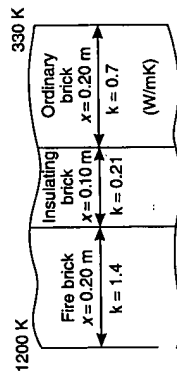


Figure 9.7. Data for Example 9.3

Solution

From equation 9.19:

$$Q = \frac{(1200 - 330)}{\frac{0.20}{1.4 \times 1} + \left(\frac{0.10}{0.21 \times 1} \right) + \left(\frac{0.20}{0.7 \times 1} \right)}$$

$$= \frac{870}{\frac{0.143}{0.476 + 0.286} + \frac{0.905}{0.905}} = 961 \text{ W/m}^2$$

The ratio (Temperature drop over firebrick)/(Total temperature drop) = $(0.143/0.905)$

∴ Temperature drop over firebrick = $\left(\frac{870 \times 0.143}{0.905} \right) = 137 \text{ deg K}$

Hence the temperature at the firebrick-insulating brick interface = $(1200 - 137) = 1063 \text{ K}$

9.3.3. Conduction through a thick-walled tube

The conditions for heat flow through a thick-walled tube when the temperatures on the inside and outside are held constant are shown in Figure 9.8. Here the area for heat flow is proportional to the radius and hence the temperature gradient is inversely proportional to the radius.

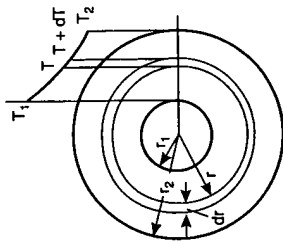


Figure 9.8. Conduction through thick-walled tube or spherical shell

The heat flow at any radius r is given by:

$$Q = -k2\pi rl \frac{dT}{dr} \quad (9.20)$$

where l is the length of tube.

Integrating between the limits r_1 and r_2 :

$$Q \int_{r_1}^{r_2} \frac{dr}{r} = -2\pi lk \int_{T_1}^{T_2} dT$$

$$Q = \frac{2\pi lk(T_1 - T_2)}{\ln(r_2/r_1)} \quad (9.21)$$

or:

This equation may be put into the form of equation 9.12 to give:

$$Q = \frac{k(2\pi r_m l)(T_1 - T_2)}{r_2 - r_1} \quad (9.22)$$

where $r_m = (r_2 - r_1) / \ln(r_2/r_1)$, is known as the *logarithmic mean radius*. For thin-walled tubes the arithmetic mean radius r_a may be used, giving:

$$Q = \frac{k(2\pi r_a l)(T_1 - T_2)}{r_2 - r_1} \quad (9.23)$$

9.3.4. Conduction through a spherical shell and to a particle

For heat conduction through a spherical shell, the heat flow at radius r is given by:

$$Q = -k4\pi r^2 \frac{dT}{dr} \quad (9.24)$$

Integrating between the limits r_1 and r_2 :

$$Q \int_{r_1}^{r_2} \frac{dr}{r^2} = -4\pi k \int_{T_1}^{T_2} dT$$

$$Q = \frac{4\pi k(T_1 - T_2)}{(1/r_1) - (1/r_2)} \quad (9.25)$$

An important application of heat transfer to a sphere is that of conduction through a stationary fluid surrounding a spherical particle or droplet of radius r as encountered for example in fluidised beds, rotary kilns, spray dryers and plasma devices. If the temperature difference $T_1 - T_2$ is spread over a very large distance so that $r_2 = \infty$ and T_1 is the temperature of the surface of the drop, then:

$$\frac{Qr}{(4\pi r^2)(T_1 - T_2)k} = 1$$

$$\frac{hd}{k} = Nu' = 2 \quad (9.26)$$

or:

where $Q/4\pi r^2(T_1 - T_2) = h$ is the heat transfer coefficient, d is the diameter of the particle or droplet and hd/k is a dimensionless group known as the *Nusselt number* (Nu') for the particle. The more general use of the Nusselt number, with particular reference to heat transfer by convection, is discussed in Section 9.4. This value of 2 for the Nusselt number is the theoretical minimum for heat transfer through a *continuous* medium. It is greater if the temperature difference is applied over a finite distance, when equation 9.25 must be used. When there is relative motion between the particle and the fluid the heat transfer rate will be further increased, as discussed in Section 9.4.6.

In this approach, heat transfer to a spherical particle by conduction through the surrounding fluid has been the prime consideration. In many practical situations the flow of heat from the surface to the internal parts of the particle is of importance. For example, if the particle is a poor conductor then the rate at which the particulate material reaches some desired average temperature may be limited by conduction inside the particle rather than by conduction to the outside surface of the particle. This problem involves unsteady state transfer of heat which is considered in Section 9.3.5.

Equations may be developed to predict the rate of change of diameter d of evaporating droplets. If the latent heat of vaporisation is provided by heat conducted through a hotter stagnant gas to the droplet surface, and heat transfer is the rate controlling step, it is shown by SPALDING⁽²⁾ that d^2 decreases linearly with time. A closely related and important practical problem is the prediction of the residence time required in a combustion chamber to ensure virtually complete burning of the oil droplets. Complete combustion is desirable to obtain maximum utilisation of energy and to minimise pollution of the atmosphere by partially burned oil droplets. Here a droplet is surrounded by a flame and heat conducted back from the flame to the droplet surface provides the heat to vaporise the oil and sustain the surrounding flame. Again d^2 decreases approximately linearly with time though the derivation of the equation is more complex due to mass transfer effects, steep temperature gradients⁽³⁾ and circulation in the drop⁽⁴⁾.

9.3.5. Unsteady state conduction

Basic considerations

In the problems which have been considered so far, it has been assumed that the conditions at any point in the system remain constant with respect to time. The case of heat transfer by conduction in a medium in which the temperature is changing with time is now considered. This problem is of importance in the calculation of the temperature distribution in a body which is being heated or cooled. If, in an element of dimensions dx by dy by dz (Figure 9.9), the temperature at the point (x, y, z) is θ and at the point $(x + dx, y + dy, z + dz)$ is $(\theta + d\theta)$, then assuming that the thermal conductivity k is constant and that no heat is generated in the medium, the rate of conduction of heat through the element is:

$$\begin{aligned}
 &= -k \, dy \, dz \left(\frac{\partial \theta}{\partial x} \right)_{yz} \quad \text{in the } x\text{-direction} \\
 &= -k \, dz \, dx \left(\frac{\partial \theta}{\partial y} \right)_{xz} \quad \text{in the } y\text{-direction} \\
 &= -k \, dx \, dy \left(\frac{\partial \theta}{\partial z} \right)_{xy} \quad \text{in the } z\text{-direction}
 \end{aligned}$$

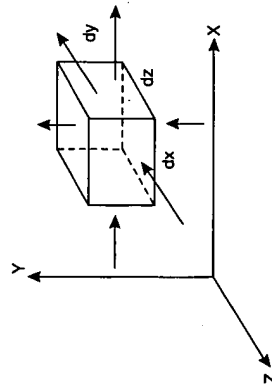


Figure 9.9. Element for heat conduction

The rate of change of heat content of the element is equal to *minus* the rate of increase of heat flow from (x, y, z) to $(x + dx, y + dy, z + dz)$. Thus the rate of change of the heat content of the element is:

$$\begin{aligned}
 &= k \, dy \, dz \left(\frac{\partial^2 \theta}{\partial x^2} \right)_{yz} \, dx + k \, dz \, dx \left(\frac{\partial^2 \theta}{\partial y^2} \right)_{xz} \, dy + k \, dx \, dy \left(\frac{\partial^2 \theta}{\partial z^2} \right)_{xy} \, dz \\
 &= k \, dx \, dy \, dz \left[\left(\frac{\partial^2 \theta}{\partial x^2} \right)_{yz} + \left(\frac{\partial^2 \theta}{\partial y^2} \right)_{xz} + \left(\frac{\partial^2 \theta}{\partial z^2} \right)_{xy} \right] \quad (9.27)
 \end{aligned}$$

The rate of increase of heat content is also equal, however, to the product of the heat capacity of the element and the rate of rise of temperature.

$$\text{Thus:} \quad k \, dx \, dy \, dz \left[\left(\frac{\partial^2 \theta}{\partial x^2} \right)_{yz} + \left(\frac{\partial^2 \theta}{\partial y^2} \right)_{xz} + \left(\frac{\partial^2 \theta}{\partial z^2} \right)_{xy} \right] = C_p \rho \, dx \, dy \, dz \, \frac{\partial \theta}{\partial t}$$

$$\begin{aligned}
 \text{or:} \quad \frac{\partial \theta}{\partial t} &= \frac{k}{C_p \rho} \left[\left(\frac{\partial^2 \theta}{\partial x^2} \right)_{yz} + \left(\frac{\partial^2 \theta}{\partial y^2} \right)_{xz} + \left(\frac{\partial^2 \theta}{\partial z^2} \right)_{xy} \right] \\
 &= D_H \left[\left(\frac{\partial^2 \theta}{\partial x^2} \right)_{yz} + \left(\frac{\partial^2 \theta}{\partial y^2} \right)_{xz} + \left(\frac{\partial^2 \theta}{\partial z^2} \right)_{xy} \right] \quad (9.28)
 \end{aligned}$$

where $D_H = k/C_p \rho$ is known as the *thermal diffusivity*.

This partial differential equation is most conveniently solved by the use of the Laplace transform of temperature with respect to time. As an illustration of the method of solution, the problem of the unidirectional flow of heat in a continuous medium will be considered. The basic differential equation for the x -direction is:

$$\frac{\partial \theta}{\partial t} = D_H \frac{\partial^2 \theta}{\partial x^2} \quad (9.29)$$

This equation cannot be integrated directly since the temperature θ is expressed as a function of two independent variables, distance x and time t . The method of solution involves transforming the equation so that the Laplace transform of θ with respect to time is used in place of θ . The equation then involves only the Laplace transform $\bar{\theta}$ and the distance x . The Laplace transform of θ is defined by the relation:

$$\bar{\theta} = \int_0^\infty \theta e^{-pt} \, dt \quad (9.30)$$

where p is a parameter.

Thus $\bar{\theta}$ is obtained by operating on θ with respect to t with x constant.

$$\text{Then:} \quad \frac{\partial^2 \bar{\theta}}{\partial x^2} = \frac{\partial^2 \theta}{\partial x^2} \quad (9.31)$$

$$\begin{aligned}
 \text{and:} \quad \frac{\partial \bar{\theta}}{\partial t} &= \int_0^\infty \frac{\partial \theta}{\partial t} e^{-pt} \, dt \\
 &= \left[\theta e^{-pt} \right]_0^\infty + p \int_0^\infty \theta e^{-pt} \, dt \\
 &= -\theta_{t=0} + p \bar{\theta} \quad (9.32)
 \end{aligned}$$

Then, taking the Laplace transforms of each side of equation 9.29:

$$\begin{aligned}
 \text{or:} \quad p \bar{\theta} - \theta_{t=0} &= D_H \frac{\partial^2 \bar{\theta}}{\partial x^2} \quad (\text{from equations 9.31 and 9.32}) \\
 \text{and:} \quad \frac{\partial^2 \bar{\theta}}{\partial x^2} - \frac{p}{D_H} \bar{\theta} &= -\frac{\theta_{t=0}}{D_H}
 \end{aligned}$$

If the temperature everywhere is constant initially, $\theta_{t=0}$ is a constant and the equation may be integrated as a normal second-order differential equation since p is not a function of x .

Thus:
$$\bar{\theta} = B_1 e^{\sqrt{(p/D_H)x}} + B_2 e^{-\sqrt{(p/D_H)x}} + \theta_{t=0} p^{-1} \quad (9.33)$$

and therefore:
$$\frac{\partial \bar{\theta}}{\partial x} = B_1 \sqrt{\frac{p}{D_H}} e^{\sqrt{(p/D_H)x}} - B_2 \sqrt{\frac{p}{D_H}} e^{-\sqrt{(p/D_H)x}} \quad (9.34)$$

The temperature θ , corresponding to the transform $\bar{\theta}$, may now be found by reference to tables of the Laplace transform. It is first necessary, however, to evaluate the constants B_1 and B_2 using the boundary conditions for the particular problem since these constants will in general involve the parameter p which was introduced in the transformation.

Considering the particular problem of the unidirectional flow of heat through a body with plane parallel faces a distance l apart, the heat flow is normal to these faces and the temperature of the body is initially constant throughout. The temperature scale will be so chosen that this uniform initial temperature is zero. At time, $t = 0$, one face (at $x = 0$) will be brought into contact with a source at a constant temperature θ' and the other face (at $x = l$) will be assumed to be perfectly insulated thermally.

The boundary conditions are therefore:

$$t = 0, \quad \theta = 0$$

$$t > 0, \quad \theta = \theta' \quad \text{when } x = 0$$

$$t > 0, \quad \frac{\partial \theta}{\partial x} = 0 \quad \text{when } x = l$$

Thus:
$$\bar{\theta}_{x=0} = \int_0^\infty \theta' e^{-pt} dt = \frac{\theta'}{p}$$

and:
$$\left(\frac{\partial \bar{\theta}}{\partial x} \right)_{x=l} = 0$$

Substitution of these boundary conditions in equations 9.33 and 9.34 gives:

$$B_1 + B_2 = \frac{\theta'}{p} \quad (9.35)$$

$$B_1 e^{\sqrt{(p/D_H)l}} - B_2 e^{-\sqrt{(p/D_H)l}} = 0$$

Hence:

$$B_1 = \frac{(\theta'/p) e^{-\sqrt{(p/D_H)l}}}{e^{\sqrt{(p/D_H)l}} + e^{-\sqrt{(p/D_H)l}}}$$

and:

$$B_2 = \frac{(\theta'/p) e^{\sqrt{(p/D_H)l}}}{e^{\sqrt{(p/D_H)l}} + e^{-\sqrt{(p/D_H)l}}}$$

Then:

$$\begin{aligned} \bar{\theta} &= \frac{e^{(l-x)\sqrt{(p/D_H)}} + e^{-(l-x)\sqrt{(p/D_H)}}}{e^{\sqrt{(p/D_H)l}} + e^{-\sqrt{(p/D_H)l}}} \frac{\theta'}{p} \\ &= \frac{\theta'}{p} \frac{(e^{(l-x)\sqrt{(p/D_H)}} + e^{-(l-x)\sqrt{(p/D_H)}})(1 + e^{-2\sqrt{(p/D_H)l}}) - (e^{-\sqrt{(p/D_H)l}})}{e^{\sqrt{(p/D_H)l}} + e^{-\sqrt{(p/D_H)l}}} \\ &= \frac{\theta'}{p} \frac{(e^{-x\sqrt{(p/D_H)}} + e^{-(2l-x)\sqrt{(p/D_H)}})(1 - e^{-2l\sqrt{(p/D_H)}}) + \dots}{1 + e^{-2l\sqrt{(p/D_H)}}} \\ &= \sum_{N=0}^{\infty} \frac{\theta'}{p} \frac{(-1)^N (e^{-(2N+x)\sqrt{(p/D_H)}} + e^{-(2(N+1)l-x)\sqrt{(p/D_H)}})}{1 + e^{-2l\sqrt{(p/D_H)}}} \quad (9.36) \end{aligned}$$

The temperature θ is then obtained from the tables of inverse Laplace transforms in the Appendix (Table 12, No 83) and is given by:

$$\theta = \sum_{N=0}^{\infty} (-1)^N \theta' \left(\operatorname{erfc} \frac{2Nl+x}{2\sqrt{D_H t}} + \operatorname{erfc} \frac{2(N+1)l-x}{2\sqrt{D_H t}} \right) \quad (9.37)$$

where:
$$\operatorname{erfc} x = \frac{2}{\sqrt{\pi}} \int_x^\infty e^{-\xi^2} d\xi$$

Values of $\operatorname{erfc} x$ ($= 1 - \operatorname{erf} x$) are given in the Appendix (Table 13) and in specialist sources.⁽⁵⁾

Equation 9.37 may be written in the form:

$$\frac{\theta}{\theta'} = \sum_{N=0}^{\infty} (-1)^N \left\{ \operatorname{erfc} \left[F_{01}^{-1/2} \left(N + \frac{1}{2} \right) \right] + \operatorname{erfc} \left[F_{01}^{-1/2} \left((N+1) - \frac{1}{2} \right) \right] \right\} \quad (9.38)$$

where $F_{01} = (D_H t/l^2)$ and is known as the *Fourier number*.

Thus:
$$\frac{\theta}{\theta'} = f \left(F_{01}, \frac{x}{l} \right) \quad (9.39)$$

The numerical solution to this problem is then obtained by inserting the appropriate values for the physical properties of the system and using as many terms in the series as are necessary for the degree of accuracy required. In most cases, the above series converge quite rapidly.

This method of solution of problems of unsteady flow is particularly useful because it is applicable when there are discontinuities in the physical properties of the material.⁽⁶⁾ The boundary conditions, however, become a little more complicated, but the problem is intrinsically no more difficult.

A general method of estimating the temperature distribution in a body of any shape consists of replacing the heat flow problem by the analogous electrical situation and measuring the electrical potentials at various points. The heat capacity per unit volume $C_p \rho$ is represented by an electrical capacitance, and the thermal conductivity k by an

electrical conductivity. This method can be used to take account of variations in the thermal properties over the body.

Example 9.4

Calculate the time taken for the distant face of a brick wall, of thermal diffusivity $D_H = 0.0043 \text{ cm}^2/\text{s}$ and thickness $l = 0.45 \text{ m}$, to rise from 295 to 375 K, if the whole wall is initially at a constant temperature of 295 K and the near face is suddenly raised to 900 K and maintained at this temperature. Assume that all the flow of heat is perpendicular to the faces of the wall and that the distant face is perfectly insulated.

Solution

The temperature at any distance x from the near face at time t is given by:

$$\theta = \sum_{N=0}^{\infty} (-1)^N \theta' \left\{ \operatorname{erfc} \left[\frac{2N+x}{2\sqrt{D_H t}} \right] + \operatorname{erfc} \left[\frac{2(N+1)l-x}{2\sqrt{D_H t}} \right] \right\} \quad (\text{equation 9.37})$$

The temperature at the distant face is therefore given by:

$$\theta = \sum_{N=0}^{\infty} (-1)^N \theta' 2 \operatorname{erfc} \left[\frac{(2N+1)l}{2\sqrt{D_H t}} \right]$$

Choosing the temperature scale so that the initial temperature is everywhere zero, then:

$$\frac{\theta}{2\theta'} = \frac{375 - 295}{2(900 - 295)} = 0.066$$

$$D_H = 4.2 \times 10^{-7} \text{ m}^2/\text{s} \quad \therefore \sqrt{D_H} = 6.5 \times 10^{-4}$$

$$\begin{aligned} \text{Thus:} \quad 0.066 &= \sum_{N=0}^{\infty} (-1)^N \operatorname{erfc} \left[\frac{0.45(2N+1)}{2 \times 6.5 \times 10^{-4} \sqrt{t}} \right] \\ &= \sum_{N=0}^{\infty} (-1)^N \operatorname{erfc} \left[\frac{346(2N+1)}{\sqrt{t}} \right] \\ &= \operatorname{erfc}(346t^{-0.5}) - \operatorname{erfc}(1038t^{-0.5}) + \operatorname{erfc}(1730t^{-0.5}) - \dots \end{aligned}$$

An approximate solution is obtained by taking the first term only, to give:

$$346t^{-0.5} = 1.30$$

from which

$$t = 70840 \text{ s}$$

$$= 70.8 \text{ ks or } 19.7 \text{ h}$$

Schmidt's method

Numerical methods have been developed by replacing the differential equation by a finite difference equation. Thus in a problem of unidirectional flow of heat:

$$\frac{\partial \theta}{\partial t} \approx \frac{\theta_{x(t+\Delta t)} - \theta_{x(t-\Delta t)}}{2\Delta t} \approx \frac{\theta_{x(t+\Delta t)} - \theta_x}{\Delta t}$$

$$\frac{\partial^2 \theta}{\partial x^2} \approx \frac{\left(\frac{\theta_{(x+\Delta x)t} - \theta_x}{\Delta x} - \frac{\theta_x - \theta_{(x-\Delta x)t}}{\Delta x} \right)}{\Delta x}$$

$$= \frac{\theta_{(x+\Delta x)t} + \theta_{(x-\Delta x)t} - 2\theta_x}{(\Delta x)^2}$$

where θ_x is the value of θ at time t and distance x from the surface, and the other values of θ are at intervals Δx and Δt as shown in Figure 9.10.

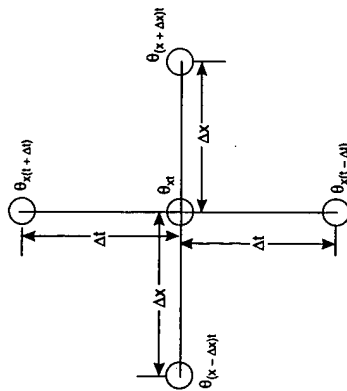


Figure 9.10. Variation of temperature with time and distance

Substituting these values in equation 9.29:

$$\theta_{x(t+\Delta t)} - \theta_{x(t-\Delta t)} = D_H \frac{2\Delta t}{(\Delta x)^2} (\theta_{(x+\Delta x)t} + \theta_{(x-\Delta x)t} - 2\theta_x) \quad (9.40)$$

and:
$$\theta_{x(t+\Delta t)} - \theta_x = D_H \frac{\Delta t}{(\Delta x)^2} (\theta_{(x+\Delta x)t} + \theta_{(x-\Delta x)t} - 2\theta_x) \quad (9.41)$$

Thus, if the temperature distribution at time t , is known, the corresponding distribution at time $t + \Delta t$ can be calculated by the application of equation 9.41 over the whole extent of the body in question. The intervals Δx and Δt are so chosen that the required degree of accuracy is obtained.

A graphical method of procedure has been proposed by SCHMIDT⁽⁷⁾. If the temperature distribution at time t is represented by the curve shown in Figure 9.11 and the points representing the temperatures at $x - \Delta x$ and $x + \Delta x$ are joined by a straight line, then the distance θ_a is given by:

$$\theta_a = \frac{\theta_{(x+\Delta x)t} + \theta_{(x-\Delta x)t}}{2} - \theta_x$$

$$= \frac{(\Delta x)^2}{2D_H \Delta t} (\theta_{x(t+\Delta t)} - \theta_x) \quad (\text{from equation 9.41}) \quad (9.42)$$

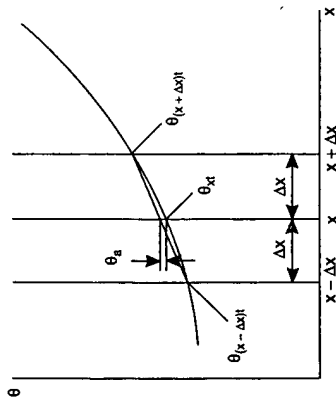


Figure 9.11. Schmidt's method

Thus, θ_a represents the change in θ_x after a time interval Δt , such that:

$$\Delta t = \frac{(\Delta x)^2}{2D_H} \quad (9.43)$$

If this simple construction is carried out over the whole of the body, the temperature distribution after time Δt is obtained. The temperature distribution after an interval $2\Delta t$ is then obtained by repeating this procedure.

The most general method of tackling the problem is the use of the *finite-element technique*⁽⁸⁾ to determine the temperature distribution at any time by using the finite difference equation in the form of equation 9.40.

Example 9.5

Solve Example 9.4 using Schmidt's method.

Solution

The development of the temperature profile is shown in Figure 9.12. At time $t = 0$ the temperature is constant at 295 K throughout and the temperature of the hot face is raised to 900 K. The problem will be solved by taking relatively large intervals for Δx .

Choosing $\Delta x = 50$ mm, the construction shown in Figure 9.12 is carried out starting at the hot face. Points corresponding to temperature after a time interval Δt are marked 1, after a time interval $2\Delta t$ by 2, and so on. Because the second face is perfectly insulated, the temperature gradient must be zero at this point. Thus, in obtaining temperatures at $x = 450$ mm, it is assumed that the temperature at $x = 500$ mm will be the same as at $x = 400$ mm, that is, horizontal lines are drawn on the diagram. It is seen that the temperature is less than 375 K after time $23\Delta t$ and greater than 375 K after time $25\Delta t$.

Thus:

$$\begin{aligned} \text{From equation 9.43:} \quad \Delta t &= 5.0^2 / (2 \times 0.0042) = 2976 \text{ s} \\ \text{Thus time required} \quad &= 24 \times 2976 = 71400 \text{ s} \end{aligned}$$

or:

$$\frac{71.4 \text{ ks}}{3600} = 19.8 \text{ h}$$

This value is quite close to that obtained by calculation, even using the coarse increments in Δx .

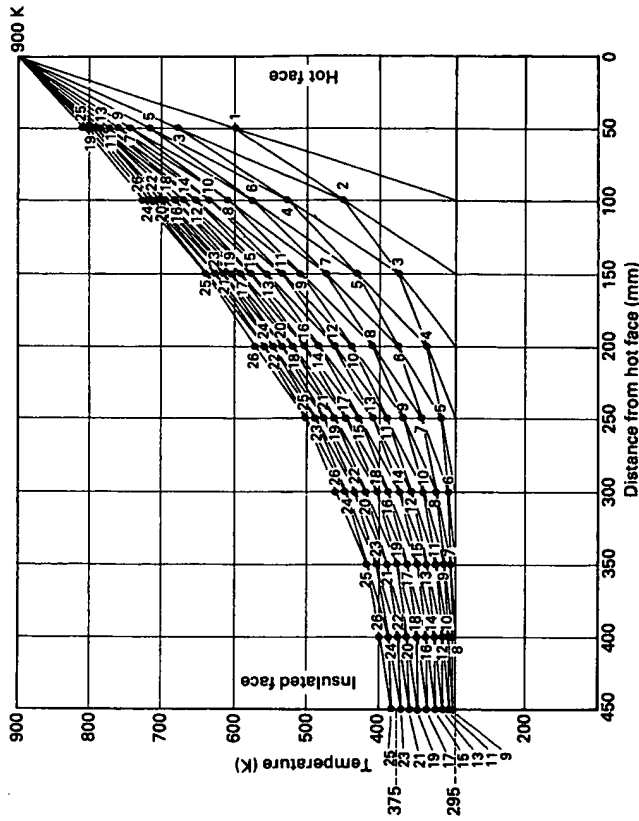


Figure 9.12. Development of temperature profile

Heating and cooling of solids and particles

The exact mathematical solution of problems involving unsteady thermal conduction may be very difficult, and sometimes impossible, especially where bodies of irregular shapes are concerned, and other methods are therefore required.

When a body of characteristic linear dimension L , initially at a uniform temperature θ_0 , is exposed suddenly to surroundings at a temperature θ' , the temperature distribution at any time t is found from dimensional analysis to be:

$$\frac{\theta' - \theta}{\theta' - \theta_0} = f\left(\frac{hL}{k}, \frac{t}{D_H^2}, \frac{x}{L}\right) \quad (9.44)$$

where D_H is the thermal diffusivity ($k_p/C_p\rho$) of the solid, x is distance within the solid body and h is the heat transfer coefficient in the fluid at the surface of the body.

Analytical solutions of equation 9.44 in the form of infinite series are available for some simple regular shapes of particles, such as rectangular slabs, long cylinders and spheres, for conditions where there is heat transfer by conduction or convection to or from the surrounding fluid. These solutions tend to be quite complex, even for simple shapes. The heat transfer process may be characterised by the value of the *Biot number* Bi where:

$$Bi = \frac{hL}{k_p} = \frac{L/k_p}{1/h} \quad (9.45)$$

where h is the external heat transfer coefficient,

L is a characteristic dimension, such as radius in the case of a sphere or long cylinder, or half the thickness in the case of a slab, and k_p is the thermal conductivity of the particle.

The Biot number is essentially the ratio of the resistance to heat transfer within the particle to that within the external fluid. At first sight, it appears to be similar in form to the Nusselt Number Nu where:

$$Nu' = \frac{hd}{k} = \frac{2hr_o}{k} \quad (9.46)$$

However, the Nusselt number refers to a single fluid phase, whereas the Biot number is related to the properties of both the fluid and the solid phases.

Three cases are now considered:

- (1) Very large Biot numbers, $Bi \rightarrow \infty$
- (2) Very low Biot numbers, $Bi \rightarrow 0$
- (3) Intermediate values of the Biot number.

(1) Bi very large. The resistance to heat transfer in the fluid is then low compared with that in the solid with the temperature of the surface of the particle being approximately equal to the bulk temperature of the fluid, and the heat transfer rate is independent of the Biot number. Equation 9.44 then simplifies to:

$$\frac{\theta' - \theta}{\theta' - \theta_0} = f\left(D_H \frac{t}{L^2}, \frac{x}{L}\right) = f\left(F_{OL}, \frac{x}{L}\right) \quad (9.47)$$

where $F_{OL} \left(= D_H \frac{t}{L^2}\right)$ is known as the *Fourier number*, using L in this case to denote the characteristic length, and x is distance from the centre of the particle. Curves connecting these groups have been plotted by a number of workers for bodies of various shapes, although the method is limited to those shapes which have been studied experimentally.

In Figure 9.13, taken from CARSLAW and JAEGER⁽⁵⁾, the value of $(\theta' - \theta_c)/(\theta' - \theta_0)$ is plotted to give the temperature θ_c at the centre of bodies of various shapes, initially at a uniform temperature θ_0 , at a time t after the surfaces have been suddenly altered to and maintained at a constant temperature θ' .

In this case (x/L) is constant at 0 and the results are shown as a function of the particular value of the Fourier number F_{OL} ($D_H t/L^2$).

(2) Bi very small. (say, <0.1). Here the main resistance to heat transfer lies within the fluid; this occurs when the thermal conductivity of the particle is very high and/or when the particle is very small. Under these conditions, the temperature within the particle is uniform and a "lumped capacity" analysis may be performed. Thus, if a solid body of volume V and initial temperature θ_0 is suddenly immersed in a volume of fluid large enough for its temperature θ to remain effectively constant, the rate of heat transfer from the body may be expressed as:

$$-\rho C_p V \frac{d\theta}{dt} = hA_s(\theta - \theta') \quad (9.48)$$

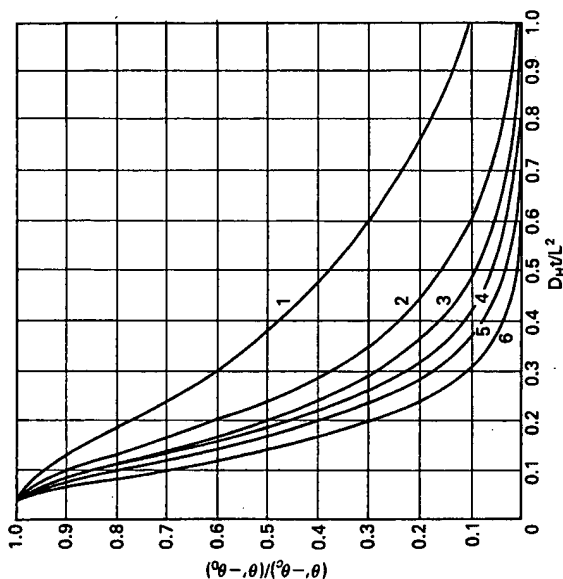


Figure 9.13. Cooling curve for bodies of various shapes: 1, slab ($2L$ = thickness); 2, square bar ($2L$ = side); 3, long cylinder (L = radius); 4, cube ($2L$ = length of side); 5, cylinder (L = radius, length = $2L$); 6, sphere (L = radius)

where A_s is the external surface area of the solid body.

$$\text{Then: } \int_{\theta_0}^{\theta} \frac{d\theta}{\theta - \theta'} = - \int_0^t \frac{hA_s}{\rho C_p V} dt$$

$$\text{i.e.: } \frac{\theta - \theta'}{\theta_0 - \theta'} = e^{-t/\tau} \quad (9.49)$$

where $\tau = \frac{\rho C_p V}{hA_s}$ is known as the *response time constant*.

It will be noted that the relevant characteristic dimension in the Biot number is defined as the ratio of the volume to the external surface area of the particle (V/A_s), and the higher the value of V/A_s , then the slower will be the response time. With the characteristic dimension defined in this way, this analysis is valid for particles of any shape at values of the Biot number less than 0.1

Example 9.6

A 25 mm diameter copper sphere and a 25 mm copper cube are both heated in a furnace to 650°C (923 K). They are then annealed in air at 95°C (368 K). If the external heat transfer coefficient h is $75\text{ W/m}^2\text{K}$ in both cases, what is temperature of the sphere and of the cube at the end of 5 minutes?

The physical properties at the mean temperature for copper are:

$$\rho = 8950 \text{ kg/m}^3 \quad C_p = 0.38 \text{ kJ/kg K} \quad k_p = 385 \text{ W/mK}$$

Solution

$$V/A_s \text{ for the sphere} = \frac{\pi d^3}{6} = \frac{d}{6} = \frac{25 \times 10^{-3}}{6} = 4.17 \times 10^{-3} \text{ m}$$

$$V/A_s \text{ for the cube} = \frac{l^3}{6l^2} = \frac{l}{6} = \frac{25 \times 10^{-3}}{6} = 4.17 \times 10^{-3} \text{ m}$$

$$Bi = \frac{h(V/A_s)}{k} = \frac{75 \times 25 \times 10^{-3}}{385 \times 6} = 8.1 \times 10^{-4} \ll 0.1$$

The use of a lumped capacity method is therefore justified.

$$\tau = \frac{\rho C_p V}{h A_s} = \frac{8950 \times 380}{75} \times \frac{25 \times 10^{-3}}{6} = 189 \text{ s}$$

Then using equation 9.49:

$$\frac{\theta - 368}{923 - 368} = \exp\left(-\frac{5 \times 60}{189}\right)$$

and:

$$\theta = 368 + 0.2045(923 - 368) = 481 \text{ K} = 208^\circ \text{C}$$

Since the sphere and the cube have the same value of V/A_s , after 5 minutes they will both attain a temperature of 208°C .

(3) *Intermediate values of Bi.* In this case the resistances to heat transfer within the solid body and the fluid are of comparable magnitude. Neither will the temperature within the solid be uniform (case 1), nor will the surface temperature be equal to that in the bulk of the fluid (case 2).

Analytical solutions in the form of infinite series can be obtained for some regular shapes (thin plates, spheres and long cylinders (length \gg radius)), and numerical solutions using *finite element methods*⁽⁸⁾ have been obtained for bodies of other shapes, both regular and irregular. Some of the results have been presented by HEISLER⁽⁹⁾ in the form of charts, examples of which are shown in Figures 9.14–9.16 for thin slabs, long cylinders and spheres, respectively. It may be noted that in this case the characteristic length L is the half-thickness of the slab and the external radius r_o of the cylinder and sphere.

Figures 9.14–9.16 enable the temperature θ_c at the centre of the solid (centre-plane, centre-line or centre-point) to be obtained as a function of the Fourier number, and hence of time, with the reciprocal of the Biot number (Bi^{-1}) as parameter.

Temperatures at off-centre locations within the solid body can then be obtained from a further series of charts given by Heisler (Figures 9.17–9.19) which link the desired temperature to the centre-temperature as a function of Biot number, with location within the particle as parameter (that is the distance x from the centre plane in the slab or radius in the cylinder or sphere). Additional charts are given by Heisler for the quantity of heat transferred from the particle in a given time in terms of the initial heat content of the particle.

Figures 9.17–9.19 clearly show that, as the Biot number approaches zero, the temperature becomes uniform within the solid, and the lumped capacity method may be used for calculating the unsteady-state heating of the particles, as discussed in section (2). The charts are applicable for Fourier numbers greater than about 0.2.

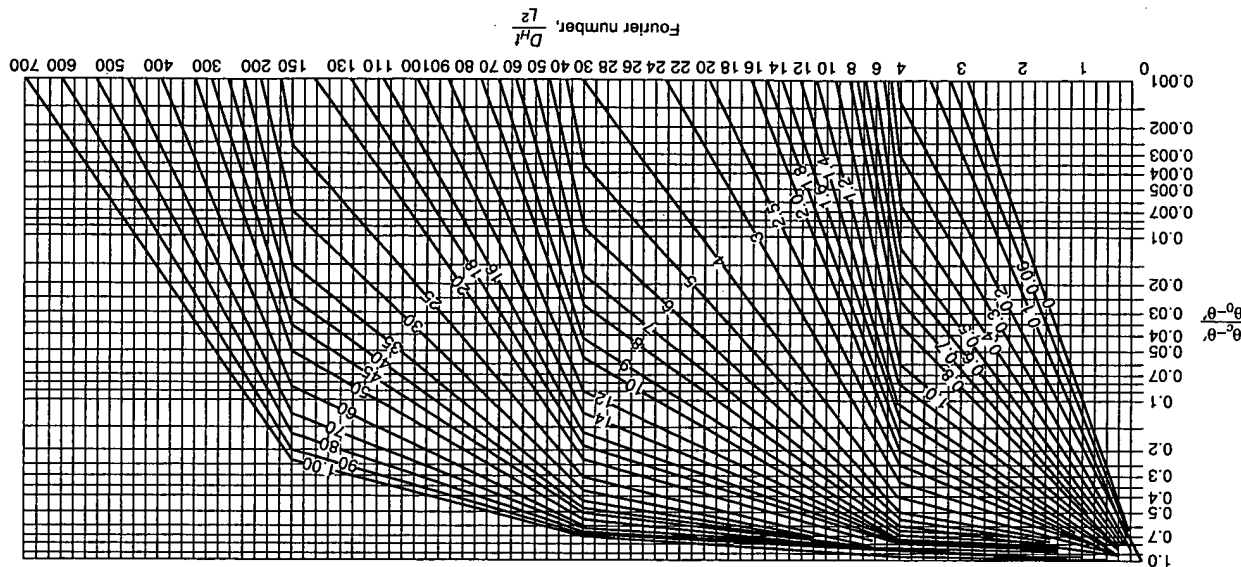


Figure 9.14. Mid-plane temperature for an infinite plate of thickness $2L$, for various values of parameters $k_p/hL (= Bi^{-1})$.

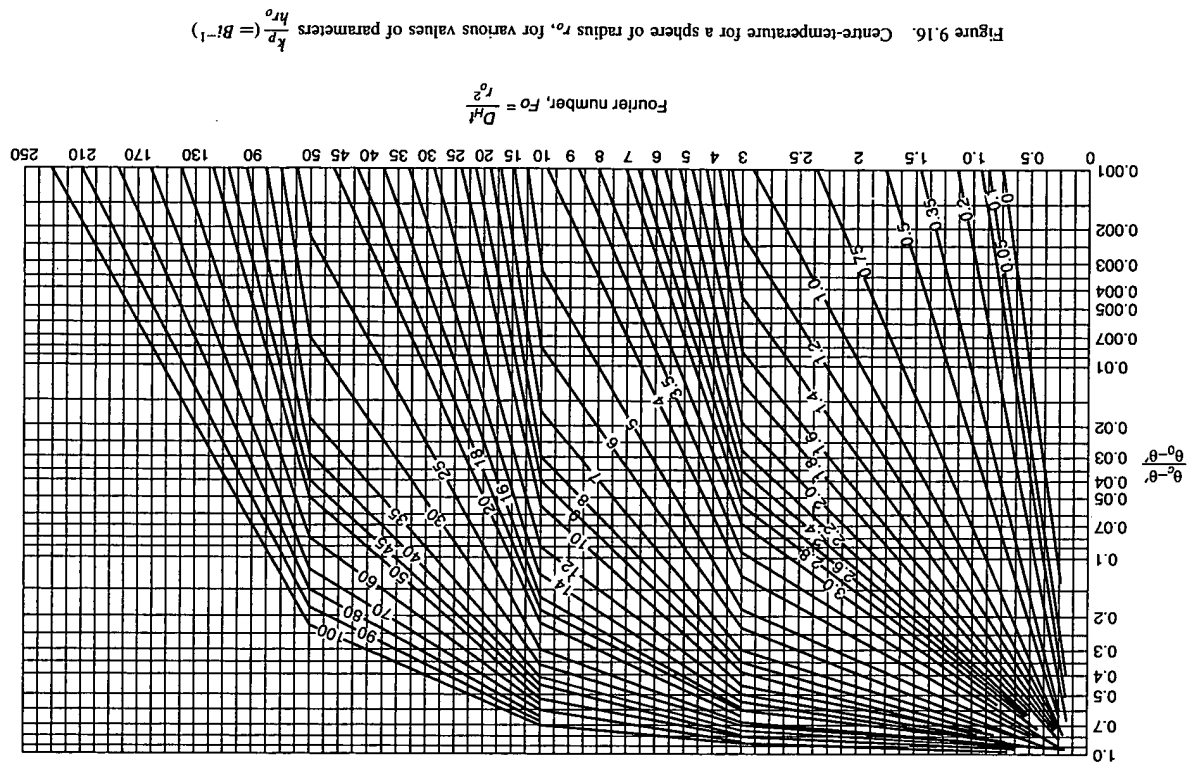
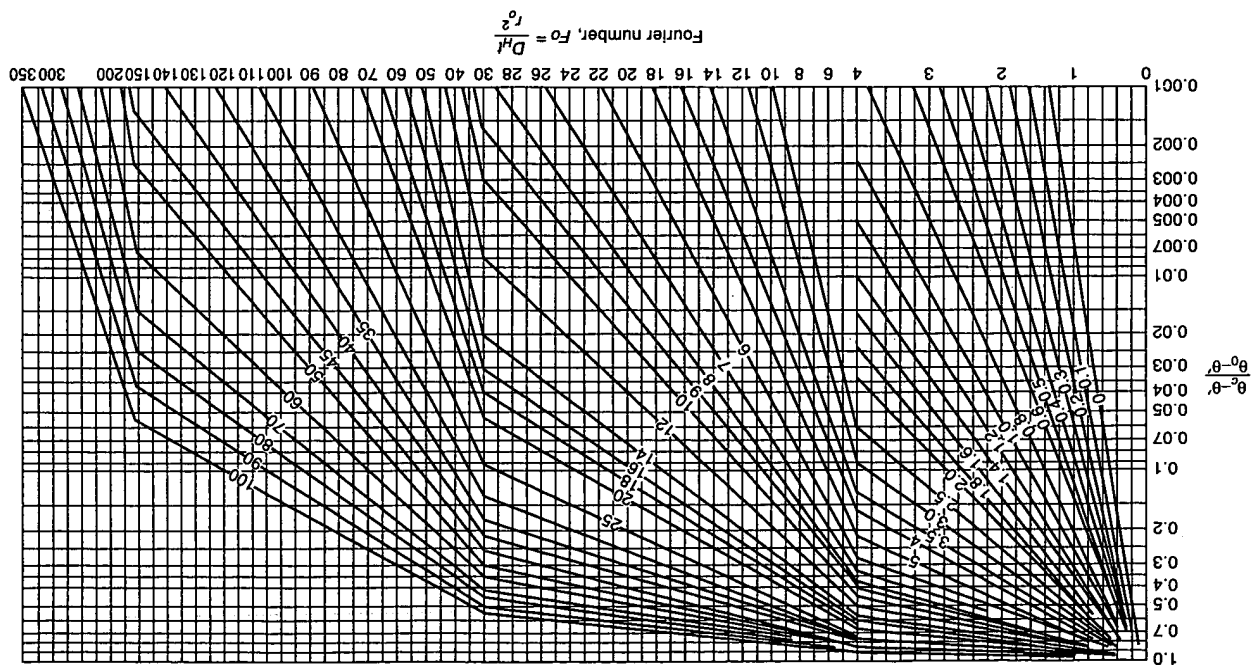
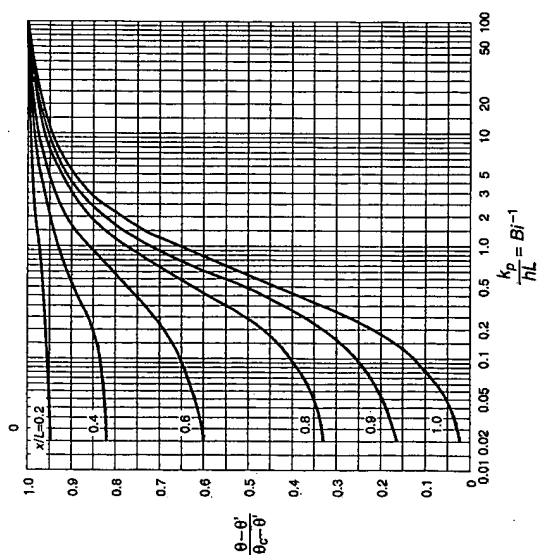
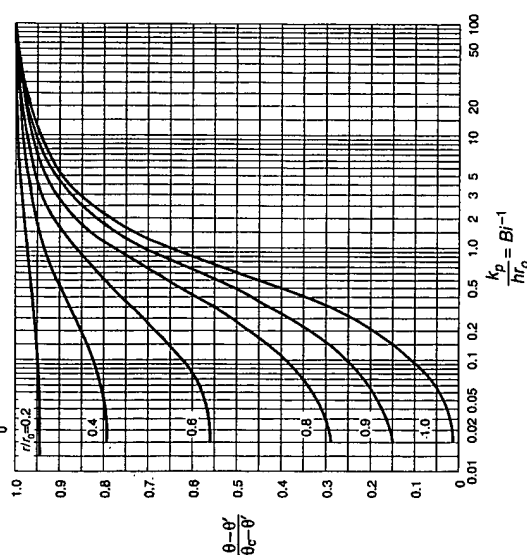
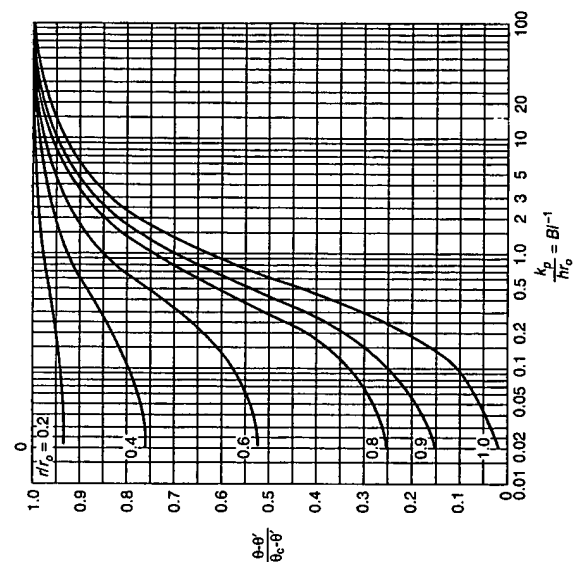


Figure 9.15. Axis temperature for an infinite cylinder of radius r_o , for various of parameters $k_p/hr_o (= Bi^{-1})$



Figure 9.17. Temperature as a function of mid-plane temperature in an infinite plate of thickness $2L$.Figure 9.18. Temperature as a function of axis temperature in an infinite cylinder of radius r_0 .Figure 9.19. Temperature as a function of centre-temperature for a sphere of radius r_0 .**Example 9.7**

A large thermoplastic sheet, 10 mm thick, at an initial temperature of 20°C (293 K), is to be heated in an oven in order to enable it to be moulded. The oven temperature is maintained at 100°C (373 K), the maximum temperature to which the plastic may be subjected, and it is necessary to ensure that the temperature throughout the whole of the sheet reaches a minimum of 80°C (353 K). Calculate the minimum length of time for which the sheet must be heated.

Thermal conductivity k_p of the plastic $= 2.5\text{ W/mK}$
 Thermal diffusivity of the surrounding fluid $D_H = 2 \times 10^{-7}\text{ m}^2/\text{s}$
 External heat transfer coefficient $h = 100\text{ W/m}^2\text{K}$

Solution

Throughout the heating process, the temperature within the sheet will be a minimum at the centre-plane ($x = 0$) and therefore the required time is that for the centre to reach 80°C (353 K).

$$\text{For this process, the Biot number } Bi = \frac{hL}{k_p} = \frac{100 \times 5 \times 10^{-3}}{2.5} = 0.2 \text{ and } Bi^{-1} = 5$$

(since L , the half-thickness of the plate is 5 mm)

$$\text{The limiting value of } \frac{\theta' - \theta_c}{\theta_i - \theta_c} = \frac{373 - 353}{373 - 293} = 0.25$$

From Figure 9.17, the Fourier number $\frac{D_{\text{eff}}}{L^2} \approx 7.7$

$$\text{Thus: } t = \frac{7.7 \times (5 \times 10^{-3})^2}{2 \times 10^{-7}} = 960 \text{ s or } \underline{\underline{16 \text{ minutes}}}$$

Heating and melting of fine particles

There are many situations in which particles are heated or cooled by a surrounding gas and these may be classified according to the degree of movement of the particle as follows:

i) Static beds

Although most beds of particles involve relatively large particle diameters, such as in pebble bed units used for the transfer of heat from flue gases to the incoming air for example, smaller particles, such as sand, are used in beds and, again, these are mainly used for heat recovery. One such application is the heating and cooling of buildings in hotter climes where the cool nocturnal air is used to cool a bed of particles which is then used to cool the incoming air during the heat of the day as it enters a building. In this way, an almost constant temperature may be achieved in a given enclosed environment in spite of the widely fluctuating ambient condition. A similar system has been used in less tropical areas where it is necessary to maintain a constant temperature in an environment in which heat is generated, such as a telephone exchange, for example. Such systems have the merit of very low capital and modest operating costs and, in most cases, the resistance to heat transfer by conduction within the solids is not dissimilar to the resistance in the gas film surrounding the particles.

ii) Partial movement of particles

The most obvious example of a process in which particles undergo only limited movement is the fluidised bed which is discussed in some detail in Volume 2. Applications here involve, not only heating and cooling, but also drying as in the case of grain dryers for example, and on occasions, chemical reaction as, for example, with fluidised-bed combustion. In such cases, conditions in the bed may, to all intents and purposes, be regarded as steady-state, with unsteady-state conduction taking place only in the entering 'process stream' which, by and large, is only a small proportion of the total bed mass in the bed.

iii) Falling particles

Particles fall by gravity through either static or moving gas streams in rotary dryers, for example, but they also fall through heating or cooling gases in specially designed columns. Examples here include the cooling of sand after it has been dried — again recovering heat in the process — salt cooling and also the spray drying of materials such as detergents which are sprayed as a concentrated solution of the material at the top of the tower and emerge as a dry powder. A similar situation occurs in fertiliser production where solid particles or granules are obtained from a spray of the molten material by counter-flow against a cooling gas stream. Convection to such materials is discussed in Section 9.4.6

One important problem involving unsteady state conduction of heat to particles is in the melting of powders in plasma spraying⁽¹⁰⁾ where Biot numbers can range from 0.005 to 5. In this case, there is initially a very high relative velocity between the fluid and the powder. The plasmas referred to here are partially ionised gases with temperatures of around 10,000 K formed by electric discharges such as arcs. There is an increasing industrial use

of the technique of plasma spraying in which powders are injected into a high-velocity plasma jet so that they are both melted and projected at velocities of several hundred metres per second onto a surface. The molten particles with diameters typically of the order 10–100 μm impinge to form an integral layer on the surface. Applications include the building up of worn shafts of pumps, for example, and the deposition of erosion-resistant ceramic layers on centrifugal pump impellers and other equipment prone to erosion damage. When a powder particle first enters the plasma jet, the relative velocity may be hundreds of metres per second and heat transfer to the particle is enhanced by convection, as discussed in Section 9.4.6. Often, and more particularly for smaller particles, the particle is quickly accelerated to essentially the same velocity as the plasma jet⁽²⁾ and conduction becomes the main mechanism of heat transfer from plasma to particle. From a design point of view, neglecting the convective contribution will ease calculations and give a more conservative and safer estimate of the size of the largest particle which can be melted before it strikes the surface. In the absence of complications due to non-continuum conditions discussed later, the value of $Nu' = hd/k$ is therefore often taken as 2, as in equation 9.26.

One complication which arises in the application of this equation to powder heating in high temperature plasmas lies in the dependence of k , the thermal conductivity of the gas or plasma surrounding the particle, on temperature. For example, the temperature of the particle surface may be 1000 K, whilst that of the plasma away from the particle may be about 10,000 K or even higher. The thermal conductivity of argon increases by a factor of about 20 over this range of temperature and that of nitrogen gas passes through a pronounced peak at about 7100 K due to dissociation–recombination effects. Thus, the temperature at which the thermal conductivity k is evaluated will have a pronounced effect on the value of the external heat transfer coefficient. A mean value of k would seem appropriate where:

$$(k)_{\text{mean}} = \frac{1}{T_2 - T_1} \int_{T_1}^{T_2} k dT \quad (\text{equation 9.16})$$

Some workers have correlated experimental data in terms of k at the arithmetic mean temperature, and some at the temperature of the bulk plasma. Experimental validation of the true effective thermal conductivity is difficult because of the high temperatures, small particle sizes and variations in velocity and temperature in plasma jets.

In view of the high temperatures involved in plasma devices and the dependence of radiation heat transfer on T^4 , as discussed in Section 9.5, it is surprising at first sight that conduction is more significant than radiation in heating particles in plasma spraying. The explanation lies in the small values of d and relatively high values of k for the gas, both of which contribute to high values of h for any given value of Nu' . Also the emissivities of most gases are, as seen later in Section 9.5, rather low.

In situations where the surrounding fluid behaves as a non-continuum fluid, for example at very high temperatures and/or at low pressures, it is possible for Nu' to be less than 2. A gas begins to exhibit non-continuum behaviour when the mean free path between collisions of gas molecules or atoms with each other is greater than about 1/100 of the characteristic size of the surface considered. The molecules or atoms are then sufficiently far apart on average for the gas to begin to lose the character of a homogeneous or continuum fluid which is normally assumed in the majority of heat transfer or fluid

dynamics problems. For example, with a particle of diameter $25\ \mu\text{m}$ as encountered in, for example, oil-burner sprays, pulverised coal flames, and in plasma spraying in air at room temperature and atmospheric pressure, the mean free path of gas molecules is about $0.06\ \mu\text{m}$ and the air then behaves as a continuum fluid. If, however, the temperature were say $1800\ \text{K}$, as in a flame, then the mean free path would be about $0.33\ \mu\text{m}$, which is greater than $1/100$ of the particle diameter. Non-continuum effects, leading to values of Nu' lower than 2 would then be likely according to theory^(11,12). The exact value of Nu' depends on the surface accommodation coefficient. This is a difficult parameter to measure for the examples considered here, and hence experimental confirmation of the theory is difficult. At the still higher temperatures that exist in thermal plasma devices, non-continuum effects should be more pronounced and there is limited evidence that values of Nu' below 1 are obtained⁽¹⁰⁾. In general, non-continuum effects, leading in particular to values of Nu' less than 2, would be more likely at high temperatures, low pressures, and small particle sizes. Thus, there is an interest in these effects in the aerospace industry when considering, for example, the behaviour of small particles present in rocket engine exhausts.

9.3.6. Conduction with internal heat source

If an electric current flows through a wire, the heat generated internally will result in a temperature distribution between the central axis and the surface of the wire. This type of problem will also arise in chemical or nuclear reactors where heat is generated internally. It is necessary to determine the temperature distribution in such a system and the maximum temperature which will occur.

If the temperature at the surface of the wire is T_o and the rate of heat generation per unit volume is Q_G , then considering unit length of a cylindrical element of radius r , the heat generated must be transmitted in an outward direction by conduction so that:

$$-k2\pi r \frac{dT}{dr} = \pi r^2 Q_G$$

Hence:

$$\frac{dT}{dr} = -\frac{Q_G r}{2k} \quad (9.50)$$

Integrating:

$$T = -\frac{Q_G r^2}{4k} + C$$

$T = T_o$ when $r = r_o$ the radius of wire and hence:

$$T = T_o + Q_G \frac{r_o^2 - r^2}{4k}$$

or:

$$T - T_o = \frac{Q_G r_o^2}{4k} \left(1 - \frac{r^2}{r_o^2}\right) \quad (9.51)$$

This gives a parabolic distribution of temperature and the maximum temperature will occur at the axis of the wire where $(T - T_o) = Q_G r_o^2 / 4k$. The arithmetic mean temperature difference, $(T - T_o)_{av} = Q_G r_o^2 / 8k$.

Since $Q_G \pi r_o^2$ is the rate of heat release per unit length of the wire then, putting T_1 as the temperature at the centre:

$$T_1 - T_o = \frac{\text{rate of heat release per unit length}}{4\pi k} \quad (9.52)$$

Example 9.8

A fuel channel in a natural uranium reactor is $5\ \text{m}$ long and has a heat release of $0.25\ \text{MW}$. If the thermal conductivity of the uranium is $33\ \text{W/mK}$, what is the temperature difference between the surface and the centre of the uranium element, assuming that the heat release is uniform along the rod?

Solution

$$\begin{aligned} \text{Heat release rate} &= 0.25 \times 10^6\ \text{W} \\ &= \frac{0.25 \times 10^6}{5} = 5 \times 10^4\ \text{W/m} \end{aligned}$$

Thus, from equation 9.52:

$$\begin{aligned} T_1 - T_o &= \frac{5 \times 10^4}{4\pi \times 33} \\ &= 121\ \text{deg K} \end{aligned}$$

It should be noted that the temperature difference is independent of the diameter of the fuel rod for a cylindrical geometry, and that the heat released per unit volume has been considered as being uniform.

In practice the assumption of the uniform heat release per unit length of the rod is not valid since the neutron flux, and hence the heat generation rate varies along its length. In the simplest case where the neutron flux may be taken as zero at the ends of the fuel element, the heat flux may be represented by a sinusoidal function, and the conditions become as shown in Figure 9.20.

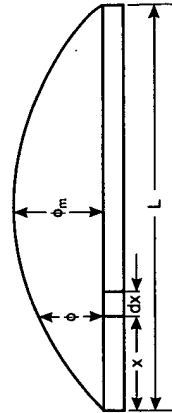


Figure 9.20. Variation of neutron flux along a length of fuel rod

Since the heat generated is proportional to the neutron flux, the heat dQ developed per unit time in a differential element of the fuel rod of length dx may be written as:

$$dQ = C \sin\left(\frac{\pi x}{L}\right) dx$$

The total heat generated by the rod Q is then given by:

$$Q = C \int_0^L \sin\left(\frac{\pi x}{L}\right) dx = \frac{2CL}{\pi}$$

Thus, $C = \pi Q/2L$. The heat release per unit length at any point is then given by:

$$\frac{dQ}{dx} = \frac{\pi Q}{2L} \sin\left(\frac{\pi x}{L}\right)$$

Substituting into equation 9.52 gives:

$$T_1 - T_o = \frac{\left(\frac{\pi Q}{2L}\right) \sin\left(\frac{\pi x}{L}\right)}{4\pi k} \quad (9.53)$$

It may be noted that when $x = 0$ or $x = L$, then $T_1 - T_o$ is zero as would be expected since the neutron flux was taken as zero at these positions.

9.4. HEAT TRANSFER BY CONVECTION

9.4.1. Natural and forced convection

Heat transfer by convection occurs as a result of the movement of fluid on a macroscopic scale in the form of eddies or circulating currents. If the currents arise from the heat transfer process itself, *natural convection* occurs, such as in the heating of a vessel containing liquid by means of a heat source situated beneath it. The liquid at the bottom of the vessel becomes heated and expands and rises because its density has become less than that of the remaining liquid. Cold liquid of higher density takes its place and a circulating current is thus set up.

In *forced convection*, circulating currents are produced by an external agency such as an agitator in a reaction vessel or as a result of turbulent flow in a pipe. In general, the magnitude of the circulation in forced convection is greater, and higher rates of heat transfer are obtained than in natural convection.

In most cases where convective heat transfer is taking place from a surface to a fluid, the circulating currents die out in the immediate vicinity of the surface and a film of fluid, free of turbulence, covers the surface. In this film, heat transfer is by thermal conduction and, as the thermal conductivity of most fluids is low, the main resistance to transfer lies there. Thus an increase in the velocity of the fluid over the surface gives rise to improved heat transfer mainly because the thickness of the film is reduced. As a guide, the film coefficient increases as (fluid velocity)ⁿ, where $0.6 < n < 0.8$, depending upon the geometry.

If the resistance to transfer is regarded as lying within the film covering the surface, the rate of heat transfer Q is given by equation 9.11 as:

$$Q = kA \frac{(T_1 - T_2)}{x}$$

The effective thickness x is not generally known and therefore the equation is usually rewritten in the form:

$$Q = hA(T_1 - T_2) \quad (9.54)$$

where h is the heat transfer coefficient for the film and $(1/h)$ is the thermal resistance.

9.4.2. Application of dimensional analysis to convection

So many factors influence the value of h that it is almost impossible to determine their individual effects by direct experimental methods. By arranging the variables in a series of dimensionless groups, however, the problem is made more manageable in that the number of groups is significantly less than the number of parameters. It is found that the heat transfer rate per unit area q is dependent on those physical properties which affect flow pattern (viscosity μ and density ρ), the thermal properties of the fluid (the specific heat capacity C_p and the thermal conductivity k) a linear dimension of the surface l , the velocity of flow u of the fluid over the surface, the temperature difference ΔT and a factor determining the natural circulation effect caused by the expansion of the fluid on heating (the product of the coefficient of cubical expansion β and the acceleration due to gravity g). Writing this as a functional relationship:

$$q = \phi[\mu, l, \rho, \mu, C_p, \Delta T, \beta g, k] \quad (9.55)$$

Noting the dimensions of the variables in terms of length L , mass M , time T , temperature θ , heat H :

q	Heat transferred/unit area and unit time	$HL^{-2}T^{-1}$
u	Velocity	LT^{-1}
l	Linear dimension	L
μ	Viscosity	$ML^{-1}T^{-1}$
ρ	Density	ML^{-3}
k	Thermal conductivity	$HT^{-1}L^{-1}\theta^{-1}$
C_p	Specific heat capacity at constant pressure	$HM^{-1}\theta^{-1}$
ΔT	Temperature difference	θ
(βg)	The product of the coefficient of thermal expansion and the acceleration due to gravity	$LT^{-2}\theta^{-1}$

It may be noted that both temperature and heat are taken as fundamental units as heat is not expressed here in terms of M, L, T .

With nine parameters and five dimensions, equation 9.55 may be rearranged in four dimensionless groups.

Using the Π -theorem for solution of the equation, and taking as the recurring set: $l, \rho, \mu, \Delta T, k$

The non-recurring variables are: $q, u, (\beta g), C_p$

Then:

$$\begin{aligned} l &\equiv L & L &= l \\ \rho &\equiv ML^{-3} & M &= \rho L^3 = \rho l^3 \\ \mu &\equiv ML^{-1}T^{-1} & T &= ML^{-1}\mu^{-1} = \rho l^3 l^{-1} \mu^{-1} = \rho l^2 \mu^{-1} \\ \Delta T &\equiv \theta & \theta &= \Delta T \\ k &\equiv HL^{-1}T^{-1}\theta^{-1} & H &= kLT\theta = kl\rho l^2 \mu^{-1} \Delta T = kl^3 \rho \mu^{-1} \Delta T \end{aligned}$$

The Π groups are then:

$$\Pi_1 = qH^{-1}L^2T = qk^{-1}l^{-3}\rho^{-1}\mu\Delta T^{-1}l^2\rho l^2\mu^{-1} = qk^{-1}l\Delta T^{-1}$$

$$\Pi_2 = uL^{-1}T = ul^{-1}\rho l^2\mu^{-1} = u\rho l\mu^{-1}$$

$$\Pi_3 = C_p H^{-1}M\theta = C_p k^{-1}l^{-3}\rho^{-1}\mu\Delta T^{-1}\rho l^3\Delta T = C_p k^{-1}\mu$$

$$\Pi_4 = \beta g L^{-1}T^2\theta = \beta g l^{-1}\rho^2 l^4\mu^{-2}\Delta T = \beta g \Delta T \rho^2 \mu^{-2} l^3$$

The relation in equation 9.55 becomes:

$$\frac{ql}{k\Delta T} = \frac{hl}{k} = \phi \left[\left(\frac{lu\rho}{\mu} \right) \left(\frac{C_p\mu}{k} \right) \left(\frac{\beta g \Delta T l^3 \rho^2}{\mu^2} \right) \right] \quad (9.56)$$

or:

$$Nu = \phi[Re, Pr, Gr]$$

This general equation involves the use of four dimensionless groups, although it may frequently be simplified for design purposes. In equation 9.56:

hl/k - is known as the *Nusselt* group Nu (already referred to in equation 9.46),

$lu\rho/\mu$ the *Reynolds* group Re ,

$C_p\mu/k$ the *Prandtl* group Pr , and

$\beta g \Delta T l^3 \rho^2 / \mu^2$ the *Grashof* group Gr

It is convenient to define other dimensionless groups which are also used in the analysis of heat transfer. These are:

$$lu\rho C_p/k \quad \text{the } \textit{Peclet} \text{ group, } Pe = RePr,$$

$$GC_p/kl \quad \text{the } \textit{Graetz} \text{ group } Gr,$$

$$h/C_p\rho u \quad \text{the } \textit{Stanton} \text{ group, } St = Nu/(RePr)$$

It may be noted that many of these dimensionless groups are ratios. For example, the *Nusselt* group $h/(k/l)$ is the ratio of the actual heat transfer to that by conduction over a thickness l , whilst the *Prandtl* group, $(\mu/\rho)/(k/C_p\rho)$ is the ratio of the kinematic viscosity to the thermal diffusivity.

For conditions in which only natural convection occurs, the velocity is dependent on the buoyancy effects alone, represented by the *Grashof* number, and the *Reynolds* group may be omitted. Again, when forced convection occurs the effects of natural convection are usually negligible and the *Grashof* number may be omitted. Thus:

$$\text{for natural convection:} \quad Nu = f(Gr, Pr) \quad (9.57)$$

$$\text{and for forced convection:} \quad Nu = f(Re, Pr) \quad (9.58)$$

For most gases over a wide range of temperature and pressure, $C_p\mu/k$ is constant and the *Prandtl* group may often be omitted, simplifying the design equations for the calculation of film coefficients with gases.

9.4.3. Forced convection in tubes

Turbulent flow

The results of a number of workers who have used a variety of gases such as air, carbon dioxide, and steam and of others who have used liquids such as water, acetone, kerosene, and benzene have been correlated by DITTUS and BOELTER⁽¹³⁾ who used mixed units for their variables. On converting their relations using consistent (SI, for example) units, they become:

for heating of fluids:

$$Nu = 0.0241Re^{0.8}Pr^{0.4} \quad (9.59)$$

and for cooling of fluids:

$$Nu = 0.0264Re^{0.8}Pr^{0.3} \quad (9.60)$$

In these equations all of the physical properties are taken at the mean bulk temperature of the fluid $(T_i + T_o)/2$, where T_i and T_o are the inlet and outlet temperatures. The difference in the value of the index for heating and cooling occurs because in the former case the film temperature will be greater than the bulk temperature and in the latter case less. Conditions in the film, particularly the viscosity of the fluid, exert an important effect on the heat transfer process.

Subsequently MCADAMS⁽¹⁴⁾ has re-examined the available experimental data and has concluded that an exponent of 0.4 for the *Prandtl* number is the most appropriate one for both heating and cooling. He also has slightly modified the coefficient to 0.023 (corresponding to Colburn's value, given below in equation 9.64) and gives the following equation, which applies for $Re > 2100$ and for fluids of viscosities not exceeding 2 mN s/m^2 :

$$Nu = 0.023Re^{0.8}Pr^{0.4} \quad (9.61)$$

WINTERTON⁽¹⁵⁾ has looked into the origins of the "Dittus and Boelter" equation and has found that there is considerable confusion in the literature concerning the origin of equation 9.61 which is generally referred to as the Dittus-Boelter equation in the literature on heat transfer.

An alternative equation which is in many ways more convenient has been proposed by COLBURN⁽¹⁶⁾ and includes the *Stanton* number ($St = h/(C_p\rho u)$) instead of the *Nusselt* number. This equation takes the form:

$$j_H = StPr^{0.67} = 0.023Re^{-0.2} \quad (9.62)$$

where j_H is known as the *j-factor* for heat transfer. It may be noted that:

$$\frac{h}{C_p\rho u} = \left(\frac{hd}{k} \right) \left(\frac{\mu}{u\rho} \right) \left(\frac{k}{C_p\mu} \right)$$

$$St = NuRe^{-1}Pr^{-1} \quad (9.63)$$

Thus, multiplying equation 9.62 by $RePr^{0.33}$:

$$Nu = 0.023Re^{0.8}Pr^{0.33} \quad (9.64)$$

which is a form of equations 9.59 and 9.60.

Again, the physical properties are taken at the bulk temperature, except for the viscosity in the Reynolds group which is evaluated at the mean film temperature taken as $(T_{\text{surface}} + T_{\text{bulk fluid}})/2$.

Writing a heat balance for the flow through a tube of diameter d and length l with a rise in temperature for the fluid from T_i to T_o :

$$h\pi d l \Delta T = \frac{\pi d^2}{4} C_p \mu \rho (T_o - T_i)$$

$$St = \frac{h}{C_p \rho u} = \frac{d(T_o - T_i)}{4l \Delta T} \quad (9.65)$$

or:

where ΔT is the mean temperature difference between the bulk fluid and the walls.

With *very viscous liquids* there is a marked difference at any position between the viscosity of the fluid adjacent to the surface and the value at the axis or at the bulk temperature of the fluid. SIEDER and TATE⁽¹⁷⁾ examined the experimental data available and suggested that a term $\left(\frac{\mu}{\mu_s}\right)^{0.14}$ be included to account for the viscosity variation and the fact that this will have opposite effects in heating and cooling. (μ is the viscosity at the bulk temperature and μ_s the viscosity at the wall or surface). They give a logarithmic plot, but do not propose a correlating equation. However, MCADAMS⁽¹⁴⁾ gives the following equation, based on Sieder and Tate's work:

$$Nu = 0.027 Re^{0.8} Pr^{0.33} \left(\frac{\mu}{\mu_s}\right)^{0.14} \quad (9.66)$$

This equation may also be written in the form of the Colburn equation (9.62).

When these equations are applied to *heating or cooling of gases* for which the Prandtl group usually has a value of about 0.74, substitution of $Pr = 0.74$ in equation 9.64 gives:

$$Nu = 0.020 Re^{0.8} \quad (9.67)$$

Water is very frequently used as the cooling medium and the effect of the variation of physical properties with temperature may be included in equation 9.64 to give a simplified equation which is useful for design purposes (Section 9.9.4).

There is a very big difference in the values of h for water and air for the same linear velocity. This is shown in Figures 9.21–9.23 and Table 9.2, all of which are based on the work of FISHENDEN and SAUNDERS⁽¹⁸⁾.

The effect of length to diameter ratio (l/d) on the value of the heat transfer coefficient may be seen in Figure 9.24. It is important at low Reynolds numbers but ceases to be significant at a Reynolds number of about 10^4 .

It is also important to note that the film coefficient varies with the distance from the entrance to the tube. This is especially important at low (l/d) ratios and an average value is given approximately by:

$$\frac{h_{\text{average}}}{h_{\infty}} = 1 + \left(\frac{d}{l}\right)^{0.7} \quad (9.68)$$

where h_{∞} is the limiting value for a very long tube.

The roughness of the surface of the inside of the pipe can have an important bearing on rates of heat transfer to the fluid, although COPE⁽¹⁹⁾, using degrees of artificial roughness

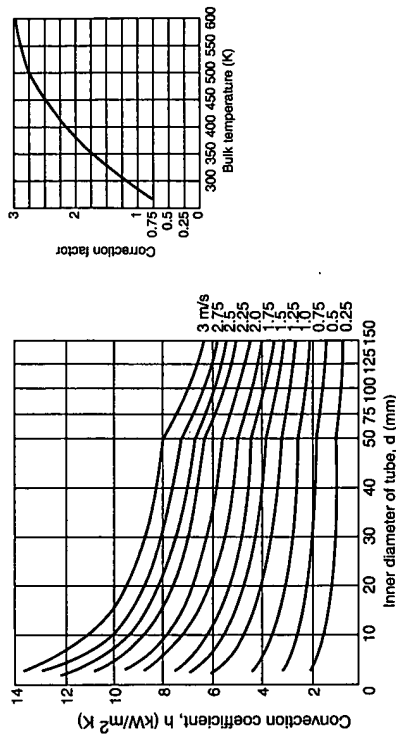


Figure 9.21. Film coefficients of convection for flow of water through a tube at 289 K

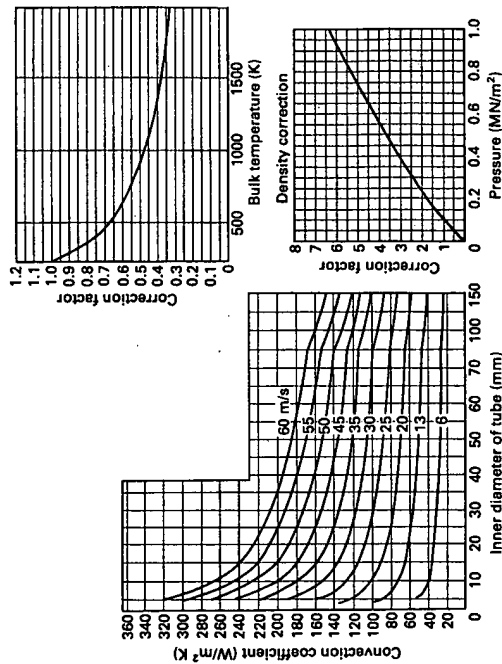


Figure 9.22. Film coefficients of convection for flow of air through a tube at various velocities (289 K, 101.3 kN/m²)

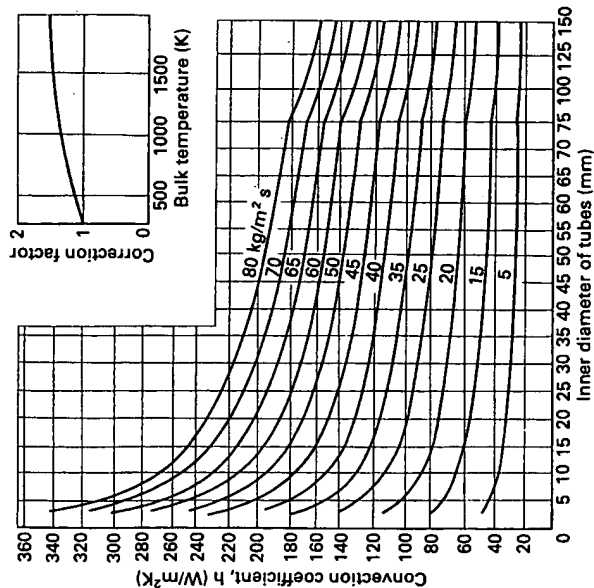


Figure 9.23. Film coefficients of convection for flow of air through a tube for various mass velocities (289 K, 101.3 kN/m²)

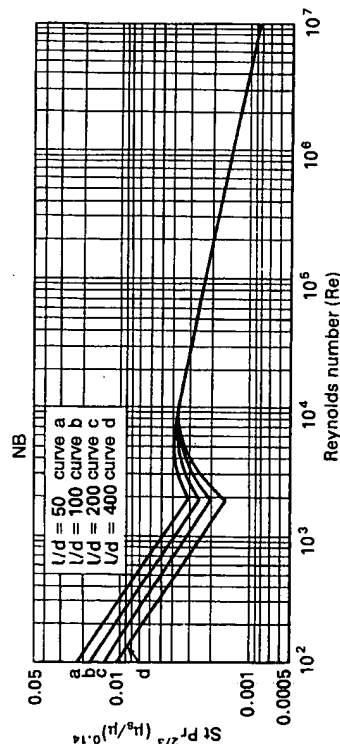


Figure 9.24. Effect of length:diameter ratio on heat transfer coefficient

ranging from 0.022 to 0.14 of the pipe diameter, found that, although the friction loss was some six times greater than for smooth tubes, the heat transfer was only 100–120 per cent higher. It was concluded that, for the same pressure drop, greater heat transfer was obtained from a smooth rather than a rough tube. The effect of a given scale deposit is usually less serious for gases than water because of the higher thermal resistance of

Table 9.2. Film coefficients for air and water (289 K and 101.3 kN/m²)

Inside diameter of tube (mm)	(in)	Velocity		Mass velocity		Film coefficient of heat transfer h	
		(m/s)	(ft/s)	(kg/m ² s)	(lb/ft ² h)	(W/m ² K) [Ref.18]	(Btu/h ft ² °F) [Ref.18]
Air	1.0	5	16.4	6.11	4530	31.2	5.5
		10	32.8	12.2	9050	50.0	8.8
		20	65.6	24.5	18,100	84.0	14.8
		40	131	48.9	36,200	146	25.7
		60	197	73.4	54,300	211	37.2
		80	263	97.9	72,400	276	49.7
	2.0	5	16.4	6.11	4530	23.8	4.2
		10	32.8	12.2	9050	44.9	7.9
		20	65.6	24.5	18,100	77.8	13.7
		40	131	48.9	36,200	127	22.4
		60	197	73.4	54,300	181	31.9
		80	263	97.9	72,400	236	41.4
Water	1.0	0.5	1.64	488	361,000	2160	380
		1.0	3.28	975	722,000	3750	660
		1.5	4.92	1460	1,080,000	5250	925
		2.0	6.55	1950	1,440,000	6520	1150
		2.5	8.18	2440	1,810,000	7780	1370
		3.0	9.81	2930	2,180,000	9040	1590
	2.0	0.5	1.64	488	361,000	1870	330
		1.0	3.28	975	722,000	3270	575
		1.5	4.92	1460	1,080,000	4540	800
		2.0	6.55	1950	1,440,000	5590	985
		2.5	8.18	2440	1,810,000	6700	1180
		3.0	9.81	2930	2,180,000	7760	1370
Water	3.0	0.5	1.64	488	361,000	1760	310
		1.0	3.28	975	722,000	3070	540
		1.5	4.92	1460	1,080,000	4200	740
		2.0	6.55	1950	1,440,000	5220	920
		2.5	8.18	2440	1,810,000	6220	1100
		3.0	9.81	2930	2,180,000	7220	1280

the gas film, although layers of dust or of materials which sublime may seriously reduce heat transfer between gas and solid by as much as 40 per cent.

Streamline flow

Although heat transfer to a fluid in streamline flow takes place solely by conduction, it is convenient to consider it here so that the results may be compared with those for turbulent flow.

In Chapter 3 it has been seen that, for streamline flow through a tube, the velocity distribution across a diameter is parabolic, as shown in Figure 9.25. If a liquid enters a section heated on the outside, the fluid near the wall will be at a higher temperature than that in the centre and its viscosity will be lower. The velocity of the fluid near the wall will therefore be greater in the heated section, and correspondingly less at the centre. The velocity distribution will therefore be altered, as shown. If the fluid enters a section where it is cooled, the same reasoning will show that the distribution in velocity will be altered

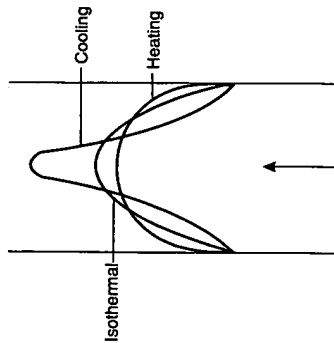


Figure 9.25. Effect of heat transfer on the velocity distribution for a liquid

to that shown. With a gas the conditions are reversed, because of the increase of viscosity with temperature. The heat transfer problem is therefore complex.

For the common problem of heat transfer between a fluid and a tube wall, the boundary layers are limited in thickness to the radius of the pipe and, furthermore, the effective area for heat flow decreases with distance from the surface. The problem can conveniently be divided into two parts. Firstly, heat transfer in the entry length in which the boundary layers are developing, and, secondly, heat transfer under conditions of fully developed flow. Boundary layer flow is discussed in Chapter 11.

For the region of fully developed flow in a pipe of length L , diameter d and radius r , the rate of flow of heat Q through a cylindrical surface in the fluid at a distance y from the wall is given by:

$$Q = -k2\pi L(r-y) \frac{d\theta}{dy} \quad (9.69)$$

Close to the wall, the fluid velocity is low and a negligible amount of heat is carried along the pipe by the flowing fluid in this region and Q is independent of y .

$$\begin{aligned} \text{Thus:} \quad \frac{d\theta}{dy} &= -\frac{Q}{k2\pi L}(r-y)^{-1} \quad \text{and} \quad \left(\frac{d\theta}{dy}\right)_{y=0} = -\frac{Q}{2\pi kLr} \\ \frac{d^2\theta}{dy^2} &= -\frac{Q}{k2\pi L}(r-y)^{-2} \quad \text{and} \quad \left(\frac{d^2\theta}{dy^2}\right)_{y=0} = -\frac{Q}{2\pi kLr^2} \end{aligned}$$

$$\text{Thus:} \quad \left(\frac{d^2\theta}{dy^2}\right)_{y=0} = r^{-1} \left(\frac{d\theta}{dy}\right)_{y=0} \quad (9.70)$$

Assuming that the temperature of the walls remains constant at the datum temperature and that the temperature at any distance y from the walls is given by a polynomial, then:

$$\begin{aligned} \theta &= a_0y + b_0y^2 + c_0y^3 \\ \frac{d\theta}{dy} &= a_0 + 2b_0y + 3c_0y^2 \quad \text{and} \quad \left(\frac{d\theta}{dy}\right)_{y=0} = a_0 \end{aligned} \quad (9.71)$$

Thus:

$$\frac{d^2\theta}{dy^2} = 2b_0 + 6c_0y \quad \text{and} \quad \left(\frac{d^2\theta}{dy^2}\right)_{y=0} = 2b_0$$

$$\text{Thus:} \quad 2b_0 = \frac{a_0}{r} \quad (\text{from equation 9.65})$$

$$\text{and:} \quad b_0 = \frac{a_0}{2r}$$

If the temperature of the fluid at the axis of the pipe is θ_s and the temperature gradient at the axis, from symmetry, is zero, then:

$$0 = a_0 + 2r \left(\frac{a_0}{2r}\right) + 3c_0r^2$$

$$\text{giving:} \quad c_0 = -\frac{2a_0}{3r^2}$$

$$\text{and:} \quad \theta_s = a_0r + r^2 \left(\frac{a_0}{2r}\right) + r^3 \left(\frac{-2a_0}{3r^2}\right)$$

$$= \frac{5}{6}a_0r$$

$$a_0 = \frac{6\theta_s}{5r}$$

$$b_0 = \frac{3\theta_s}{5r^2}$$

$$\text{and:} \quad c_0 = -\frac{4\theta_s}{5r^3}$$

$$\text{Thus:} \quad \frac{\theta}{\theta_s} = \frac{6y}{5r} + \frac{3}{5} \left(\frac{y}{r}\right)^2 - \frac{4}{5} \left(\frac{y}{r}\right)^3 \quad (9.72)$$

Thus the rate of heat transfer per unit area at the wall:

$$\begin{aligned} q &= -k \left(\frac{d\theta}{dy}\right)_{y=0} \\ &= -\frac{6k\theta_s}{5r} \end{aligned} \quad (9.73)$$

In general, the temperature θ_s at the axis is not known, and the heat transfer coefficient is related to the temperature difference between the walls and the bulk fluid. The bulk temperature of the fluid is defined as the ratio of the heat content to the heat capacity of the fluid flowing at any section. Thus the bulk temperature θ_B is given by:

$$\theta_B = \frac{\int_0^r C_p \rho u_x 2\pi(r-y) dy}{\int_0^r C_p \rho u_x 2\pi(r-y) dy}$$

$$= \frac{\int_0^r \theta u_x (r-y) dy}{\int_0^r u_x (r-y) dy} \quad (9.74)$$

From Poiseuille's law (equation 3.30):

$$u_x = \frac{-\Delta P}{4\mu L} [r^2 - (r-y)^2] = \frac{-\Delta P}{4\mu L} (2ry - y^2)$$

Hence:

$$u_s = \frac{-\Delta P}{4\mu L} r^2 \quad (9.75)$$

where u_s is the velocity at the pipe axis,

$$\text{and:} \quad \frac{u_x}{u_s} = \frac{2y}{r} - \left(\frac{y}{r}\right)^2 \quad (9.76)$$

$$\begin{aligned} \text{Thus:} \quad \int_0^r u_x (r-y) dy &= r^2 u_s \int_0^1 \left[2\frac{y}{r} - \left(\frac{y}{r}\right)^2 \right] \left(1 - \frac{y}{r}\right) d\left(\frac{y}{r}\right) \\ &= r^2 u_s \int_0^1 \left[2\left(\frac{y}{r}\right) - 3\left(\frac{y}{r}\right)^2 + \left(\frac{y}{r}\right)^3 \right] d\left(\frac{y}{r}\right) \\ &= \frac{1}{4} r^2 u_s \quad (9.77) \end{aligned}$$

Since:

$$\frac{\theta}{\theta_s} = \frac{6y}{5r} + \frac{3}{5} \left(\frac{y}{r}\right)^2 - \frac{4}{5} \left(\frac{y}{r}\right)^3 \quad (\text{equation 9.72})$$

$$\begin{aligned} \int_0^r \theta u_x (r-y) dy &= r^2 u_s \theta_s \int_0^1 \left[\frac{6y}{5r} + \frac{3}{5} \left(\frac{y}{r}\right)^2 - \frac{4}{5} \left(\frac{y}{r}\right)^3 \right] \left[2\left(\frac{y}{r}\right) - 3\left(\frac{y}{r}\right)^2 + \left(\frac{y}{r}\right)^3 \right] d\left(\frac{y}{r}\right) \\ &= r^2 u_s \theta_s \int_0^1 \left[\frac{12}{5} \left(\frac{y}{r}\right)^2 - \frac{12}{5} \left(\frac{y}{r}\right)^3 - \frac{11}{5} \left(\frac{y}{r}\right)^4 + 3\left(\frac{y}{r}\right)^5 - \frac{4}{5} \left(\frac{y}{r}\right)^6 \right] d\left(\frac{y}{r}\right) \\ &= r^2 u_s \theta_s \left(\frac{4}{5} - \frac{3}{5} + \frac{11}{25} + \frac{1}{2} - \frac{4}{35} \right) \\ &= \frac{51}{350} r^2 u_s \theta_s \quad (9.78) \end{aligned}$$

Substituting from equations 9.77 and 9.78 in equation 9.74:

$$\begin{aligned} \theta_B &= \frac{\frac{51}{350} r^2 u_s \theta_s}{\frac{1}{4} r^2 u_s} \\ &= \frac{102}{175} \theta_s = 0.583 \theta_s \quad (9.79) \end{aligned}$$

The heat transfer coefficient h is then given by:

$$h = -\frac{q}{\theta_B}$$

where q is the rate of heat transfer per unit area of tube.

Thus, from equations 9.73 and 9.79:

$$h = \frac{6k\theta_s/5r}{0.583\theta_s} = \frac{2.06k}{r} = 4.1 \frac{k}{d}$$

and:

$$Nu = \frac{hd}{k} = 4.1 \quad (9.80)$$

This expression is applicable only to the region of fully developed flow. The heat transfer coefficient for the inlet length can be calculated approximately, using the expressions given in Chapter 11 for the development of the boundary layers for the flow over a plane surface. It should be borne in mind that it has been assumed throughout that the physical properties of the fluid are not appreciably dependent on temperature and therefore the expressions will not be expected to hold accurately if the temperature differences are large and if the properties vary widely with temperature.

For values of $(RePr d/l)$ greater than 12, the following empirical equation is applicable:

$$Nu = 1.62 \left(RePr \frac{d}{l} \right)^{1/3} = 1.75 \left(\frac{GC_p}{kl} \right)^{1/3} \quad (9.81)$$

where $G = (\pi d^2/4) \rho u$, i.e. the mass rate of flow.

The product $RePr$ is termed the Peclet number Pe .

$$\text{Thus:} \quad Pe = \frac{ud\rho C_p \mu}{\mu k} = \frac{C_p \rho u d}{k} \quad (9.82)$$

Equation 9.81 may then be written:

$$Nu = 1.62 \left(Pe \frac{d}{l} \right)^{1/3} \quad (9.83)$$

In this equation the temperature difference is taken as the arithmetic mean of the terminal values, that is:

$$\frac{(T_w - T_1) + (T_w - T_2)}{2}$$

where T_w is the temperature of the tube wall which is taken as constant.

If the liquid is heated almost to the wall temperature T_w (that is when GC_p/kl is very small) then, on equating the heat gained by the liquid to that transferred from the pipe:

$$GC_p(T_2 - T_1) = \pi d l h \frac{T_2 - T_1}{2}$$

or:

$$h = \frac{2 GC_p}{\pi dl} \quad (9.84)$$

For values of $(RePr d/l)$ less than about 17, the Nusselt group becomes approximately constant at 4.1; the value given in equation 9.80.

Experimental values of h for viscous oils are greater than those given by equation 9.81 for heating and less for cooling. This is due to the large variation of viscosity with temperature and the correction introduced for turbulent flow may also be used here, giving:

$$Nu \left(\frac{\mu_s}{\mu} \right)^{0.14} = 1.86 \left(RePr \frac{d}{l} \right)^{1/3} = 2.01 \left(\frac{GC_p}{kl} \right)^{1/3} \quad (9.85)$$

$$\text{or: } Nu \left(\frac{\mu_2}{\mu} \right)^{0.14} = 1.86 \left(Pe \frac{d}{l} \right)^{1/3} \quad (9.86)$$

When $(G C_p / kl) < 10$, the outlet temperature closely approaches that of the wall and equation 9.84 applies. These equations have been obtained with tubes about 10 mm to 40 mm in diameter, and the length of unheated tube preceding the heated section is important. The equations are not entirely consistent since for very small values of ΔT the constants in equations 9.81 and 9.85 would be expected to be the same. It is important to note, when using these equations for design purposes, that the error may be as much as ± 25 per cent for turbulent flow and greater for streamline conditions.

With laminar flow there is a marked influence of tube length and the curves shown in Figure 9.24 show the parameter l/d from 50 to 400.

Whenever possible, streamline conditions of flow are avoided in heat exchangers because of the very low heat transfer coefficients which are obtained. With very viscous liquids, however, turbulent conditions can be produced only if a very high pressure drop across the plant is permissible. In the processing industries, streamline flow in heat exchangers is most commonly experienced with heavy oils and brines at low temperatures. Since the viscosity of these materials is critically dependent on temperature, the equations would not be expected to apply with a high degree of accuracy.

9.4.4. Forced convection outside tubes

Flow across single cylinders

If a fluid passes at right angles across a single tube, the distribution of velocity around the tube will not be uniform. In the same way the rate of heat flow around a hot pipe across which air is passed is not uniform but is a maximum at the front and rear, and a minimum at the sides, where the rate is only some 40 per cent of the maximum. The general picture is shown in Figure 9.26 but for design purposes reference is made to the average value.

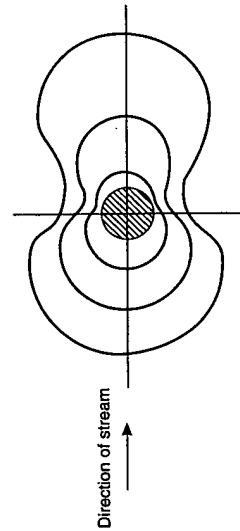


Figure 9.26. Distribution of the film heat transfer coefficient round a cylinder with flow normal to the axis for three different values of Re

A number of workers, including, REIHER⁽²⁰⁾, HILPERT⁽²¹⁾, GRIFFITHS and AWBERRY⁽²²⁾, have studied the flow of a hot gas past a single cylinder, varying from a thin wire to a

tube of 150 mm diameter. Temperatures up to 1073 K and air velocities up to 30 m/s have been used with Reynolds numbers $(d_o u \rho / \mu)$ from 1000 to 100,000 (where d_o is the cylinder diameter, or the outside tube diameter). The data obtained may be expressed by:

$$Nu = 0.26 Re^{0.6} Pr^{0.3} \quad (9.87)$$

Taking Pr as 0.74 for gases, this reduces to

$$Nu = 0.24 Re^{0.6} \quad (9.88)$$

DAVIS⁽²³⁾ has also worked with water, paraffin, and light oils and obtained similar results. For very low values of Re (from 0.2 to 200) with liquids the data are better represented by the equation:

$$Nu = 0.86 Re^{0.43} Pr^{0.3} \quad (9.89)$$

In each case the physical properties of the fluid are measured at the mean film temperature T_f , taken as the average of the surface temperature T_w and the mean fluid temperature T_m ; where $T_m = (T_1 + T_2)/2$.

Flow at right angles to tube bundles

One of the great difficulties with this geometry is that the area for flow is continually changing. Moreover the degree of turbulence is considerably less for banks of tubes in line, as at (a), than for staggered tubes, as at (b) in Figure 9.27. With the small bundles which are common in the processing industries, the selection of the true mean area for flow is further complicated by the change in number of tubes in the rows.

The results of a number of workers for heat transfer to and from gases flowing across tube banks may be expressed by the equation:

$$Nu = 0.33 C_h Re_{\max}^{0.6} Pr^{0.3} \quad (9.90)$$

where C_h depends on the geometrical arrangement of the tubes, as shown in Table 9.3. GRIMMOND⁽²⁴⁾ proposed this form of expression to correlate the data of HUGG⁽²⁵⁾ and PIERSON⁽²⁶⁾ who worked with small electrically heated tubes in rows of ten deep. Other workers have used similar equations. Some correction factors have been given by PIERSON⁽²⁶⁾ for bundles with less than ten rows although there are insufficient reported data from commercial exchangers to fix these values with accuracy. Thus for five rows a factor of 0.92 and for eight rows 0.97 is suggested.

These equations are based on the maximum velocity through the bundle. Thus for an in-line arrangement as is shown in Figure 9.27a, $G'_{\max} = G'Y/(Y - d_o)$, where Y is the pitch of the pipes at right-angles to direction of flow; it is more convenient here to use the mass flowrate per unit area G' in place of velocity. For staggered arrangements the maximum velocity may be based on the distance between the tubes in a horizontal line or on the diagonal of the tube bundle, whichever is the less.

It has been suggested that, for in-line arrangements, the constant in equation 9.90 should be reduced to 0.26, but there is insufficient evidence from commercial exchangers to confirm this.

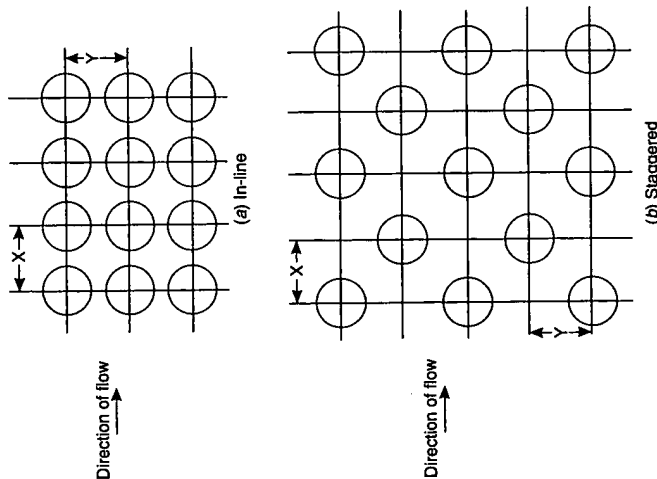


Figure 9.27. Arrangements of tubes in heat exchangers

Table 9.3.(18) Values of C_h and C_f

Re_{max}	$X = 1.25d_o$				$X = 1.5d_o$			
	In-line		Staggered		In-line		Staggered	
	C_h	C_f	C_h	C_f	C_h	C_f	C_h	C_f
2000	1.06	1.68	1.21	2.52	1.06	1.74	1.16	2.58
20,000	1.00	1.44	1.06	1.56	1.00	1.56	1.05	1.74
40,000	1.00	1.20	1.03	1.26	1.00	1.32	1.02	1.50
$Y = 1.25d_o$								
2000	0.95	0.79	1.17	1.80	0.95	0.97	1.15	1.80
20,000	0.96	0.84	1.04	1.10	0.96	0.96	1.02	1.16
40,000	0.96	0.74	0.99	0.88	0.96	0.85	0.98	0.96
$Y = 1.5d_o$								

With liquids the same equation may be used, although for Re less than 2000, there is insufficient published work to justify an equation. McADAMS,⁽²⁷⁾ however, has given a curve for h for a bundle with staggered tubes ten rows deep. An alternative approach has been suggested by KERN⁽²⁸⁾ who worked in terms of the hydraulic mean diameter d_e for flow *parallel* to the tubes:

i.e.:

$$d_e = 4 \times \frac{\text{Free area for flow}}{\text{Wetted perimeter}}$$

$$= 4 \left(\frac{Y^2 - (\pi d_o^2/4)}{\pi d_o} \right)$$

for a square pitch as shown in Figure 9.28. The maximum cross-flow area A_s is then given by:

$$A_s = \frac{d_s l_B C'}{Y}$$

where C' is the clearance, l_B the baffle spacing, and d_s the internal diameter of the shell.

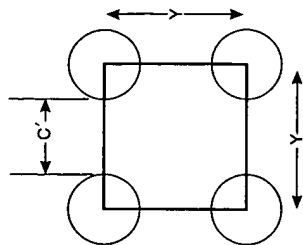


Figure 9.28. Clearance and pitch for tube layouts

The mass rate of flow per unit area G'_s is then given as rate of flow divided by A_s , and the film coefficient is obtained from a Nusselt type expression of the form:

$$\frac{h_o d_e}{k} = 0.36 \left(\frac{d_e G'_s}{\mu} \right)^{0.55} \left(\frac{C_p \mu}{k} \right)^{1/3} \left(\frac{\mu}{\mu_s} \right)^{0.14} \quad (9.91)$$

There are insufficient published data to assess the relative merits of equations 9.90 and 9.91.

For 19 mm tubes on 25 mm square pitch:

$$d_e = 4 \frac{[25^2 - (\pi/4)19^2]}{\pi \times 19}$$

$$= 22.8 \text{ mm or } 0.023 \text{ m}$$

Example 9.9

14.4 tonne/h (4.0 kg/s) of nitrobenzene is to be cooled from 400 to 315 K by heating a stream of benzene from 305 to 345 K.

Two tubular heat exchangers are available each with a 0.44 m i.d. shell fitted with 166 tubes, 19.0 mm o.d. and 15.0 mm i.d., each 5.0 m long. The tubes are arranged in two passes on 25 mm square pitch with a baffle spacing of 150 mm. There are two passes on the shell side and operation is to be countercurrent. With benzene passing through the tubes, the anticipated film coefficient on the tube side is 1000 W/m²·K.

Assuming true cross-flow prevails in the shell, what value of scale resistance could be allowed if these units were used?
For nitrobenzene: $C_p = 2380 \text{ J/kg K}$, $k = 0.15 \text{ W/m K}$, $\mu = 0.70 \text{ mN s/m}^2$

Solution

(i) Tube side coefficient.

$$h_i = 1000 \text{ W/m}^2 \text{ K based on inside area}$$

$$\frac{1000 \times 15.0}{19.0} = 790 \text{ W/m}^2 \text{ K based on outside area}$$

or:

(ii) Shell side coefficient.

$$\text{Area for flow} = \text{shell diameter} \times \text{baffle spacing} \times \text{clearance/pitch}$$

$$= \frac{0.44 \times 0.150 \times 0.006}{0.025} = 0.0158 \text{ m}^2$$

$$\text{Hence: } G'_s = \frac{4.0}{0.0158} = 253.2 \text{ kg/m}^2 \text{ s}$$

Taking $\mu/\mu_s = 1$ in equation 9.91:

$$h_o = 0.36 \frac{k}{d_e} \left(\frac{d_e G'_s}{\mu} \right)^{0.55} \left(\frac{C_p \mu}{k} \right)^{0.33}$$

The hydraulic mean diameter,

$$d_e = 4 \left[\frac{25^2 - \frac{\pi \times 19.0^2}{4}}{\pi \times 19.0} \right] = 22.8 \text{ mm or } 0.023 \text{ m}$$

$$\text{and here: } h_o = \left(\frac{0.15}{0.023} \right) 0.36 \left(\frac{0.023 \times 253.2}{0.70 \times 10^{-3}} \right)^{0.55} \left(\frac{2380 \times 0.70 \times 10^{-3}}{0.15} \right)^{0.33}$$

$$= 2.35 \times 143 \times 2.23 = 750 \text{ W/m}^2 \text{ K}$$

(iii) Overall coefficient.

The logarithmic mean temperature difference is given by:

$$\Delta T_m = \frac{(400 - 345) - (315 - 305)}{\ln(400 - 345)/\ln(315 - 305)}$$

$$= 26.4 \text{ deg K}$$

The corrected mean temperature difference is then $\Delta T_m \times F = 26.4 \times 0.8 = 21.1 \text{ deg K}$
(Details of the correction factor for ΔT_m are given in Section 9.9.3)

$$\text{Heat load: } Q = 4.0 \times 2380(400 - 315) = 8.09 \times 10^5 \text{ W}$$

The surface area of each tube

$$U_o = \frac{Q}{A_o \Delta T_m F} = \frac{8.09 \times 10^5}{2 \times 166 \times 5.0 \times 0.0598 \times 21.1}$$

$$= 386.2 \text{ W/m}^2 \text{ K}$$

Thus:

(iv) Scale resistance.

If scale resistance is R_d , then:

$$R_d = \frac{1}{386.2} - \frac{1}{750} - \frac{1}{1000} = 0.00026 \text{ m}^2 \text{ K/W}$$

This is a rather low value, though the heat exchangers would probably be used for this duty.

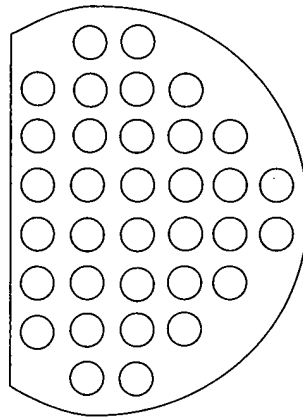


Figure 9.29. Baffle for heat exchanger

As discussed in Section 9.9 it is common practice to fit *baffles* across the tube bundle in order to increase the velocity over the tubes. The commonest form of baffle is shown in Figure 9.29 where it is seen that the cut-away section is about 25 per cent of the total area. With such an arrangement, the flow pattern becomes more complex and the extent of leakage between the tubes and the baffle, and between the baffle and the inside of the shell of the exchanger, complicates the problem, as discussed further in Section 9.9.6. Reference may also be made in Volume 6 and to the work of SHORR⁽²⁹⁾, DONOHUE⁽³⁰⁾, and TINKER⁽³¹⁾. The various methods are all concerned with developing a method of calculating the true area of flow and of assessing the probable influence of leaks. When using baffles, the value of h_o , as found from equation 9.89, is commonly multiplied by 0.6 to allow for leakage although more accurate approaches have been developed as discussed in Section 9.9.6.

The *drop in pressure* for the flow of a fluid across a tube bundle may be important because of the small pressure head available and because by good design it is possible to get a better heat transfer for the same drop in pressure. $-\Delta P_f$ depends on the velocity u_i through the minimum area of flow and in Chapter 3 an equation proposed by GRIMISON⁽²⁴⁾ is given as:

$$-\Delta P_f = \frac{C_f j \rho u_i^2}{6} \quad (\text{equation 3.83})$$

Table 9.4. (18) Ratio of heat transfer to friction for tube bundles ($Re_{\max} = 20,000$)

	$X = 1.25d_o$			$X = 1.5d_o$		
	C_h	C_f	C_h/C_f	C_h	C_f	C_h/C_f
In-line						
$Y = 1.25d_o$	1	1.44	0.69	1	1.56	0.64
$Y = 1.5d_o$	0.96	0.84	1.14	0.96	0.96	1.0
Staggered						
$Y = 1.25d_o$	1.06	1.56	0.68	1.05	1.74	0.60
$Y = 1.5d_o$	1.04	1.10	0.95	1.02	1.16	0.88

where C_f depends on the geometry of the tube layout and j is the number of rows of tubes. It is found that the ratio of C_h , the heat transfer factor in equation 9.90, to C_f

is greater for the in-line arrangement but that the actual heat transfer is greater for the staggered arrangement, as shown in Table 9.4.

The drop in pressure $-\Delta P_f$ over the tube bundles of a heat exchanger is also given by:

$$-\Delta P_f = \frac{f' G_s^2 (n+1) d_v}{2 \rho d_e} \quad (9.92)$$

where f' is the friction factor given in Figure 9.30, G_s' the mass velocity through bundle, n the number of baffles in the unit, d_v the inside shell diameter, ρ the density of fluid, d_e the equivalent diameter, and $-\Delta P_f$ the drop in pressure.

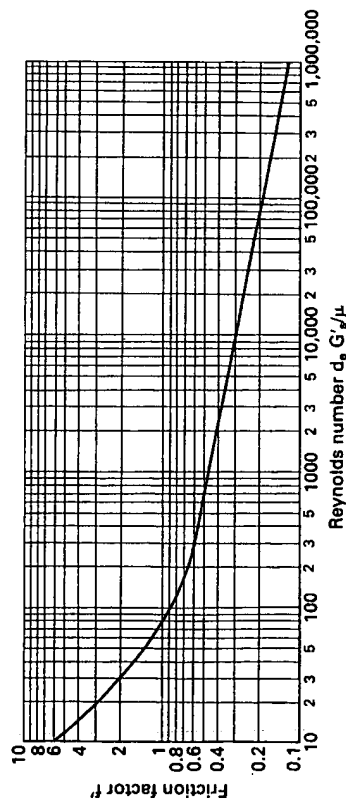


Figure 9.30. Friction factor for flow over tube bundles

Example 9.10

54 tonne/h (15 kg/s) of benzene is cooled by passing the stream through the shell side of a tubular heat exchanger, 1 m i.d., fitted with 5 m tubes, 19 mm o.d. arranged on a 25 mm square pitch with 6 mm clearance. If the baffle spacing is 0.25 m (19 baffles), what will be the pressure drop over the tube bundle? ($\mu \approx 0.5 \text{ mN s/m}^2$).

Solution

Cross-flow area: $A_s = \frac{1.0 \times 0.25 \times 0.006}{0.025} = 0.06 \text{ m}^2$

Mass flow: $G_s' = \frac{15}{0.06} = 250 \text{ kg/m}^2 \text{ s}$

Equivalent diameter: $d_e = \frac{4[0.025^2 - (\pi/4)0.019^2]}{\pi \times 0.019} = 0.0229 \text{ m}$

Reynolds number through the tube bundle = $\frac{250 \times 0.0229}{0.5 \times 10^{-3}} = 11450$

From Figure 9.29: $f' = 0.280$

Density of benzene = 881 kg/m^3

From equation 9.92:

$$-\Delta P_f = \frac{0.280 \times 250^2 \times 20 \times 1.0}{2 \times 881 \times 0.0229} = 8674 \text{ N/m}^2$$

or: $\frac{8674}{881 \times 9.81} = 1.00 \text{ m of benzene}$

9.4.5. Flow in non-circular sections Rectangular ducts

For the heat transfer for fluids flowing in non-circular ducts, such as rectangular ventilating ducts, the equations developed for turbulent flow inside a circular pipe may be used if an equivalent diameter, such as the hydraulic mean diameter d_e discussed previously, is used in place of d .

The data for heating and cooling water in turbulent flow in rectangular ducts are reasonably well correlated by the use of equation 9.59 in the form:

$$\frac{hd_e}{k} = 0.023 \left(\frac{d_e G'}{\mu} \right)^{0.8} \left(\frac{C_p \mu}{k} \right)^{0.4} \quad (9.93)$$

Whilst the experimental data of COPE and BAILEY⁽³²⁾ are somewhat low, the data of WASHINGTON and MARKS⁽³³⁾ for heating air in ducts are well represented by this equation.

Annular sections between concentric tubes

Concentric tube heat exchangers are widely used because of their simplicity of construction and the ease with which additions may be made to increase the area. They also give turbulent conditions at low volumetric flowrates.

In presenting equations for the film coefficient in the annulus, one of the difficulties is in selecting the best equivalent diameter to use. When considering the film on the outside of the inner tube, DAVIS⁽³⁴⁾ has proposed the equation:

$$\frac{hd_1}{k} = 0.031 \left(\frac{d_1 G'}{\mu} \right)^{0.8} \left(\frac{C_p \mu}{k} \right)^{0.33} \left(\frac{\mu}{\mu_s} \right)^{0.14} \left(\frac{d_2}{d_1} \right)^{0.15} \quad (9.94)$$

where d_1 and d_2 are the outer diameter of the inner tube, and the inner diameter of the outer tube, respectively.

CARPENTER *et al.*⁽³⁵⁾ suggest using the hydraulic mean diameter $d_e = (d_2 - d_1)$ in the Sieder and Tate equation (9.66) and recommend the equation:

$$\frac{hd_e}{k} \left(\frac{\mu_s}{\mu} \right)^{0.14} = 0.027 \left(\frac{d_e G'}{\mu} \right)^{0.8} \left(\frac{C_p \mu}{k} \right)^{0.33} \quad (9.95)$$

Their data, which were obtained using a small annulus, are somewhat below those given by equation 9.95 for values of $d_e G'/\mu$ less than 10,000, although this may be because the flow was not fully turbulent: with an index on the Reynolds group of 0.9, the equation fitted the data much better. There is little to choose between these two equations, but they both give rather high values for h .

For the viscous region, Carpenter's results are reasonably well correlated by the equation:

$$\frac{hd_e}{k} \left(\frac{\mu_s}{\mu} \right)^{0.14} = 2.01 \left(\frac{GC_p}{kl} \right)^{0.33} \quad (9.96)$$

$$= 1.86 \left[\left(\frac{d_e G'}{\mu} \right) \left(\frac{C_p \mu}{k} \right) \left(\frac{d_1 + d_2}{l} \right) \right]^{1/3} \quad (9.97)$$

Equations 9.96 and 9.97 are the same as equations 9.85 and 9.86, with d_e replacing d . These results have all been obtained with small units and mainly with water as the fluid in the annulus.

Flow over flat plates

For the turbulent flow of a fluid over a flat plate the Colburn type of equation may be used with a different constant:

$$j_h = 0.037 Re_x^{-0.2} \quad (9.98)$$

where the physical properties are taken as for equation 9.64 and the characteristic dimension in the Reynolds group is the actual distance x along the plate. This equation therefore gives a point value for j_h .

9.4.6. Convection to spherical particles

In Section 9.3.4, consideration is given to the problem of heat transfer by conduction through a surrounding fluid to spherical particles or droplets. Relative motion between the fluid and particle or droplet causes an increase in heat transfer, much of which may be due to convection. Many investigators have correlated their data in the form:

$$Nu' = 2 + \beta' Re^n Pr^m \quad (9.99)$$

where values of β' , a numerical constant, and exponents n and m are found by experiment. In this equation, $Nu' = hd/k$ and $Re' = d\rho\mu$, the Reynolds number for the particle, u is the relative velocity between particle and fluid, and d is the particle diameter. As the relative velocity approaches zero, Re' tends to zero and the equation reduces to $Nu' = 2$ for pure conduction.

ROWE *et al.* (36), having analysed a large number of previous studies in this area and provided further experimental data, have concluded that for particle Reynolds numbers in the range 20–2000, equation 9.99 may be written as:

$$Nu' = 2.0 + \beta' Re^{0.5} Pr^{0.33} \quad (9.100)$$

where β' lies between 0.4 and 0.8 and has a value of 0.69 for air and 0.79 for water. In some practical situations the relative velocity between particle and fluid may change due to particle acceleration or deceleration, and the value of Nu' can then be time-dependent.

For mass transfer, which is considered in more detail in Chapter 10, an analogous relation (equation 10.233) applies, with the Sherwood number replacing the Nusselt number and the Schmidt number replacing the Prandtl number.

9.4.7. Natural convection

If a beaker containing water rests on a hot plate, the water at the bottom of the beaker becomes hotter than that at the top. Since the density of the hot water is lower than that of the cold, the water in the bottom rises and heat is transferred by natural convection. In the same way air in contact with a hot plate will be heated by natural convection currents, the air near the surface being hotter and of lower density than that some distance away. In both of these cases there is no external agency providing forced convection currents, and the transfer of heat occurs at a correspondingly lower rate since the natural convection currents move rather slowly.

For these processes which depend on buoyancy effects, the rate of heat transfer might be expected to follow a relation of the form:

$$Nu = f(Gr, Pr) \quad (\text{equation 9.57})$$

Measurements by SCHMIDT⁽³⁷⁾ of the upward air velocity near a 300 mm vertical plate show that the velocity rises rapidly to a maximum at a distance of about 2 mm from the plate and then falls rapidly. However, the temperature evens out at about 10 mm from the plate. Temperature measurements around horizontal cylinders have been made by RAY⁽³⁸⁾.

Natural convection from horizontal surfaces to air, nitrogen, hydrogen, and carbon dioxide, and to liquids (including water, aniline, carbon tetrachloride, glycerol) has been studied by several workers, including DAVIS⁽³⁹⁾, ACKERMANN⁽⁴⁰⁾, FISHENDEN and SAUNDERS⁽¹⁸⁾ and SAUNDERS⁽⁴¹⁾. Most of the results are for thin wires and tubes up to about 50 mm diameter; the temperature differences used are up to about 1100 deg K with gases and about 85 deg K with liquids. The general form of the results is shown in Figure 9.31, where $\log Nu$ is plotted against $\log (Pr Gr)$ for streamline conditions. The curve can be represented by a relation of the form:

$$Nu = C'(Gr Pr)^n \quad (9.101)$$

Numerical values of C' and n , determined experimentally for various geometries, are given in Table 9.5⁽⁴²⁾. Values of coefficients may then be predicted using the equation:

$$\frac{hl}{k} = C' \left(\frac{\beta g \Delta T l^3 \rho^2 C_p \mu}{\mu^2 k} \right)^n \quad \text{or} \quad h = C' \left(\frac{\Delta T}{l} \right)^n \left(\frac{\beta g \rho^2 C_p}{\mu k} \right)^n \quad (9.102)$$

Table 9.5. Values of C' , C'' and n for use in equations 9.102 and 9.105⁽⁴²⁾

Geometry	$GrPr$	C'	n	C'' (SI units) (for air at 294 K)
Vertical surfaces (l = vertical dimension < 1 m)	$< 10^4$	1.36	0.20	
	$10^4 - 10^9$	0.59	0.25	1.37
	$> 10^9$	0.13	0.33	1.24
Horizontal cylinders (l = diameter < 0.2 m)	$10^{-5} - 10^{-3}$	0.71	0.04	
	$10^{-3} - 1.0$	1.09	0.10	
	$1.0 - 10^4$	1.09	0.20	
	$10^4 - 10^9$	0.53	0.25	1.32
	$> 10^9$	0.13	0.33	1.24
Horizontal flat surfaces (facing upwards) (facing downwards)	$10^5 - 2 \times 10^7$	0.54	0.25	1.86
	$2 \times 10^7 - 3 \times 10^{10}$	0.14	0.33	
	$3 \times 10^{10} - 3 \times 10^{16}$	0.27	0.25	0.88

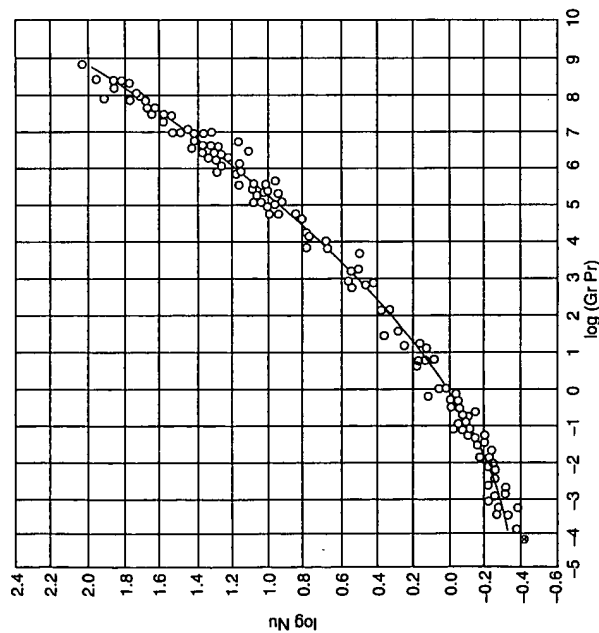


Figure 9.31. Natural convection from horizontal tubes

where the physical properties are at the mean of the surface and bulk temperatures and, for gases, the coefficient of cubical expansion β is taken as $1/T$, where T is the absolute temperature.

For vertical plates and cylinders, KATO *et al.*⁽⁴³⁾ have proposed the following equations for situations where $1 < Pr < 40$:

$$\text{For } Gr > 10^9: \quad Nu = 0.138 Gr^{0.36} (Pr^{0.175} - 0.55) \quad (9.103)$$

$$\text{and for } Gr < 10^9: \quad Nu = 0.683 Gr^{0.25} Pr^{0.25} \left(\frac{Pr}{0.861 + Pr} \right)^{0.25} \quad (9.104)$$

Natural convection to air

Simplified dimensional equations have been derived for air, water and organic liquids by grouping the fluid properties into a single factor in a rearrangement of equation 9.102 to give:

$$h = C'' (\Delta T)^n / \nu^{3n-1} \quad (\text{W/m}^2\text{K}) \quad (9.105)$$

Values of C'' (in SI units) are also given in Table 9.5 for air at 294 K. Typical values for water and organic liquids are 127 and 59 respectively.

Example 9.11

Estimate the heat transfer coefficient for natural convection from a horizontal pipe 0.15 m diameter, with a surface temperature of 400 K to air at 294 K

Solution

Over a wide range of temperature, $k'(\beta g \rho^2 C_p / \mu k) = 36.0$

For air at a mean temperature of $0.5(400 + 294) = 347$ K, $k = 0.0310$ W/m K (Table 6, Appendix A.1)

$$\text{Thus:} \quad \frac{\beta g \rho^2 C_p}{\mu k} = \frac{36.0}{0.0310^4} = 3.9 \times 10^7$$

From Equation 9.102:

$$\begin{aligned} Gr Pr &= 3.9 \times 10^7 (400 - 294) \times 0.15^3 \\ &= 1.39 \times 10^7 \end{aligned}$$

From Table 9.5:

$$n = 0.25 \quad \text{and} \quad C'' = 1.32$$

Thus, in Equation 9.104:

$$\begin{aligned} h &= 1.32(400 - 294)^{0.25} (0.15)^{(3 \times 0.25) - 1} \\ &= 1.32 \times 106^{0.25} \times 0.15^{-0.25} \\ &= \underline{\underline{6.81 \text{ W/m}^2 \text{ K}}} \end{aligned}$$

Fluids between two surfaces

For the transfer of heat from a hot surface across a thin layer of fluid to a parallel cold surface:

$$\frac{Q}{Q_k} = \frac{h \Delta T}{(k/x) \Delta T} = \frac{hx}{k} = Nu \quad (9.106)$$

where Q_k is the rate at which heat would be transferred by pure thermal conduction between the layers, a distance x apart, and Q is the actual rate.

For $(Gr Pr) = 10^3$, the heat transferred is approximately equal to that due to conduction alone, though for $10^4 < Gr Pr < 10^6$, the heat transferred is given by:

$$\frac{Q}{Q_k} = 0.15 (Gr Pr)^{0.25} \quad (9.107)$$

which is noted in Figure 9.32. In this equation the characteristic dimension to be used for the Grashof group is x , the distance between the planes, and the heat transfer is independent of surface area, provided that the linear dimensions of the surfaces are large compared with x . For higher values of $(Gr Pr)$, Q/Q_k is proportional to $(Gr Pr)^{1/3}$, showing that the heat transferred is not entirely by convection and is not influenced by the distance x between the surfaces.

A similar form of analysis has been given by KRAUSSOLD⁽⁴⁴⁾ for air between two concentric cylinders. It is important to note from this general analysis that a single layer of air will not be a good insulator because convection currents set in before it becomes 25 mm thick. The good insulating properties of porous materials are attributable to the

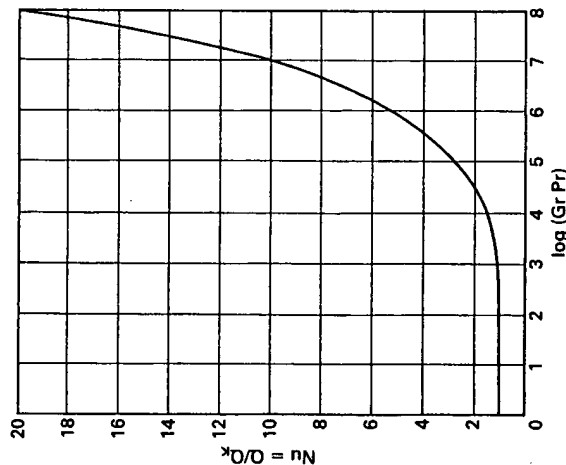


Figure 9.32. Natural convection between surfaces

fact that they offer a series of very thin layers of air in which convection currents are not present.

9.5. HEAT TRANSFER BY RADIATION

9.5.1. Introduction

It has been seen that heat transfer by conduction takes place through either a solid or a stationary fluid and heat transfer by convection takes place as a result of either forced or natural movement of a hot fluid. The third mechanism of heat transfer, radiation, can take place without either a solid or a fluid being present, that is through a vacuum, although many fluids are transparent to radiation, and it is generally assumed that the emission of thermal radiation is by "waves" of wavelengths in the range $0.1 - 100 \mu\text{m}$ which travel in straight lines. This means that direct radiation transfer, which is the result of an interchange between various radiating bodies or surfaces, will take place only if a straight line can be drawn between the two surfaces; a situation which is often expressed in terms of one surface "seeing" another. Having said this, it should be noted that opaque surfaces sometimes cast shadows which inhibit radiation exchange and that indirect transfer by radiation can take place as a result of partial reflection from other surfaces. Although all bodies at temperatures in excess of absolute zero radiate energy in all directions, radiation is of especial importance from bodies at high temperatures such as those encountered in furnaces, boilers and high temperature reactors, where in addition to radiation from hot surfaces, radiation from reacting flame gases may also be a consideration.

9.5.2. Radiation from a black body

In thermal radiation, a so-called *black body* absorbs all the radiation falling upon it, regardless of wavelength and direction, and, for a given temperature and wavelength, no surface can emit more energy than a black body. The radiation emitted by a black body, whilst a function of wavelength and temperature, is regarded as *diffuse*, that is, it is independent of direction. In general, most rough surfaces and indeed most engineering materials may be regarded as being diffuse. A black body, because it is a perfect emitter or absorber, provides a standard against which the radiation properties of real surfaces may be compared.

If the *emissive power* E of a radiation source—that is the energy emitted per unit area per unit time—is expressed in terms of the radiation of a single wavelength λ , then this is known as the *monochromatic* or *spectral emissive power* E_{λ} , defined as that rate at which radiation of a particular wavelength λ is emitted per unit surface area, per unit wavelength in all directions. For a black body at temperature T , the spectral emissive power of a wavelength λ is given by *Planck's Distribution Law*:

$$E_{\lambda,b} = C_1 / \lambda^5 (\exp(C_2 / \lambda T) - 1) \quad (9.108)$$

where, in SI units, $E_{\lambda,b}$ is in W/m^3 and $C_1 = 3.742 \times 10^{-16} \text{ W/m}^2$ and $C_2 = 1.439 \times 10^{-2} \text{ mK}$ are the respective radiation constants. Equation 9.108 permits the evaluation of the emissive power from a black body for a given wavelength and absolute temperature and values obtained from the equation are plotted in Figure 9.33 which is based on the work of INCROPERA and DE WITT⁽⁴⁵⁾. It may be noted that, at a given wavelength, the radiation from a black body increases with temperature and that, in general, short wavelengths are associated with high temperature sources.

Example 9.12

What is the temperature of a surface coated with carbon black if the emissive power at a wavelength of $1.0 \times 10^{-6} \text{ m}$ is $1.0 \times 10^9 \text{ W/m}^2$? How would this be affected by a +2 per cent error in the emissive power measurement?

Solution

From equation 9.108 $\exp(C_2 / \lambda T) = [C_1 / E_{\lambda,b} \lambda^5] + 1$

$$\text{or: } \exp(1.439 \times 10^{-2} / (1.0 \times 10^{-6} T)) = [3.742 \times 10^{-16} / (1 \times 10^{-9} \times (1.0 \times 10^{-6})^5)] + 1$$

$$= 3.742 \times 10^5$$

$$\text{Thus: } (1.439 \times 10^4) / T = \ln(3.742 \times 10^5) = 12.83$$

$$\text{and: } T = (1.439 \times 10^4) / 12.83 = \underline{\underline{1121 \text{ K}}}$$

With an error of +2 per cent, the correct value is given by:

$$E_{\lambda,b} = (100 - 2)(1 \times 10^9) / 100 = 9.8 \times 10^8 \text{ W/m}^2$$

$$9.8 \times 10^8 = (3.742 \times 10^{-16}) / ((1 \times 10^{-6})^5)$$

$$(\exp(1.439 \times 10^{-2} / (1.0 \times 10^{-6} T)) - 1)$$

$$T = \underline{\underline{1120 \text{ K}}}$$

Thus, the error in the calculated temperature of the surface is only 1 K.

The wavelength at which maximum emission takes place is related to the absolute temperature by *Wein's Displacement Law*, which states that the wavelength for maximum emission varies inversely with the absolute temperature of the source, or:

$$\lambda_{\max} T = \text{constant}, C_3 (= 2.898 \times 10^{-3} \text{ mK in SI units}) \quad (9.109)$$

Thus, combining equations 9.108 and 9.109:

$$E_{\lambda \max, b} = C_1 / [(C_3/T)^5 [\exp(C_2/C_3) - 1]] \quad (9.110)$$

$$E_{\lambda \max, b} = C_4 T^5$$

where, in SI units, the fourth radiation constant, $C_4 = 12.86 \times 10^{-6} \text{ W/m}^2 \text{ K}^5$. Values of the maximum emissive power are shown by the broken line in Figure 9.33.

An interesting feature of Figure 9.33 is that it illustrates the well-known *greenhouse effect* which depends on the ability of glass to transmit radiation from a hot source over only a limited range of wavelengths. This warms the air in the greenhouse, though to a much lower temperature than that of the external source, the sun; a temperature at which the wavelength will be much longer, as seen from Figure 9.33, and one at which the glass will not transmit radiation. In this way, radiation outwards from within a greenhouse is considerably reduced and the air within the enclosure retains its heat. Much the same

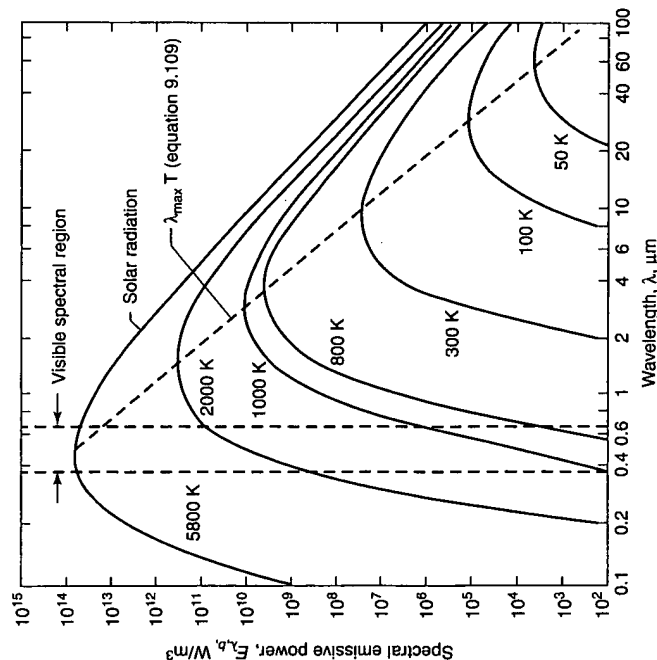


Figure 9.33. Spectral black-body emissive power⁽⁴⁵⁾

phenomenon occurs in the gases above the earth's surface which will transmit incoming radiation from the sun at a given wavelength though not radiation from the earth which, because it is at a lower temperature, emits at a longer wavelength. The passage of radiation through gases and indeed through glass is one example of a situation where the transmissivity τ , discussed in Section 9.5.3, is not zero.

The *total emissive power* E is defined as the rate at which radiation energy is emitted per unit time per unit area of surface over all wavelengths and in all directions. This may be determined by making a summation of all the radiation at all wavelengths, that is by determining the area corresponding to a particular temperature under the Planck distribution curve, Figure 9.33. In this way, from equation 9.108, the total emissive power is given by:

$$E_b = \int_0^\infty C_1 d\lambda / [\lambda^5 (\exp(C_2/\lambda T) - 1)] \quad (9.111)$$

which is known as the *Stefan-Boltzmann Law*. This may be integrated for any constant value of T to give:

$$E_b = \sigma T^4 \quad (9.112)$$

where, in SI units, the Stefan-Boltzmann constant $\sigma = 5.67 \times 10^{-8} \text{ W/m}^2 \text{ K}^4$.

Example 9.13

Electrically-heated carbide elements, 10 mm in diameter and 0.5 m long, radiating essentially as black bodies, are to be used in the construction of a heater in which thermal radiation from the surroundings is negligible. If the surface temperature of the carbide is limited to 1750 K, how many elements are required to provide a radiated thermal output of 500 kW?

Solution

From equation 9.112, the total emissive power is given by:

$$E_b = \sigma T^4 = (5.67 \times 10^{-8} \times 1750^4) = 5.32 \times 10^5 \text{ W/m}^2$$

$$\text{The area of one element} = \pi(10/1000)(0.5) = 1.571 \times 10^{-2} \text{ m}^2$$

$$\text{and: Power dissipated by one element} = (5.32 \times 10^5 \times 1.571 \times 10^{-2}) = 8.367 \times 10^3 \text{ W}$$

$$\text{Thus: Number of elements required} = (500 \times 1000) / (8.357 \times 10^3) = 59.8 \text{ say } 60$$

9.5.3. Radiation from real surfaces

The *emissivity* of a material is defined as the ratio of the radiation per unit area emitted from a "real" or from a grey surface (one for which the emissivity is independent of wavelength) to that emitted by a black body at the same temperature. Emissivities of "real" materials are always less than unity and they depend on the type, condition and roughness of the material, and possibly on the wavelength and direction of the emitted radiation as well. For diffuse surfaces where emissivities are independent of direction, the emissivity, which represents an average over all directions, is known as the *hemispherical emissivity*. For a particular wavelength λ this is given by:

$$e_\lambda = E_\lambda / E_b \quad (9.113)$$

and, similarly, the total hemispherical emissivity, an average over all wavelengths, is given by:

$$e = E/E_b \quad (9.114)$$

Equation 9.114 leads to *Kirchoff's Law* which states that the absorptivity, or fraction of incident radiation absorbed, and the emissivity of a surface are equal. If two bodies **A** and **B** of areas A_1 and A_2 are in a large enclosure from which no energy is lost, then the energy absorbed by **A** from the enclosure is $A_1 a_1 I$ where I is the rate at which energy is falling on unit area of **A** and a_1 is the absorptivity. The energy given out by **A** is $E_1 A_1$ and, at equilibrium, these two quantities will be equal or:

$$I A_1 a_1 = A_1 E_1$$

and, for **B**:

$$I A_2 a_2 = A_2 E_2$$

Thus:

$$E_1/a_1 = E_2/a_2 = E/a \text{ for any other body.}$$

Since $E/a = E_b/a_b$, then, from equation 9.114:

$$e = E/E_b = a/a_b$$

and, as by definition, $a_b = 1$, the emissivity of any body is equal to its absorptivity, or:

$$e = a \quad (9.115)$$

For most industrial, non-metallic surfaces and for non-polished metals, e is usually about 0.9, although values as low as 0.03 are more usual for highly polished metals such

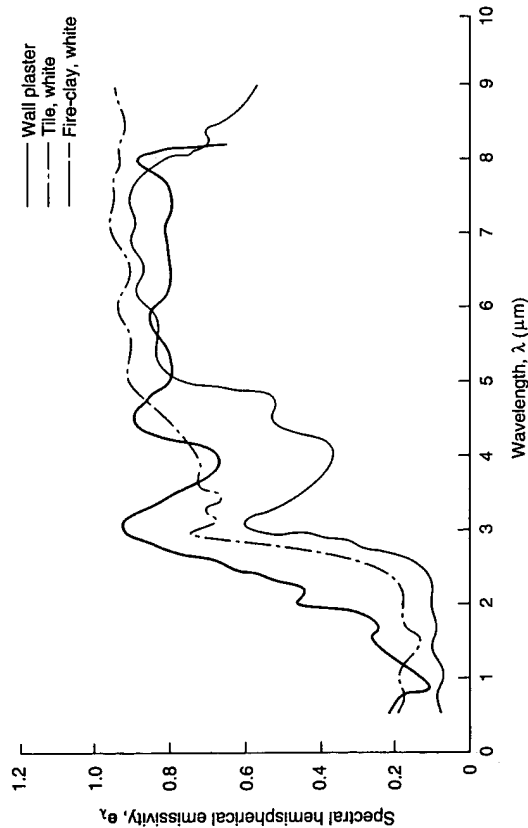


Figure 9.34. Spectral emissivity of non-conductors as a function of wavelength⁽⁴⁵⁾

as copper or aluminium. As explained later, a small cavity in a body acts essentially as a black body with an effective emissivity of unity. The variation of emissivity with wavelength is illustrated in Figure 9.34⁽⁴⁵⁾ and typical values are given in Table 9.6 which is based on the work of HOTTTEL and SAROFIM⁽⁴⁶⁾. More complete data are available in Appendix A1, Table 10. If equation 9.113 is written as:

$$E_\lambda = e_\lambda E_{\lambda,b} \quad (9.116)$$

then the spectral emissive power of a grey surface may be obtained from the spectral emissivity, e_λ and the spectral emissive power of a black body $E_{\lambda,b}$ given by equation 9.108. As shown in Figure 9.35, for a temperature of 2000 K for example, the emission curve for a real material may have a complex shape because of the variation of emissivity with wavelength. If, however, the ordinate of the black body curve $E_{\lambda,b}$ at a particular wavelength is multiplied by the spectral emissivity of the source at that wavelength, the ordinates on the curve for the real surface are obtained, and the total emissive power of the real surface is obtained by integrating E_λ over all possible wavelengths to give:

$$E = \int_0^\infty E_\lambda d\lambda = \int_0^\infty e_\lambda E_{\lambda,b} d\lambda \quad (9.117)$$

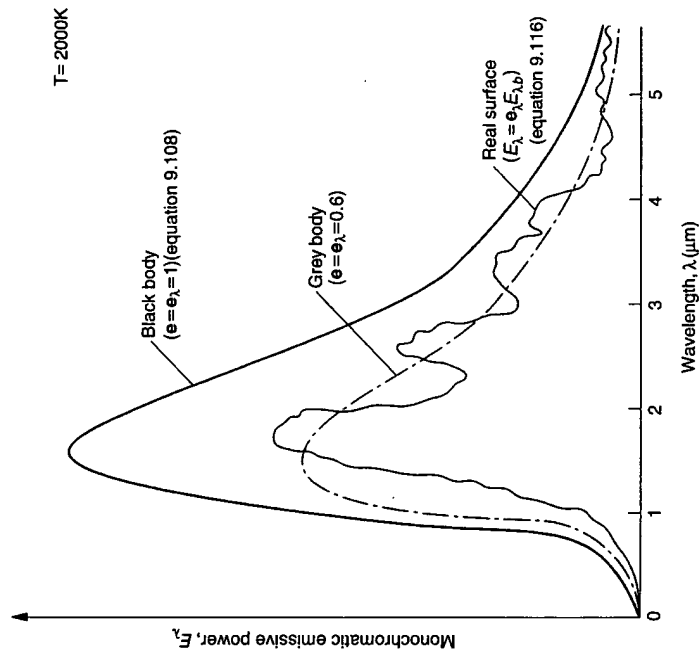


Figure 9.35. Comparison of black body, grey body and real surface radiation at 2000 K.⁽⁴⁵⁾

This integration may be carried out numerically or graphically, though this approach, which has been considered in some detail by INCROPERA and DE WIT⁽⁴⁵⁾, can be difficult, especially where the spectral distribution of radiation arrives at a surface of complex structure. The amount of calculation involved cannot often be justified in practical situations and it is more usual to use a mean spectral emissivity for the surface which is assumed to be constant over a range of wavelengths. Where the spectral emissivity does not vary with wavelength then the surface is known as a *grey body*, and, for a diffuse grey body, ϵ_λ can be replaced by e in equations 9.112 and 9.114 to give:

$$E = eE_b = e\sigma T^4 \quad (9.118)$$

In this way, the emissive power of a grey body is a constant proportion of the power emitted by the black body, resulting in the curve shown in Figure 9.35 where, for example, $e = 0.6$. The assumption that the surface behaves as a grey body is valid for most engineering calculations if the value of emissivity is taken as that for the dominant temperature of the radiation.

From equation 9.117, it is seen that the rate of heat transfer by radiation from a hot body at temperature T_1 to a cooler one at temperature T_2 is then given by:

$$q = Q/A = e\sigma(T_1^4 - T_2^4) = e\sigma(T_1 - T_2)(T_1^3 + T_1^2T_2 + T_1T_2^2 + T_2^3)$$

The quantity $q/(T_1 - T_2)$ is a heat transfer coefficient as used in convective heat transfer, and here it may be designated h_r , the heat transfer coefficient for radiation heat transfer where:

$$h_r = q/(T_1 - T_2) = \frac{e\sigma(T_1^4 - T_2^4)}{T_1 - T_2} = e\sigma(T_1^3 + T_1^2T_2 + T_1T_2^2 + T_2^3) \quad (9.119)$$

It may be noted that if $(T_1 - T_2)$ is very small, that is T_1 and T_2 are virtually equal, then:

$$h_r = 4e\sigma T^3$$

Example 9.14

What is the emissivity of a grey surface, 10 m² in area, which radiates 1000 kW at 1500 K? What would be the effect of increasing the temperature to 1600 K?

Solution

The emissive power

$$E = (1000 \times 1000)/10 = 100,000 \text{ W/m}^2$$

From equation 9.118:

$$\begin{aligned} e &= E/\sigma T^4 \\ &= 100,000/(5.67 \times 10^{-8} \times 1500^4) = 0.348 \end{aligned}$$

At 1600 K:

$$\begin{aligned} E &= e\sigma T^4 \\ &= (0.348 \times 5.67 \times 10^{-8} \times 1600^4) = 1295 \text{ kW} \end{aligned}$$

an increase of 29.5 per cent for a 100 deg K increase in temperature.

Table 9.6. Typical emissivity values⁽⁴⁶⁾

Surface	TK	Emissivity e
<i>(A) Metals and metallic oxides</i>		
Aluminium		
Polished plate	296	0.040
Rough plate	299	0.055
Polished	311-589	0.096
Polished	390	0.023
Copper		
Plate, oxidised	498	0.78
Gold		
Highly polished	500-900	0.018-0.35
Polished iron	700-1300	0.144-0.377
Cast iron, newly turned	295	0.435
Smooth sheet iron	1172-1311	0.55-0.60
Sheet steel, oxidised	295	0.657
Iron		
Steel plate, rough	373	0.736
311-644		0.94-0.97
Pure, unoxidised	400-500	0.057-0.075
Grey, oxidised	297	0.281
Lead		
Mercury	273-373	0.09-0.12
Molybdenum	1000-2866	0.096-0.292
Monel	472-872	0.41-0.46
Nickel		
Polished	500-600	0.07-0.087
Wire	460-1280	0.096-0.186
Plate, oxidised	472-872	0.37-0.48
Chromonickel	325-1308	0.64-0.76
Nickel alloys		
Nickel, grey oxidised	294	0.262
Pure, polished plate	500-900	0.054-0.104
Strip	1200-1900	0.12-0.17
Platinum		
Filament	300-1600	0.036-0.192
Wire	500-1600	0.073-0.182
Polished	310-644	0.0221-0.0312
Filament	1600-3272	0.194-0.31
Bright tinned iron sheet	298	0.043-0.064
Tin		
Filament	3588	0.39
Tungsten		
Pure, polished	500-600	0.045-0.053
Zinc		
Galvanised sheet	297	0.276
<i>(B) Refractories, building materials, paints etc.</i>		
Asbestos		
Board	297	0.96
Brick		
Red, rough	294	0.93
Silica, unglazed	1275	0.80
Filament	1311-1677	0.526
Carbon		
Candle soot	372-544	0.952
Lampblack	311-644	0.945
White fused on iron	292	0.897
Enamel		
Glass	295	0.937
Paints, lacquers,		
Smooth	296	0.906
Snow-white enamel	296	0.906
Black, shiny lacquer	298	0.875
Black matt shellac	350-420	0.91
Plaster,		
Porcelain,		
Glazed	283-361	0.91
Refractory materials		
Poor radiators	295	0.924
Good radiators	872-1272	0.65-0.75
Hard, glossy plate	872-1272	0.80-0.90
Rubber		
Soft, grey, rough	296	0.945
Water		
Soft, grey, rough	298	0.859
	273-373	0.95-0.963

In a real situation, radiation incident upon a surface may be absorbed, reflected and transmitted and the properties, *absorptivity*, *reflectivity* and *transmissivity* may be used to describe this behaviour. In theory, these three properties will vary with the direction and wavelength of the incident radiation, although, with diffuse surfaces, directional variations may be ignored and mean, *hemispherical* properties used.

If the *absorptivity* a , the fraction of the incident radiation absorbed by the body is defined on a spectral basis, then:

$$a_\lambda = I_{\lambda, \text{abs}} / I_\lambda \quad (9.120)$$

and the total absorptivity, the mean over all wavelengths, is defined as:

$$a = I_{\text{abs}} / I \quad (9.121)$$

Since a black body absorbs all incident radiation then for a black body:

$$a_\lambda = a = 1$$

The absorptivity of a grey body is therefore less than unity.

In a similar way, the *reflectivity*, r , the fraction of incident radiation which is reflected from the surface, is defined as:

$$r = I_{\text{ref}} / I \quad (9.122)$$

and the *transmissivity*, t , the fraction of incident radiation which is transmitted through the body, as:

$$t = I_{\text{trans}} / I \quad (9.123)$$

Since, as shown in Figure 9.36, all the incident radiation is absorbed, reflected or transmitted, then:

$$I_{\text{abs}} + I_{\text{ref}} + I_{\text{trans}} = I$$

$$a + r + t = 1$$

or:

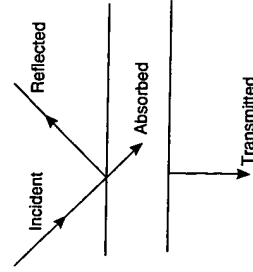


Figure 9.36. Reflection, absorption, and transmission of radiation

Since most solids are opaque to thermal radiation, $t = 0$ and therefore:

$$a + r = 1 \quad (9.124)$$

Kirchoff's Law, discussed previously, states that, at any wavelength, the emissivity and the absorptivity are equal. If this is extended to total properties, then, at a given temperature:

$$e = a \quad (\text{equation 9.115})$$

For a grey body, the emissivity and the absorptivity are, by definition, independent of temperature and hence equation 9.115 may be applied more generally showing that, where one radiation property (a , r or e) is specified for an opaque body, the other two may be obtained from equations 9.115 and 9.124. Kirchoff's Law explains why a cavity with a small aperture approximates to a black body in that radiation entering is subjected to repeated internal absorption and reflection so that only a negligible amount of the incident radiation escapes through the aperture. In this way, $a = e = 1$ and, at T K, the emissive power of the aperture is σT^4 .

9.5.4. Radiation transfer between black surfaces

Since radiation arriving at a black surface is completely absorbed, no problems arise from multiple reflections. Radiation is emitted from a diffuse surface in all directions and therefore only a proportion of the radiation leaving a surface arrives at any other given surface. This proportion depends on the relative geometry of the surfaces and this may be taken into account by the *view factor*, *shape factor* or *configuration factor*, which is normally written as F_{ij} for radiation arriving at surface j from surface i . In this way, F_{ij} , which is, of course, completely independent of the surface temperature, is the fraction of radiation leaving i which is directly intercepted by j .

If radiant heat transfer is taking place between two black surfaces, 1 and 2, then:

radiation emitted by surface 1 = $A_1 E_{b1}$

where A_1 and E_{b1} are the area and black body emissive power of surface 1, respectively. The fraction of this radiation which arrives at and is totally absorbed by surface 2 is F_{12} and the heat transferred is then:

$$Q_{1 \rightarrow 2} = A_1 F_{12} E_{b1}$$

Similarly, the radiation leaving surface 2 which arrives at 1 is given by:

$$Q_{2 \rightarrow 1} = A_2 F_{21} E_{b2}$$

and the net radiation transfer between the two surfaces is $Q_{12} = (Q_{1 \rightarrow 2} - Q_{2 \rightarrow 1})$ or:

$$Q_{12} = A_1 F_{12} E_{b1} - A_2 F_{21} E_{b2}$$

$$= \sigma A_1 F_{12} T_1^4 - \sigma A_2 F_{21} T_2^4 \quad (9.125)$$

When the two surfaces are at the same temperature, $T_1 = T_2$, $Q_{12} = 0$

and thus: $Q_{12} = 0 = \sigma T_1^4 (A_1 F_{12} - A_2 F_{21})$

Since the temperature T_1 can have any value so that, in general $T_1 \neq 0$, then:

$$A_1 F_{12} = A_2 F_{21} \quad (9.126)$$

Equation 9.126, known as the *reciprocity relationship* or *reciprocal rule*, then leads to the equation:

$$Q_{12} = \sigma A_1 F_{12} (T_1^4 - T_2^4) = \sigma A_2 F_{21} (T_1^4 - T_2^4) \quad (9.127)$$

The product of an area and an appropriate view factor is known as the *exchange area* which, in SI units, is expressed in m^2 . In this way, $A_1 F_{12}$ is known as exchange area 1-2.

Example 9.15

Calculate the view factor, F_{21} and the net radiation transfer between two black surfaces, a rectangle 2 m by 1 m (area A_1) at 1500 K and a disc 1 m in diameter (area A_2) at 750 K, if the view factor, $F_{12} = 0.25$.

Solution

$$A_1 = (2 \times 1) = 2 \text{ m}^2$$

$$A_2 = (\pi \times 1^2)/4 = 0.785 \text{ m}^2$$

From equation 9.126:

$$A_1 F_{12} = A_2 F_{21}$$

or:

$$(2 \times 0.25) = 0.785 F_{21}$$

and:

$$F_{21} = 0.637$$

In equation 9.127:

$$Q_{12} = \sigma A_1 F_{12} (T_1^4 - T_2^4)$$

$$Q_{12} = (5.67 \times 10^{-8} \times 2 \times 0.25)(1500^4 - 750^4) \\ = 5.38 \times 10^5 \text{ W or } \underline{538 \text{ kW}}$$

View factors, the values of which determine heat transfer rates, are dependent on the geometrical configuration of each particular system. As a simple example, radiation may be considered between elemental areas dA_1 and dA_2 of two irregular-shaped flat bodies, well separated by a distance L between their mid-points as shown in Figure 9.37. If α_1 and α_2 are the angles between the imaginary line joining the mid-points and the normals, the rate of heat transfer is then given by:

$$Q_{12} = \sigma (T_1^4 - T_2^4) \int_{A_1}^{A_2} (\cos \alpha_1 \cos \alpha_2 dA_1 dA_2) / \pi L^2 \quad (9.128)$$

Equation 9.128 may be extended to much larger surfaces by subdividing these into a series of smaller elements, each of exchange area $A_i F_{ij}$, and summing the exchange areas between each pair of elements to give:

$$A_i F_{ij} = A_j F_{ji} = \int_{A_i} \int_{A_j} (\cos \alpha_i \cos \alpha_j dA_i dA_j) / \pi L^2 \quad (9.129)$$

In this procedure, the value of the integrand can be determined numerically for every pair of elements and the double integral, approximately the sum of these values, then becomes:

$$\int_{A_j} \int_{A_i} (\cos \alpha_i \cos \alpha_j dA_i dA_j) / \pi L^2 = \sum_{A_i} \sum_{A_j} (\cos \alpha_i \cos \alpha_j dA_i dA_j) / \pi L^2 \quad (9.130)$$

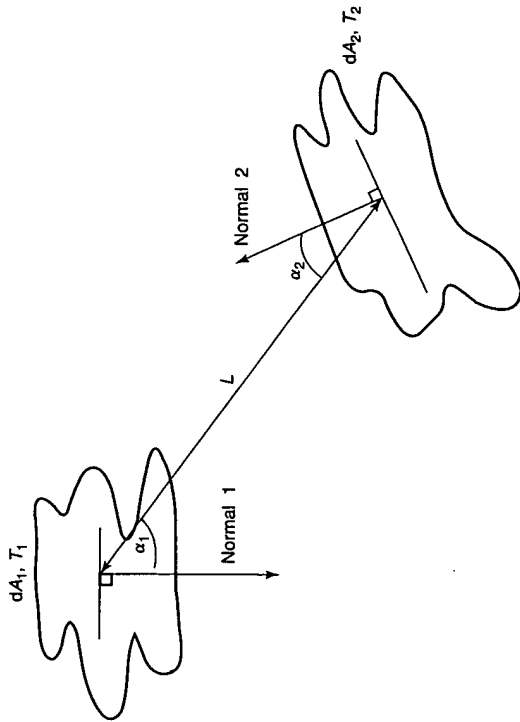


Figure 9.37. Determination of view factor

The amount of calculation involved here can be very considerable and use of a computer is usually required. A simpler approach is to make use of the many expressions, graphs and tables available in the heat transfer literature. Typical data, presented by INCROPERA and DE WITT⁽⁴⁵⁾ and by HOWELL⁽⁴⁷⁾, are shown in Figures 9.38-9.40, where it will be seen that in many cases, the values of the view factors approach unity. This means that nearly all the radiation leaving one surface arrives at the second surface as, for example, when a sphere is contained within a second larger sphere. Wherever a view factor approaches zero, only a negligible part of one surface can be seen by the other surface.

It is important to note here that if an element does not radiate directly to any part of its own surface, the shape factor with respect to itself, F_{11} , F_{22} and so on, is zero. This applies to any convex surface for which, therefore, $F_{11} = 0$.

Example 9.16

What are the view factors, F_{12} and F_{21} , for (a) a vertical plate, 3 m high by 4 m long, positioned at right angles to one edge of a second, horizontal plate, 4 m wide and 6 m long, and (b) a 1 m diameter sphere positioned within a 2 m diameter sphere?

Solution

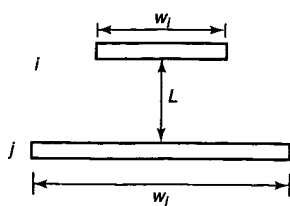
(a) Using the nomenclature in Figure 9.40 iii:

$$Y/X = (6/4) = 1.5 \text{ and } Z/X = (3/4) = 0.75$$

From the figure:

$$F_{12} = 0.12$$

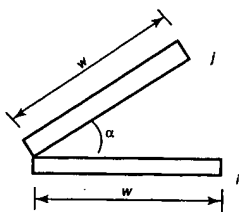
(i) Parallel plates with mid-lines connected by perpendicular



$$F_{ij} = \{[(W_i + W_j)^2 + 4]^{0.5} - [(W_i - W_j)^2 + 4]^{0.5}\} / 2W_i$$

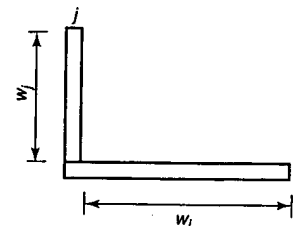
where: $W_i = W_i/L$ and $W_j = W_j/L$

(ii) Inclined parallel plates of equal width and a common edge



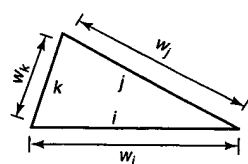
$$F_{ij} = 1 - \sin(\alpha/2)$$

(iii) Perpendicular plates with a common edge



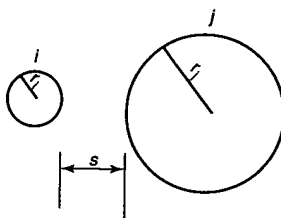
$$F_{ij} = \{1 + (w_i/w_j) - [1 + (w_i/w_j)^2]^{0.5}\} / 2$$

(iv) Three-sided enclosure



$$F_{ij} = (w_i + w_j - w_k) / 2w_i$$

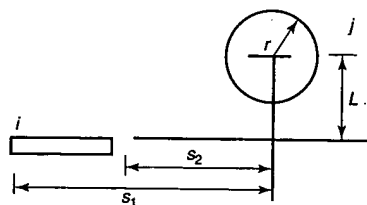
(v) Parallel cylinders of different radius



$$F_{ij} = (1/2\pi) \{ -\pi + [C^2 - (R+1)^2]^{0.5} - [C^2 - (R-1)^2]^{0.5} + (R-1) \cos^{-1}[(R/C) - (1/C)] - (R+1) \cos^{-1}[(R/C) + (1/C)] \}$$

where: $R = r_i/r_j$, $S = s/r_i$ and $C = 1 + R + S$

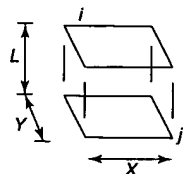
(vi) Cylinder and parallel rectangle



$$F_{ij} = [r/(s_1 - s_2)] [\tan^{-1}(s_1/L) - \tan^{-1}(s_2/L)]$$

Figure 9.38. View Factors for two-dimensional geometries.⁽⁴⁵⁾

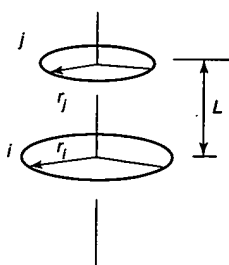
(i) Aligned parallel rectangles



$$F_{ij} = [2/(\pi \bar{X} \bar{Y})] \{ \ln[(1 + \bar{X}^2)(1 + \bar{Y}^2)/(1 + \bar{X}^2 + \bar{Y}^2)]^{0.5} + \bar{X}(1 + \bar{Y}^2)^{0.5} \tan^{-1}[\bar{X}/(1 + \bar{Y}^2)^{0.5}] + \bar{Y}(1 + \bar{X}^2)^{0.5} \tan^{-1}[\bar{Y}/(1 + \bar{X}^2)^{0.5}] - \bar{X} \tan^{-1} \bar{X} - \bar{Y} \tan^{-1} \bar{Y} \}$$

where: $\bar{X} = X/L$ and $\bar{Y} = Y/L$

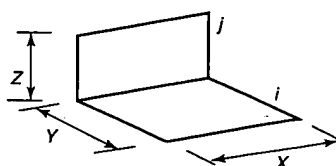
(ii) Coaxial parallel discs



$$F_{ij} = 0.5 \{ S^2 - 4(R_i/r_j)^2 \}^{0.5}$$

where: $R_i = r_i/L$, $R_j = r_j/L$ and $S = 1 + (R_i^2 + R_j^2)/R_i^2$

(iii) Perpendicular rectangles with a common edge



$$F_{ij} = (1/\pi W) \{ W \tan^{-1}(1/W) + H \tan^{-1}(1/H) - (H^2 + W^2)^{0.5} \tan^{-1}(H^2 + W^2)^{-0.5} + 0.25 \ln[(1 + W^2)(1 + H^2)/(1 + W^2 + H^2)] [W^2(1 + W^2 + H^2)/(1 + W^2)(W^2 + H^2)] \times [H^2(1 + H^2 + W^2)/(1 + H^2)(H^2 + W^2)] H^2 \}$$

where: $H = Z/X$ and $W = Y/X$

Figure 9.39. View factors for three-dimensional geometries.⁽⁴⁵⁾

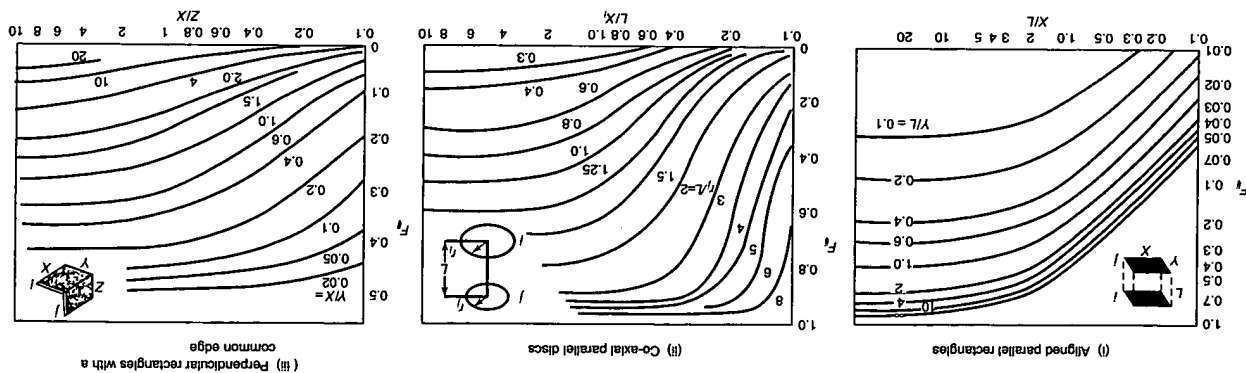
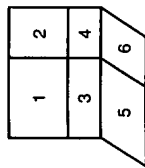


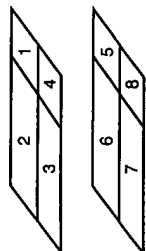
Figure 9.40. View factors for three-dimensional geometries⁽⁴⁵⁾

- (i) Two perpendicular rectangles
– between surfaces 1 and 6



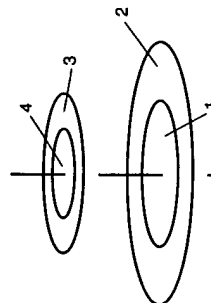
$$F_{16} = (A_6/A_1)[(1/2A_6)(A_{1+2+3+4})F_{1+2+3+4}(5+6) \\ + A_6F_{6(2+4)} - A_5F_{5(1+3)} - (1/2A_6)(A_{3+4})F_{3+4}(5+6) \\ - A_6F_{6A} - A_5F_{53}]$$

- (ii) Two parallel rectangles
– between surfaces 1 and 7



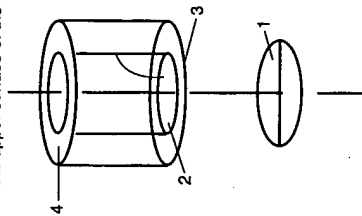
$$F_{17} = (1/4A_1)[A_{1+2+3+4})F_{1+2+3+4}(5+6+7+8) + A_1F_{5+6+7+8} \\ + A_5F_{3+7} + A_4F_{48}] - (1/4A_1)[A_{1+2})F_{1+2}(5+6) + A_{1+4})F_{1+4}(5+8) \\ + A_{3+4})F_{3+4}(7+8) + A_{2+3})F_{2+3}(6+7)]$$

- (iii) Two parallel circular rings
– between surfaces 2 and 3



$$F_{23} = (A_{1+2}/A_2)[F_{1+2}(3+4) - F_{1+2}4] \\ + (A_1/A_2)[F_{1(3+4)} - F_{14}]$$

- (iv) A circular tube and a disc between surface 3,
the inner wall of the tube of radius x_3 and surface 1,
the upper surface of the disc of radius x_1 .



$$F_{13} = F_{12} - F_{14} \\ F_{31} = (x_3^2/x_1^2)(F_{12} + F_{14})$$

Figure 9.41. View factors obtained by using the summation rule⁽⁴⁷⁾

From equation 9.126:

$$A_1 F_{12} = A_2 F_{21}$$

$$(3 \times 4)0.12 = (4 \times 6)F_{21}$$

$$F_{21} = 0.06$$

and:

(b) For the two spheres: $F_{12} = 1$ and $F_{21} = (r_1/r_2)^2 = (1/2)^2 = 0.25$

$$F_{22} = 1 - (r_1/r_2)^2 = 1 - 0.25 = 0.75$$

For a given geometry, view factors are related to each other, one example being the reciprocity relationship given in equation 9.126. Another important relationship is the *summation rule* which may be applied to the surfaces of a complete enclosure. In this case, all the radiation leaving one surface, say i , must arrive at all other surfaces in the enclosure so that, for n surfaces:

$$F_{i1} + F_{i2} + F_{i3} + \dots + F_{in} = 1$$

or: $F_{ij} = 1$ (9.131)

from which: $A_i F_{ij} = A_j$ (9.132)

This means that the sum of the exchange areas associated with a surface in an enclosure must be same as the area of that surface. The principle of the summation rule may be extended to other geometries such as, for example, radiation from a vertical rectangle (area 1) to an adjacent horizontal rectangle (area 2), as shown in Figure 9.40iii, where they are joined to a second horizontal rectangle of the same width (area 3). In effect area 3 is an extension of area 2 but has a different view factor.

In this case:

$$A_1 F_{1(2+3)} = A_1 F_{12} + A_1 F_{13}$$

or: $A_1 F_{13} = A_1 F_{1(2+3)} - A_1 F_{12}$ (9.133)

Equation 9.133 allows F_{13} to be determined from the view factors F_{12} and $F_{1(2+3)}$ which can be obtained directly from Figure 9.40iii. Typical data obtained by using this technique are shown in Figure 9.41 which is based on the work of HOWELL⁽⁴⁷⁾.

Example 9.17

What is the view factor F_{23} for the two parallel rings shown in Figure 9.41iii if the inner and outer radii of the two rings are: upper = 0.2 m and 0.3 m, lower = 0.3 m and 0.4 m and the rings are 0.2 m apart?

Solution

From Figure 9.41iii:

$$F_{23} = (A_{(1+2)}/A_2)(F_{(1+2)(3+4)} - F_{(1+2)4}) - (A_1/A_2)(F_{1(3+4)} - F_{14})$$

Laying out the data in tabular form and obtaining F from Figure 9.40ii, then,

For:	r_i (m)	r_j (m)	L (m)	(r_i/L)	(r_j/L)	(L/r_i)	F
$F_{(1+2)(3+4)}$	0.4	0.3	0.2	1.5	0.5	0.5	0.40
$F_{1(2+3)}$	0.4	0.2	0.2	1.0	0.5	0.5	0.22
$F_{1(3+4)}$	0.3	0.3	0.2	1.5	0.67	0.55	0.55
F_{14}	0.3	0.2	0.2	1.0	0.67	0.67	0.30

$$A_{(1+2)}/A_2 = 0.4^2/(0.4^2 - 0.3^2) = 2.29$$

$$A_1/A_2 = 0.3^2/(0.4^2 - 0.3^2) = 1.29$$

and hence:

$$F_{23} = 2.29(0.40 - 0.22) + 1.29(0.55 - 0.30) = 0.74$$

Equation 9.127 may be extended in order to determine the net rate of radiation heat transfer from a surface in an enclosure. If the enclosure contains n black surfaces, then the net heat transfer by radiation to surface i is given by:

$$Q_i = Q_{i1} + Q_{i2} + Q_{i3} + \dots + Q_{in}$$

or: $Q_i = \sum_{j=1}^{j=n} \sigma A_j F_{ji} (T_j^4 - T_i^4)$ (9.134)

or, applying the reciprocity relationship:

$$Q_i = \sum_{j=1}^{j=n} \sigma A_i F_{ij} (T_j^4 - T_i^4)$$

Example 9.18

A plate, 1 m in diameter at 750 K, is to be heated by placing it beneath a hemispherical dome of the same diameter at 1200 K; the distance between the plate and the bottom of the dome being 0.5 m, as shown in Figure 9.42. If the surroundings are maintained at 290 K, the surfaces may be regarded as black bodies and heat transfer from the underside of the plate is negligible, what is the net rate of heat transfer by radiation to the plate?

Solution

Taking area 1 as that of the plate, area 2 as the underside of the hemisphere, area 3 as an imaginary cylindrical surface linking the plate and the underside of the dome which represents the black surroundings and area 4 as an imaginary disc sealing the hemisphere and parallel to the plate, then, from equation 9.134, the net radiation to the surface of the plate 1 is given by:

$$Q_1 = \sigma A_2 F_{21} (T_2^4 - T_1^4) + \sigma A_3 F_{31} (T_3^4 - T_1^4)$$

or, using the reciprocity rule:

$$Q_1 = \sigma A_1 F_{12} (T_2^4 - T_1^4) + \sigma A_1 F_{13} (T_3^4 - T_1^4)$$

All radiation from the disc 1 to the dome 2 is intercepted by the imaginary disc 4 and hence $F_{12} = F_{14}$, which may be obtained from Figure 9.39ii, with i and j representing areas 1 and 4 respectively. Thus:

$$R_1 = r_1/L = (0.5/0.5) = 1; R_4 = r_4/L = (0.5/0.5) = 1$$

$$S = 1 + (1 + R_4^2)/(R_1^2) = 1 + (1 + 1.0)/(1.0) = 3.0$$

and:

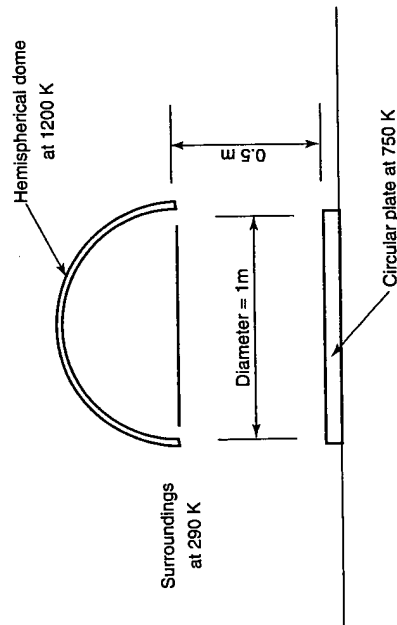


Figure 9.42. Data for Example 9.18

$$\text{Thus: } F_{14} = 0.5 \left[S - \left[(S^2 - 4(r_4/r_1)^2)^{0.5} \right] \right] = 0.5 \left[3 - \left[(3^2 - 4(0.5/0.5)^2)^{0.5} \right] \right] = 0.38$$

$$\text{and: } F_{12} = F_{14} = 0.38$$

The summation rule states that:

$$F_{11} + F_{12} + F_{13} = 1$$

and since, for a plane surface, $F_{11} = 0$, then:

$$F_{13} = (1 - 0.38) = 0.62$$

$$A_1 = (\pi 1.0^2)/4 = 0.785 \text{ m}^2$$

and hence:

$$\begin{aligned} Q_1 &= (5.67 \times 10^{-8} \times 0.785 \times 0.38)(1200^4 - 750^4) + (5.67 \times 10^{-8} \times 0.785 \times 0.62)(290^4 - 750^4) \\ &= (1.691 \times 10^{-8} \times 1.757 \times 10^{12}) - (2.760 \times 10^{-8} \times 3.093 \times 10^{11}) \\ &= 2.12 \times 10^4 \text{ W} = \underline{\underline{21.2 \text{ kW}}} \end{aligned}$$

Radiation between two black surfaces may be increased considerably by introducing a third surface which acts in effect as a re-radiator. For example, if a surface 1 of area A_1 at temperature T_1 is radiating to a second surface 2 of area A_2 at temperature T_2 joined to it as shown in Figure 9.39iii, then adding a further surface R consisting of insulating material so as to form a triangular enclosure will reduce the heat transfer to the surroundings considerably. Even though some heat will be conducted through the insulation, this will usually be small and most of the energy absorbed by the insulated surface will be re-radiated back into the enclosure.

The net rate of heat transfer to surface 2 is given by:

$$Q_2 = \sigma A_1 F_{12} (T_1^4 - T_2^4) + \sigma A_R F_{R2} (T_R^4 - T_2^4) \quad (9.135)$$

where T_R is the mean temperature of the insulation, though, in practice, there will be a temperature distribution across this surface. At steady-state, the net rate of radiation to

surface R is equal to the heat loss from it to the surroundings, Q_{surr} , or:

$$Q_{\text{surr}} = \sigma A_1 F_{1R} (T_1^4 - T_R^4) + \sigma A_2 F_{2R} (T_2^4 - T_R^4) \quad (9.136)$$

If Q_{surr} is negligible, that is, the surface may be treated as adiabatic, then from equation 9.136:

$$\sigma A_1 F_{1R} (T_1^4 - T_R^4) + \sigma A_2 F_{2R} (T_2^4 - T_R^4) = 0$$

Rearranging:

$$T_R^4 = (A_1 F_{1R} T_1^4 + A_2 F_{2R} T_2^4) / (A_1 F_{1R} + A_2 F_{2R})$$

Substituting for T_R from this equation in equation 9.135 and noting, from the reciprocity relationship, that $A_2 F_{2R} = A_R F_{R2}$, then:

$$Q_2 = \sigma (T_1^4 - T_2^4) \{ A_1 F_{12} + [(1 / (A_1 F_{1R}) + (1 / (A_R F_{R2})))]^{-1} \} \quad (9.137)$$

Example 9.19

A flat-bottomed cylindrical vessel, 2 m in diameter, containing boiling water at 373 K, is mounted on a cylindrical section of insulating material, 1 m deep and 2 m ID at the base of which is a radiant heater, also 2 m in diameter, with a surface temperature of 1500 K. If the vessel base and the heater surfaces may be regarded as black bodies and conduction through the insulation is negligible, what is the rate of radiant heat transfer to the vessel? How would this be affected if the insulation were removed so that the system was open to the surroundings at 290 K?

Solution

If area 1 is the radiant heater surface and area 2 the under-surface of the vessel, with R the insulated cylinder, then:

$$A_1 = A_2 = (\pi \times 2^2 / 4) = 3.14 \text{ m}^2$$

$$A_R = (\pi \times 2.0 \times 1.0) = 6.28 \text{ m}^2$$

From Figure 9.40ii, with $i = 1$, $j = 2$, $r_i = 1.0 \text{ m}$, $r_j = 1.0 \text{ m}$ and $L = 1.0 \text{ m}$,

$$(L/r_i) = (1.0/1.0) = 1.0; \quad \text{and } (r_j/L) = (1.0/1.0) = 1.0$$

and:

$$F_{12} = 0.40$$

[The view factor may also be obtained from Figure 9.39ii as follows:
Using the nomenclature of Figure 9.39:

$$R_1 = (r_1/L) = (1.0/1.0) = 1.0$$

$$R_2 = (r_2/L) = (1.0/1.0) = 1.0$$

$$S = 1 + [(1 + R_2^2)/R_1^2] = 1 + [(1 + 1^2)/1^2] = 3.0$$

$$\text{and: } F_{12} = 0.5[S - \{S^2 - 4(r_2/r_1)^2\}^{0.5}] = 0.5[3 - \{3^2 - (4 \times 1^2)\}^{0.5}] = 0.382]$$

The summation rule states that:

$$F_{11} + F_{12} + F_{1R} = 1$$

and since, for a plane surface, $F_{11} = 0$, then: $F_{1R} = (1 - 0.382) = 0.618$

Since $A_1 = A_2$:

$$F_{21} = F_{12} \text{ and } F_{2R} = F_{1R} = 0.618$$

Also $A_1 F_{12} = A_2 F_{21}$ and hence, from equation 9.137:

$$\begin{aligned} Q_2 &= [A_1 F_{12} + ((1/A_1 F_{1R}) + (1/A_2 F_{2R}))^{-1}] \sigma (T_1^4 - T_2^4) \\ &= [(3.14 \times 0.382) H(1/(3.14 \times 0.618) H(1/(3.14 \times 0.618)))^{-1}] (5.67 \times 10^{-8}) (1500^4 - 373^4) \\ &= 6.205 \times 10^5 \text{ W or } \underline{\underline{620 \text{ kW}}} \end{aligned}$$

If the surroundings without insulation are surface 3 at $T_3 = 290 \text{ K}$, then $F_{23} = F_{2R} = 0.618$ and, from equation 9.135:

$$\begin{aligned} Q_2 &= \sigma A_1 F_{12} (T_1^4 - T_2^4) + \sigma A_2 F_{23} (T_3^4 - T_2^4) \\ &= (5.67 \times 10^{-8} \times 3.14 \times 0.382) (1500^4 - 373^4) + (5.67 \times 10^{-8} \times 3.14 \times 0.618) (290^4 - 373^4) \\ &= 3.42 \times 10^5 \text{ W or } \underline{\underline{342 \text{ kW}}}; \text{ a reduction of 45 per cent.} \end{aligned}$$

9.5.5 Radiation transfer between grey surfaces

Since the absorptivity of a grey surface is less than unity, not all the incident radiation is absorbed and some is reflected diffusely causing multiple reflections to occur. This makes radiation between grey surfaces somewhat complex compared with black surfaces since, with grey surfaces, reflectivity as well as the geometrical configuration must be taken into account. With grey bodies, it is convenient to consider the total radiation leaving a surface Q_o , that is the emitted plus the reflected components. The equivalent flux, $Q_o/A = Q_o$ is termed *radiosity* and the total radiosity Q_{oi} , which in the SI system has the units W/m^2 , is the rate at which radiation leaves per unit area of surface i over the whole span of wavelengths. If the incident radiation arriving at a grey surface i in an enclosure is Q_{ii} , corresponding to a flux $q_{ii} = Q_{ii}/A_i$, then the reflected flux, that is, energy per unit area, is $r_i q_{ii}$. The emitted flux is $e_i E_{bi} = e_i \sigma T_i^4$ and the radiosity is then given by:

$$q_{oi} = e_i E_{bi} + r_i q_{ii} \quad (9.138)$$

The net radiation from the surface is given by:

$$\begin{aligned} Q_i &= (\text{rate at which energy leaves the surface}) \\ &\quad - (\text{rate at which energy arrives at the surface}) \end{aligned}$$

or:

$$Q_i = q_{oi} - Q_{ii} = A_i (q_{oi} - q_{ii}) \quad (9.139)$$

Substituting from equation 9.138 in equation 9.139 and noting that $(e_i + r_i) = 1$, then:

$$\begin{aligned} Q_i &= A_i e_i E_{bi} / r_i + (A_i / r_i) [q_{oi} (1 - e_i) - q_{oi}] \\ &= (A_i e_i / r_i) (E_{bi} - q_{oi}) \end{aligned} \quad (9.140)$$

If the temperature of a grey surface is known, then the net heat transfer to or from the surface may be determined from the value of the radiosity q_o . With regard to signs, the usual convention is that a positive value of Q_i indicates heat transfer from grey surfaces.

Example 9.20

Radiation arrives at a grey surface of emissivity 0.75 at a constant temperature of 400 K, at the rate of 3 kW/m². What is the radiosity and the net rate of radiation transfer to the surface? What coefficient of heat transfer is required to maintain the surface temperature at 300 K if the rear of the surface is perfectly insulated and the front surface is cooled by convective heat transfer to air at 295 K?

Solution

Since $e + r = 1$: $r = 0.25$

From equation 9.118: $E_b = (5.67 \times 10^{-8} \times 400^4) = 1452 \text{ W/m}^2$

From equation 9.138: $q_o = e E_b + r q_i$
 $= (0.75 \times 1452) + (0.25 \times 3000) = 1839 \text{ W/m}^2$

From equation 9.140: $Q/A = q = (1.0 \times 0.75/0.25)(1452 - 1839) = -1161 \text{ W/m}^2$

where the negative value indicates heat transfer to the surface.

For convective heat transfer from the surface:

$$\begin{aligned} q_c &= h(T_s - T_{\text{ambient}}) \\ h_c &= q_c / (T_s - T_{\text{ambient}}) = 1161 / (400 - 295) = 11.1 \text{ W/m}^2 \text{ K} \end{aligned}$$

and:

For the simplest case of a *two-surface enclosure* in which surfaces 1 and 2 exchange radiation with each other only, then, assuming $T_1 > T_2$, Q_{12} is the net rate of transfer from 1, Q_1 or the rate of transfer to 2, Q_2 .

Thus:

$$Q_{12} = Q_1 = -Q_2 \quad (9.141)$$

Substituting from equation 9.139:

$$Q_1 = A_1 (q_{o1} - q_{i1}) \quad (9.142)$$

$$q_{i1} A_1 = q_{o1} A_1 F_{11} + q_{o2} A_2 F_{21} \quad (9.143)$$

that is:

$$\begin{aligned} &(\text{rate of energy incident upon surface 1}) \\ &= (\text{rate of energy arriving at surface 1 from itself}) \\ &\quad + (\text{rate of energy arriving at surface 1 from surface 2}) \end{aligned}$$

From equations 9.142 and 9.143 and using $A_1 F_{12} = A_2 F_{21}$, then:

$$Q_1 = q_{o1} (A_1 - A_1 F_{11}) - q_{o2} A_1 F_{12} \quad (9.144)$$

Since, by the summation rule, $(A_1 - A_1 F_{11}) = A_1 F_{12}$, then:

$$Q_1 = (A_1 F_{12}) (q_{o1} - q_{o2}) \quad (9.145)$$

From equation 9.140:

$$Q_1 = (A_1 e_1 / r_1) (E_{b1} - q_{o1}) \text{ and } -Q_2 = (A_2 e_2 / r_2) (E_{b2} - q_{o2}) \quad (9.146)$$

Substituting from equation 9.146 into equation 9.145 and using the relationships in equation 9.141 gives:

$$Q_{12}[(1/A_1 F_{12}) + (r_1/A_1 e_1) + (r_2/A_2 e_2)] = (E_{b1} - E_{b2})$$

and hence $Q_{12} = (E_{b1} - E_{b2})/[(1/A_1 F_{12}) + (r_1/A_1 e_1) + (r_2/A_2 e_2)]$ (9.147)

Since $r = 1 - e$, then, writing $E_{b1} = \sigma T_1^4$ and $E_{b2} = \sigma T_2^4$:

$$Q_{12} = [\sigma(T_1^4 - T_2^4)]/[(1/A_1 F_{12}) + (1 - e_1)/(A_1 e_1) + (1 - e_2)/(A_2 e_2)] \quad (9.148)$$

Equation 9.148 is the same as equation 9.127 for black body exchange with two additional terms $(1 - e_1)/(A_1 e_1)$ and $(1 - e_2)/(A_2 e_2)$ introduced in the denominator for surfaces 1 and 2.

Radiation between parallel plates

For two large parallel plates of equal areas, and separated by a small distance, it may be assumed that all of the radiation leaving plate 1 falls on plate 2, and similarly all of the radiation leaving plate 2 falls on plate 1.

$$\text{Thus: } F_{12} = F_{21} = 1$$

$$\text{and: } A_1 = A_2$$

Substituting in equation 9.148:

$$Q_{12} = \frac{A_1 \sigma (T_1^4 - T_2^4)}{1 + (1 - e_1)/e_1 + (1 - e_2)/e_2} \quad (9.149)$$

$$\text{and: } \frac{Q_{12}}{A_1} = q_{12} = \frac{\sigma (T_1^4 - T_2^4)}{\frac{1}{e_1} + \frac{1}{e_2} - 1}$$

Other cases of interest include radiation between:

- (i) two concentric spheres
- (ii) two concentric cylinders where the length: diameter ratio is large.

In both of these cases, the inner surface 1 is convex, and all the radiation emitted by it falls on the outer surface 2.

$$\text{Thus: } F_{12} = 1$$

and from the reciprocal rule:

$$F_{21} = F_{12} \frac{A_1}{A_2} = \frac{A_1}{A_2} \quad (\text{equation 9.126})$$

Substituting in equation 9.148:

$$Q_{12} = \frac{A_1 \sigma (T_1^4 - T_2^4)}{1 + [(1 - e_1)/e_1] + [(1 - e_2)/e_2] \frac{A_1}{A_2}}$$

$$= \frac{A_1 \sigma (T_1^4 - T_2^4)}{\frac{1}{e_1} + \frac{1}{e_2} (1 - e_2) \frac{A_1}{A_2}}$$

$$\text{and: } \frac{Q_{12}}{A_1} = q_{12} = \frac{\sigma (T_1^4 - T_2^4)}{\frac{1}{e_1} + \left[\frac{(1 - e_2) A_1}{e_2 A_2} \right]} \quad (9.150)$$

For radiation from surface 1 to extensive surroundings ($A_1/A_2 \rightarrow 0$), then:

$$q_{12} = e_1 \sigma (T_1^4 - T_2^4) \quad (9.151)$$

Radiation shield

The rate of heat transfer by radiation between two surfaces may be reduced by inserting a shield, so that radiation from surface 1 does not fall directly on surface 2, but instead is intercepted by the shield at a temperature T_{sh} (where $T_1 > T_{sh} > T_2$) which then re-radiates to surface 2. An important application of this principle is in a furnace where it is necessary to protect the walls from high-temperature radiation.

The principle of the radiation shield may be illustrated by considering the simple geometric configuration in which surfaces 1 and 2 and the shield may be represented by large planes separated by a small distance as shown in Figure 9.43.

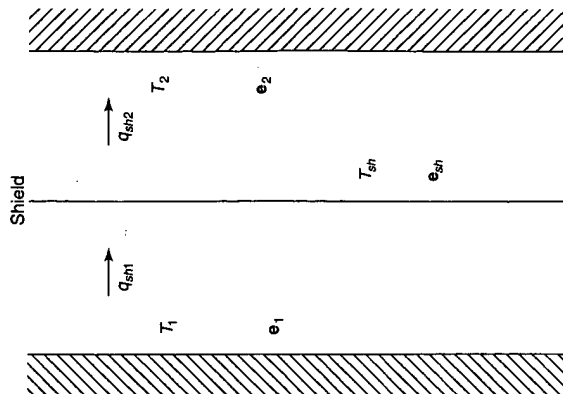


Figure 9.43. Radiation shield

Neglecting any temperature drop across the shield (which has a surface emissivity ϵ_{sh}), then in the steady state, the transfer rate of radiant heat to the shield from the surface 1 must equal the rate at which heat is radiated from the shield to surface 2. Application of equation 9.149 then gives:

$$q_{sh} = q_{sh1} (= q_{sh2}) = \frac{\sigma(T_1^4 - T_{sh}^4)}{\left(\frac{1}{\epsilon_1}\right) + \left(\frac{1}{\epsilon_{sh}}\right) - 1} = \frac{\sigma(T_{sh}^4 - T_2^4)}{\left(\frac{1}{\epsilon_{sh}}\right) + \left(\frac{1}{\epsilon_2}\right) - 1} \quad (9.152)$$

Eliminating T_{sh}^4 in terms of T_1^4 and T_2^4 from equation 9.152:

$$T_1^4 - T_{sh}^4 = \frac{q_{sh}}{\sigma} \left(\frac{1}{\epsilon_1} + \frac{1}{\epsilon_{sh}} - 1 \right)$$

$$T_{sh}^4 - T_2^4 = \frac{q_{sh}}{\sigma} \left(\frac{1}{\epsilon_{sh}} + \frac{1}{\epsilon_2} - 1 \right)$$

Adding:
$$T_1^4 - T_2^4 = \frac{q_{sh}}{\sigma} \left(\frac{1}{\epsilon_1} + \frac{2}{\epsilon_{sh}} + \frac{1}{\epsilon_2} - 2 \right)$$

and:
$$q_{sh} = \frac{\sigma(T_1^4 - T_2^4)}{\left(\frac{1}{\epsilon_1}\right) + \left(\frac{2}{\epsilon_{sh}}\right) + \left(\frac{1}{\epsilon_2}\right) - 2} \quad (9.153)$$

Then from equations 9.149 and 9.153:

$$\frac{q_{sh}}{q_{12}} = \frac{\left(\frac{1}{\epsilon_1}\right) + \left(\frac{1}{\epsilon_2}\right) - 1}{\frac{1}{\epsilon_1} + \frac{2}{\epsilon_{sh}} + \frac{1}{\epsilon_2} - 2} \quad (9.154)$$

For the special case where all the emissivities are equal ($\epsilon_1 = \epsilon_{sh} = \epsilon_2$):

$$\frac{q_{sh}}{q_{12}} = 1/2$$

Similarly, it can be shown that if n shields are arranged in series, then:

$$\frac{q_{sh}}{q_{12}} = \frac{1}{n+1}$$

In practice, as a result of introducing the radiation shield, the temperature T_2 will fall because a heat balance must hold for surface 2, and the heat transfer rate from it to the surroundings will have been reduced to q_{sh} . The extent to which T_2 is reduced depends on the heat transfer coefficient between surface 2 and the surroundings.

Multi-sided enclosures

For the more complex case of a *multi-sided enclosure* formed from n surfaces, the radiosities may be obtained from an energy balance for each surface in turn in the enclosure. Thus the energy falling on a typical surface i in an enclosure formed from

n surfaces is:

$$A_i q_{ii} = q_{01} A_1 F_{1i} + q_{02} A_2 F_{2i} + q_{03} A_3 F_{3i} + \dots + q_{0n} A_n F_{ni} \quad (9.155)$$

where $A_i q_{ii} = Q_i$ is the energy incident upon surface i , $q_{01} A_1 F_{1i}$ is the energy leaving surface 1 which is intercepted by surface i and $q_{0n} A_n F_{ni}$ is the energy leaving surface n which is intercepted by surface i . $q_{01} A_1 = q_{01}$ is the energy leaving surface 1 and F_{1i} is the fraction of this which is intercepted by surface i .

From equation 9.138:

$$q_{ii} = (q_{0i} - \epsilon_i E_{bi}) / r_i$$

Substituting for q_{ii} into equation 9.155 gives:

$$A_i (q_{0i} - \epsilon_i E_{bi}) / r_i = A_1 F_{1i} q_{01} + A_2 F_{2i} q_{02} + A_3 F_{3i} q_{03} + \dots + A_j F_{ji} q_{0j} + \dots + A_n F_{ni} q_{0n} \quad (9.156)$$

Noting, for example, that for surface 2, $i = 2$, then:

$$A_2 (q_{02} - \epsilon_2 E_{b2}) / r_2 = A_1 F_{12} q_{01} + A_2 F_{22} q_{02} + A_3 F_{32} q_{03} + \dots + A_j F_{j2} q_{0j} + \dots + A_n F_{n2} q_{0n} \quad (9.157)$$

Rearranging:

$$A_1 F_{12} q_{01} + [A_2 F_{22} - (A_2 / r_2)] q_{02} + A_3 F_{32} q_{03} + \dots + A_j F_{j2} q_{0j} + \dots + A_n F_{n2} q_{0n} = (A_2 \epsilon_2 / r_2) E_{b2} \quad (9.158)$$

Equations similar to equation 9.158 may be obtained for each of the surfaces in an enclosure, $i = 1, i = 2, i = 3, i = n$ and the resulting set of simultaneous equations may then be solved for the unknown radiosities, $q_{01}, q_{02}, \dots, q_{0n}$. The radiation heat transfer is then obtained from equation 9.140. This approach requires data on the areas and view factors for all pairs of surfaces in the enclosure and the emissivity, reflectivity and the black body emissive power for each surface. Should any surface be well insulated, then, in this case, $Q_i = 0$ and:

$$A_i (\epsilon_i / r_i) (E_{bi} - q_{0i}) = 0$$

Since, in general, $A_i (\epsilon_i / r_i) \neq 0$, then $E_{bi} = q_{0i}$.

If a surface has a specified net thermal input flux, say q_{ii} , then, from equation 9.140:

$$E_{bi} = (r_i / (A_i \epsilon_i)) q_{ii} + q_{0i}$$

It may be noted that this approach assumes that the surfaces are grey and diffuse, that emissivity and reflectivity do not vary across a surface and that the temperature, irradiation and radiosity are constant over a surface. Since the technique uses average values over a surface, the subdivision of the enclosure into surfaces must be undertaken with care, noting that a number of surfaces may be regarded as a single surface, that it may be necessary to split one surface up into a number of smaller surfaces and also possibly to introduce an imaginary surface into the system, to represent the surroundings, for example. In a real situation, there may be both grey and black surfaces present and, for the latter, r_i tends to zero and (A_i / r_i) and $(A_i \epsilon_i / r_i)$ become very large.

Example 9.21

A horizontal circular plate, 1.0 m in diameter, is to be maintained at 500 K by placing it 0.20 m directly beneath a horizontal electrically heated plate, also 1.0 m in diameter, maintained at 1000 K. The assembly is exposed to black surroundings at 300 K, and convection heat transfer is negligible. Estimate the electrical input to the heater and the net rate of heat transfer to the plate if the emissivity of the heater is 0.75 and the emissivity of the plate 0.5.

Solution

Taking surface 1 as the heater, surface 2 as the heated plate and surface 3 as an imaginary enclosure consisting of a vertical cylindrical surface representing the surroundings, then, for each surface:

Surface	A (m ²)	e	r	(A/r) (m ²)	(Ae/r) (m ²)
1	1.07	0.75	0.25	4.28	3.21
2	1.07	0.50	0.50	2.14	1.07
3	0.628	1.0	0		

For surface 1:

For a plane surface: $F_{11} = 0$ and $A_1 F_{11} = 0$

Using the nomenclature of Figure 9.39:

For co-axial parallel discs with $r_1 = r_2 = 0.5$ m and $L = 0.2$ m:

$$R_1 = r_1/L = (0.5/0.20) = 2.5$$

$$R_2 = r_2/L = (0.5/0.20) = 2.5$$

$$\text{and: } S = 1 + (1 + R_2^2)/R_1^2 = 1 + (1 + 2.5^2)/2.5^2 = 2.16$$

$$F_{12} = 0.5[S - \{S^2 - 4(r_2/r_1)^2\}^{0.5}]$$

$$= 0.5 \times \{2.16 - [(2.16^2 - 4(0.5/0.5)^2)^{0.5}]\} = 0.672$$

$$A_1 F_{12} = (1.07 \times 0.672) = 0.719 \text{ m}^2$$

and, from the summation rule:

$$A_1 F_{13} = A_1 - (A_1 F_{11} + A_1 F_{12}) = 1.07 - (0 + 0.719) = 0.350 \text{ m}^2$$

For surface 2:

For a plane surface:

$$A_2 F_{22} = 0$$

and by the reciprocity rule:

$$A_2 F_{21} = A_1 F_{12} = 0.719 \text{ m}^2$$

By symmetry:

$$A_2 F_{23} = A_1 F_{13} = 0.350 \text{ m}^2$$

For surface 3:

By the reciprocity rule:

$$A_3 F_{31} = A_1 F_{13} = 0.350 \text{ m}^2$$

$$A_3 F_{32} = A_2 F_{23} = 0.350 \text{ m}^2$$

and:

From the summation rule:

$$A_3 F_{33} = A_3 - (A_3 F_{31} + A_3 F_{32})$$

$$= 0.785 - (0.350 + 0.350) = 0.085 \text{ m}^2$$

From equation 9.12:

$$E_{b1} = \sigma T_1^4 = (5.67 \times 10^{-8} \times 1000^4)$$

$$= 5.67 \times 10^4 \text{ W/m}^2 \text{ or } 56.7 \text{ kW/m}^2$$

HEAT TRANSFER

$$E_{b2} = \sigma T_2^4 = (5.67 \times 10^{-8} \times 500^4)$$

$$= 3.54 \times 10^3 \text{ W/m}^2 \text{ or } 3.54 \text{ kW/m}^2$$

$$E_{b3} = \sigma T_3^4 = (5.67 \times 10^{-8} \times 300^4)$$

$$= 0.459 \times 10^3 \text{ W/m}^2 \text{ or } 0.459 \text{ kW/m}^2$$

$$q_{03} = E_{b3} = 0.459 \text{ kW/m}^2$$

Since surface 3 is a black body,

From equations 9.157 and 9.158:

$$\begin{aligned} (A_1 F_{11} - A_1/r_1)q_{01} + A_2 F_{21}q_{02} + A_3 F_{31}q_{03} &= -E_{b1}A_1e_1/r_1 \\ &\times (0 - 4.28)q_{01} + 0.719q_{02} + (0.350 \times 0.459) \\ &= -(56.7 \times 1.07 \times 0.75)/0.25 \end{aligned}$$

$$\text{or: } 0.719q_{02} - 4.28q_{01} = -182 \quad (1)$$

$$\text{and: } (A_1 F_{12}q_{01}) + (A_2 F_{22} - A_2/r_2)q_{02} = -E_{b2}A_2e_2/r_2$$

$$0.719q_{01} + (0 - 1.07/0.5)q_{02} = -(3.54 \times 1.07 \times 0.5)/0.5$$

$$\text{or: } 0.719q_{01} - 2.14q_{02} = -3.79 \quad (2)$$

Solving equations 1 and 2 simultaneously gives:

$$q_{01} = 45.42 \text{ kW/m}^2 \text{ and } q_{02} = 17.16 \text{ kW/m}^2$$

power input to the heater = rate of heat transfer from the heater

From equation 9.140:

$$Q_1 = (A_1 e_1/r_1)(E_{b1} - q_{01}) = (1.07 \times 0.75/0.25)(56.7 - 45.42) = \underline{\underline{36.2 \text{ kW}}}$$

Again, from equation 9.140, the rate of heat transfer to the plate is:

$$Q_2 = (A_2 e_2/r_2)(E_{b2} - q_{02}) = (1.07 \times 0.5/0.25)(3.54 - 17.16) = \underline{\underline{-14.57 \text{ kW}}}$$

where the negative sign indicates heat transfer to the plate.

9.5.6. Radiation from gases

In the previous discussion surfaces have been considered which are *isothermal, opaque and grey* which *emit and reflect diffusely* and are characterised by *uniform surface radiosity* and the medium separating the surfaces has been assumed to be *non-participating*, in that it neither absorbs nor scatters the surface radiation nor does it emit radiation itself. Whilst, in most cases, such assumptions are valid and permit reasonably accurate results to be calculated, there are occasions where such assumptions do not hold and more refined techniques are required such as those described in the specialist literature^(45,48-53). For *non-polar gases* such as N_2 and O_2 , the foregoing assumptions are largely valid, since the gases do not emit radiation and they are essentially transparent to incident radiation. This is not the case with *polar molecules* such as CO_2 and H_2O vapour, NH_3 and hydrocarbon gases, however, since these not only emit and absorb over a wide temperature range, but also radiate in specific wavelength intervals called *bands*. Furthermore, gaseous radiation is a volumetric rather than a surface phenomenon.

Whilst the calculation of the radiant heat flux from a gas to an adjoining surface embraces inherent spectral and directional effects, a simplified approach has been developed by HOTTEL and MANGLESDORF⁽⁵⁴⁾, which involves the determination of radiation emission from a hemispherical mass of gas of radius L , at temperature T_g to a surface element, dA_1 , near the centre of the base of the hemisphere. Emission from the gas per unit area of the surface is then:

$$E_g = e_g \sigma T_g^4 \quad (9.159)$$

where the gas emissivity e_g is a function of T_g , the total pressure of the gas P , the partial pressure of the radiating gas P_g and the radius of the hemisphere L .

Data on the emissivity of water vapour at a total pressure of 101.3 kN/m^2 are plotted in Figure 9.44 for different values of the product of the vapour partial pressure P_w and the hemisphere radius L . For other values of the total pressure, the correction factor C_p also given in the figure must be used. Similar data for carbon dioxide are given in Figure 9.45. Although these data refer to water vapour or carbon dioxide alone in a mixture of non-radiating gases, they may be extended to situations where both are present in such a mixture by expressing the total emissivity as:

$$e_g = e_w + e_c - \Delta e \quad (9.160)$$

where Δe is a correction factor, shown in Figure 9.46, which allows for the reduction in emission associated with mutual absorption of radiation between the two species.

Although these data provide the emissivity of a hemispherical gas mass of radius L radiating to an element at the centre of the base, they may be extended to other geometries by using the concept of *mean beam length* L_e which correlates the dependence of gas emissivity with both the size and shape of the gas geometry in terms of a single parameter. Essentially the mean beam length is the radius of the hemisphere of gas whose emissivity is equivalent to that in the particular geometry considered, and typical values of L_e which are then used to replace L in Figures 9.38–40 are shown in Table 9.7. Using these data and Figures 9.38–9.40, the rate of transfer of radiant heat to a surface of area A_s due to emission from an adjoining gas is given by:

$$Q = e_g A_s \sigma T_g^4 \quad (9.161)$$

A black surface will not only absorb all of this radiation but will also emit radiation, and the net rate at which radiation is exchanged between the gas and the surface at temperature T_s is given by:

$$Q_{\text{net}} = A_s \sigma (e_g T_g^4 - a_g T_s^4) \quad (9.162)$$

In this equation, the absorptivity a_g may be obtained from the emissivity using expressions of the form⁽⁵⁴⁾:

water:

$$a_w = C_w e_w (T_g/T_s)^{0.45} \quad (9.163)$$

carbon dioxide:

$$a_c = C_c e_c (T_g/T_s)^{0.65} \quad (9.164)$$

where e_w and C_w and e_c and C_c are obtained from Figures 9.38 and 9.39 respectively, noting that T_g is replaced by T_s and $(P_w L_e)$ or $(P_c L_e)$ by $[P_w L_e (T_s/T_g)]$ or $[P_c L_e (T_s/T_g)]$.

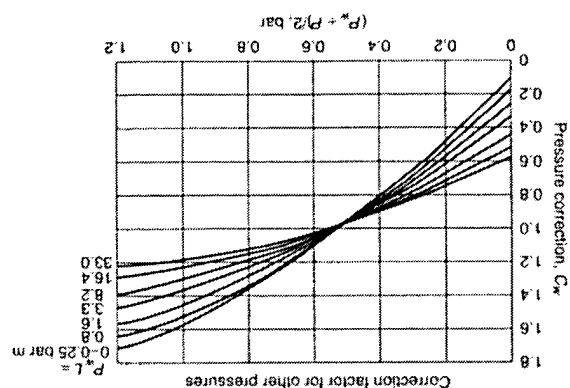
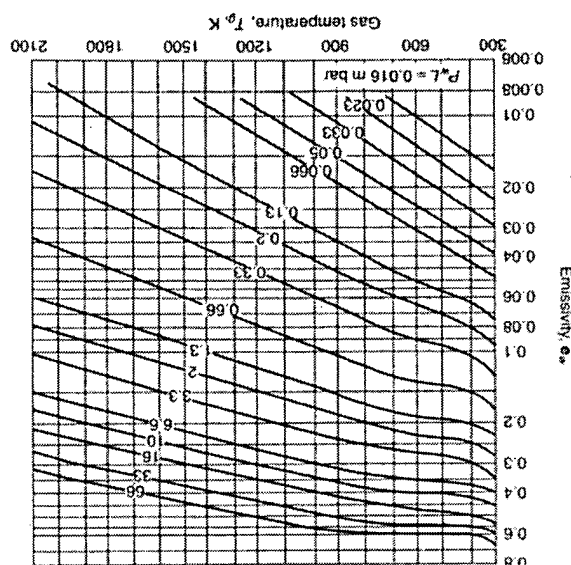


Figure 9.44. Emissivity of water vapour in a mixture of non-radiating gases at 101.3 kN/m^2 (54)



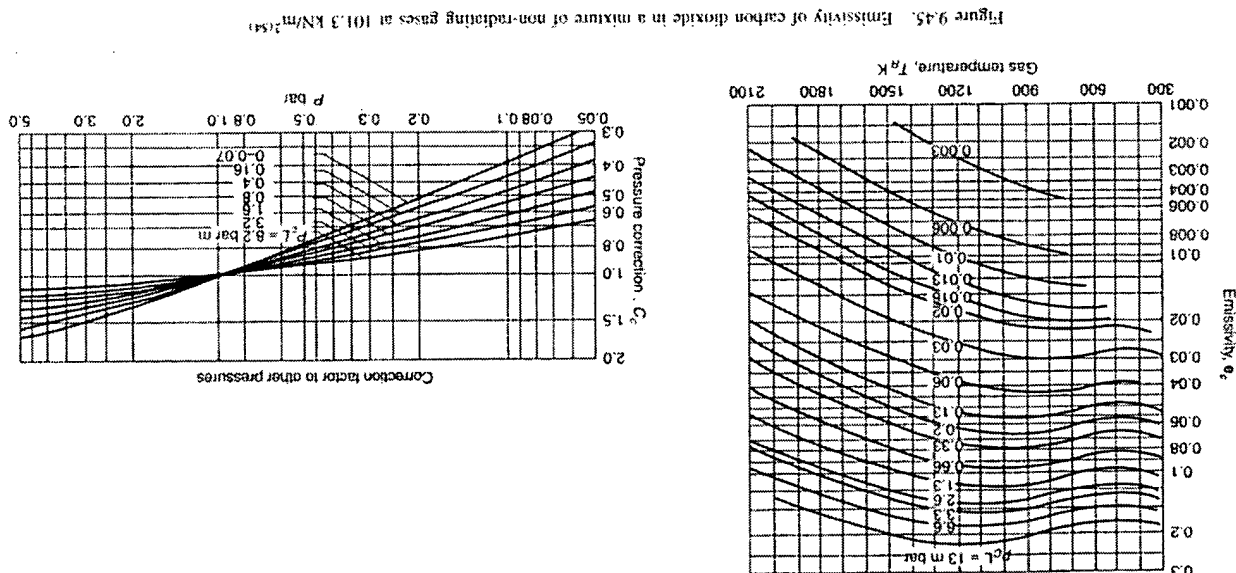


Figure 9.45. Emissivity of carbon dioxide in a mixture of non-radiating gases at 101.3 kN/m² (54)

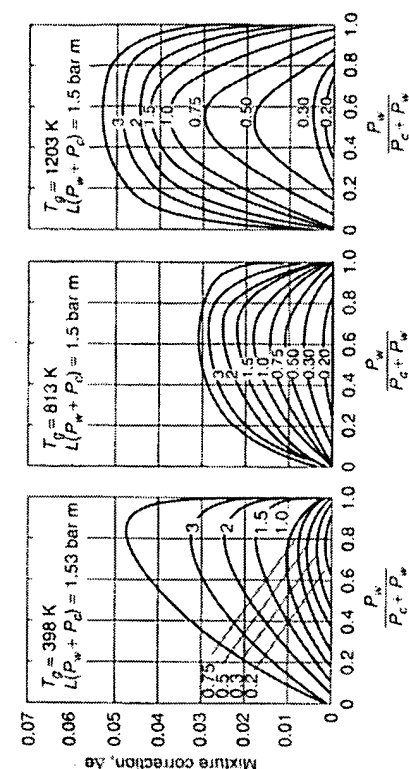


Figure 9.46. Correction factor for water vapour-carbon dioxide mixtures (54)

respectively. It may be noted that, in the presence of both water vapour and carbon dioxide, the total absorptivity is given by:

$$a_g = a_w + a_c - \Delta a \quad (9.165)$$

where $\Delta a = \Delta \epsilon$ is obtained from Figure 9.46. If the surrounding surface is grey, some of the radiation may be reflected and equation 9.162 may be modified by a factor, $e_g/[1 - (1 - a_g)(1 - e_g)]$ to take this into account. This leads to the following equation for the heat transferred per unit time from the gas to the surface:

$$Q = \sigma \epsilon_s A_s (e_g T_g^4 - a_g T_s^4) / [1 - (1 - a_g)(1 - e_g)] \quad (9.166)$$

Table 9.7. Mean beam lengths for various geometries (54)

Geometry	Characteristic length	Mean beam length, L_p
Sphere — radiation to surface		
Infinite circular cylinder — radiation to curved surface	Diameter, D	$0.65D$
Semi-infinite cylinder — radiation to base	Diameter, D	$0.95D$
Cylinder of equal height and diameter — radiation to entire surface	Diameter, D	$0.65D$
Infinite parallel planes — radiation to planes	Diameter, D	$0.60D$
Cube — radiation to any surface	Spacing between planes, L	$1.80L$
Shape of volume, V — radiation to surface of area, A	Side, L	$0.66L$
	Ratio: volume/area, (V/A)	$3.6(V/A)$

Example 9.22

The walls of a combustion chamber, 0.5 m in diameter and 2 m long, have an emissivity of 0.5 and are maintained at 750 K. If the combustion products containing 10 per cent carbon dioxide and 10 per cent water vapour are at 150 kN/m² and 1250 K, what is the net rate of radiation to the walls?

Solution

The partial pressures of carbon dioxide (P_c) and of water (P_w) are:

$$P_c = P_w = (10/100)150 = 15.0 \text{ kN/m}^2 \text{ or } (15.0/100) = 0.15 \text{ bar}$$

From Table 9.7:

$$L_w = 3.6 \text{ V/A} = 3.6(\pi/4 \times 0.5^2 \times 2)/(2\pi/4 \times 0.5^2) + (0.5\pi \times 2.0) = 0.4 \text{ m}$$

For water vapour:

$$P_w L_w = (0.15 \times 0.4) = 0.06 \text{ bar m}$$

and from Figure 9.44, $e_w = 0.075$

$$P = (150/100) = 1.5 \text{ bar, } P_w = 0.15 \text{ bar and: } 0.5(P_w + P) = 0.825 \text{ bar}$$

Since $P_w L_w = 0.06 \text{ bar m}$, then from Figure 9.44:

$$C_w = 1.4 \text{ and } e_w = (1.4 \times 0.075) = 0.105$$

For carbon dioxide:

$$P_c L_w = (0.15 \times 0.4) = 0.06 \text{ bar m}$$

and from Figure 9.45, $e_c = 0.037$

Since $P = 1.5 \text{ bar}$, $P_c = 0.15 \text{ bar}$ and $P_c L_w = 0.06 \text{ bar m}$, then, from Figure 9.38:

$$C_c = 1.2 \text{ and } e_c = (1.2 \times 0.037) = 0.044$$

$$(P_w + P_c) L_w = (0.15 + 0.15)0.4 = 0.12 \text{ bar m}$$

$$P_c/(P_c + P_w) = 0.15/(0.15 + 0.15) = 0.5$$

Thus, from Figure 9.45 for $T_g > 1203 \text{ K}$, $\Delta e = 0.001$

and, from equation 9.160:

$$e_g = e_w - \Delta e = (0.105 + 0.044 - 0.001) = 0.148$$

For water vapour:

$$P_w L_w (T_g/T_g) = 0.06(750/1250) = 0.036 \text{ bar m}$$

and, from Figure 9.44 at 750 K, $e_w = 0.12$

Since $0.5(P_w + P) = 0.825 \text{ bar}$ and $P_w L_w (T_g/T_g) = P_c L_w (T_g/T_g) = 0.036 \text{ bar m}$,

then, from Figure 9.44: $C_w = 1.40$ and $e_w = (0.12 \times 1.40) = 0.168$

and the absorptivity, from equation 9.163 is:

$$a_w = e_w (T_g/T_g)^{0.45} = 0.168(1250/750)^{0.45} = 0.212$$

For carbon dioxide:

From Figure 9.45 at 750 K, $e_c = 0.08$

From Figure 9.45 at $P = 1.5 \text{ bar}$ and $P_c L_w (T_g/T_g) = 0.036 \text{ bar m}$:

$$C_c = 1.02 \text{ and } e_c = (0.08 \times 1.02) = 0.082$$

and the absorptivity, from equation 9.164 is:

$$a_c = e_c (T_g/T_g)^{0.65} = 0.082(1250/750)^{0.65} = 0.114$$

$$P_w/(P_c + P_w) = 0.5 \text{ and } (P_c + P_w) L_w (T_g/T_g) = (0.036 + 0.036) = 0.072 \text{ bar m}$$

Thus, from Figure 9.46, for $T_g = 813 \text{ K}$, $\Delta e = \Delta a < 0.01$ and this may be neglected.

$$a_g = a_w + a_c - \Delta a = (0.212 + 0.114 - 0) = 0.326$$

If the surrounding surface is black, then:

$$\begin{aligned} Q &= nA_s(e_g T_g^4 - a_g T_w^4) \\ &= (5.67 \times 10^{-8})[(2\pi/4)(0.5^2) + (0.5\pi \times 2.0)](0.148 \times 1250^4) - (0.326 \times 750^4) \\ &= 5.03 \times 10^4 \text{ W} = \underline{\underline{50.3 \text{ kW}}} \end{aligned} \quad (\text{equation 9.162})$$

For grey walls, the correction factor allowing for multiple reflection of incident radiation is:

$$C_g = e_g/[1 - (1 - e_g)(1 - e_g)] = 0.5/[1 - (1 - 0.326)(1 - 0.5)] = 0.754$$

and hence: net radiation to the walls, $Q_w = (50.3 \times 0.754) = \underline{\underline{37.9 \text{ kW}}}$

Radiation from gases containing suspended particles

The estimation of the radiation from pulverised-fuel flames, from dust particles in flames and from flames made luminous as a result of the thermal decomposition of hydrocarbons to soot, involves an evaluation of radiation from clouds of particles. In pulverised-fuel flames, the mean particle size is typically $25 \mu\text{m}$ and the composition varies from a very high carbon content to virtually pure ash. In contrast, the suspended matter in luminous flames, resulting from soot formation due to incomplete mixing of hydrocarbons with air before being heated, consists of carbon together with very heavy hydrocarbons with an initial particle size of some $0.3 \mu\text{m}$. In general, pulverised-fuel particles are sufficiently large to be substantially opaque to incident radiation, whilst the particles in a luminous flame are so small that they act as semi-transparent bodies with respect to thermal or long wavelength radiation.

According to SCHACK⁽⁵⁵⁾, a single particle of soot transmits approximately 95 per cent of the incident radiation and a cloud must contain a very large number of particles before an appreciable emission can occur. If the concentration of particles is K' , then the product of K' and the thickness of the layer L is equivalent to the product $P_g L_g$ in the radiation of gases. For a known or measured emissivity of the flame e_f , the heat transfer rate per unit time to a wall is given by:

$$Q = e_f e_s \sigma (T_f^4 - T_w^4) \quad (9.167)$$

where e_s is the effective emissivity of the wall, and T_f and T_w are the temperatures of the flame and wall respectively. e_f varies, not only from point to point in a flame, but also depends on the type of fuel, the shape of the burner and combustion chamber, and on the air supply and the degree of preheating of the air and fuel.

9.6. HEAT TRANSFER IN THE CONDENSATION OF VAPOURS**9.6.1. Film coefficients for vertical and inclined surfaces**

When a saturated vapour is brought into contact with a cool surface, heat is transferred from the vapour to the surface and a film of condensate is produced.

In considering the heat that is transferred, the method first put forward by NUSSELT⁽⁵⁶⁾ and later modified by subsequent workers is followed. If the vapour condenses on a vertical surface, the condensate film flows downwards under the influence of gravity, although it is retarded by the viscosity of the liquid. The flow will normally be streamline and the heat flows through the film by conduction. In Nusselt's work it is assumed that the temperature of the film at the cool surface is equal to that of the surface, and at the other side was at the temperature of the vapour. In practice, there must be some small difference in temperature between the vapour and the film, although this may generally be neglected except where non-condensable gas is present in the vapour.

It is shown in Chapter 3, that the mean velocity of a fluid flowing down a surface inclined at an angle ϕ to the horizontal is given by:

$$u = \frac{\rho g \sin \phi s^2}{3\mu} \quad (\text{equation 3.87})$$

For a vertical surface: $\sin \phi = 1$ and $u = \frac{\rho g s^2}{3\mu}$

The maximum velocity u_s which occurs at the free surface is:

$$u_s = \frac{\rho g \sin \phi s^2}{2\mu} \quad (\text{equation 3.88})$$

and this is 1.5 times the mean velocity of the liquid.

Since the liquid is produced by condensation, the thickness of the film will be zero at the top and will gradually increase towards the bottom. Under stable conditions the difference in the mass rates of flow at distances x and $x + dx$ from the top of the surface will result from condensation over the small element of the surface of length dx and width w , as shown in Figure 9.47.

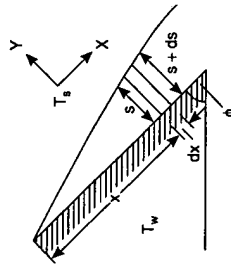


Figure 9.47. Condensation on an inclined surface

If the thickness of the liquid film increases from s to $s + ds$ in that distance, the increase in the mass rate of flow of liquid dG is given by:

$$\begin{aligned} \frac{d}{ds} \left(\frac{\rho^2 g \sin \phi s^3 w}{3\mu} \right) ds \\ = \frac{\rho^2 g \sin \phi}{\mu} w s^2 ds \end{aligned}$$

If the vapour temperature is T_s and the wall temperature is T_w , the heat transferred by thermal conduction to an element of surface of length dx is:

$$\frac{k(T_s - T_w)}{s} w dx$$

where k is the thermal conductivity of the condensate.

Thus the mass rate of condensation on this small area of surface is:

$$\frac{k(T_s - T_w)}{s\lambda} w dx$$

where λ is the latent heat of vaporisation of the liquid.

$$\frac{k(T_s - T_w)}{s\lambda} w dx = \frac{\rho^2 g \sin \phi}{\mu} w s^2 ds$$

Thus:

$$\mu k(T_s - T_w)x = \frac{1}{2} \rho^2 g \sin \phi s^4 \lambda$$

On integration:

since $s = 0$ when $x = 0$.

$$s = \sqrt[4]{\frac{4\mu kx(T_s - T_w)}{g \sin \phi \lambda \rho^2}} \quad (9.168)$$

Thus:

Now the heat transfer coefficient h at $x = x$, $= k/s$, and hence:

$$h = \sqrt[4]{\frac{\rho^2 g \sin \phi \lambda k^3}{4\mu x(T_s - T_w)}} \quad (9.169)$$

Thus:

$$Nu = \frac{hx}{k} = \sqrt[4]{\frac{\rho^2 g \sin \phi \lambda x^3}{4\mu k(T_s - T_w)}} \quad (9.170)$$

and:

These expressions give point values of h and Nu_x at $x = x$. It is seen that the coefficient decreases from a theoretical value of infinity at the top as the condensate film thickens. The mean value of the heat transfer coefficient over the whole surface, between $x = 0$ and $x = x$ is given by:

$$\begin{aligned} h_m &= \frac{1}{x} \int_0^x h dx = \frac{1}{x} \int_0^x Kx^{-1/4} dx \quad (\text{where } K \text{ is independent of } x) \\ &= \frac{1}{x} K \frac{x^{3/4}}{3/4} = \frac{4}{3} Kx^{-1/4} = \frac{4}{3} h \\ &= 0.943 \sqrt[4]{\frac{\rho^2 g \sin \phi \lambda k^3}{\mu x \Delta T_f}} \end{aligned} \quad (9.171)$$

where ΔT_f is the temperature difference across the condensate film. For a vertical surface, $\sin \phi = 1$ and:

$$h_m = 0.943 \sqrt[4]{\frac{\rho^2 g \lambda k^3}{\mu x \Delta T_f}} \quad (9.172)$$

9.6.2. Condensation on vertical and horizontal tubes

The Nusselt equation

If vapour condenses on the outside of a vertical tube of diameter d_o , then the hydraulic mean diameter for the film is:

$$\frac{4 \times \text{flow area}}{\text{wetted perimeter}} = \frac{4S}{b} \quad (\text{say})$$

If G is the mass rate of flow of condensate, the mass rate of flow per unit area G' is G/S and the Reynolds number for the condensate film is then given by:

$$Re = \frac{(4S/b)(G/S)}{\mu} = \frac{4G}{\mu b} = \frac{4M}{\mu} \quad (9.173)$$

where M is the mass rate of flow of condensate per unit length of perimeter, or:

$$M = \frac{G}{\pi d_o}$$

For streamline conditions in the film, $4M/\mu \neq 2100$ and:

$$h_m = \frac{Q}{A \Delta T_f} = \frac{G \lambda}{b \Delta T_f} = \frac{\lambda M}{l \Delta T_f}$$

From equation 9.172:

$$h_m = 0.943 \left(\frac{k^3 \rho^2 g \lambda}{\mu l \Delta T_f} \right)^{1/4} = 0.943 \left(\frac{k^3 \rho^2 g h_m}{\mu M} \right)^{1/4}$$

and hence:

$$h_m \left(\frac{\mu^2}{k^3 \rho^2 g} \right)^{1/3} = 1.47 \left(\frac{4M}{\mu} \right)^{-1/3} \quad (9.174)$$

For horizontal tubes, Nusselt proposes the equation:

$$h_m = 0.72 \left(\frac{k^3 \rho^2 g \lambda}{d_o \mu \Delta T_f} \right)^{1/4} \quad (9.175)$$

This may be rearranged to give:

$$h_m \left(\frac{\mu^2}{k^3 \rho^2 g} \right)^{1/3} = 1.51 \left(\frac{4M}{\mu} \right)^{-1/3} \quad (9.176)$$

where M is the mass rate of flow per unit length of tube.

This is approximately the same as equation 9.173 for vertical tubes and is a universal equation for condensation, noting that for vertical tubes $M = G/\pi d_o$ and for horizontal tubes $M = G/l$, where l is the length of the tube. Comparison of the two equations shows that, provided the length is more than three times the diameter, the horizontal tube will give a higher transfer coefficient for the same temperature conditions.

For j vertical rows of horizontal tubes, equation 9.175 may be modified to give:

$$h_m = 0.72 \left(\frac{k^3 \rho^2 g \lambda}{j d_o \mu \Delta T_f} \right)^{1/4} \quad (9.177)$$

KERN⁽²⁸⁾ suggests that, based on the performance of commercial exchangers, this equation is too conservative and that the exponent of j should be nearer $-\frac{1}{6}$ than $-\frac{1}{4}$. This topic is discussed in Volume 6, Chapter 12.

Experimental values

In testing Nusselt's equation it is important to ensure that the conditions comply with the requirements of the theory. In particular, it is necessary for the condensate to form a uniform film on the tubes, for the drainage of this film to be by gravity, and the flow streamline. Although some of these requirements have probably not been entirely fulfilled, results for pure vapours such as steam, benzene, toluene, diphenyl, ethanol, and so on, are sufficiently close to give support to the theory. Some data obtained by HASELDEN and PROSAD⁽⁵⁷⁾ for condensing oxygen and nitrogen vapours on a vertical surface, where precautions were taken to see that the conditions were met, are in very good agreement with Nusselt's theory. The results for most of the workers are within 15 per cent for horizontal tubes, although they tend to be substantially higher than the theoretical for vertical tubes. Typical values are given in Table 9.8 taken from McADAMS⁽²⁷⁾ and elsewhere.

Table 9.8. Average values of film coefficients h_m for condensation of pure saturated vapours on horizontal tubes

Vapour	Value of h_m (W/m ² K)	Value of h_m (Btu/h ft ² °F)	Range of ΔT_f (deg K)
Steam	10,000–28,000	1700–5000	1–11
Steam	18,000–37,000	3200–6500	4–37
Benzene	1400–2200	240–380	23–37
Diphenyl	1300–2300	220–400	4–15
Toluene	1100–1400	190–240	31–40
Methanol	2800–3400	500–600	8–16
Ethanol	1800–2600	320–450	6–22
Propanol	1400–1700	250–300	13–20
Oxygen	3300–8000	570–1400	0.08–2.5
Nitrogen	2300–5700	400–1000	0.15–3.5
Ammonia	6000	1000	—
Freon-12	1100–2200	200–400	—

When considering commercial equipment, there are several factors which prevent the true conditions of Nusselt's theory being met. The temperature of the tube wall will not be constant, and for a vertical condenser with a ratio of ΔT at the bottom to ΔT at the top of five, the film coefficient should be increased by about 15 per cent.

Influence of vapour velocity

A high vapour velocity upwards tends to increase the thickness of the film and thus reduce h , though the film may sometimes be disrupted mechanically as a result of the formation of small waves. For the downward flow of vapour, TEN BOSCH⁽⁵⁸⁾ has shown that h increases considerably at high vapour velocities and may increase to two or three times the value given by the Nusselt equation. It must be remembered that when a large

fraction of the vapour is condensed, there may be a considerable change in velocity over the surface.

Under conditions of high vapour velocity CARPENTER and COLBURN⁽⁵⁹⁾ have shown that turbulence may occur with low values of the Reynolds number, in the range 200–400. When the vapour velocity is high, there will be an appreciable drag on the condensate film and the expression obtained for the heat transfer coefficient is difficult to manage.

Carpenter and Colburn have put forward a simple correlation of their results for condensation at varying vapour velocities on the inner surface of a vertical tube which takes the form:

$$h_m = 0.065 G'_m \sqrt{\frac{C_p \rho k (R' / \rho_0 \mu^2)}{\mu \rho_0}} \quad (9.178)$$

where:

$$G'_m = \sqrt{\frac{(G_1^2 + G_1' G_2' + G_2^2)}{3}}$$

and u is the velocity calculated from G'_m . In this equation C_p , k , ρ , and μ are properties of the condensate and ρ_0 refers to the vapour. G'_1 is the mass rate of flow per unit area at the top of the tube and G'_2 the corresponding value at the bottom. R' is the shear stress at the free surface of the condensate film.

As pointed out by COLBURN⁽⁶⁰⁾, the group $C_p \rho k / \mu \rho_0$ does not vary very much for a number of organic vapours so that a plot of h_m and G'_m will provide a simple approximate correlation with separate lines for steam and for organic vapours as shown in Figure 9.48^(60,61). Whilst this must be regarded as an empirical approximation it is very useful for obtaining a good indication of the effect of vapour velocity.

Turbulence in the film

If Re is greater than 2100 during condensation on a vertical tube the mean coefficient h_m will increase as a result of turbulence. The data of KIRKBRIDE⁽⁶²⁾ and BADGER^(63,64) for the condensation of diphenyl vapour and Dowtherm on nickel tubes are expressed in the form:

$$h_m \left(\frac{\mu^2}{k^3 \rho^2 g} \right)^{1/3} = 0.0077 \left(\frac{4M}{\mu} \right)^{0.4} \quad (9.179)$$

Comparing equation 9.176 for streamline flow of condensate and equation 9.179 for turbulent flow, it is seen that, with increasing Reynolds number, h_m decreases with streamline flow but increases with turbulent flow. These results are shown in Figure 9.49.

Design equations are given in Volume 6, Chapter 12, for condensation both inside and outside horizontal and vertical tubes, and the importance of avoiding flooding in vertical tubes is stressed.

9.6.3. Dropwise condensation

In the discussion so far, it is assumed that the condensing vapour, on coming into contact with the cold surface, wets the tube so that a continuous film of condensate is formed. If the droplets initially formed do not wet the surface, after growing slightly

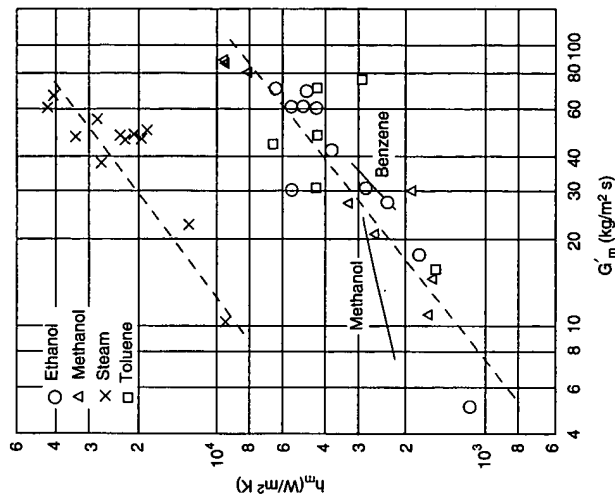


Figure 9.48. Average heat transfer data of CARPENTER and COLBURN⁽⁵⁹⁾ (shown as points) compared with those of TEPE and MUELLER⁽⁶¹⁾ (shown as solid lines). Dashed lines represent equation 9.178

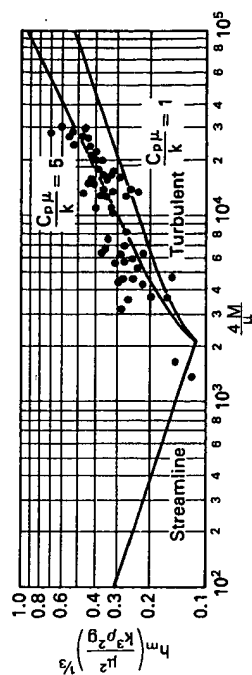


Figure 9.49. Effects of turbulence in condensate film

they will fall from the tube exposing fresh condensing surface. This is known as dropwise condensation and, since the heat does not have to flow through a film by conduction, much higher transfer coefficients are obtained. Steam is the only pure vapour for which definite dropwise condensation has been obtained, and values of h from 40 to 114 kW/m² K have been obtained, with much higher values on occasions. This question has been discussed by DREW, NAGLE and SMITH⁽⁶⁵⁾ who have shown that there are many materials which make the surface non-wettable although, of these, only those which are firmly held to the

surface are of any practical use. Mercaptans and oleic acid have been used to promote dropwise condensation, but at present there is little practical application of this technique. Exceptionally high values of h will not give a corresponding increase in the overall coefficient, since for a condenser with steam, a value of about $11 \text{ kW/m}^2 \text{ K}$ can be obtained with film condensation. On the other hand, it may be helpful in experimental work to reduce the thermal resistance on one side of a surface to a negligible value.

9.6.4. Condensation of mixed vapours

In the previous discussion it has been assumed that the vapour is a pure material, such as steam or organic vapour. If it contains a proportion of non-condensable gas and is cooled below its dew point, a layer of condensate is formed on the surface with a mixture of non-condensable gas and vapour above it. The heat flow from the vapour to the surface then takes place in two ways. Firstly, sensible heat is passed to the surface because of the temperature difference. Secondly, since the concentration of vapour in the main stream is greater than that in the gas film at the condensate surface, vapour molecules diffuse to the surface and condense there, giving up their latent heat. The actual rate of condensation is then determined by the combination of these two effects, and its calculation requires a knowledge of mass transfer by diffusion, as discussed in Chapter 10.

In the design of a cooler-condenser for a mixture of vapour and a permanent gas, the method of COLBURN and HOUGEN⁽⁶⁶⁾ is considered. This requires a point-to-point calculation of the condensate-vapour interface conditions T_c and P_s . A trial and error solution is required of the equation:

$$q_v + q_\lambda = q_c \quad (9.180)$$

$$h_g(T_s - T_c) + k_G \lambda (P_g - P_s) = h_o(T_c - T_{cm}) = U \Delta T \quad (9.181)$$

where the first term q_v represents the sensible heat transferred to the condensing surface, the second term q_λ the latent heat transferred by the diffusing vapour molecules, and the third term q_c the heat transferred from the condensing surface through the pipe wall, dirt and scales, and water film to the cooling medium. h_g is the heat transfer coefficient over the gas film, h_o the conductance of the combined condensate film, tube wall, dirt and scale films, and the cooling medium film and U the overall heat transfer coefficient. T_s is the vapour temperature, T_c the temperature of the condensate, T_{cm} the cooling medium temperature, ΔT the overall temperature difference $= (T_s - T_{cm})$, P_g is the partial pressure of diffusing vapour, P_s the vapour pressure at T_c , λ the latent heat of vaporisation per unit mass, and k_G the mass transfer coefficient in mass per unit time, unit area and unit partial pressure difference.

To evaluate the required condenser area, point values of the group $U \Delta T$ as a function of q_c must be determined by a trial and error solution of equation 9.181. Integration of a plot of q_c against $1/U \Delta T$ will then give the required condenser area. This method takes into account point variations in temperature difference, overall coefficient and mass velocities and consequently produces a reasonably accurate value for the surface area required.

The individual terms in equation 9.181 are now examined to enable a trial solution to proceed. Values for h_g and k_G are most conveniently obtained from the CHILTON and

COLBURN⁽⁶⁷⁾ analogy discussed in Chapter 10.

$$h_g = \frac{j_h G' C_p}{(C_p \mu / k)^{0.67}} \quad (9.182)$$

Thus:

$$k_G = \frac{j_d G'}{P_{Bm} (\mu / \rho D)^{0.67}} \quad (9.183)$$

Values of j_h and j_d are obtained from a knowledge of the Reynolds number at a given point in the condenser. The combined conductance h_o is evaluated by determining the condensate film coefficient h_c from the Nusselt equation and combining this with the dirt and tube wall conductances and a cooling medium film conductance predicted from the Sieder-Tate relationships. Generally, h_o may be considered to be constant throughout the exchanger.

From a knowledge of h_g , k_G , and h_o and for a given T_s and T_{cm} values of the condensate surface temperature T_c are estimated until equation 9.181 is satisfied. The calculations are repeated, and in this manner several point values of the group $U \Delta T$ throughout the condenser may be obtained.

The design of a cooler condenser for the case of condensation of two vapours is more complicated than the preceding single vapour-permanent gas case⁽⁶⁸⁾, and an example has been given by JEFFREYS⁽⁶⁹⁾.

For the condensation of a vapour in the presence of a non-condensable gas, the following example is considered which is based on an the work of KERN⁽²⁸⁾.

Example 9.23

A mixture of 0.57 kg/s of steam and 0.20 kg/s of carbon dioxide at 308 kN/m^2 and its dew point enters a heat exchanger consisting of 246 tubes, 19 mm o.d., wall thickness 1.65 mm , 3.65 m long, arranged in four passes on 25 mm square pitch in a 0.54 m diameter shell and leaves at 322 K . Condensation is effected by cooling water entering and leaving the unit at 300 and 319 K respectively. If the diffusivity of steam-carbon dioxide mixtures is $0.000011 \text{ m}^2/\text{s}$ and the group $(\mu / \rho D)^{0.67}$ may be taken to be constant at 0.62 , estimate the overall coefficient of heat transfer and the dirt factor for the condenser.

Solution

In the steam entering the condenser, there is $\frac{0.57}{18} = 0.032 \text{ kmol water}$
 and $\frac{0.20}{44} = 0.0045 \text{ kmol CO}_2$ } total = 0.0365 kmol .

Hence the partial pressure of water = $(308 \times 0.032 / 0.0365) = 270 \text{ kN/m}^2$ and from Table 11A in the Appendix, the dew point = 404 K .

Mean molecular weight of the mixture = $(0.57 + 0.20) / 0.0365 = 21.1 \text{ kg/kmol}$.

At the inlet: vapour pressure of water = 270 kN/m^2 } total = 308 kN/m^2
 inert pressure = $(308 - 270) = 38 \text{ kN/m}^2$

At the outlet: partial pressure of water at $322 \text{ K} = 11.7 \text{ kN/m}^2$ } total = 308 kN/m^2
 inert pressure = $(308 - 11.7) = 296.3 \text{ kN/m}^2$

steam at the outlet = $\frac{0.0045 \times 11.7}{296.3} = 0.000178 \text{ kmol}$

and: steam condensed = $(0.032 - 0.000178) = 0.03182 \text{ kmol}$.

The heat load is now estimated at each interval between the temperatures 404, 401, 397, 380, 339 and 322 K.

For the interval 404 to 401 K

From Table 11A in the Appendix, the partial pressure of steam at 401 K = 252.2 kN/m² and hence the partial pressure of CO₂ = (308 - 252.2) = 55.8 kN/m². Steam remaining = (0.0045 × 252.2/55.8) = 0.0203 kmol.

∴ Steam condensed = (0.032 - 0.0203) = 0.0117 kmol

Heat of condensation = (0.0117 × 18)(2180 + 1.93(404 - 401)) = 466 kW

Heat from uncondensed steam = (0.0203 × 18 × 1.93(404 - 401)) = 1.9 kW

Heat from carbon dioxide = (0.020 × 0.92(404 - 401)) = 0.5 kW

and the total for the interval = 468.4 kW

Repeating the calculation for the other intervals of temperature gives the following results:

Interval (K)	Heat load (kW)
404-401	468.4
401-397	323.5
397-380	343.5
380-339	220.1
339-322	57.9
Total	1407.3

and the flow of water = 1407.3/(4.187(319 - 300)) = 17.7 kg/s.

With this flow of water and a flow area per pass of 0.0120 m², the mass velocity of water is 1425 kg/m²s, equivalent to a velocity of 1.44 m/s at which $h_i = 6.36$ kW/m² K. Basing this on the outside area, $h_{io} = 5.25$ kW/m² K.

Shell-side coefficient for entering gas mixture:

$$\text{The mean specific heat, } C_p = \frac{(0.20 \times 0.92) + (0.57 \times 1.93)}{0.77} = 1.704 \text{ kJ/kg K.}$$

Similarly, the mean thermal conductivity $k = 0.025$ kW/m K and the mean viscosity $\mu = 0.015$ mN s/m²

The area for flow through the shell = 0.0411 m² and the mass velocity on the shell side

$$= \frac{0.20 + 0.57}{0.0411} = 18.7 \text{ kg/m}^2\text{s}$$

Taking the equivalent diameter as 0.024 m, $Re = 29,800$

and: $h_g = 0.107$ kW/m² K or 107 W/m² K.

$$\text{Now: } \left(\frac{\mu}{\rho D}\right)^{0.67} = 0.62, \left(\frac{C_p \mu}{k}\right)^{0.67} = 1.01$$

$$\text{and: } k_G = \frac{h_g (C_p \mu / k)^{0.67}}{C_p P_r (\mu / \rho D)^{0.67}} = \frac{107 \times 1.01}{1704 P_r \times 0.62} = \frac{0.102}{P_r}$$

At point 1

Temperature of the gas $T = 404$ K, partial pressure of steam $P_g = 270$ kN/m², partial pressure of the inert $P_i = 38$ kN/m², water temperature $T_w = 319$ K and $\Delta T = (404 - 319) = 85$ K. An estimate is now made for the temperature of the condensate film of $T_c = 391$ K. In this case $P_g = 185.4$ kN/m² and $P_i = (308 - 185.4) = 122.6$ kN/m².

$$P_{iF} = \frac{122.6 - 38}{\ln(122.6/38)} = 72.2 \text{ kN/m}^2.$$

Thus:

In equation 9.181:

$$h_g(T_s - T_c) + k_G \lambda (P_g - P_i) = h_{i0}(T_c - T_{cm})$$

$$0.107(404 - 391) + \left(\frac{0.102}{72.2}\right) 2172(270 - 185.4) = 5.25(391 - 319)$$

$$259 = 378 \quad \text{i.e. there is no balance.}$$

Try $T_c = 378$ K, $P_g = 118.5$ kN/m², $P_i = (308 - 118.5) = 189.5$ kN/m²

$$P_{iF} = \frac{189.5 - 38}{\ln(189.5/38)} = 94.2 \text{ kN/m}^2$$

and:

$$0.107(404 - 378) + \left(\frac{0.102}{94.2}\right) 2172(270 - 118.5) = 5.25(378 - 319)$$

$$310 = 308 \quad \text{which agrees well}$$

$$U \Delta T = 309 \text{ kW/m}^2 \quad \text{and} \quad U = \frac{309}{(404 - 319)} = 3.64 \text{ kW/m}^2 \text{ K.}$$

Repeating this procedure at the various temperature points selected, the heat-exchanger area may then be obtained as the area under a plot of Σq vs. $1/U \Delta T$, or as $A = \Sigma q / U \Delta T$ according to the following tabulation:

Point	T_s (K)	T_c (K)	$U \Delta T$ (kW/m ²)	$(U \Delta T)_{\log}$ (kW/m ²)	Q (kW)	$A = Q / (U \Delta T)_{\log}$ (m ²)	ΔT (K)	ΔT_{\log} (K)	$Q / \Delta T_{\log}$ (kW/K)
1	404	378	309	—	—	—	84.4	—	—
2	401	356	228	268.5	468.4	1.75	88.1	86.3	5.42
3	397	336	145	186.5	323.5	1.74	88.6	88.4	3.66
4	380	312	40.6	88.1*	343.5	3.89	76.7	82.7	4.15
5	339	302	5.4	17.5*	220.1	12.58	38.1	55.2*	4.00
6	322	300	2.1	3.5*	51.9	14.83	22.2	29.6*	1.75
Total:					1407.3	34.8			18.98

*based on LMTD.

If no condensation takes place, the logarithmic mean temperature difference is 46.6 K. In practice the value is $(1407.3/18.98) = 74.2$ K.

Assuming no scale resistance, the overall coefficient is $\frac{1407.3}{34.8 \times 74.2} = 0.545$ kW/m² K.

The available surface area on the outside of the tubes = 0.060 m²/m

$$\text{or } (246 \times 3.65 \times 0.060) = 53.9 \text{ m}^2$$

The actual coefficient is therefore $\frac{1407.3}{53.9 \times 74.2} = 0.352$ kW/m² K

$$\text{and the dirt factor is } \frac{(0.545 - 0.352)}{(0.545 \times 0.352)} = 1.01 \text{ m}^2\text{K/kW.}$$

As shown in Figure 9.50, the clean coefficient varies from 3.64 kW/m² K at the inlet to 0.092 kW/m² K at the outlet.

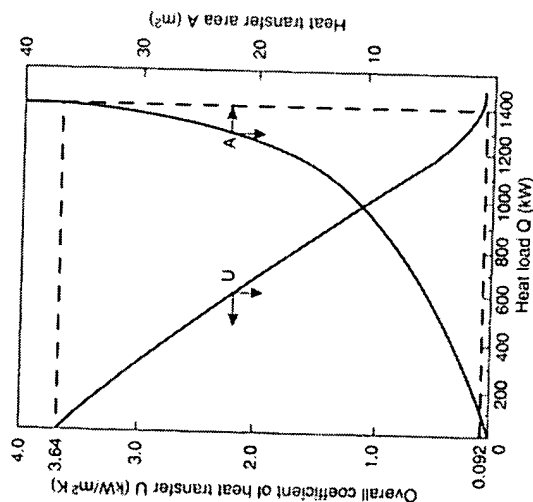


Figure 9.50. Results for Example 9.23

Condensation of mixed vapours is considered further in Volume 6, Chapter 12, where it is suggested that the local heat transfer coefficient may be expressed in terms of the local gas-film and condensate-film coefficients. For partial condensation where:

- (i) *non-condensables* < 0.5 per cent; their effect can be ignored,
- (ii) *non-condensables* > 70 per cent; the heat transfer can be taken as being by forced convection alone, and
- (iii) *non-condensables* 0.5–70 per cent; both mechanisms are effective.

9.7. BOILING LIQUIDS

9.7.1 Conditions for boiling

In processing units, liquids are boiled either on submerged surfaces or on the inside of vertical tubes. Mechanical agitation may be applied in the first case and, in the second, the liquid may be driven through the tubes by means of an external pump. The boiling of liquids under either of these conditions normally leads to the formation of vapour first in the form of bubbles and later as a distinct vapour phase above a liquid interface. The conditions for boiling on the submerged surface are discussed here and the problems arising with boiling inside tubes are considered in Volume 2. Much of the fundamental work on the ideas of boiling has been presented by WESTWATER⁽⁷⁰⁾ and JAKOB⁽⁷¹⁾, and subsequently by ROHSENOW and CLARK⁽⁷²⁾ and ROHSENOW⁽⁷³⁾ and by

FORSTER⁽⁷⁴⁾. The boiling of solutions in which a solid phase is separated after evaporation has proceeded to a sufficient extent is considered in Volume 2.

For a bubble to be formed in a liquid, such as steam in water, for example, it is necessary for a surface of separation to be produced. Kelvin has shown that, as a result of the surface tension between the liquid and vapour, the vapour pressure on the inside of a concave surface will be less than that at a plane surface. As a result, the vapour pressure P_v inside the bubble is less than the saturation vapour pressure P_s at a plane surface. The relation between P_v and P_s is:

$$P_v = P_s - \left(\frac{2\sigma}{r} \right) \quad (9.184)$$

where r is the radius of curvature of the bubble, and σ is the surface tension.

Hence the liquid must be superheated near the surface of the bubble, the extent of the superheat increasing with decrease in the radius of the bubble. On this basis it follows that very small bubbles are difficult to form without excessive superheat. The formation of bubbles is made much easier by the fact that they will form on curved surfaces or on irregularities on the heating surface, so that only a small degree of superheat is normally required.

Nucleation at much lower values of superheat is believed to arise from the presence of existing nuclei such as non-condensing gas bubbles, or from the effect of the shape of the cavities in the surface. Of these, the current discussion on the influence of cavities is the most promising. In many cavities the angle θ will be greater than 90° and the effective contact angle, which includes the contact angle of the cavity β , will be considerably greater [$= \theta + (180 - \beta)/2$], so that a much-reduced superheat is required to give nucleation. Thus the size of the mouth of the cavity and the shape of the cavity plays a significant part in nucleation⁽⁷⁵⁾.

It follows that for boiling to occur a small difference in temperature must exist between the liquid and the vapour. JAKOB and FRITZ⁽⁷⁶⁾ have measured the temperature distribution for water boiling above an electrically heated hot plate. The temperature dropped very steeply from about 383 K on the actual surface of the plate to 374 K about 0.1 mm from it. Beyond this point the temperature was reasonably constant until the water surface was reached. The mean superheat of the water above the temperature in the vapour space was about 0.5 deg K and this changed very little with the rate of evaporation. At higher pressures this superheating became smaller becoming 0.2 deg K at 5 MN/m² and 0.05 deg K at 101 MN/m². The temperature drop from the heating surface depends, however, very much on the rate of heat transfer and on the nature of the surface. Thus in order to maintain a heat flux of about 25.2 kW/m², a temperature difference of only 6 deg K was required with a rough surface as against 10.6 deg K with a smooth surface. The heat transfer coefficient on the boiling side is therefore dependent on the nature of the surface and on the difference in temperature available. For water boiling on copper plates JAKOB and FRITZ⁽⁷⁶⁾ give the following coefficients for a constant temperature difference of 5.6 deg K, with different surfaces:

- (1) Surface after 8 h (28.8 ks) use and 48 h (172.8 ks) immersion in water

$$h = 8000 \text{ W/m}^2 \text{ K}$$

$$h = 3900 \text{ W/m}^2 \text{ K}$$

$$h = 2600 \text{ W/m}^2 \text{ K}$$

- (2) Freshly sandblasted

- (3) Sandblasted surface after long use

(4) Chromium plated

$$h = 2000 \text{ W/m}^2 \text{ K}$$

The initial surface, with freshly cut grooves, gave much higher figures than case (1). The nature of the surface will have a marked effect on the physical form of the bubble and the area actually in contact with the surface, as shown in Figure 9.51.

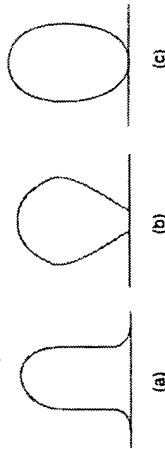


Figure 9.51. Shapes of bubbles (a) screen surface—thin oil layer (b) chromium plated and polished surface (c) screen surface—clean

The three cases are:

- Non-wettable surface*, where the vapour bubbles spread out thus reducing the area available for heat transfer from the hot surface to the liquid.
- Partially wettable surface*, which is the commonest form, where the bubbles rise from a larger number of sites and the rate of transfer is increased.
- Entirely wetted surface*, such as that formed by a screen. This gives the minimum area of contact between vapour and surface and the bubbles leave the surface when still very small. It therefore follows that if the liquid has detergent properties this may give rise to much higher rates of heat transfer.

9.7.2. Types of boiling

Interface evaporation

In boiling liquids on a submerged surface it is found that the heat transfer coefficient depends very much on the temperature difference between the hot surface and the boiling liquid. The general relation between the temperature difference and heat transfer coefficient was first presented by NUKIYAMA⁽⁷⁷⁾ who boiled water on an electrically heated wire. The results obtained have been confirmed and extended by others, and Figure 9.52 shows the data of FARBER and SCORAH⁽⁷⁸⁾. The relationship here is complex and is best considered in stages.

In interface evaporation, the bubbles of vapour formed on the heated surface move to the vapour-liquid interface by natural convection and exert very little agitation on the liquid. The results are given by:

$$Nu = 0.61(Gr Pr)^{1/4} \quad (9.185)$$

which may be compared with the expression for natural convection:

$$Nu = C'(Gr Pr)^n \quad (\text{equation 9.101})$$

where $n = 0.25$ for streamline conditions and $n = 0.33$ for turbulent conditions.

HEAT TRANSFER

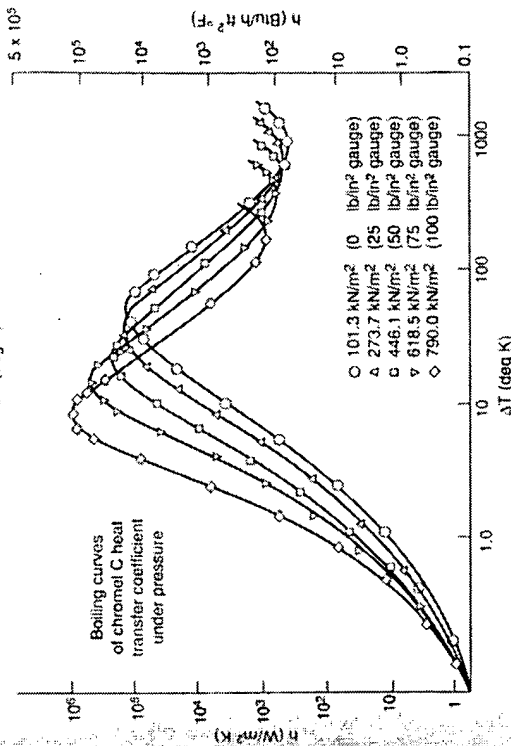
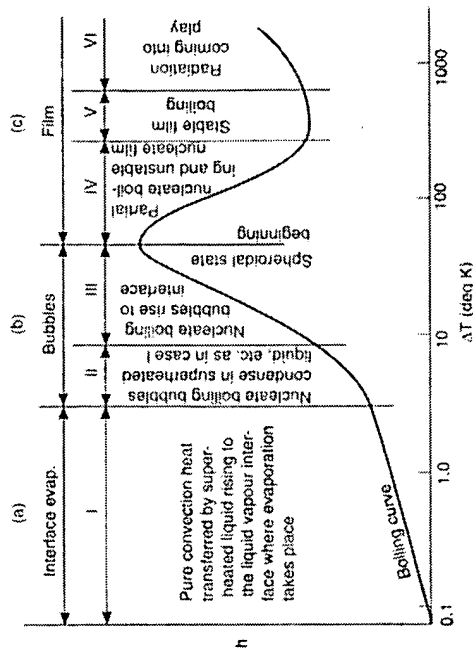


Figure 9.52. Heat transfer results of FARBER and SCORAH⁽⁷⁸⁾

Nucleate boiling

At higher values of ΔT the bubbles form more rapidly and form more centres of nucleation. Under these conditions the bubbles exert an appreciable agitation on the liquid and the heat transfer coefficient rises rapidly. This is the most important region for boiling in industrial equipment.

Film boiling

With a sufficiently high value of ΔT , the bubbles are formed so rapidly that they cannot get away from the hot surface, and they therefore form a blanket over the surface. This means that the liquid is prevented from flowing on to the surface by the bubbles of vapour and the coefficient falls. The maximum coefficient occurs during nucleate boiling although this is an unstable region for operation. In passing from the *nucleate boiling* region to the *film boiling* region, two critical changes occur in the process. The first manifests itself in a decrease in the heat flux, the second is the prelude to stable film boiling. The intermediate region is generally known as the *transition* region. It may be noted that the first change in the process is an important hydrodynamic phenomenon which is common to other two-phase systems, such as flooding in countercurrent gas-liquid or vapour-liquid systems, for example.

With very high values of ΔT , the heat transfer coefficient rises again because of heat transfer by radiation. These very high values are rarely achieved in practice and usually the aim is to operate the plant at a temperature difference a little below the value giving the maximum heat transfer coefficient.

9.7.3. Heat transfer coefficients and heat flux

The values of the heat transfer coefficients for low values of temperature difference are given by equation 9.185. Figure 9.53 shows the values of h and for q for water boiling on a submerged surface. Whilst the actual values vary somewhat between investigations, they all give a maximum for a temperature difference of about 22 deg K. The maximum value of h is about 50 kW/m² K and the maximum flux is about 1100 kW/m².

Similar results have been obtained by BONILLA and PERRY⁽⁷⁹⁾, INSINGER and BLISS⁽⁸⁰⁾ and others for a number of organic liquids such as benzene, alcohols, acetone, and carbon tetrachloride. The data in Table 9.9 for liquids boiling at atmospheric pressure show that the maximum heat flux is much smaller with organic liquids than with water and the temperature difference at this condition is rather higher. In practice the critical value of ΔT may be exceeded. SAUER *et al.*⁽⁸¹⁾ found that the overall transfer coefficient U for boiling ethyl acetate with steam at 377 kN/m² was only 14 per cent of that when the steam pressure was reduced to 115 kN/m².

Table 9.9. Maximum heat flux for various liquids boiling at atmospheric pressure

Liquid	Surface	Critical ΔT (deg K)	Maximum flux (kW/m ²)
Water	Chromium	25	910
50 mol% ethanol-water	Chromium	29	595
Ethanol	Chromium	33	455
n-Butanol	Chromium	44	455
Acetone	Nickel	44	370
iso-Propanol	Chromium	25	455
Carbon tetrachloride	Chromium	33	340
Benzene	Copper	—	180
	Copper	—	170–230

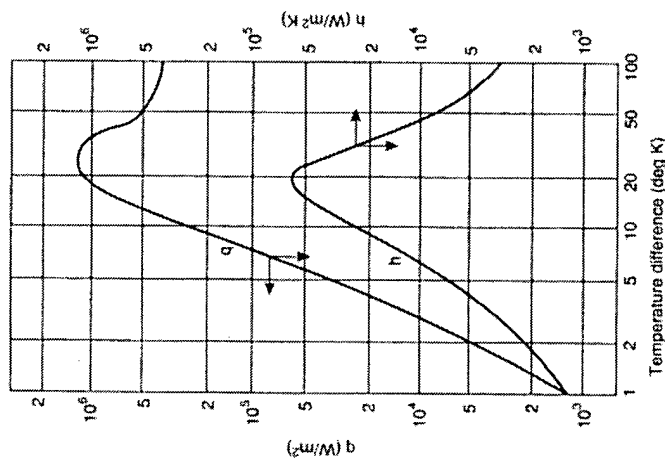


Figure 9.53. Effect of temperature difference on heat flux and heat transfer coefficient to water boiling at 373 K on a submerged surface

In considering the problem of nucleate boiling, the nature of the surface, the pressure, and the temperature difference must be taken into account as well as the actual physical properties of the liquid.

Apart from the question of scale, the nature of the clean surface has a pronounced influence on the rate of boiling. Thus BONILLA and PERRY⁽⁷⁹⁾ boiled ethanol at atmospheric pressure and a temperature difference of 23 deg K, and found that the heat flux at atmospheric pressure was 850 kW/m² for polished copper, 450 for gold plate, and 370 for fresh chromium plate, and only 140 for old chromium plate. This wide fluctuation means that care must be taken in anticipating the heat flux, since the high values that may be obtained initially may not persist in practice because of tarnishing of the surface.

Effect of temperature difference

CRUYDER and FINALBORGIO⁽⁸²⁾ boiled a number of liquids on a horizontal brass surface, both at atmospheric and at reduced pressure. Some of their results are shown in Figure 9.54, where the coefficient for the boiling liquid h is plotted against the temperature difference between the hot surface and the liquid. The points for the various liquids in Figure 9.54

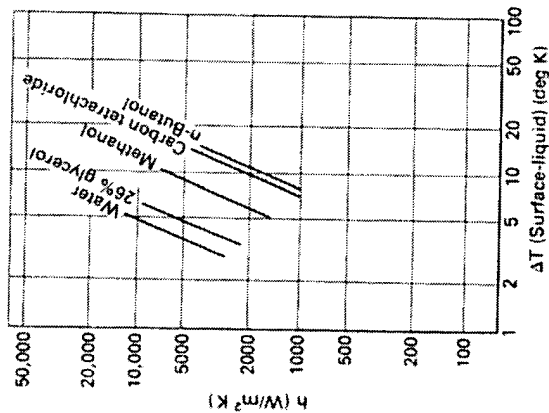


Figure 9.54. Effect of temperature difference on the heat transfer coefficient for boiling liquids (CRYDER and FINALBORGO⁽⁸²⁾)

lie on nearly parallel straight lines, which may be represented by:

$$h = \text{constant} \times \Delta T^{2.5} \quad (9.186)$$

This value for the index of ΔT has been found by other workers, although LINK⁽⁸³⁾ found values as high as 4 for some of their work. It is important to note that this value of 2.5 is true only for temperature differences up to 19 deg K.

In some ways it is more convenient to show the results in the form of heat flux versus temperature difference, as shown in Figure 9.55, where some results from a number of workers are given.

Effect of pressure

CRYDER and FINALBORGO⁽⁸²⁾ found that h decreased uniformly as the pressure and hence the boiling point was reduced, according to the relation $h = \text{constant} \times B^{n'}$, where T'' is numerically equal to the temperature in K and B is a constant. Combining this with equation 9.186, their results for h were expressed in the empirical form:

$$h = \text{constant} \times \Delta T^{2.5} B^{n'} \quad (9.187)$$

$$\text{or, using SI units: } \log \left(\frac{h}{5.67} \right) = a' + 2.5 \log \Delta T + b' (T'' - 273)$$

where $(T'' - 273)$ is in °C.

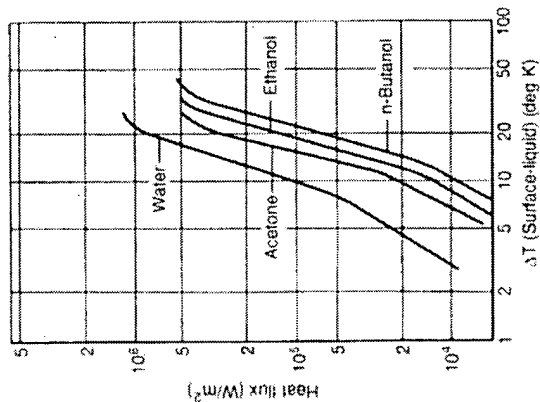


Figure 9.55. Effect of temperature difference on heat flux to boiling liquids (BONILLA and PERRY⁽⁷⁹⁾)

If a' and b' are given the following values, h is expressed in $\text{W/m}^2 \text{K}$:

	a'	b'	a'	b'
Water	-0.96	0.025	-4.13	0.022
Methanol	-1.11	0.027	-1.47	0.029
CCl_4	-1.55	0.022	-2.43	0.031

The values of a' will apply only to a particular apparatus although a value of b' of 0.025 is of more general application. If h_n is the coefficient at some standard boiling point T_n , and h at some other temperature T , equation 9.187 may be rearranged to give:

$$\log \frac{h}{h_n} = 0.025 (T'' - T_n'') \quad (9.188)$$

for a given material and temperature difference.

As the pressure is raised above atmospheric pressure, the film coefficient increases for a constant temperature difference. CICHETTI and BONILLA⁽⁸⁴⁾ have examined this problem for pressures up to the critical value for the vapour, and have shown that ΔT for maximum rate of boiling decreases with the pressure. They obtained a single curve, shown in Figure 9.56, by plotting q_{max}/P_c against P/P_c , where P_c is the critical pressure and P the reduced pressure $= P/P_c$. This curve represents the data for water, ethanol, benzene, propane, n-heptane, and several mixtures with water. For water the results cover only a small range of P/P_c , because of the high value of P_c . For the organic liquids

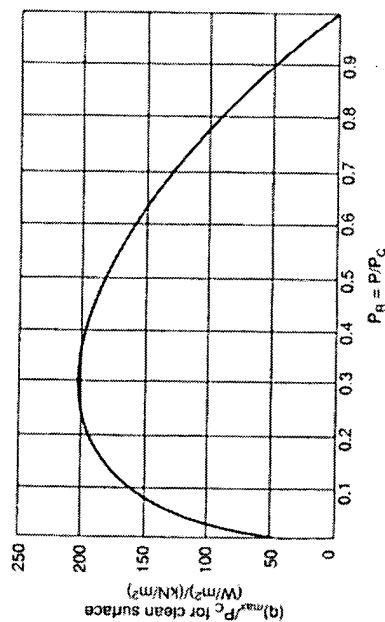


Figure 9.56. Effect of pressure on the maximum heat flux in nucleate boiling

investigated, it was shown that the maximum value of heat flux q occurs at a pressure P of about one-third of the critical pressure P_c . As shown in Table 9.10, the range of physical properties of the organic liquids is not wide and further data are required to substantiate the previous relation.

Table 9.10. Heat transfer coefficients for boiling liquids

Liquid	Boiling point (deg K)	h	
		(W/m² K)	(Btu/h ft² °F)
Water	372	9000	1600
	372	2700	500
	326	4700	850
	326	1300	250
Methanol	337	4800	850
	337	1500	250
	306	3000	500
	306	900	150
Carbon tetrachloride	349	3500	600
	349	1100	200
	315	2000	400
	315	700	100

9.7.4. Analysis based on bubble characteristics

It is a matter speculation as to why such high values of heat flux are obtained with the boiling process. It was once thought that the bubbles themselves were carriers of latent heat which was added to the liquid by their movement. It has now been shown, by determining the numbers of bubbles, that this mechanism would result in the transfer of only a moderate part of the heat that is actually transferred. The current views are that the high flux arises

from the agitation produced by the bubbles, and two rather different explanations have been put forward. ROHSENOW and CLARK⁽⁷²⁾ and ROHSENOW⁽⁷³⁾ base their argument on the condition of the bubble on leaving the hot surface. By calculating the velocity and size of the bubble an expression may be derived for the heat transfer coefficient in the form of a Nusselt type equation, relating the Nusselt group to the Reynolds and Prandtl groups. FORSTER and ZUBER^(85,86), however, argue that the important velocity is that of the growing bubble, and this is the term used to express the velocity. In either case the bubble movement is vital in obtaining a high flux. The liquid adjacent to the surface is agitated and exerts a mixing action by pushing hot liquid from the surface to the bulk of the stream.

Considering in more detail the argument proposed by ROHSENOW and CLARK⁽⁷²⁾ and ROHSENOW⁽⁷³⁾, the size of a bubble at the instant of breakaway from the surface has been determined by FRITZ⁽⁸⁷⁾ who has shown that d_b is given by:

$$d_b = C_1 \phi \left(\frac{2\sigma}{g(\rho_l - \rho_v)} \right)^{1/2} \quad (9.189)$$

where σ is the surface tension, ρ_l and ρ_v the density of the liquid and vapour, ϕ is the contact angle, and C_1 is a constant depending on conditions.

The flowrate of vapour per unit area as bubbles u_b is given by:

$$u_b = \frac{f n \pi d_b^3}{6} \quad (9.190)$$

where f is the frequency of bubble formation at each bubble site and n is the number of sites of nucleation per unit area.

The heat transferred by the bubbles q_b is to a good approximation given by:

$$q_b = \frac{1}{6} \pi d_b^3 f n \rho_v \lambda \quad (9.191)$$

where λ is the latent heat of vaporisation.

It has been shown that for heat flux rates up to 3.2 kW/m² the product $f d_b$ is constant and that the total heat flow per unit area q is proportional to n . From equation 9.191 it is seen that q_b is proportional to n at a given pressure, so that $q \propto q_b$.

Hence:

$$q = C_2 \frac{\pi}{6} d_b^3 f n \rho_v \lambda \quad (9.192)$$

Substituting from equations 9.190 and 9.192, the mass flow per unit area:

$$\rho_v u_b = f n \frac{\pi}{6} d_b^3 \rho_v = \frac{q}{C_2 \lambda} \quad (9.193)$$

A Reynolds number for the bubble flow which represents the term for agitation may be defined as:

$$\begin{aligned} Re_b &= \frac{d_b \rho_v u_b}{\mu_l} \\ &= C_1 \phi \left(\frac{2\sigma}{g(\rho_l - \rho_v)} \right)^{1/2} \left(\frac{q}{C_2 \lambda} \right) \frac{1}{\mu_l} \end{aligned}$$

$$= C_3 \phi \frac{q}{\lambda_l \mu_l} \left(\frac{\sigma}{g(\rho_l - \rho_v)} \right)^{1/2} \quad (9.194)$$

$$\begin{aligned} \text{The Nusselt group for bubble flow, } Nu_b &= h_b C_1 \frac{\phi}{k_l} \left(\frac{2\sigma}{g(\rho_l - \rho_v)} \right)^{1/2} \\ &= C_4 h_b \frac{\phi}{k_l} \left(\frac{\sigma}{g(\rho_l - \rho_v)} \right)^{1/2} \end{aligned} \quad (9.195)$$

and hence a final correlation is obtained of the form:

$$Nu_b = \text{constant } Re_b^n Pr^m \quad (9.196)$$

$$\text{or: } Nu_b = \text{constant} \left[\frac{C_3 \phi q}{\mu_l \lambda_l} \left(\frac{\sigma}{g(\rho_l - \rho_v)} \right)^{1/2} \right]^n \left(\frac{C_l \mu_l}{k_l} \right)^m \quad (9.197)$$

where n and m have been found experimentally to be 0.67 and -0.7 respectively and the constant, which depends on the metal surface, ranges from 67–100 for polished chromium, 77 for platinum wire and 166 for brass.^[73]

A comprehensive study of nucleate boiling of a wide range of liquids on thick plates of copper, aluminium, brass and stainless steel has been carried out by PIORO⁽⁸⁸⁾ who has evaluated the constants in equation 9.197 for different combinations of liquid and surface.

FORSTER and ZUBER^(85,86) who employed a similar basic approach, although the radial rate of growth dr/dt was used for the bubble velocity in the Reynolds group, showed that:

$$\frac{dr}{dt} = \frac{\Delta T C_l \rho_l}{2\lambda_l \rho_v} \left(\frac{\pi D_{bl}}{r} \right)^{1/2} \quad (9.198)$$

where D_{bl} is the thermal diffusivity ($k_l/C_l \rho_l$) of the liquid. Using this method, a final correlation in the form of equation 9.196 has been presented.

Although these two forms of analysis give rise to somewhat similar expressions, the basic terms are evaluated in quite different ways and the final expressions show many differences. Some data fit the Rohsenow equation reasonably well⁽⁸⁸⁾, and other data fit Forster's equation.

These expressions all indicate the importance of the bubbles on the rate of transfer, although as yet they have not been used for design purposes. INSINGER and BLISS⁽⁸⁹⁾ made the first approach by dimensional analysis and MCNELLY⁽⁸⁹⁾ has subsequently obtained a more satisfactory result. The influence of ΔT is taken into account by using the flux q , and the last term allows for the change in volume when the liquid vaporises. The following expression was obtained in which the numerical values of the indices were deduced from existing data:

$$\frac{hd}{k_l} = 0.225 \left(\frac{C_l \mu_l}{k_l} \right)^{0.69} \left(\frac{qd}{\lambda_l \mu} \right)^{0.69} \left(\frac{p_d}{\sigma} \right)^{0.31} \left(\frac{\rho_l}{\rho_v} - 1 \right) \quad (9.199)$$

9.7.5. Sub-cooled boiling

If bubbles are formed in a liquid which is much below its boiling point, then the bubbles will collapse in the bulk of the liquid. Thus if a liquid flows over a very hot surface, then

the bubbles formed are carried away from the surface by the liquid and sub-cooled boiling occurs. Under these conditions a very large number of small bubbles are formed and a very high heat flux is obtained. Some results for these conditions are given in Figure 9.57.

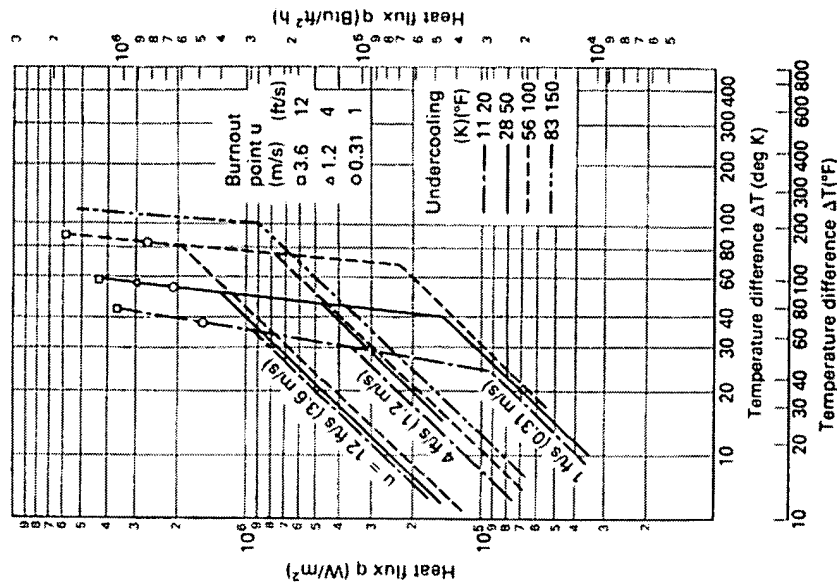


Figure 9.57. Heat flux in sub-cooled boiling

If a liquid flows through a tube heated on the outside then the heat flux q will increase with ΔT as shown in Figure 9.57. Beyond a certain value of ΔT the increase in q is very rapid. If the velocity through the tube is increased, then a similar plot is obtained with a higher value of q at low values of ΔT and then the points follow the first line. Over the first section, forced convection boiling exists where an increase in Reynolds number does not bring about a very great increase in q because the bubbles are themselves producing agitation in the boundary layer near the wall. Over the steep section, sub-cooled boiling exists where the velocity is not important provided it is sufficient to remove the bubbles

rapidly from the surface. In the same way, mechanical agitation of a liquid boiling on a submerged surface will not markedly increase the heat flux.

9.7.6. Design considerations

In the design of vaporisers and reboilers, two types of boiling are important — nucleate boiling in a pool of liquid as in a kettle-type reboiler or a jacketed vessel, and convective boiling which occurs where the vaporising liquid flows over a heated surface and heat transfer is by both forced convection and nucleate boiling as, for example, in forced circulation or thermosiphon reboilers. The discussion here is a summary of that given in Volume 6 where a worked example is given.

In the absence of experimental data, the correlation given by FORSTER and ZUBER⁽⁸⁶⁾ may be used to estimate *pool boiling* coefficients, although the following reduced pressure correlation given by MOSTINSKI⁽⁹⁰⁾ is much simpler to use and gives reliable results for h (in $\text{W/m}^2 \text{K}$):

$$h = 0.104 P_c^{0.69} q^{0.7} \left[1.8 \left(\frac{P}{P_c} \right)^{0.17} + 4 \left(\frac{P}{P_c} \right)^{1.2} + 10 \left(\frac{P}{P_c} \right)^{10} \right] \quad (9.200)$$

In this equation, P_c and P are the critical and operating pressures (bar), respectively, and q is the heat flux (W/m^2). Both equations are for single component fluids, although they may also be used for close-boiling mixtures and for wider boiling ranges with a factor of safety. In reboiler and vaporiser design, it is important that the heat flux is well below the critical value. A correlation is given for the heat transfer coefficient for the case where film-boiling takes place on tubes submerged in the liquid.

Convective boiling, which occurs when the boiling liquid flows through a tube or over a tube bundle, depends on the state of the fluid at any point. The effective heat transfer coefficient can be considered to be made up of the convective and nucleate boiling components. The convective boiling coefficient is estimated using an equation for single-phase forced-convection heat transfer (equation 9.64, for example) modified by a factor to allow for the effects of two-phase flow. Similarly, the nucleate boiling coefficient is obtained from the Forster and Zuber or Mostinski correlation, modified by a factor dependent on the liquid Reynolds number and on the effects of two-phase flow. The estimation of convective boiling coefficients is illustrated by means of an example in Volume 6.

One of the most important areas of application of heat transfer to boiling liquids is in the use of evaporators to effect an increase in the concentration of a solution. This topic is considered in Volume 2.

For vaporising the liquid at the bottom of a distillation column a reboiler is used, as shown in Figure 9.58. The liquid from the still enters the boiler at the base, and, after flowing over the tubes, passes out over a weir. The vapour formed, together with any entrained liquid, passes from the top of the unit to the column. The liquid flow may be either by gravity or by forced circulation. In such equipment, provision is made for expansion of the tubes either by having a floating head as shown, or by arranging the tubes in the form of a hairpin bend (Figure 9.59). A vertical reboiler may also be used with steam condensing on the outside of the tube bundle. With all systems it is undesirable

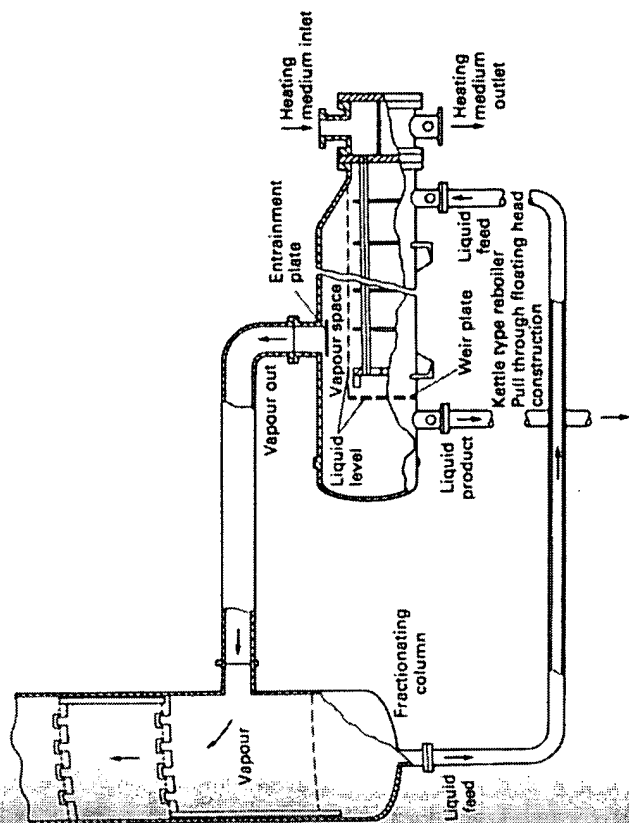


Figure 9.58. Reboiler installed on a distillation column

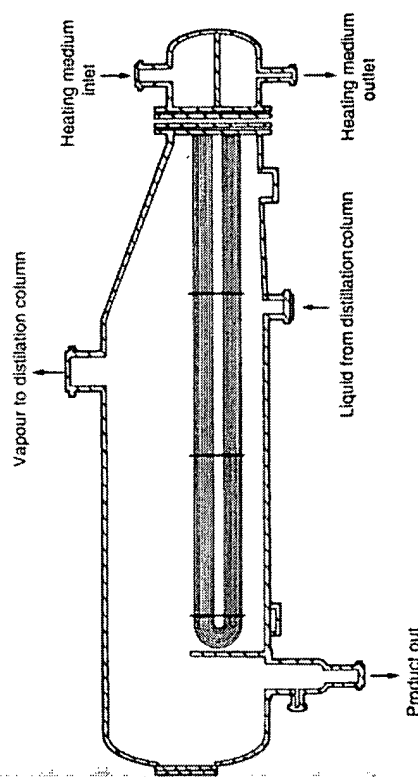


Figure 9.59. Kettle reboiler with hairpin tubes

to vaporise more than a small percentage of the feed since a good liquid flow over the tubes is necessary to avoid scale formation.

In the design of *forced convection* reboilers, the normal practice is to calculate the heat transfer coefficient on the assumption that heat is transferred by forced convection only, and this gives safe values. KERN⁽²⁸⁾ recommends that the heat flux should not exceed 60 kW/m² for organics and 90 kW/m² for dilute aqueous solutions. In *thermosyphon reboilers*, the fluid circulates at a rate at which the pressure losses in the system are just balanced by the hydrostatic head and the design involves an iterative procedure based on an assumed circulation rate through the exchanger. *Kettle reboilers*, such as that shown in Figure 9.59, are essentially pool boiling devices and their design, based on nucleate boiling data, uses the Zuber equation for single tubes, modified by a tube-density factor. This general approach is developed further in Volume 6.

9.8. HEAT TRANSFER IN REACTION VESSELS

9.8.1. Helical cooling coils

A simple jacketed pan or kettle is very commonly used in the processing industries as a reaction vessel. In many cases, such as in nitration or sulphonation reactions, heat has to be removed or added to the mixture in order either to control the rate of reaction or to bring it to completion. The addition or removal of heat is conveniently arranged by passing steam or water through a jacket fitted to the outside of the vessel or through a helical coil fitted inside the vessel. In either case some form of agitator is used to obtain even distribution in the vessel. This may be of the anchor type for very thick pastes or a propeller or turbine if the contents are not too viscous.

In such a vessel, the thermal resistances to heat transfer arise from the water film on the inside of the coil, the wall of the tube, the film on the outside of the coil, and any scale that may be present on either surface. The overall transfer coefficient may be expressed by:

$$\frac{1}{UA} = \frac{1}{h_i A_i} + \frac{x_w}{k_w A_w} + \frac{1}{h_o A_o} + \frac{R_o}{A_o} + \frac{R_i}{A_i} \quad (9.201)$$

where R_o and R_i are the scale resistances and the other terms have the usual definitions.

Inside film coefficient

The value of h_i may be obtained from a form of equation 9.64:

$$\frac{h_i d}{k} = 0.023 \left(\frac{d u \rho}{\mu} \right)^{0.8} \left(\frac{C_p \mu}{k} \right)^{0.33} \quad (9.202)$$

if water is used in the coil, and the Sieder and Tate equation (equation 9.66) if a viscous brine is used for cooling.

These equations have been obtained for straight tubes; with a coil somewhat greater transfer is obtained for the same physical conditions. JESCHKE⁽⁹¹⁾ cooled air in a 31 mm steel tube wound in the form of a helix and expressed his results in the form:

$$h_i(\text{coil}) = h_i(\text{straight pipe}) \left(1 + 3.5 \frac{d}{d_c} \right) \quad (9.203)$$

where d is the inside diameter of the tube and d_c the diameter of the helix. PRAATT⁽⁹²⁾ has examined this problem in greater detail for liquids and has given almost the same result. Combining equations 9.202 and 9.203, the inside film coefficient h_i for the coil may be calculated.

Outside film coefficient

The value of h_o is determined by the physical properties of the liquor and by the degree of agitation achieved. This latter quantity is difficult to express in a quantitative manner and the group $L^2 N \rho / \mu$ has been used both for this problem and for the allied one of power used in agitation, as discussed in Chapter 7. In this group L is the length of the paddle and N the revolutions per unit time. CHILTON, DREW and JEBENS⁽⁹³⁾, working with a small tank only 0.3 m in diameter d_v , expressed their results by:

$$\frac{h_o d_v}{k} \left(\frac{\mu_s}{\mu} \right)^{0.14} = 0.87 \left(\frac{C_p \mu}{k} \right)^{1/3} \left(\frac{L^2 N \rho}{\mu} \right)^{0.62} \quad (9.204)$$

where the factor $(\mu_s/\mu)^{0.14}$ allows for the difference between the viscosity adjacent to the coil (μ_s) and that in the bulk of the liquor. A wide range of physical properties was achieved by using water, two oils, and glycerol.

PRAATT⁽⁹²⁾ used both circular and square tanks up to 0.6 m in size and a series of different arrangements of a simple paddle as shown in Figure 9.60. The effect of altering the arrangement of the coil was investigated and the tube diameter d_o , the gap between the turns d_g , the diameter of the helix d_c , the height of the coil d_p , and the width of the stirrer W were all varied. The final equations tanks were:

For cylindrical tanks

$$\frac{h_o d_o}{k} = 34 \left(\frac{L^2 N \rho}{\mu} \right)^{0.5} \left(\frac{C_p \mu}{k} \right)^{0.3} \left(\frac{d_g}{d_p} \right)^{0.8} \left(\frac{W}{d_c} \right)^{0.25} \left(\frac{L^2 d_o}{d_c^3} \right)^{0.1} \quad (9.205)$$

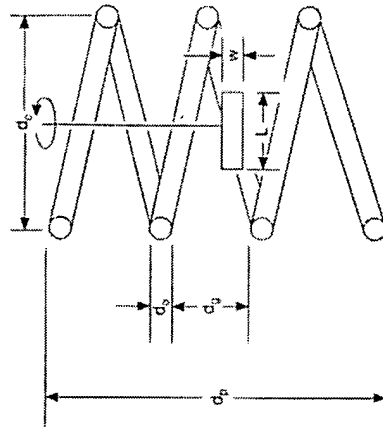


Figure 9.60. Arrangement of coil in Pratt's work⁽⁷⁹⁾

For square tanks:

$$\frac{h_o l_o}{k} = 39 \left(\frac{L^2 N \rho}{\mu} \right)^{0.5} \left(\frac{C_p \mu}{k} \right)^{0.3} \left(\frac{d_g}{d_p} \right)^{0.8} \left(\frac{W}{d_c} \right)^{0.25} \left(\frac{L^2 l_o}{d_p^3} \right)^{0.1} \quad (9.206)$$

where l_o is the length of the side of the vessel.

These give almost the same results as the earlier equations over a wide range of conditions. CUMMINGS and WEST⁽⁹⁴⁾ have tested these results with a much larger tank of 0.45 m³ capacity and have given an expression similar to equation 9.204 but with a constant of 1.01 instead of 0.87. A retreating blade turbine impeller was used, and in many cases a second impeller was mounted above the first, giving an agitation which is probably more intense than that attained by the other workers. A constant of 0.9 seems a reasonable average from existing work.

Example 9.24

Toluene is continuously nitrated to mononitrotoluene in a cast-iron vessel, 1 m diameter, fitted with a propeller agitator 0.3 m diameter rotating at 2.5 Hz. The temperature is maintained at 310 K by circulating 0.5 kg/s cooling water through a stainless steel coil 25 mm o.d. and 22 mm i.d. wound in the form of a helix, 0.80 m in diameter. The conditions are such that the reacting material may be considered to have the same physical properties as 75 per cent sulphuric acid. If the mean water temperature is 290 K, what is the overall coefficient of heat transfer?

Solution

The overall coefficient U_o based on the outside area of the coil is given by equation 9.201:

$$\frac{1}{U_o} = \frac{1}{h_o} + \frac{x_w d_o}{k_w d_w} + \frac{d_o}{h_i d} + R_o + \frac{R_i d_o}{d}$$

where d_w is the mean diameter of the pipe.

From equations 9.202 and 9.203, the inside film coefficient for the water is given by:

$$h_i = \frac{k}{d} \left(1 + 3.5 \frac{d}{d_c} \right) 0.023 \left(\frac{d u \rho}{\mu} \right)^{0.8} \left(\frac{C_p \mu}{k} \right)^{0.4}$$

In this equation:

$$\rho u = \frac{0.5}{(\pi/4) \times 0.022^2} = 1315 \text{ kg/m}^2 \text{ s}$$

$d = 0.022 \text{ m}$, $d_c = 0.80 \text{ m}$, $k = 0.59 \text{ W/m K}$, $\mu = 1.08 \text{ mN s/m}^2$ or $1.08 \times 10^{-3} \text{ N s/m}^2$, and $C_p = 4.18 \times 10^3 \text{ J/kg K}$

$$\begin{aligned} \text{Thus: } h_i &= \frac{0.59}{0.022} \left(1 + 3.5 \times \frac{0.022}{0.80} \right) 0.023 \left(\frac{0.022 \times 1315}{1.08 \times 10^{-3}} \right)^{0.8} \left(\frac{4.18 \times 10^3 \times 1.08 \times 10^{-3}}{0.59} \right)^{0.4} \\ &= 0.680(26.780)^{0.8}(7.65)^{0.4} = 5490 \text{ W/m}^2 \text{ K} \end{aligned}$$

The external film coefficient is given by equation 9.204:

$$\frac{h_o d_o}{k} \left(\frac{\mu_s}{\mu} \right)^{0.14} = 0.87 \left(\frac{C_p \mu}{k} \right)^{0.33} \left(\frac{L^2 N \rho}{\mu} \right)^{0.62}$$

For 75 per cent sulphuric acid:

$k = 0.40 \text{ W/m K}$, $\mu_s = 8.6 \times 10^{-3} \text{ N s/m}^2$ at 300 K, $\mu = 6.5 \times 10^{-3} \text{ N s/m}^2$ at 310 K, $C_p = 1.88 \times 10^3 \text{ J/kg K}$, and $\rho = 1666 \text{ kg/m}^3$

$$\text{Thus: } \frac{h_o \times 1.0}{0.40} \left(\frac{8.6}{6.5} \right)^{0.14} = 0.87 \left(\frac{1.88 \times 10^3 \times 6.5 \times 10^{-3}}{0.40} \right)^{0.33} \left(\frac{0.3^2 \times 2.5 \times 1666}{6.5 \times 10^{-3}} \right)^{0.62}$$

$$2.5 h_o \times 1.04 = 0.87 \times 3.09 \times 900$$

$$h_o = 930 \text{ W/m}^2 \text{ K}$$

and:

Taking $k_w = 15.9 \text{ W/m K}$ and R_o and R_i as 0.0004 and 0.0002 m² K/W, respectively:

$$\frac{1}{U_o} = \frac{1}{930} + \frac{0.0015 \times 0.025}{15.9 \times 0.0235} + \frac{0.025}{5490 \times 0.022} + 0.0004 + \frac{0.0002 \times 0.025}{0.022}$$

$$= 0.00107 + 0.00010 + 0.00021 + 0.00040 + 0.00023 = 0.00201$$

$$U_o = 498 \text{ W/m}^2 \text{ K}$$

and:

In this calculation a mean area of surface might have been used with sufficient accuracy. It is important to note the great importance of the scale terms which together form a major part of the thermal resistance.

9.8.2. Jacketed vessels

In many cases, heating or cooling of a reaction mixture is most satisfactorily achieved by condensing steam in a jacket or passing water through it—an arrangement which is often used for organic reactions where the mixture is too viscous for the use of coils and a high-speed agitator. CHILTON *et al.*⁽⁹³⁾ and CUMMINGS and WEST⁽⁹⁴⁾ have measured the transfer coefficients for this case by using an arrangement as shown in Figure 9.61, where heat is supplied to the jacket and simultaneously removed by passing water through the coil. Chilton measured the temperatures of the inside of the vessel wall, the bulk liquid, and the surface of the coil by means of thermocouples and thus obtained the film heat transfer coefficients directly. Cummings and West used an indirect method to give the film coefficient from measurements of the overall coefficients.

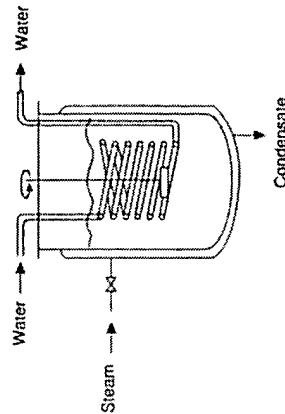


Figure 9.61. Reaction vessel with jacket and coil

CHILTON *et al.*⁽⁹³⁾ expressed their results by:

$$\frac{h_p d_o}{k} \left(\frac{\mu_s}{\mu} \right)^{0.14} = 0.36 \left(\frac{L^2 N \rho}{\mu} \right)^{0.67} \left(\frac{C_p \mu}{k} \right)^{0.33} \quad (9.207)$$

where h_b is the film coefficient for the liquor adjacent to the wall of the vessel. CUMMINGS and WEST⁽⁹⁴⁾ used the same equation although the coefficient was 0.40. Considering that Chilton's vessel was only 0.3 m in diameter and fitted with a single paddle of 150 mm length, and that Cummings and West used a 0.45 m³ vessel with two turbine impellers, agreement between their results is remarkably good. The group $(\mu_s/\mu)^{0.14}$ is again used to allow for the difference in the viscosities at the surface and in the bulk of the fluid.

BROWN *et al.*⁽⁹⁵⁾ have given data on the performance of 1.5 m diameter sulphphonators and nitrators of 3.4 m³ capacity as used in the dyestuffs industry. The sulphphonators were of cast iron and had a wall thickness of 25.4 mm; the annular space in the jacket being also 25.4 mm. The agitator of the sulphphonator was of the anchor type with a 127 mm clearance at the walls and was driven at 0.67 Hz. The nitrators were fitted with four-bladed propellers of 0.61 m diameter driven at 2 Hz. For cooling, the film coefficient h_b for the inside of the vessel was given by:

$$\frac{h_b d_v}{k} \left(\frac{\mu_s}{\mu} \right)^{0.14} = 0.55 \left(\frac{L^2 N \rho}{\mu} \right)^{0.67} \left(\frac{C_p \mu}{k} \right)^{0.25} \quad (9.208)$$

which is very similar to that given by equation 9.207.

The film coefficients for the water jacket were in the range 635–1170 W/m² K for water rates of 1.44–9.23 l/s, respectively. It may be noted that 7.58 l/s corresponds to a vertical velocity of only 0.061 m/s and to a Reynolds number in the annulus of 5350. The thermal resistance of the wall of the pan was important, since with the sulphphonator it accounted for 13 per cent of the total resistance at 323 K and 31 per cent at 403 K. The change in viscosity with temperature is important when considering these processes, since, for example, the viscosity of the sulphphonation liquors ranged from 340 mN s/m² at 323 K to 22 mN s/m² at 403 K.

In discussing equations 9.207 and 9.208 FLETCHER⁽⁹⁶⁾ has summarised correlations obtained for a wide range of impeller and agitator designs in terms of the constant before the Reynolds number and the index on the Reynolds number as shown in Table 9.11.

Table 9.11. Data on common agitators for use in equations 9.207 and 9.208

Type of agitator	Constant	Index
Flat blade disc turbine unbaffled, or baffled vessel, $Re < 400$	0.54	0.67
baffled, $Re > 400$	0.74	0.67
Retreating-blade turbine with three blades, jacked and baffled vessel, $Re = 2 \times 10^3$ to 2×10^6		
glassed steel impeller	0.33	0.67
alloy steel impeller	0.37	0.67
Propeller with three blades baffled vessel, $Re = 5500$ to 37,000	0.64	0.67
Flat blade paddle		
baffled or unbaffled vessel, $Re \geq 4000$	0.36	0.67
Anchor		
$Re = 30$ to 300	1.00	0.50
$Re = 300$ to 5000	0.38	0.67

9.8.3. Time required for heating or cooling

It is frequently necessary to heat or cool the contents of a large batch reactor or storage tank. In this case the physical constants of the liquor may alter and the overall transfer coefficient may change during the process. In practice, it is often possible to assume an average value of the transfer coefficient so as to simplify the calculation of the time required for heating or cooling. The heating of the contents of a storage tank is commonly effected by condensing steam, either in a coil or in some form of hairpin tube heater.

In the case of a storage tank with liquor of mass m and specific heat C_p , heated by steam condensing in a helical coil, it may be assumed that the overall transfer coefficient U is constant. If T_s is the temperature of the condensing steam, T_1 and T_2 the initial and final temperatures of the liquor, and A the area of heat transfer surface, and T is the temperature of the liquor at any time t , then the rate of transfer of heat is given by:

$$\begin{aligned} Q &= m C_p \frac{dT}{dt} = UA(T_s - T) \\ \frac{dT}{dt} &= \frac{UA}{m C_p} (T_s - T) \\ \int_{T_1}^{T_2} \frac{dT}{T_s - T} &= \frac{UA}{m C_p} \int_0^t dt \\ \ln \frac{T_s - T_1}{T_s - T_2} &= \frac{UA}{m C_p} t \end{aligned} \quad (9.209)$$

From this equation, the time t of heating from T_1 to T_2 , may be calculated. The same analysis may be used if the steam condenses in a jacket of a reaction vessel.

This analysis does not allow for any heat losses during the heating, or, for that matter, cooling operation. Obviously the higher the temperature of the contents of the vessel, the greater are the heat losses and, in the limit, the heat supplied to the vessel is equal to the heat losses, at which stage no further rise in the temperature of the contents of the vessel is possible. This situation is illustrated in Example 9.25.

The heating-up time can be reduced by improving the rate of heat transfer to the fluid, by agitating of the fluid for example, and by reducing heat losses from the vessel by insulation. In the case of a large vessel there is a limit to the degree of agitation possible, and circulation of the fluid through an external heat exchanger is an attractive alternative.

Example 9.25

A vessel contains 1 tonne (1 Mg) of a liquid of specific heat capacity 4.0 kJ/kg K. The vessel is heated by steam at 393 K which is fed to a coil immersed in the agitated liquid and heat is lost to the surroundings at 293 K from the outside of the vessel. How long does it take to heat the liquid from 293 to 353 K and what is the maximum temperature to which the liquid can be heated? When the liquid temperature has reached 353 K, the steam supply is turned off for 2 hours (7.2 ks) and the vessel cools. How long will it take to reheat the material to 353 K? The surface area of the coil is 0.5 m² and the overall coefficient of heat transfer to the liquid may be taken as 600 W/m² K. The outside area of the vessel is 6 m² and the coefficient of heat transfer to the surroundings may be taken as 10 W/m² K.

Solution

If T K is the temperature of the liquid at time t s, then a heat balance on the vessel gives:

$$(1000 \times 4000) \frac{dT}{dt} = (600 \times 0.5)(393 - T) - (10 \times 6)(T - 293)$$

$$\text{or: } 4,000,000 \frac{dT}{dt} = 135,480 - 360T$$

$$\text{and: } 11,111 \frac{dT}{dt} = 376.3 - T$$

The equilibrium temperature occurs when $dT/dt = 0$,

that is when:

$$T = \underline{\underline{376.3 \text{ K}}}$$

In heating from 293 to 353 K, the time taken is:

$$\begin{aligned} t &= 11,111 \int_{293}^{353} \frac{dT}{(376.3 - T)} \\ &= 11,111 \ln \left(\frac{83.3}{23.3} \right) \\ &= \underline{\underline{14,155 \text{ s (or 3.93 h)}}} \end{aligned}$$

The steam is turned off for 7200 s and during this time a heat balance gives:

$$\begin{aligned} (1000 \times 4000) \frac{dT}{dt} &= -(10 \times 6)(T - 293) \\ 66,700 \frac{dT}{dt} &= 293 - T \end{aligned}$$

The change in temperature is then given by:

$$\begin{aligned} \int_{353}^T \frac{dT}{(293 - T)} &= \frac{1}{66,700} \int_0^{7200} dt \\ \ln \frac{-60}{293 - T} &= \frac{7200}{66,700} = 0.108 \\ T &= \underline{\underline{346.9 \text{ K}}} \end{aligned}$$

The time taken to reheat the liquid to 353 K is then given by:

$$\begin{aligned} t &= 11,111 \int_{346.9}^{353} \frac{dT}{(376.3 - T)} \\ &= 11,111 \ln \left(\frac{29.4}{23.3} \right) \\ &= \underline{\underline{2584 \text{ s (0.72 h)}}} \end{aligned}$$

9.9. SHELL AND TUBE HEAT EXCHANGERS

9.9.1. General description

Since shell and tube heat exchangers can be constructed with a very large heat transfer surface in a relatively small volume, fabricated from alloy steels to resist corrosion and

be used for heating, cooling and for condensing a very wide range of fluids, they are the most widely used form of heat transfer equipment. Figures 9.62-9.64 show various forms of construction and a tube bundle is shown in Figure 9.65. The simplest type of unit, shown in Figure 9.62, has fixed tube plates at each end into which the tubes are expanded. The tubes are connected so that the internal fluid makes several passes up and

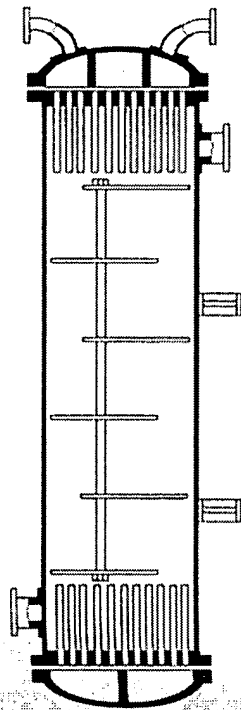


Figure 9.62. Heat exchanger with fixed tube plates (four tube, one shell-pass)

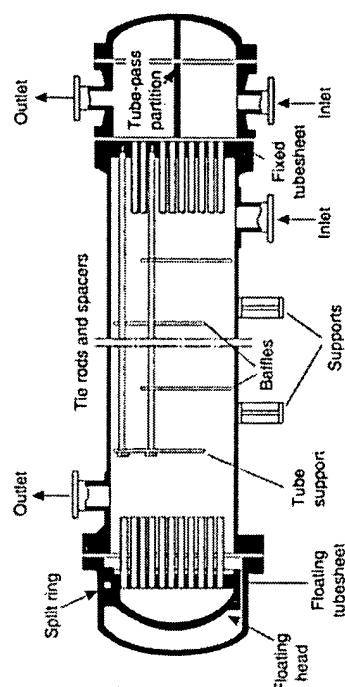


Figure 9.63. Heat exchanger with floating head (two tube-pass, one shell-pass)

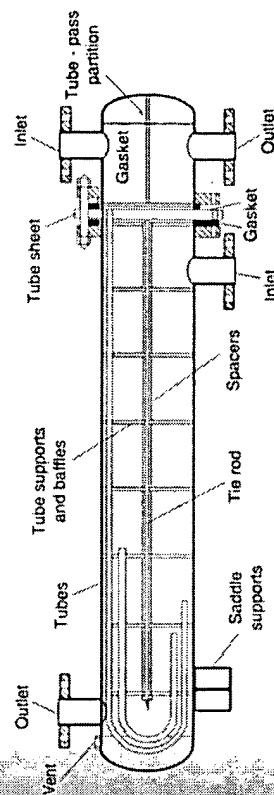


Figure 9.64. Heat exchanger with hairpin tubes

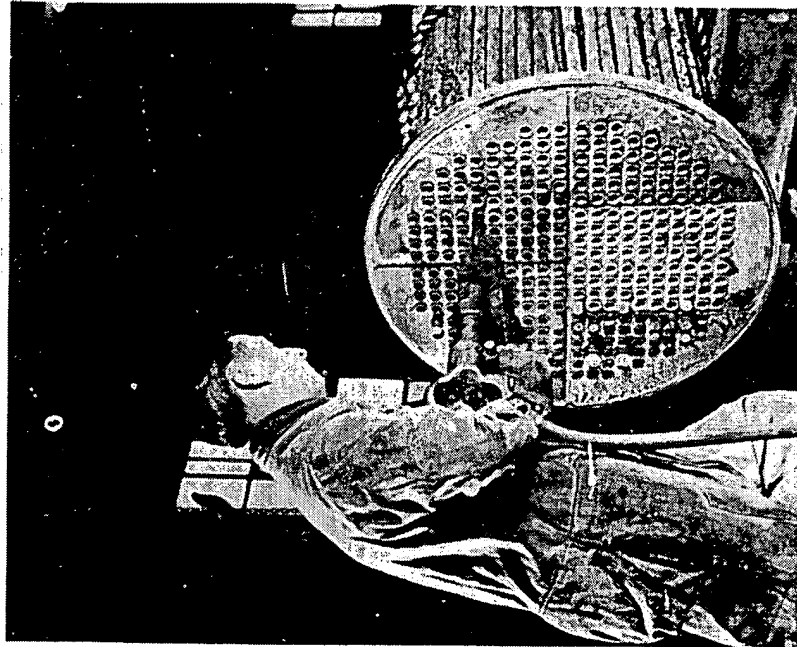


Figure 9.65. Expanding the ends of the tubes into the tube plate of a heat exchanger bundle

down the exchanger thus enabling a high velocity of flow to be obtained for a given heat transfer area and throughput of fluid. The fluid flowing in the shell is made to flow first in one sense and then in the opposite sense across the tube bundle by fitting a series of baffles along the length. These baffles are frequently of the segmental form with about 25 per cent cut away, as shown in Figure 9.29 to provide the free space to increase the velocity of flow across the tubes, thus giving higher rates of heat transfer. One problem with this type of construction is that the tube bundle cannot be removed for cleaning and although an expansion joint may be fitted to the shell.

In order to allow for the removal of the tube bundle and for considerable expansion of the tubes, a floating head exchanger is used, as shown in Figure 9.63. In this arrangement one tube plate is fixed as before, but the second is bolted to a floating head cover so that the tube bundle can move relative to the shell. This floating tube sheet is clamped

between the floating head and a split backing flange in such a way that it is relatively easy to break the flanges at both ends and to draw out the tube bundle. It may be noted that the shell cover at the floating head end is larger than that at the other end. This enables the tubes to be placed as near as possible to the edge of the fixed tube plate, leaving very little unused space between the outer ring of tubes and the shell.

Another arrangement which provides for expansion involves the use of hairpin tubes, as shown in Figure 9.64. This design is very commonly used for the reboilers on large fractionating columns where steam is condensed inside the tubes.

In these designs there is one pass for the fluid on the shell-side and a number of passes on the tube-side. It is often an advantage to have two or more shell-side passes, although this considerably increases the difficulty of construction and, very often therefore, several smaller exchangers are connected together to obtain the same effect.

The essential requirements in the design of a heat exchanger are, firstly, the provision of a unit which is reliable and has the desired capacity, and secondly, the need to provide an exchanger at minimum overall cost. In general, this involves using standard components and fittings and making the design as simple as possible. In most cases, it is necessary to balance the capital cost in terms of the depreciation against the operating cost. Thus in a condenser, for example, a high heat transfer coefficient is obtained and hence a small exchanger is required if a higher water velocity is used in the tubes.

Against this, the cost of pumping increases rapidly with increase in velocity and an economic balance must be struck. A typical graph showing the operating costs, depreciation and the total cost plotted as a function of the water velocity in the tubes is shown in Figure 9.66.

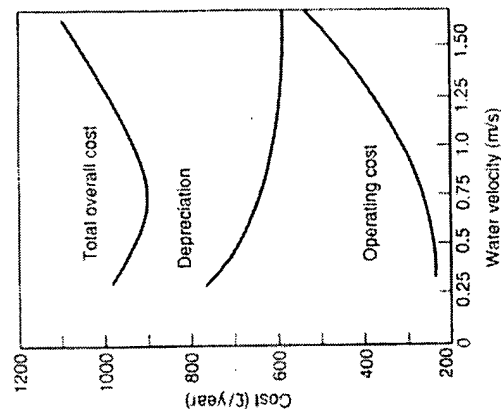


Figure 9.66. Effect of water velocity on annual operating cost of condenser

9.9.2. Basic components

The various components which make up a shell and tube heat exchanger are shown in Figures 9.63 and 9.64 and these are now considered. Many different mechanical arrangements are used and it is convenient to use a basis for classification. The standard published by the Tubular Exchanger Manufacturer's Association (TEMA⁽⁹⁷⁾) is outlined here. It should be added that noting that SAUNDERS⁽⁹⁸⁾ has presented a detailed discussion of design codes and problems in fabrication.

Of the various *shell types* shown in Figure 9.67, the simplest, with entry and exit nozzles at opposite ends of a single pass exchanger, is the TEMA E-type on which most design methods are based, although these may be adapted for other shell types by allowing for the resulting velocity changes. The TEMA F-type has a longitudinal baffle giving two shell passes and this provides an alternative arrangement to the use of two shells required in order to cope with a close temperature approach or low shell-side flowrates. The pressure drop in two shells is some eight times greater than that encountered in the E-type design although any potential leakage between the longitudinal baffle and the shell in the F-type design may restrict the range of application. The so-called "split-flow" type of unit with a longitudinal baffle is classified as the TEMA G-type whose performance is superior although the pressure drop is similar to the E-type. This design is used mainly for reboilers and only occasionally for systems where there is no change of phase. The so-called "divided-flow" type, the TEMA J-type, has one inlet and two outlet nozzles and with a pressure drop some one-eighth of the E-type, finds application in gas coolers and condensers operating at low pressures. The TEMA X-type shell has no cross baffles and hence the shell-side fluid is in pure counterflow giving extremely low pressure drops and again, this type of design is used for gas cooling and condensation at low pressures.

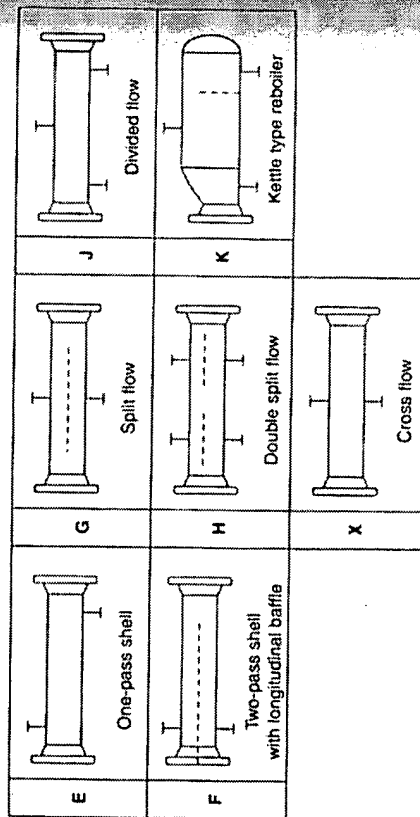


Figure 9.67. TEMA shell types

The *shell* of a heat exchanger is commonly made of carbon steel and standard pipes are used for the smaller sizes and rolled welded plate for the larger sizes (say 0.4–1.0 m).

The thickness of the shell may be calculated from the formula for thin-walled cylinders and a minimum thickness of 9.5 mm is used for shells over 0.33 m o.d. and 11.1 mm for shells over 0.9 m o.d. Unless the shell is designed to operate at very high pressures, the calculated wall thickness is usually less than these values although a corrosion allowance of 3.2 mm is commonly added to all carbon steel parts and thickness is determined more by rigidity requirements than simply internal pressure. The minimum shell thickness for various materials is given in BS3274⁽⁹⁹⁾. A shell diameter should be such as to give as close a fit to the tube bundle as practical in order to reduce bypassing round the outside of the bundle. Typical values for the clearance between the outer tubes in the bundle and the inside diameter of the shell are given in Figure 9.68 for various types of exchanger.

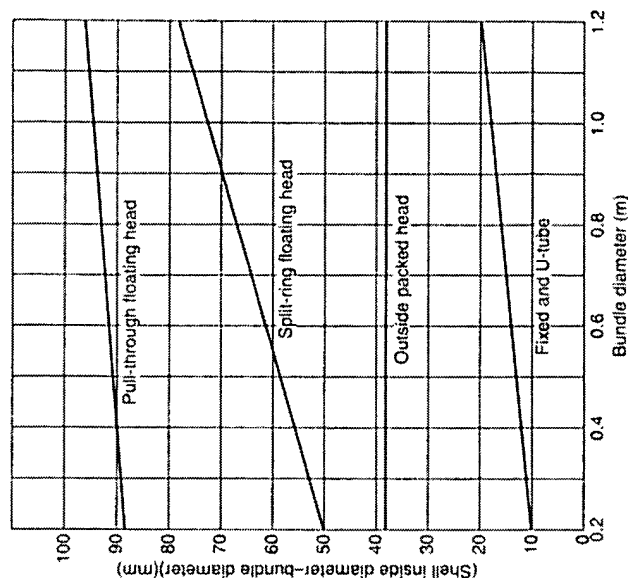


Figure 9.68. Shell-bundle clearance

The detailed design of the *tube bundle* must take into account both shell-side and tube-side pressures since these will both affect any potential leakage between the tube bundle and the shell which cannot be tolerated where high purity or uncontaminated materials are required. In general, tube bundles make use of a fixed tubesheet, a floating-head or U-tubes which are shown in Figures 9.62, 9.63 and 9.64 respectively. It may be noted here that the thickness of the fixed tubesheet may be obtained from a relationship of the form:

$$d_t = d_G \sqrt{0.25P/f} \quad (9.210)$$

where d_G is the diameter of the gasket (m), P the design pressure (MN/m^2), f the allowable working stress (MN/m^2) and d_i the thickness of the sheet measured at the bottom of the partition plate grooves. The thickness of the floating head tubesheet is very often calculated as $\sqrt{2d_i}$.

In selecting a tube diameter, it may be noted that smaller tubes give a larger heat transfer area for a given shell, although 19 mm o.d. tubes are normally the minimum size used in order to permit adequate cleaning. Although smaller diameters lead to shorter tubes, more holes have to be drilled in the tubesheet which adds to the cost of construction and increases the likelihood of tube vibration. Heat exchanger tubes are usually in the range 16 mm ($\frac{5}{8}$ in) to 50 mm (2 in) O.D.; the smaller diameter usually being preferred as these give more compact and therefore cheaper units. Against this, larger tubes are easier to clean especially by mechanical methods and are therefore widely used for heavily fouling fluids. The tube thickness or gauge must be such as to withstand the internal pressure and also to provide an adequate corrosion allowance. Details of steel tubes used in heat exchangers are given in BS3606⁽¹⁰⁰⁾ and summarised in Table 9.12, and standards for other materials are given in BS3274⁽⁹⁹⁾.

Table 9.12. Standard dimensions of steel tubes

Outside diameter d_o (mm)	Wall thickness (mm)	Cross sectional area for flow		Surface area per unit length	
		(m^2)	(ft^2)	(m^2/m)	(ft^2/ft)
16	0.630	0.001145	0.00156	0.0503	0.165
	1.6	0.00129	0.00139		
	2.0	0.00113	0.00122		
20	0.787	0.00222	0.00239	0.0628	0.206
	1.6	0.00201	0.00216		
	2.0	0.00172	0.00185		
25	0.984	0.00373	0.00402	0.0785	0.258
	1.6	0.00346	0.00373		
	2.0	0.00308	0.00331		
30	1.181	0.00564	0.00607	0.0942	0.309
	1.6	0.00531	0.00572		
	2.0	0.00483	0.00512		
38	1.496	0.00937	0.01010	0.1194	0.392
	2.0	0.00845	0.00910		
	2.6	0.00784	0.00844		
50	1.969	0.01662	0.01789	0.1571	0.515
	2.0	0.01576	0.01697		
	2.6	0.01493	0.01607		

In general, the larger the tube length, the lower is the cost of an exchanger for a given surface area due to the smaller shell diameter, the thinner tube sheets and flanges and the smaller number of holes to be drilled, and the reduced complexity. Preferred tube lengths are 1.83 m (6 ft), 2.44 m (8 ft), 3.88 m (12 ft) and 4.88 m (16 ft); larger sizes are used where the total tube-side flow is low and fewer, longer tubes are required in order to obtain a required velocity. With the number of tubes per tube-side pass fixed in order to obtain a required velocity, the total length of tubes per tube-side pass is determined by the heat transfer surface required. It is then necessary to fit the tubes into a suitable shell

to give the desired shell-side velocity. It may be noted that with long tube lengths and relatively few tubes in a shell, it may be difficult to arrange sufficient baffles for adequate support of the tubes. For good all-round performance, the ratio of tube length to shell diameter is usually in the range 5–10.

Tube layout and pitch. considered in Section 9.4.4 and shown in Figure 9.69, make use of equilateral triangular, square and staggered square arrays. The triangular layout gives a robust tube sheet although, because the vertical and horizontal distances between adjacent tubes is generally greater in a square layout compared with the equivalent triangular pitch design, the square array simplifies maintenance and particularly cleaning on the shell-side. Good practice requires a minimum pitch of 1.25 times the tube diameter and/or a minimum web thickness between tubes of about 3.2 mm to ensure adequate strength for tube rolling. In general, the smallest pitch in triangular 30° layout is used for clean fluids in both laminar and turbulent flow and a 90° or 45° layout with a 6.4 mm clearance where mechanical cleaning is required. The bundle diameter, d_b , may be estimated from the following empirical equation which is based on standard tube layouts:

$$\text{Number of tubes, } N_t = a(d_b/d_o)^b \quad (9.211)$$

where the values of the constants a and b are given in Table 9.13. Tables giving the number of tubes that can be accommodated in standard shells using various tube sizes, pitches and numbers of passes for different exchanger types are given, for example, in KERN⁽²⁸⁾ and LUDWIG⁽¹⁰¹⁾.

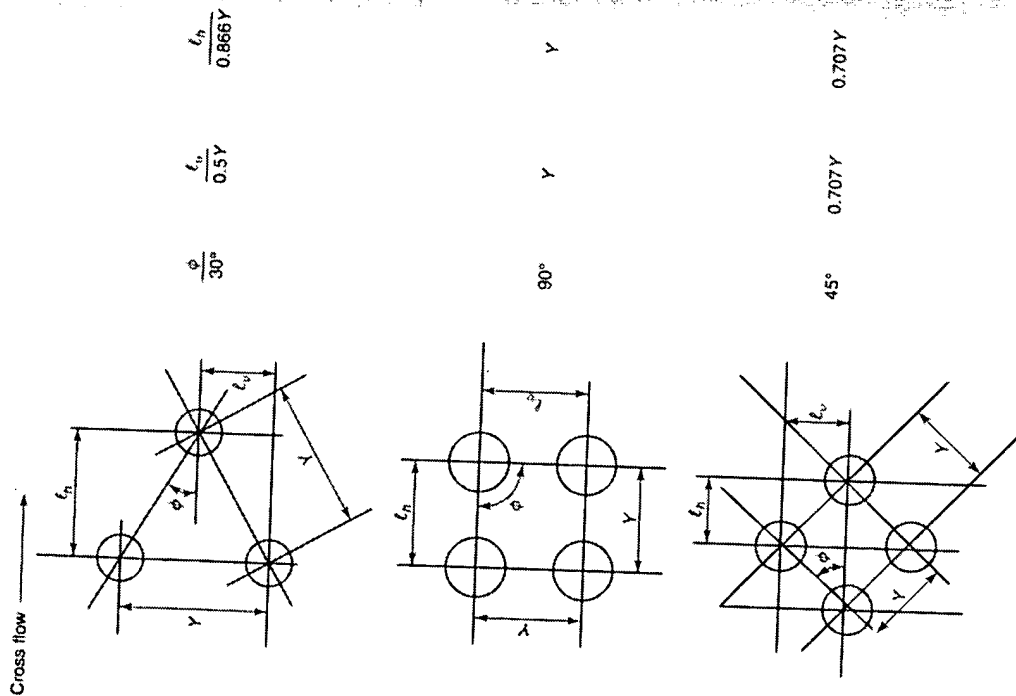
Table 9.13. Constants for use with equation 9.211.

Number of passes	Constants for use with equation 9.211.					
	1	2	4	6	8	
Triangular pitch*	a	0.319	0.249	0.175	0.0743	0.0365
	b	2.142	2.207	2.285	2.499	2.675
Square pitch*	a	0.215	0.156	0.158	0.0402	0.0331
	b	2.207	2.291	2.263	1.617	2.643

*Pitch = $1.25d_o$

Various baffle designs are shown in Figure 9.70. The cross-baffle is designed to direct the flow of the shell-side fluid across the tube bundle and to support the tubes against sagging and possible vibration, and the most common type is the segmental baffle which provides a baffle window. The ratio, baffle spacing/baffle cut, is very important in maximising the ratio of heat transfer rate to pressure drop. Where very low pressure drops are required, double segmental or "disc and doughnut" baffles are used to reduce the pressure drop by some 60 per cent. Triple segmental baffles and designs in which all the tubes are supported by all the baffles provide for low pressure drops and minimum tube vibration.

With regard to baffle spacing, TEMA⁽⁹⁷⁾ recommends that segmental baffles should not be spaced closer than 20 per cent of the shell inside diameter or 50 mm whichever is the greater and that the maximum spacing should be such that the unsupported tube lengths, given in Table 9.14, are not exceeded. It may be noted that the majority of failures due to vibration occur when the unsupported tube length is in excess of 80 per cent of the TEMA maximum; the best solution is to avoid having tubes in the baffle window.

Figure 9.69. Examples of tube arrays.⁽⁹⁷⁾

9.9.3. Mean temperature difference in multipass exchangers

In an exchanger with one shell pass and several tube-side passes, the fluids in the tubes and shell will flow co-currently in some of the passes and countercurrently in the others. For given inlet and outlet temperatures, the mean temperature difference for countercurrent flow is greater than that for co-current or parallel flow, and there is no easy way of

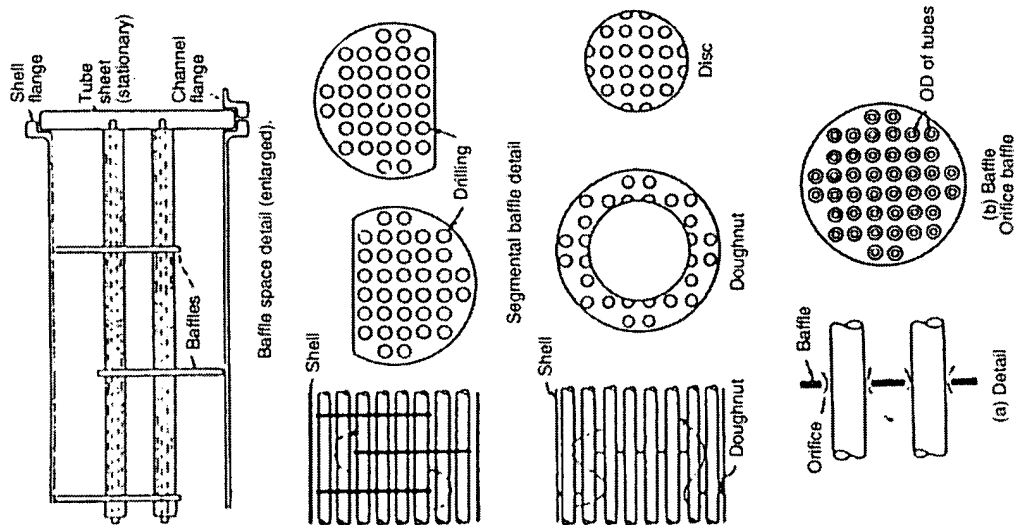


Figure 9.70. Baffle designs

finding the true temperature difference for the unit. The problem has been investigated by UNDERWOOD⁽¹⁰²⁾ and by BOWMAN *et al.*⁽¹⁰³⁾ who have presented graphical methods for calculating the true mean temperature difference in terms of the value of θ_m which would be obtained for countercurrent flow, and a correction factor F . Provided the following conditions are maintained or assumed, F can be found from the curves shown in Figures 9.71–9.74.

Table 9.14. Maximum unsupported spans for tubes

Approximate tube OD, (mm)	Maximum unsupported span (mm)	
	Materials group A	Materials group B
19	1520	1321
25	1880	1626
32	2240	1930
38	2540	2210
50	3175	2794

Materials

Group A: Carbon and high alloy steel, low alloy steel, nickel-copper, nickel, nickel-chromium-iron.
 Group B: Aluminium and aluminium alloys, copper and copper alloys, titanium and zirconium.

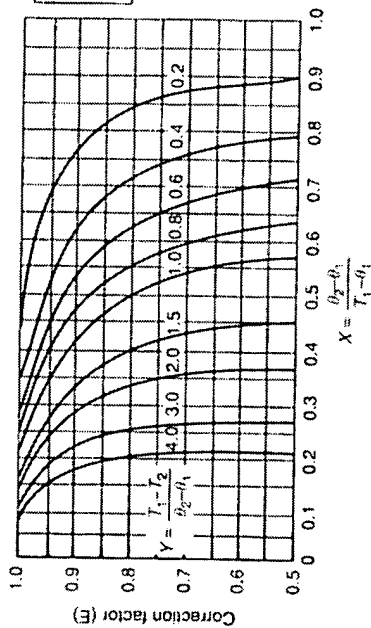


Figure 9.71. Correction for logarithmic mean temperature difference for single shell pass exchanger

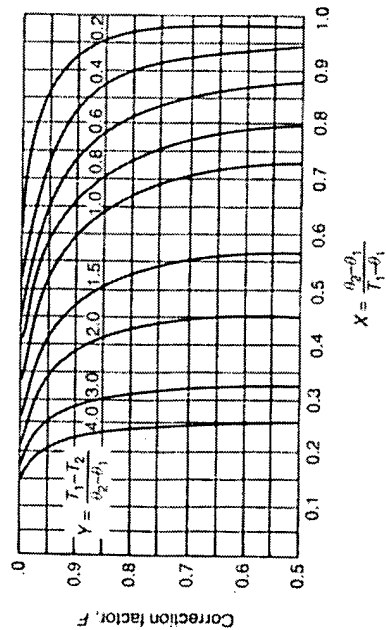


Figure 9.72. Correction for logarithmic mean temperature difference for double shell pass exchanger

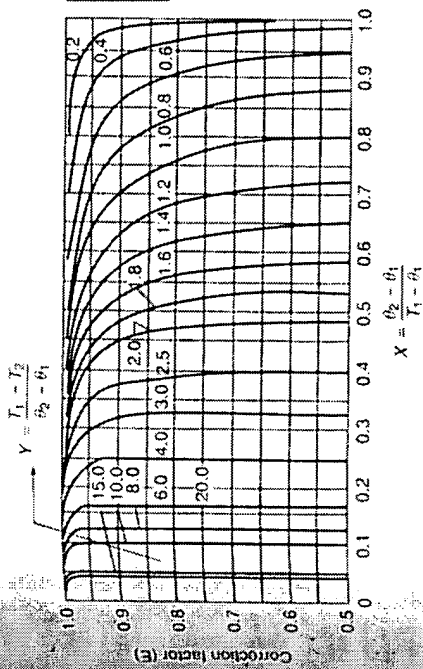


Figure 9.73. Correction for logarithmic mean temperature difference for three shell pass exchanger

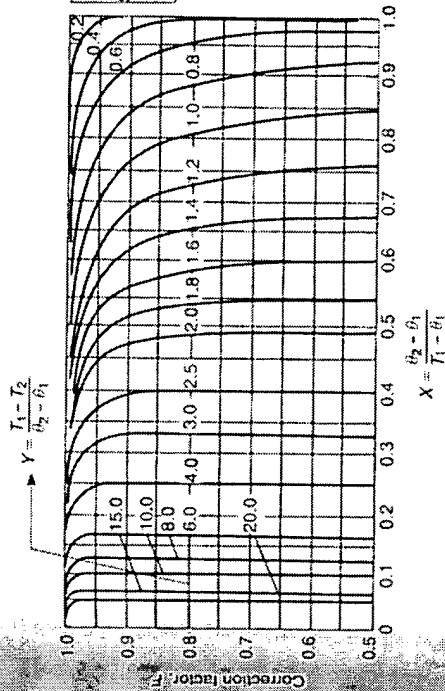


Figure 9.74. Correction for logarithmic mean temperature difference for four shell pass exchanger

- The shell fluid temperature is uniform over the cross-section considered as constituting a pass.
- There is equal heat transfer surface in each pass.
- The overall heat transfer coefficient U is constant throughout the exchanger.
- The heat capacities of the two fluids are constant over the temperature range.
- There is no change in phase of either fluid.
- Heat losses from the unit are negligible.

Then:

$$Q = UAF\theta_m \quad (9.212)$$

F is expressed as a function of two parameters:

$$X = \frac{\theta_2 - \theta_1}{T_1 - \theta_1} \quad \text{and} \quad Y = \frac{T_1 - T_2}{\theta_2 - \theta_1} \quad (9.213)$$

If a one shell-side system is used Figure 9.71 applies, for two shell-side passes Figure 9.72, for three shell-side passes Figure 9.73, and for four shell-side passes Figure 9.74. For the case of a single shell-side pass and two tube-side passes illustrated in Figures 9.75a and 9.75b, the temperature profile is as shown. Because one of the passes constitutes a parallel flow arrangement, the exit temperature of the cold fluid θ_2 cannot closely approach the hot fluid temperature T_1 . This is true for the conditions shown in Figures 9.75a and 9.75b and UNDERWOOD⁽¹⁰²⁾ has shown that F is the same in both cases.

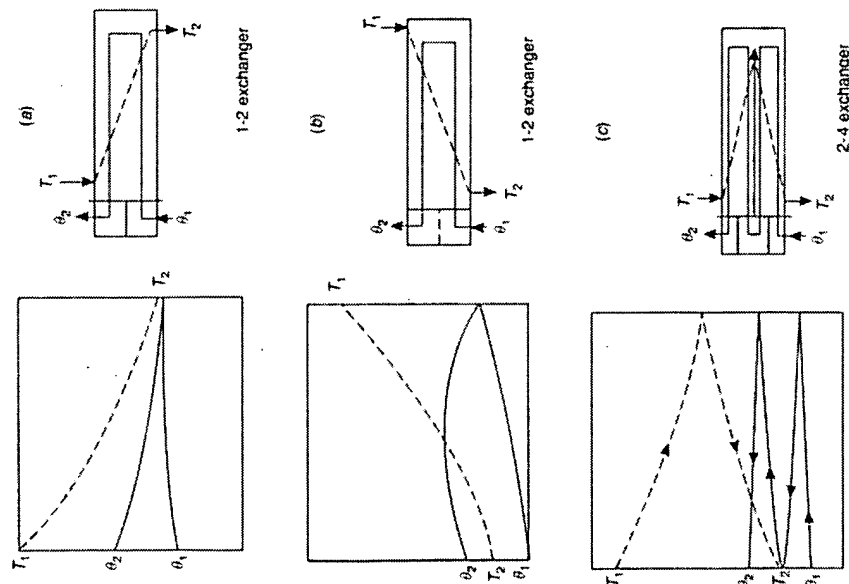


Figure 9.75. Temperature profiles in single and double shell pass exchangers

if, for example, an exchanger is required to operate over the following temperatures:

$$T_1 = 455 \text{ K}, \quad T_2 = 372 \text{ K}$$

$$\theta_1 = 283 \text{ K}, \quad \theta_2 = 388 \text{ K}$$

$$X = \frac{\theta_2 - \theta_1}{T_1 - \theta_1} = \frac{388 - 283}{455 - 283} = 0.6$$

Then:

$$Y = \frac{T_1 - T_2}{\theta_2 - \theta_1} = \frac{455 - 372}{388 - 283} = 0.8$$

and:

For a single shell pass arrangement, from Figure 9.71 F is 0.65 and, for a double shell pass arrangement, from Figure 9.72 F is 0.95. On this basis, a two shell-pass design would be used.

In order to obtain maximum heat recovery from the hot fluid, θ_2 should be as high as possible. The difference $(T_2 - \theta_2)$ is known as the *approach temperature* and, if $\theta_2 > T_2$, then a *temperature cross* is said to occur; a situation where the value of F decreases very rapidly when there is but a single pass on the shell-side. This implies that, in parts of the heat exchanger, heat is actually being transferred in the wrong direction. This may be illustrated by taking as an example the following data where equal ranges of temperature are considered:

Case	T_1	T_2	θ_1	θ_2	Approach	X	Y	F
1	613	513	363	463	($T_2 - \theta_2$)	0.4	1	0.92
2	573	473	373	473	0	0.5	1	0.80
3	543	443	363	463	cross of 20	0.55	1	0.66

If a temperature cross occurs with a single pass on the shell-side, a unit with two shell passes should be used. It is seen from Figure 9.75b that there may be some point where the temperature of the cold fluid is greater than θ_2 so that beyond this point the stream will be cooled rather than heated. This situation may be avoided by increasing the number of shell passes. The general form of the temperature profile for a two shell-side unit is as shown in Figure 9.75c. Longitudinal shell-side baffles are rather difficult to fit and there is a serious chance of leakage. For this reason, the use of two exchangers arranged in series, one below the other, is to be preferred. It is even more important to employ separate exchangers when three passes on the shell-side are required. On the very largest installations it may be necessary to link up a number of exchangers in parallel arranged as, say, sets of three in series as shown in Figure 9.76. This arrangement is preferable for any very large unit which would be unwieldy as a single system. When the total surface area is much greater than 250 m², consideration should be given to using multiple smaller units even though the initial cost may be higher.

In many processing operations there may be a large number of process streams, some of which need to be heated and others cooled. An overall heat balance will indicate whether, in total, there is a net surplus or deficit of heat available. It is of great economic importance to achieve the most effective match of the hot and cold streams in the heat exchanger network so as to reduce to a minimum both the heating and cooling duties placed on the works utilities, such as supplies of steam and cooling water. This necessitates making the best use of the temperature driving forces. In considering the overall requirements there will be some point where the temperature difference between the hot and cold streams is a

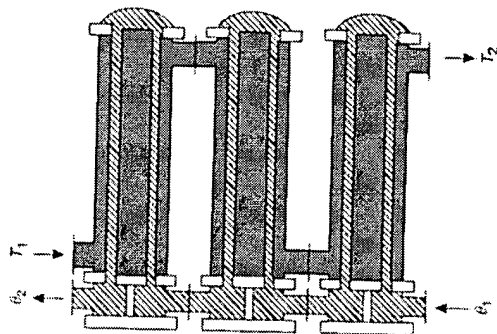


Figure 9.76. Set of three heat exchangers in series

minimum and this is referred to as the *pinch*. The lower the temperature difference at the pinch point, the lower will be the demand on the utilities, although it must be remembered that a greater area, (and hence cost) will be involved and an economic balance must therefore be struck. Heat exchanger networks are discussed in Volume 6 and, in detail, in the User Guide published by the Institution of Chemical Engineers⁽¹⁰⁵⁾. Subsequently, LINNHOFF⁽¹⁰⁵⁾ has given an overview of the industrial application of pinch analysis to the design of networks in order to reduce both capital costs and energy requirements.

Example 9.26

Using the data of Example 9.1, calculate the surface area required to effect the given duty using a multipass heat exchanger in which the cold water makes two passes through the tubes and the hot water makes a single pass through the shell.

Solution

As in Example 9.1, the heat load = 1672 kW

With reference to Figure 9.71: $T_1 = 360$ K, $T_2 = 340$ K

and hence: $X = \frac{\theta_2 - \theta_1}{T_1 - \theta_1} = \frac{316 - 300}{360 - 300} = 0.267$

and: $Y = \frac{T_1 - T_2}{\theta_2 - \theta_1} = \frac{360 - 340}{316 - 300} = 1.25$

from Figure 9.58: $F = 0.97$

HEAT TRANSFER

$$F\theta_m = (41.9 \times 0.97) = 40.6 \text{ K}$$

and hence:

$$A = \frac{1672}{2 \times 40.6} = 20.6 \text{ m}^2$$

The heat transfer area is then:

9.9.4. Film coefficients

Practical values

In any item of heat transfer equipment, the required area of heat transfer surface for a given load is determined by the overall temperature difference θ_m , the overall heat transfer coefficient U and the correction factor F in equation 9.212. The determination of the individual film coefficients which determine the value of U has proved difficult even for simple cases, and it is quite common for equipment to be designed on the basis of practical values of U rather than from a series of film coefficients. For the important case of the transfer of heat from one fluid to another across a metal surface, two methods have been developed for measuring film coefficients. The first requires a knowledge of the temperature difference across each film and therefore involves measuring the temperatures of both fluids and the surface of separation. With a concentric tube system, it is very difficult to insert a thermocouple into the thin tube and to prevent the thermocouple connections from interfering with the flow of the fluid. Nevertheless, this method is commonly adopted, particularly when electrical heating is used. It must be noted that when the heat flux is very high, as with boiling liquids, there will be an appreciable temperature drop across the tube wall and the position of the thermocouple is then important. For this reason, working with stainless steel, which has a relatively low thermal conductivity, is difficult.

The second method uses a technique proposed by WILSON⁽¹⁰⁶⁾. If steam is condensing on the outside of a horizontal tube through which water is passed at various velocities, then the overall and film transfer coefficients are related by:

$$\frac{1}{U} = \frac{1}{h_o} + \frac{x_w}{k_w} + R_i + \frac{1}{h_i} \quad (\text{from equation 9.201})$$

provided that the transfer area on each side of the tube is approximately the same.

For conditions of turbulent flow the transfer coefficient for the water side, $h_i = \epsilon \mu^{0.8}$, R_i the scale resistance is constant, and h_o the coefficient for the condensate film is almost independent of the water velocity. Thus, equation 9.201 reduces to:

$$\frac{1}{U} = (\text{constant}) + \frac{1}{\epsilon \mu^{0.8}}$$

If $1/U$ is plotted against $1/\mu^{0.8}$ a straight line, known as a Wilson plot, is obtained with a slope of $1/\epsilon$ and an intercept equal to the value of the constant. For a clean tube R_i should be nil, and hence h_o can be found from the value of the intercept, as x_w/k_w will generally be small for a metal tube. h_i may also be obtained at a given velocity from the difference between $1/U$ at that velocity and the intercept.

This technique has been applied by RHODES and YOUNGER⁽¹⁰⁷⁾ to obtain the values of h_o for condensation of a number of organic vapours, by PRATT⁽⁹²⁾ to obtain the inside coefficient for coiled tubes, and by COULSON and MEHTA⁽¹⁰⁸⁾ to obtain the coefficient for

Table 9.15. Thermal resistance of heat exchanger tubes

Gauge (BWG)	Thickness (mm)	Values of x_w/k_w ($m^2 K/KW$)		
		Copper	Steel	Aluminum
18	1.24	0.0031	0.019	0.083
16	1.65	0.0042	0.025	0.109
14	2.10	0.0055	0.032	0.141
12	2.77	0.0072	0.042	0.176
Values of x_w/k_w ($ft^2 h^2/Btu$)				
18	0.049	0.000018	0.00011	0.00047
16	0.065	0.000024	0.00014	0.00062
14	0.083	0.000031	0.00018	0.00086
12	0.109	0.000041	0.00024	0.0011

Table 9.16. Thermal resistances of scale deposits from various fluids

Water*	m ² /KW	ft ² h ² /Btu		m ² /KW	ft ² h ² /Btu
		good quality, oil-free	poor quality, oil-free		
distilled sea	0.09	0.0005	0.0012	0.052	0.0003
clear river	0.21	0.0015	0.0033	0.09	0.0005
untreated cooling tower	0.58	0.0015	0.0015	0.18	0.001
treated cooling tower	0.26	0.0015	0.0015	0.27	0.0015
treated boiler feed	0.26	0.0015	0.0015	0.18	0.001
hard well	0.58	0.0033	0.0033	1.0	0.006
Gases				2.0	0.01
air	0.25-0.50	0.0015-0.003	0.0015-0.003		
solvent vapours	0.14	0.0008	0.0008		

*For a velocity of 1 m/s (≈ 3 ft/s) and temperatures of less than 320 K (122°F)

an annulus. If the results are repeated over a period of time, the increase in the value of R_f can also be obtained by this method.

Typical values of thermal resistances and individual and overall heat transfer coefficients are given in Tables 9.15-9.18.

Correlated data

Heat transfer data for turbulent flow inside conduits of uniform cross-section are usually correlated by a form of equation 9.66;

$$Nu = C Re^{0.5} Pr^{0.33} (\mu/\mu_s)^{0.14} \quad (9.214)$$

where, based on the work of SIEDER and TATE⁽¹⁷⁾, the index for the viscosity correction term is usually 0.14 although higher values have been reported. Using values of C of 0.021 for gases, 0.023 for non-viscous liquids and 0.027 for viscous liquids, equation 9.214 is sufficiently accurate for design purposes, and any errors are far outweighed by uncertainties in predicting shell-side coefficients. Rather more accurate tube-side data

Table 9.17. Approximate overall heat transfer coefficients U for shell and tube equipment

	Hot side	Cold side	Overall U	
			$W/m^2 K$	$Btu/h ft^2 ^\circ F$
Condensers				
Steam (pressure)		Water	2000-4000	350-750
Steam (vacuum)		Water	1700-3400	300-600
Saturated organic solvents (atmospheric)		Water	600-1200	100-200
Saturated organic solvents (vacuum some non-condensable)		Water-brine	300-700	50-120
Organic solvents (atmospheric and high non-condensable)		Water-brine	100-500	20-80
Organic solvents (vacuum and high non-condensable)		Water-brine	60-300	10-50
Low boiling hydrocarbons (atmospheric)		Water	400-1200	80-200
High boiling hydrocarbons (vacuum)		Water	60-200	10-30
Heaters				
Steam		Water	1500-4000	250-750
Steam		Light oils	300-900	50-150
Steam		Heavy oils	60-400	10-80
Steam		Organic solvents	600-1200	100-200
Steam		Gases	30-300	5-50
Dowtherm		Gases	20-200	4-40
Dowtherm		Heavy oils	50-400	8-60
Evaporators				
Steam		Water	2000-4000	350-750
Steam		Organic solvents	600-1200	100-200
Steam		Light oils	400-1000	80-180
Steam		Heavy oils (vacuum)	150-400	25-75
Water		Refrigerants	400-900	75-150
Organic solvents		Refrigerants	200-600	30-100
Heat exchangers (no change of state)				
Water		Water	900-1700	150-300
Organic solvents		Water	300-900	50-150
Gases		Water	20-300	3-50
Light oils		Water	400-900	60-160
Heavy oils		Water	60-300	10-50
Organic solvents		Light oil	100-400	20-70
Water		Brine	600-1200	100-200
Organic solvents		Brine	200-500	30-90
Gases		Brine	20-300	3-50
Organic solvents		Organic solvents	100-400	20-60
Heavy oils		Heavy oils	50-300	8-50

may be obtained by using correlations given by the Engineering Sciences Data Unit and, based on this work, BUTTERWORTH⁽¹⁰⁹⁾ offers the equation:

$$St = E Re^{-0.205} Pr^{-0.505} \quad (9.215)$$

where:

$$\text{the Stanton Number } St = Nu Re^{-1} Pr^{-1}$$

$$E = 0.22 \exp[-0.0225(\ln Pr)^2]$$

and

Equation 9.215 is valid for Reynolds Numbers in excess of 10,000. Where the Reynolds Number is less than 2000, the flow will be laminar and, provided natural convection effects

Table 9.18. Approximate film coefficients for heat transfer

No. change of state	h_i or h_o	
	$W/m^2 \cdot K$	$Btu/ft^2 \cdot h \cdot ^\circ F$
<i>No change of state</i>		
water	1700–11,000	300–2000
gases	20–300	3–50
organic solvents	350–3000	60–500
oils	60–700	10–120
<i>Condensation</i>		
steam	6000–17,000	1000–3000
organic solvents	900–2800	150–500
light oils	1200–2300	200–400
heavy oils (vacuum)	120–300	20–50
ammonia	3000–6000	500–1000
<i>Evaporation</i>		
water	2000–12,000	30–200
organic solvents	600–2000	100–300
ammonia	1100–2300	200–400
light oils	800–1700	150–300
heavy oils	60–300	10–50

are negligible, film coefficients may be estimated from a form of equation 9.85 modified to take account of the variation of viscosity over the cross-section:

$$Nu = 1.86(RePr)^{0.33} (d/l)^{0.33} (\mu/\mu_s)^{0.14} \quad (9.216)$$

The minimum value of the Nusselt Number for which equation 9.216 applies is 35. Reynolds Numbers in the range 2000–10,000 should be avoided in designing heat exchangers as the flow is then unstable and coefficients cannot be predicted with any degree of accuracy. If this cannot be avoided, the lesser of the values predicted by Equations 9.214 and 9.216 should be used.

As discussed in Section 9.4.3, heat transfer data are conveniently correlated in terms of a heat transfer factor j_h , again modified by the viscosity correction factor:

$$j_h = StPr^{0.67} (\mu/\mu_s)^{-0.14} \quad (9.217)$$

which enables data for laminar and turbulent flow to be included on the same plot, as shown in Figure 9.77. Data from Figure 9.77 may be used together with equation 9.217 to estimate coefficients with heat exchanger tubes and commercial pipes although, due to a higher roughness, the values for commercial pipes will be conservative. Equation 9.217 is rather more conveniently expressed as:

$$Nu = (hd/k) = j_h Re Pr^{0.33} (\mu/\mu_s)^{-0.14} \quad (9.218)$$

It may be noted that whilst Figure 9.77 is similar to Figure 9.24, the values of j_h differ due to the fact that KERN⁽²⁸⁾ and other workers define the heat transfer factor as:

$$j_H = Nu Pr^{-0.33} (\mu/\mu_s)^{-0.14} \quad (9.219)$$

Thus the relationship between j_h and j_H is:

$$j_h = j_H / Re \quad (9.220)$$

As discussed in Section 9.4.3, by incorporating physical properties into equations 9.214 and 9.216, correlations have been developed specifically for water and equation 9.221, based on data from EAGLE and FERGUSON⁽¹⁰⁾ may be used:

$$h = 4280(0.00488T - 1)t^{0.8}/d^{0.2} \quad (9.221)$$

which is in SI units, with h (film coefficient) in $W/m^2 \cdot K$, T in K , t in m/s and d in m .

Example 9.27

Estimate the heat transfer area required for the system considered in Examples 9.1 and 9.26, assuming that no data on the overall coefficient of heat transfer are available.

Solution

As in the previous examples,

$$\text{heat load} = 1672 \text{ kW}$$

and

$$\text{corrected mean temperature difference, } F\theta_m = 40.6 \text{ deg } K$$

In the tubes:

$$\text{mean water temperature, } T = 0.5(360 + 340) = 350 \text{ K}$$

Assuming a tube diameter, $d = 19 \text{ mm}$ or 0.0019 m and a water velocity, $u = 1 \text{ m/s}$, then, in equation 9.221:

$$h_i = 4280(0.00488 \times 350 - 1)t^{0.8}/(0.0019)^{0.2} = 10610 \text{ W/m}^2 \cdot K \text{ or } 10.6 \text{ kW/m}^2 \cdot K$$

From Table 9.18, an estimate of the shell-side film coefficient is:

$$h_o = 0.5(1700 + 11000) = 6355 \text{ W/m}^2 \cdot K \text{ or } 6.35 \text{ kW/m}^2 \cdot K$$

For steel tubes of a wall thickness of 1.6 mm, the thermal resistance of the wall, from Table 9.15 is:

$$x_w/k_w = 0.025 \text{ m}^2 \cdot K/kW$$

and the thermal resistance for treated water, from Table 9.16, is $0.26 \text{ m}^2 \cdot K/kW$ for both layers of scale. Thus, in Equation 9.201:

$$\begin{aligned} (1/U) &= (1/h_o) + (x_w/k_w) + R_f + R_o + (1/h_i) \\ &= (1/6.35) + 0.025 + 0.52 + (1/10.6) = 0.797 \text{ m}^2 \cdot K/kW \end{aligned}$$

and:

$$U = 1.25 \text{ kW/m}^2 \cdot K$$

The heat transfer area required is then:

$$A = Q/F\theta_m U = 1672/(40.6 \times 1.25) = 32.9 \text{ m}^2$$

As discussed in Section 9.4.4, the complex flow pattern on the *shell-side* and the great number of variables involved make the prediction of coefficients and pressure drop very difficult, especially if leakage and bypass streams are taken into account. Until about 1960, empirical methods were used to account for the difference in the performance

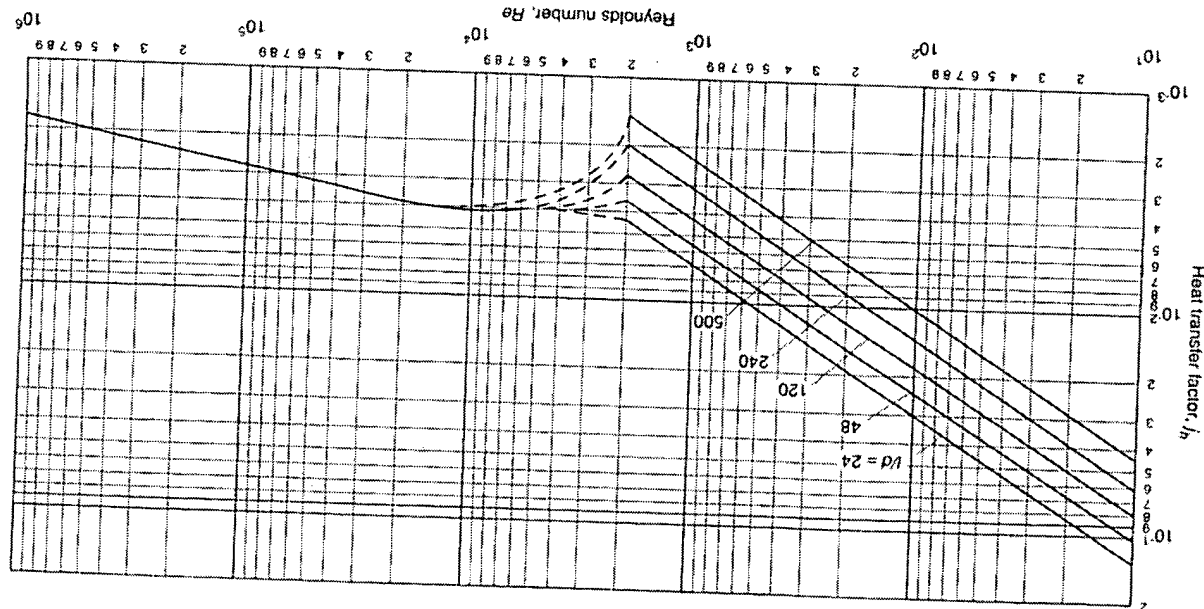


Figure 9.77. Heat transfer factor for flow inside tubes

of real exchangers as compared with that for cross-flow over ideal tube banks. The methods of KERN⁽²⁸⁾ and DONOHUE⁽¹¹⁾ are typical of these "bulk flow" methods and their approach, together with more recent methods involving an analysis of the contribution to heat transfer by individual streams in the shell, are discussed in Section 9.9.6.

Special correlations have also been developed for liquid metals, used in recent years in the nuclear industry with the aim of reducing the volume of fluid in the heat transfer circuits. Such fluids have high thermal conductivities, though in terms of heat capacity per unit volume, liquid sodium, for example, which finds relatively widespread application, has a value of $C_p\rho$ of only $1275 \text{ kJ/m}^3 \text{ K}$.

Although water has a much greater value, it is unsuitable because of its high vapour pressure at the desired temperatures and the corresponding need to use high-pressure piping. Because of their high thermal conductivities, liquid metals have particularly low values of the Prandtl number (about 0.01) and they behave rather differently from normal fluids under conditions of forced convection. Some values for typical liquid metals are given in Table 9.19.

Table 9.19. Prandtl numbers of liquid metals

Metal	Temperature (K)	Prandtl number Pr
Potassium	975	0.003
Sodium	975	0.004
Na/K alloy (56:44)	975	0.06
Mercury	575	0.008
Lithium	475	0.065

The results of work on sodium, lithium, and mercury for forced convection in a pipe have been correlated by the expression:

$$Nu = 0.625(RePr)^{0.4} \quad (9.222)$$

although the accuracy of the correlation is not very good. With values of Reynolds number of about 18,000 it is quite possible to obtain a value of h of about $11 \text{ kW/m}^2 \text{ K}$ for flow in a pipe.

9.9.5. Pressure drop in heat exchangers

Tube-side

Pressure drop on the tube-side of a shell and tube exchanger is made up of the friction loss in the tubes and losses due to sudden contractions and expansions and flow reversals experienced by the tube-side fluid. The friction loss may be estimated by the methods outlined in Section 3.4.3 from which the basic equation for isothermal flow is given by equation 3.18 which can be written as:

$$-\Delta P_f = 4j_f(l/d_i)(\rho u^2) \quad (9.223)$$

where j_f is the dimensionless friction factor. Clearly the flow is not isothermal and it is usual to incorporate an empirical correction factor to allow for the change in physical

properties, particularly viscosity, with temperature to give:

$$-\Delta P_t = 4j_f(l/d_i)(\rho u^2)(\mu/\mu_s)^m \quad (9.22)$$

where $m = -0.25$ for laminar flow ($Re < 2100$) and -0.14 for turbulent flow ($Re > 2100$). Values of j_f for heat exchanger tubes are given in Figure 9.78 which is based on Figure 3.7.

There is no entirely satisfactory method for estimating losses due to contraction of the tube inlets, expansion at the exits and flow reversals, although KERN⁽²⁸⁾ suggests adding four velocity heads per pass, FRANK⁽¹¹²⁾ recommends 2.5 velocity heads, BUTTERWORTH⁽¹¹³⁾ 1.8, LORD *et al.*⁽¹¹⁴⁾ suggests that the loss per pass is equivalent to a tube length of 300 diameters for straight tubes and 200 for U-tubes, whilst EVANS⁽¹¹⁵⁾ recommends the addition of 67 tube diameters per pass. Another approach is to estimate the number of velocity heads by using factors for pipe-fittings as discussed in Section 3.4, and given in Table 3.2. With four tube passes, for example, there will be four contractions equivalent to a loss of $(4 \times 0.5) = 2$ velocity heads, four expansions equivalent to a loss of $(4 \times 1.0) = 4$ velocity heads and three 180° bends equivalent to a loss of $(3 \times 1.5) = 4.5$ velocity heads. In this way, the total loss is 10.5 velocity heads, or 2.6 per pass, giving support to Frank's proposal of 2.5. Using this approach, equation 9.224 becomes:

$$-\Delta P_{\text{total}} = N_P [4j_f(l/d_i)(\mu/\mu_s)^m + 1.25](\rho u^2) \quad (9.225)$$

where N_P is the number of tube-side passes. Additionally, there will be expansion and contraction losses at the inlet and outlet nozzles respectively, and these losses may be estimated by adding one velocity head for the inlet, and 0.5 of a velocity head for the outlet, based on the nozzle velocities. Losses in the nozzles are only significant for gases at pressures below atmospheric.

Shell-side

As discussed in Section 9.4.4, the prediction of pressure drop, and indeed heat transfer coefficients, in the shell is very difficult due to the complex nature of the flow pattern in the segmentally baffled unit. Whilst the baffles are intended to direct fluid across the tubes, the actual flow is a combination of cross-flow between the baffles and axial or parallel flow in the baffle windows as shown in Figure 9.79, although even this does not represent the actual flow pattern because of leakage through the clearances necessary for the fabrication and assembly of the unit. This more realistic flow pattern is shown in Figure 9.80 which is based on the work of TINKER⁽¹¹⁶⁾ who identifies the various streams in the shell as follows:

- A—fluid flowing through the clearance between the tube and the hole in the baffle.
- B—the actual cross-flow stream.
- C—fluid flowing through the clearance between the outer tubes and the shell.
- E—fluid flowing through the clearance between the baffle and the shell.
- F—fluid flowing through the gap between the tubes because of any pass-partition plates. This is especially significant with a vertical gap.

Because stream A does not bypass the tubes, it is the pressure drop rather than the heat transfer which is affected. Streams C, E and F bypass the tubes, thus reducing the effective

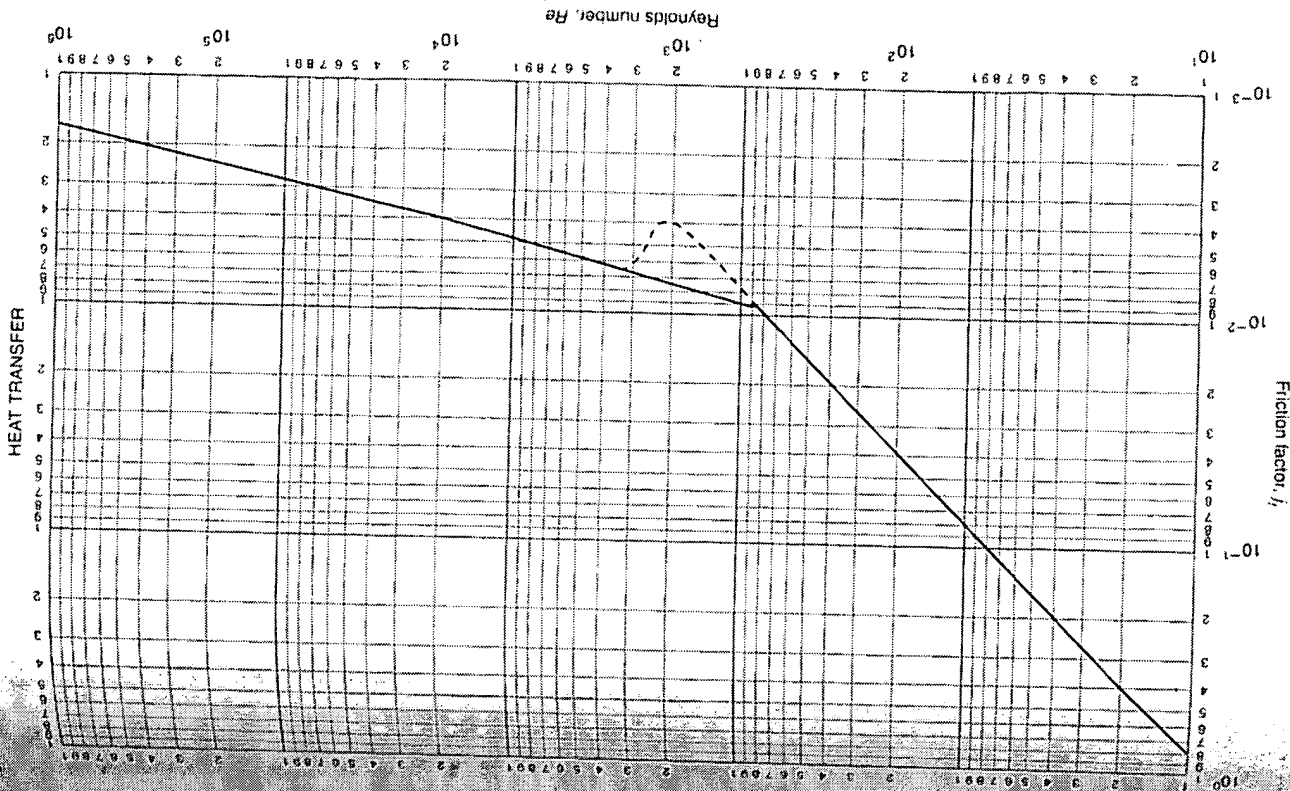


Figure 9.78. Tube-side friction factors⁽²⁸⁾.

Note: The friction factor j_f is the same as the friction factor for pipes ($f = R/\mu u^2$), defined in Chapter 3.

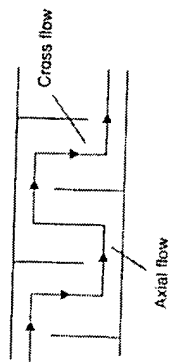
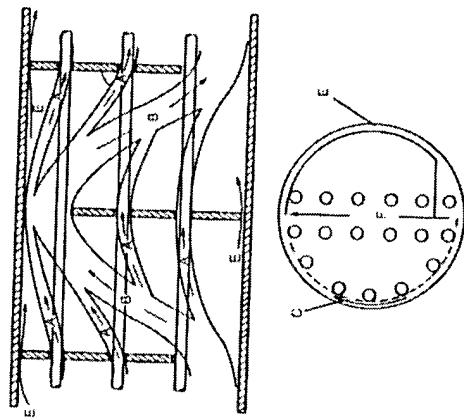


Figure 9.79. Idealised main stream flow

Figure 9.80. Shell-side leakage and by-pass paths⁽¹⁾⁽⁶⁾

heat transfer area. Stream C, the main bypass stream, is most significant in pull-through bundle units where there is of necessity a large clearance between the bundle and its shell, although this can be reduced by using horizontal sealing strips. In a similar way the flow of stream F may be reduced by fitting dummy tubes. As an exchanger becomes fouled, clearances tend to plug and this increases the pressure drop. The whole question of shell-side pressure drop estimation in relation to design procedures is now discussed.

9.9.6. Heat exchanger design

Process conditions

A first-stage consideration in the design process is the allocation of fluids to either shell or tubes and, by and large, the more corrosive fluid is passed through the tubes to reduce the costs of expensive alloys and clad components. Similarly, the fluid with the greatest fouling tendency is also usually passed through the tubes where cleaning is easier. Furthermore, velocities through the tubes are generally higher and more readily controllable and can be adjusted to reduce fouling. Where special alloys are in contact with hot fluids (the

fluids should be passed through the tubes to reduce costs. In addition the shell temperature is lowered, thus reducing lagging costs. Passing hazardous materials through the tubes leads to greater safety and, because high pressure tubes are cheaper than a high pressure shell, streams at high pressure are best handled on the tube-side. In a similar way, where a very low pressure drop is required as in vacuum operation for example, the fluids involved are best handled on the tube-side where higher film heat transfer coefficients are obtained for a given pressure drop. Provided the flow is turbulent, a higher heat transfer coefficient is usually obtained with a more viscous liquid in the shell because of the more complex flow patterns although, because the tube-side coefficient can be predicted with greater accuracy, it is better to place the fluid in the tubes if turbulent flow in the shell is not possible. Normally, the most economical design is achieved with the fluid with the lower flowrate in the shell.

In selecting a design velocity, it should be recognised that at high velocities high rates of heat transfer are achieved and fouling is reduced, but pressure drops are higher. Normally, the velocity must not be so high as to cause erosion which can be reduced at the tube inlet by fitting plastic inserts, and yet be such that any solids are kept in suspension. For process liquids, velocities are usually 0.3–1.0 m/s in the shell and 1.0–2.0 m/s in the tubes, with a maximum value of 4.0 m/s when fouling must be reduced. Typical water velocities are 1.5–2.5 m/s. For vapours, velocities lie in the range 5–10 m/s with high pressure fluids and 50–70 m/s with vacuum operation, the lower values being used for materials of high molecular weight.

In general, the higher of the temperature differences between the outlet temperature of one stream and the inlet temperature of the other should be 20 deg K and the lower temperature difference should be 5–7 deg K for water coolers and 3–5 deg K when using refrigerated brines, although optimum values can only be determined by an economic analysis of alternative designs.

Similar considerations apply to the selection of pressure drops where there is freedom of choice, although a full economic analysis is justified only in the case of very expensive units. For liquids, typical values in optimised units are 35 kN/m² where the viscosity is less than 1 mN s/m² and 50–70 kN/m² where the viscosity is 1–10 mN s/m²; for gases, 0.4–0.8 kN/m² for high vacuum operation, 50 per cent of the system pressure at 100–200 kN/m², and 10 per cent of the system pressure above 1000 kN/m². Whatever pressure drop is used, it is important that erosion and flow-induced tube vibration caused by high velocity fluids are avoided.

Design methods

It is shown in Section 9.9.5 that, with the existence of various bypass and leakage streams in practical heat exchangers, the flow patterns of the shell-side fluid, as shown in Figure 9.79, are complex in the extreme and far removed from the idealised cross-flow situation discussed in Section 9.4.4. One simple way of using the equations for cross-flow presented in Section 9.4.4, however, is to multiply the shell-side coefficient obtained from these equations by the factor 0.6 in order to obtain at least an estimate of the shell-side coefficient in a practical situation. The pioneering work of KERN⁽²⁸⁾ and DONOHUE⁽¹¹⁾, who used correlations based on the total stream flow and empirical methods to allow for the performance of real exchangers compared with that for cross-flow over ideal tube banks, went much further and,

although their early design method does not involve the calculation of bypass and leakage streams, it is simple to use and quite adequate for preliminary design calculations.

The method, which is based on experimental work with a great number of commercial exchangers with standard tolerances, gives a reasonably accurate prediction of heat transfer coefficients for standard designs, although predicted data on pressure drop is less satisfactory as it is more affected by leakage and bypassing. Using a similar approach to that for tube-side flow, shell-side heat transfer and friction factors are correlated using a hypothetical shell diameter and shell-side velocity where, because the cross-sectional area for flow varies across the shell diameter, linear and mass velocities are based on the maximum area for cross-flow; that is at the shell equator. The shell equivalent diameter is obtained from the flow area between the tubes taken parallel to the tubes, and the wetted perimeter, as outlined in Section 9.9.4 and illustrated in Figure 9.28. The shell-side factors, j_h and j_f , for various baffle cuts and tube arrangements based on the data given by KERN⁽²⁸⁾ and LUDWIG⁽¹⁰¹⁾ are shown in Figures 9.81 and 9.82.

The general approach is to calculate the area for cross-flow for a hypothetical row of tubes at the shell equator from the equation given in Section 9.4.4:

$$A_s = d_s l_B C' / Y \quad (9.226)$$

where d_s is the shell diameter, l_B is the baffle length and (C'/Y) is the ratio of the clearance between the tubes and the distance between tube centres. The mass flow divided by the area A_s gives the mass velocity G'_s , and the linear velocity on the shell-side u_s is obtained by dividing the mass velocity by the mean density of the fluid. Again using the equations in Section 9.4.4, the shell-side equivalent or hydraulic diameter is given by:

$$\begin{aligned} \text{For square pitch: } d_e &= 4(Y^2 - \pi d_o^2/4)/\pi d_o = 1.27(Y^2 - 0.785d_o^2)/d_o \quad (9.227) \\ \text{and for triangular pitch: } d_e &= 4[(0.87Y \times Y/2) - (0.5\pi d_o^2/4)/(\pi d_o/2)] \\ &= 1.10(Y^2 - 0.917d_o^2)/d_o \quad (9.228) \end{aligned}$$

Using this equivalent diameter, the shell-side Reynolds number is then:

$$Re_s = G'_s d_e / \mu = u_s d_e \rho / \mu \quad (9.229)$$

where G'_s is the mass flowrate per unit area. Hence j_h may be obtained from Figure 9.81. The shell-side heat transfer coefficient is then obtained from a re-arrangement of equation 9.220:

$$Nu = (h_s d_e / k_f) = j_h Re P_r^{0.33} (\mu / \mu_s)^{0.14} \quad (9.230)$$

In a similar way, the factor j_f is obtained from Figure 9.82 and the pressure drop estimated from a modified form of equation 9.224:

$$-\Delta P_s = 4 j_f (d_s / d_e) (l / l_B) (\rho l_B^2) (\mu / \mu_s)^{-0.14} \quad (9.231)$$

where (l/l_B) is the number of times the flow crosses the tube bundle $(= n + 1)$.

The pressure drop over the shell nozzles should be added to this value although this is usually only significant with gases. In general, the nozzle pressure loss is 1.5 velocity heads for the inlet and 0.5 velocity heads for the outlet, based on the nozzle area or the

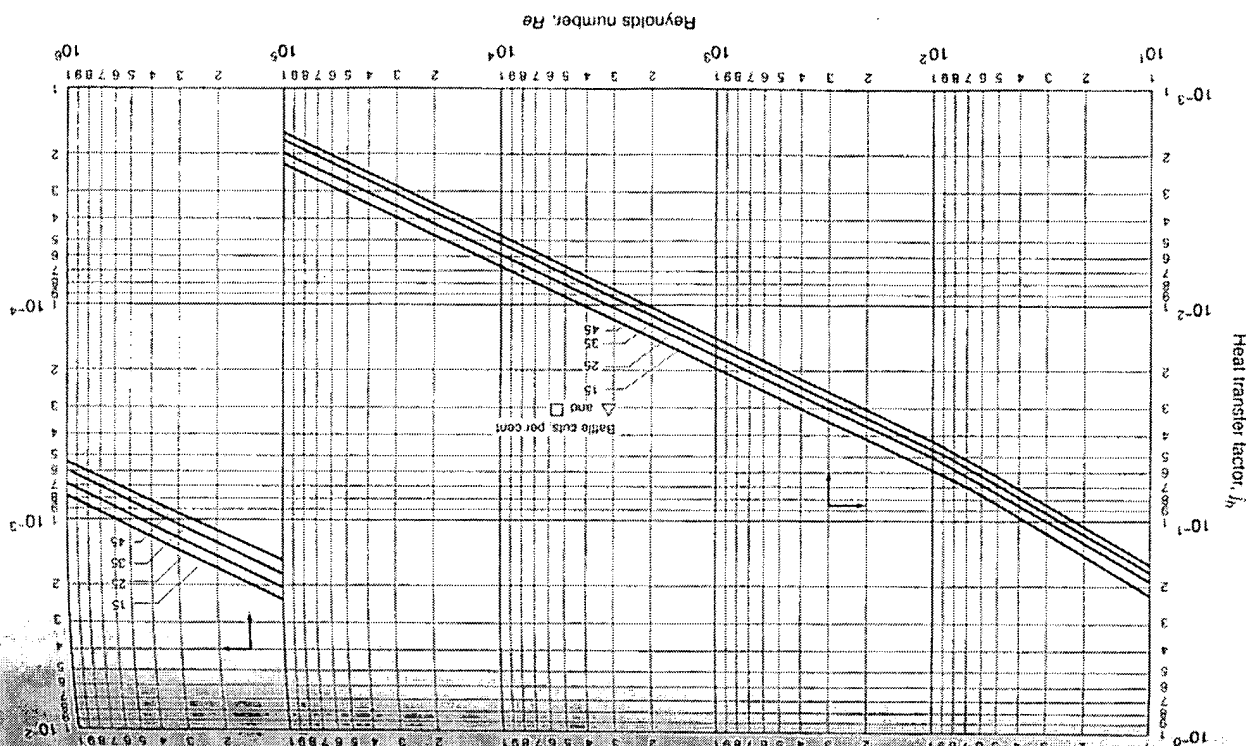


Figure 9.81. Shell-side heat-transfer factors with segmental baffles.⁽²⁸⁾

free area between the tubes in the row adjacent to the nozzle, whichever is the least. Kern's method is now illustrated in the following example.

Example 9.28

Using Kern's method, design a shell and tube heat exchanger to cool 30 kg/s of butyl alcohol from 370 to 315 K using treated water as the coolant. The water will enter at 300 K and leave at 315 K.

Solution

Since it is corrosive, the water will be passed through the tubes.

At a mean temperature of $0.5(370 + 315) = 343$ K, from Table 3, Appendix A1, the thermal capacity of butyl alcohol = 2.90 kJ/kg K and hence:

$$\text{Heat load} = (30 \times 2.90)(370 - 315) = 4785 \text{ kW}$$

If the heat capacity of water is 4.18 kJ/kg K, then:

$$\text{Flow of cooling water} = 4785/(4.18(315 - 300)) = 76.3 \text{ kg/s}$$

The logarithmic mean temperature difference,

$$\theta_m = [(370 - 315) - (315 - 300)] / \ln[(370 - 315)/(315 - 300)] = 30.7 \text{ deg K}$$

With one shell-side pass and two tube-side passes, then from equation 9.213:

$$X = (370 - 315)/(315 - 300) = 3.67 \text{ and } Y = (315 - 300)/(370 - 300) = 0.21$$

and from Figure 9.75:

$$F = 0.85 \text{ and } F\theta_m = (0.85 \times 30.7) = 26.1 \text{ deg K}$$

From Table 9.17, an estimated value of the overall coefficient is $U = 500 \text{ W/m}^2\text{K}$ and hence, the provisional area, from equation 9.212, is:

$$A = (4785 \times 10^3)/(26.1 \times 500) = 367 \text{ m}^2$$

It is convenient to use 20 mm OD, 16 mm ID tubes, 4.88 m long which, allowing for the tube-sheets, would provide an effective tube length of 4.83 m. Thus:

$$\text{Surface area of one tube} = \pi(20/1000) = 0.303 \text{ m}^2$$

$$\text{Number of tubes required} = (367/0.303) = 1210$$

With a clean shell-side fluid, 1.25 triangular pitch may be used and, from equation 9.211:

$$1210 = 0.249(d_b/20)^2 \cdot 207$$

from which:

$$d_b = 937 \text{ mm}$$

Using a split-ring floating head unit, then, from Figure 9.71, the diametrical clearance between the shell and the tubes = 68 mm and:

$$\text{Shell diameter, } d_s = (937 + 68) = 1005 \text{ mm}$$

which approximates to the nearest standard pipe size of 1016 mm.

Tube-side coefficient

The water-side coefficient may now be calculated using equation 9.218, although here, use will be made of the factor:

$$\text{Cross-sectional area of one tube} = (\pi/40) \times 16^2 = 201 \text{ mm}^2$$

$$\text{Number of tubes/pass} = (1210/2) = 605$$

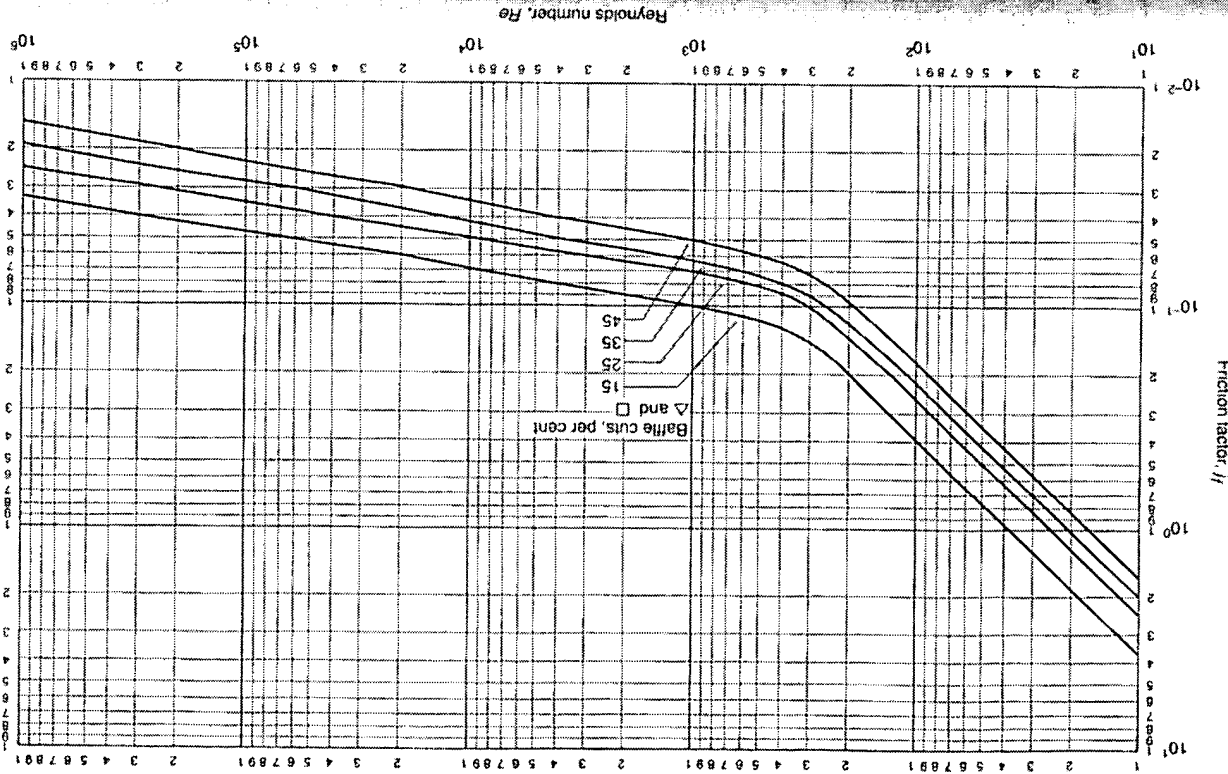


Figure 9.57 Shell-side friction factors with segmental baffles (25)

Thus:

$$\text{Tube-side flow area} = (605 \times 20) \times 10^{-6} = 0.122 \text{ m}^2$$

$$\text{Mass velocity of the water} = (76.3/0.122) = 625 \text{ kg/m}^2\text{s}$$

Thus, for a mean water density of 995 kg/m^3 :

$$\text{Water velocity, } u = (625/995) = 0.63 \text{ m/s}$$

At a mean water temperature of $0.5(315 + 300) = 308 \text{ K}$, viscosity, $\mu = 0.8 \text{ mN s/m}^2$ and thermal conductivity, $k = 0.59 \text{ W/m K}$.

Thus:

$$Re = du\rho/\mu = (16 \times 10^{-3} \times 0.63 \times 995)/(0.8 \times 10^{-3}) = 12540$$

$$Pr = C_p \mu/k = (4.18 \times 10^3 \times 0.8 \times 10^{-3})/0.59 = 5.67$$

$$1/d_i = 4.83/(16 \times 10^{-3}) = 302$$

Thus, from Figure 9.77, $j_h = 3.7 \times 10^{-3}$, and, in equation 9.218, neglecting the viscosity term:

$$(h_i \times 16 \times 10^{-3})/0.59 = (3.7 \times 10^{-3} \times 12540 \times 5.67^{0.33})$$

$$h_i = 3030 \text{ W/m}^2\text{K}$$

and:

Shell-side coefficient

The baffle spacing will be taken as 20 per cent of the shell diameter or $(1005 \times 20/100) = 201 \text{ mm}$. The tube pitch $= (1.25 \times 20) = 25 \text{ mm}$ and, from equation 9.226:

$$\text{Cross-flow area, } A_s = [(25 - 20)/25](1005 \times 20) \times 10^{-6} = 0.040 \text{ m}^2$$

$$\text{Mass velocity in the shell, } G_s = (30/0.040) = 750 \text{ kg/m}^2\text{s}$$

Thus:

From equation 9.228:

$$\text{Equivalent diameter, } d_e = 1.10(25^2 - (0.917 \times 20^2)/20) = 14.2 \text{ mm}$$

At a mean shell-side temperature of $0.5(370 + 315) = 343 \text{ K}$, from Appendix A1:

density of butyl alcohol, $\rho = 780 \text{ kg/m}^3$, viscosity, $\mu = 0.75 \text{ mN s/m}^2$, heat capacity, $C_p = 3.1 \text{ kJ/kg K}$ and thermal conductivity, $k = 0.16 \text{ W/m K}$. Thus, from equation 9.229:

$$Re = G_s d_e/\mu = (750 \times 14.2 \times 10^{-3})/(0.75 \times 10^{-3}) = 14200$$

$$Pr = C_p \mu/k = (3.1 \times 10^3 \times 0.75 \times 10^{-3})/0.16 = 14.5$$

Thus, with a 25 per cent segmental cut, from Figure 9.81, $j_h = 5.0 \times 10^{-3}$

Neglecting the viscosity correction term in equation 9.230:

$$(h_s \times 14.2 \times 10^{-3})/0.16 = 5.0 \times 10^{-3} \times 14200 \times 14.5^{0.33}$$

$$h_s = 1933 \text{ W/m}^2\text{K}$$

and:

The mean butanol temperature $= 343 \text{ K}$, the mean water temperature $= 308 \text{ K}$ and hence the mean wall temperature may be taken as $0.5(343 + 308) = 326 \text{ K}$ at which $\mu_s = 1.1 \text{ mN s/m}^2$

$$(\mu_s/\mu_s)^{0.14} = (0.75/1.1)^{0.14} = 0.95$$

showing that the correction for a low viscosity fluid is negligible.

Overall coefficient

The thermal conductivity of cupro-nickel alloys $= 50 \text{ W/m K}$ and, from Table 9.16, scale resistances will be taken as $0.00020 \text{ m}^2\text{K/W}$ for the water and $0.00018 \text{ m}^2\text{K/W}$ for the organic.

Based on the outside area, the overall coefficient is given by:

$$1/U = 1/h_o + R_o + s_w/k_w + R_i/(d_o d_i) + (1/h_i)(d_o d_i)$$

$$= (1/1933) + 0.00020 + [0.5(20 - 16) \times 10^{-3}/50] + (0.00015 \times 20)/16 + 20/(3030 \times 16) \\ = 0.00052 + 0.00020 + 0.00004 + 0.000225 + 0.00041 = 0.00140 \text{ m}^2\text{K/W}$$

$$\text{and: } U = 717 \text{ W/m}^2\text{K}$$

which is well in excess of the assumed value of $500 \text{ W/m}^2\text{K}$.

Pressure drop

On the tube-side, $Re = 12450$ and from Figure 9.78, $f_f = 4.5 \times 10^{-3}$. Neglecting the viscosity correction term, equation 9.225 becomes:

$$\Delta P_t = 2(4 \times 4.5 \times 10^{-3})(4830/16) + 1.25(995 \times 0.63^3) = 5279 \text{ N/m}^2 \text{ or } 5.28 \text{ kN/m}^2$$

which is low, permitting a possible increase in the number of tube passes.

On the shell-side, the linear velocity, $(G_s/\rho) = (750/780) = 0.96 \text{ m/s}$

From Figure 9.82, when $Re = 14200$, $f_f = 4.6 \times 10^{-3}$

Neglecting the viscosity correction term, in equation 9.231:

$$-\Delta P_s = (4 \times 4.6 \times 10^{-3})(1005/14.2)(4830/20)(780 \times 0.96^2) \\ = 224950 \text{ N/m}^2 \text{ or } 225 \text{ kN/m}^2$$

This value is very high and thought should be given to increasing the baffle spacing. If this is doubled, this will reduce the pressure drop by approximately $(1/2)^2 = 1/4$ and:

$$-\Delta P_s = (225/4) = 56.2 \text{ kN/m}^2 \text{ which is acceptable.}$$

Since $h_o \propto Re^{0.8} \propto u^{0.8}$,

$$h_o = 1933(1/2)^{0.8} = 1110 \text{ W/m}^2\text{K}$$

which gives an overall coefficient of $561 \text{ W/m}^2\text{K}$ which is still in excess of the assumed value of $500 \text{ W/m}^2\text{K}$. Further detailed discussion of Kern's method together with a worked example is presented in Volume 6.

Whilst Kern's method provides a simple approach and one which is quite adequate for preliminary design calculations, much more reliable predictions may be achieved by taking into account the contribution to heat transfer and pressure drop made by the various idealised flow streams shown in Figure 9.80. Such an approach was originally taken by TINKER⁽¹⁶⁾ and many of the methods subsequently developed have been based on his model which unfortunately is difficult to follow and tedious to use. The approach has been simplified by DEVORE⁽¹¹⁷⁾, however, who, in using standard tolerances for commercial exchangers and a limited number of baffle designs, gives nomographs which enable the method to be used with simple calculators. Devore's method has been further simplified by MUELLER⁽¹¹⁸⁾ who gives an illustrative example. PALEN and TABOREK⁽¹¹⁹⁾ and GRANT⁽¹²⁰⁾ have described how both Heat Transfer Inc. and Heat Transfer and Fluid Flow Services have used Tinker's method to develop proprietary computer-based methods.

Using Tinker's approach, BELL^(121,122) has described a semi-analytical method, based on work at the University of Delaware, which allows for the effects of major bypass and leakage streams, and which is suitable for use with calculators. In this procedure, the heat transfer coefficient and the pressure drop are obtained from correlations for flow over ideal tube banks, applying correction factors to allow for the effects of leakage, bypassing and flow

in the window zone. This approach gives more accurate predictions than Kern's method and can be used to determine the effects of constructional tolerances and the use of sealing tapes. This method is discussed in some detail in Volume 6, where an illustrative example is offered.

A more recent approach is that offered by WILLS and JOHNSTON⁽¹²³⁾ who have developed a simplified version of Tinker's method. This has been adopted by the Engineering Sciences Data Unit, ESDU⁽¹²⁴⁾, and it gives a useful calculation technique for providing realistic checks on 'black box' computer predictions. The basis of this approach is shown in Figure 9.83 which shows fluid flowing from A to B in two streams—over the tubes in cross-flow, and bypassing the tube bundle—which then combine to form a single stream. In addition, leakage occurs between the tubes and the baffle and between the baffle and the shell, as shown. For each of these streams, a coefficient is defined which permits the pressure drop for each stream to be expressed in terms of the square of the mass velocity for that stream. A knowledge of the coefficients for each stream and the sum of the pressure drops in each zone enables the coefficients for each stream to be estimated by an iterative procedure, and the flowrate of each stream to be obtained. The estimation of the heat transfer coefficient and the pressure drop is then a relatively simple operation. This method is of especial value in investigating the effect of various shell-to-baffle and baffle-to-tube tolerances on the performance of a heat exchanger, both in terms of heat transfer rates and the pressure losses incurred.

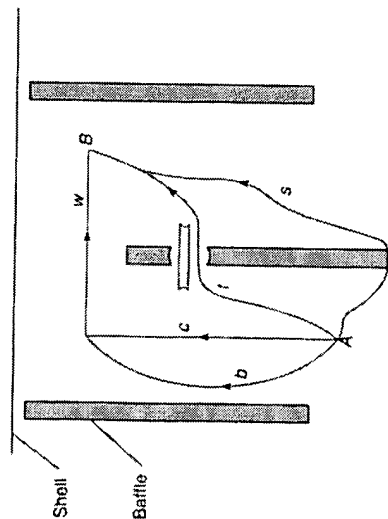


Figure 9.83. Flow streams in the Wills and Johnston method⁽¹²³⁾.

9.9.7. Heat exchanger performance

One of the most useful methods of evaluating the performance of an existing heat exchanger or to assess a proposed design is to determine its *effectiveness* η , which is defined as the ratio of the actual rate of heat transfer Q to the maximum rate Q_{\max} that is thermodynamically possible or:

$$\eta = \frac{Q}{Q_{\max}} \quad (9.232)$$

Q_{\max} is the heat transfer rate which would be achieved if it were possible to bring the outlet temperature of the stream with the lower heat capacity to the inlet temperature of the other stream. Using the nomenclature in Figure 9.84, and taking stream 1 as having the lower value of GC_p , then:

$$Q_{\max} = G_1 C_{p1} (T_{11} - T_{21}) \quad (9.233)$$

An overall heat balance gives:

$$Q = G_1 C_{p1} (T_{11} - T_{12}) = G_2 C_{p2} (T_{22} - T_{21})$$

Thus, based on stream 1:

$$\eta = \frac{G_1 C_{p1} (T_{11} - T_{12})}{G_1 C_{p1} (T_{11} - T_{21})} = \frac{T_{11} - T_{12}}{T_{11} - T_{21}} \quad (9.234)$$

and, based on stream 2:

$$\eta = \frac{G_2 C_{p2} (T_{22} - T_{21})}{G_1 C_{p1} (T_{11} - T_{21})} \quad (9.235)$$

In calculating temperature differences, the positive value should always be taken.

Example 9.29

A flow of 1 kg/s of an organic liquid of heat capacity 2.0 kJ/kg K is cooled from 350 to 330 K by a stream of water flowing countercurrently through a double-pipe heat exchanger. Estimate the effectiveness of the unit if the water enters the exchanger at 290 K and leaves at 320 K.

Solution

Heat load, $Q = 1 \times 2.0(350 - 330) = 40 \text{ kW}$

Flow of water, $G_{\text{cool}} = \frac{40}{4.187(320 - 290)} = 0.318 \text{ kg/s}$

For organic: $(GC_p)_{\text{hot}} = (1 \times 2.0) = 2.0 \text{ kW/K} (= G_2 C_{p2})$

For water: $(GC_p)_{\text{cold}} = (0.318 \times 4.187) = 1.33 \text{ kW/K} (= G_1 C_{p1})$

From equation 9.235:

$$\begin{aligned} \text{effectiveness } \eta &= \frac{2.0(350 - 330)}{1.33(350 - 290)} \\ &= 0.50 \end{aligned}$$

9.9.8. Transfer units

The concept of a *transfer unit* is useful in the design of heat exchangers and in assessing their performance, since its magnitude is less dependent on the flowrate of the fluids than the heat transfer coefficient which has been used so far. The number of transfer units N is defined by:

$$N = \frac{UA}{(GC_p)_{\min}} \quad (9.236)$$

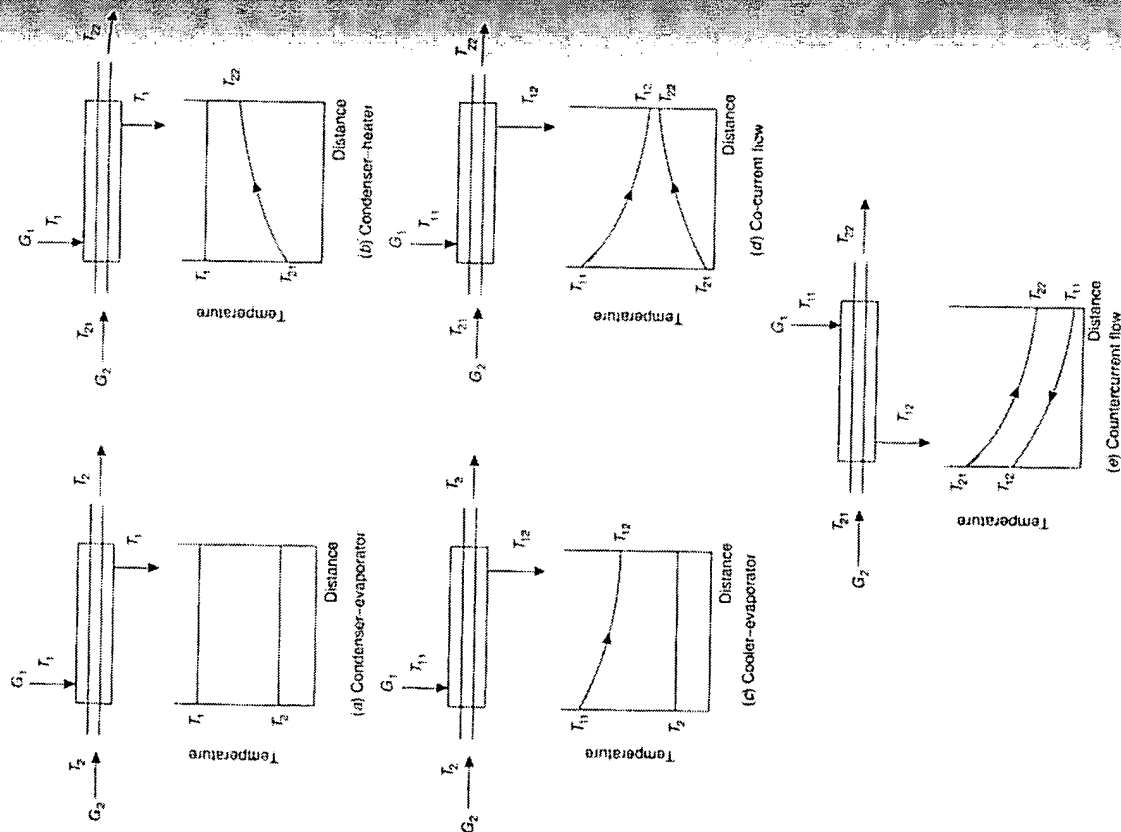


Figure 9.84. Nomenclature for effectiveness of heat exchangers

where $(GC_p)_{\min}$ is the lower of the two values $G_1 C_{p1}$ and $G_2 C_{p2}$. N is the ratio of the heat transferred for a unit temperature driving force to the heat absorbed by the fluid stream when its temperature is changed by 1 deg K. Thus, the number of transfer units gives a measure of the amount of heat which the heat exchanger can transfer. The relation for the effectiveness of the heat exchanger in terms of the heat capacities of the streams is now given for a number of flow conditions. The relevant nomenclature is given in Figure 9.84.

Transfer units are also used extensively in the calculation of mass transfer rates in countercurrent columns and reference should be made to Chapter 10.

Considering *co-current* flow as shown in Figure 9.84d, for an elemental area dA of a heat exchanger, the rate of transfer of heat dQ is given by:

$$dQ = U dA (T_1 - T_2) = U dA \theta \quad (9.237)$$

where T_1 and T_2 are the temperatures of the two streams and θ is the point value of the temperature difference between the streams.

In addition: $dQ = G_2 C_{p2} dT_2 = -G_1 C_{p1} dT_1$

$$\text{Thus: } dT_2 = \frac{dQ}{G_2 C_{p2}} \quad \text{and} \quad dT_1 = \frac{-dQ}{G_1 C_{p1}}$$

$$\text{and: } dT_1 - dT_2 = d(T_1 - T_2) = d\theta = -dQ \left(\frac{1}{G_1 C_{p1}} + \frac{1}{G_2 C_{p2}} \right)$$

Substituting from equation 9.237 for dQ :

$$\frac{d\theta}{\theta} = -U dA \left[\frac{1}{G_1 C_{p1}} + \frac{1}{G_2 C_{p2}} \right] \quad (9.238)$$

Integrating:

$$\ln \frac{\theta_2}{\theta_1} = -UA \left[\frac{1}{G_1 C_{p1}} + \frac{1}{G_2 C_{p2}} \right]$$

or:

$$\ln \frac{T_{12} - T_{22}}{T_{11} - T_{21}} = \frac{UA}{G_1 C_{p1}} \left[1 + \frac{G_1 C_{p1}}{G_2 C_{p2}} \right] \quad (9.239)$$

If $G_1 C_{p1} < G_2 C_{p2}$, $G_1 C_{p1} = (GC_p)_{\min}$

From equation 9.236:

$$N = \frac{UA}{G_1 C_{p1}}$$

Thus:

$$\frac{T_{12} - T_{22}}{T_{11} - T_{21}} = \exp \left[-N \left(1 + \frac{G_1 C_{p1}}{G_2 C_{p2}} \right) \right] \quad (9.240)$$

From equations 9.234 and 9.235:

$$T_{11} - T_{12} = \eta (T_{11} - T_{21})$$

$$T_{22} - T_{21} = \eta \frac{G_1 C_{p1}}{G_2 C_{p2}} (T_{11} - T_{21})$$

Adding:
$$T_{11} - T_{12} + T_{22} - T_{21} = \eta \left(1 + \frac{G_1 C_{p1}}{G_2 C_{p2}} \right) (T_{11} - T_{21})$$

$$1 - \frac{T_{12} - T_{22}}{T_{11} - T_{21}} = \eta \left(1 + \frac{G_1 C_{p1}}{G_2 C_{p2}} \right)$$

Substituting in equation 9.240:

$$\eta = \frac{1 - \exp \left[-N \left(1 + \frac{G_1 C_{p1}}{G_2 C_{p2}} \right) \right]}{1 + \frac{G_1 C_{p1}}{G_2 C_{p2}}} \quad (9.241)$$

For the particular case where $G_1 C_{p1} = G_2 C_{p2}$:

$$\eta = 0.5[1 - \exp(-2N)] \quad (9.242)$$

For a very large exchanger ($N \rightarrow \infty$), $\eta \rightarrow 0.5$.

A similar procedure may be followed for *countercurrent flow* (Figure 9.84e), although it should be noted that, in this case, $\theta_1 = T_{11} - T_{22}$ and $\theta_2 = T_{12} - T_{21}$. The corresponding equation for the effectiveness factor η is then:

$$\eta = \frac{1 - \exp \left[-N \left(1 - \frac{G_1 C_{p1}}{G_2 C_{p2}} \right) \right]}{1 - \frac{G_1 C_{p1}}{G_2 C_{p2}} \exp \left[-N \left(1 - \frac{G_1 C_{p1}}{G_2 C_{p2}} \right) \right]} \quad (9.243)$$

For the case where $G_1 C_{p1} = G_2 C_{p2}$, it is necessary to expand the exponential terms to give:

$$\eta = \frac{N}{1 + N} \quad (9.244)$$

In this case, for a very large exchanger ($N \rightarrow \infty$), $\eta \rightarrow 1$.

If one component is merely undergoing a *phase change at constant temperature* (Figure 9.84b, c) $G_1 C_{p1}$ is effectively zero and both equations 9.241 and 9.243 reduce to:

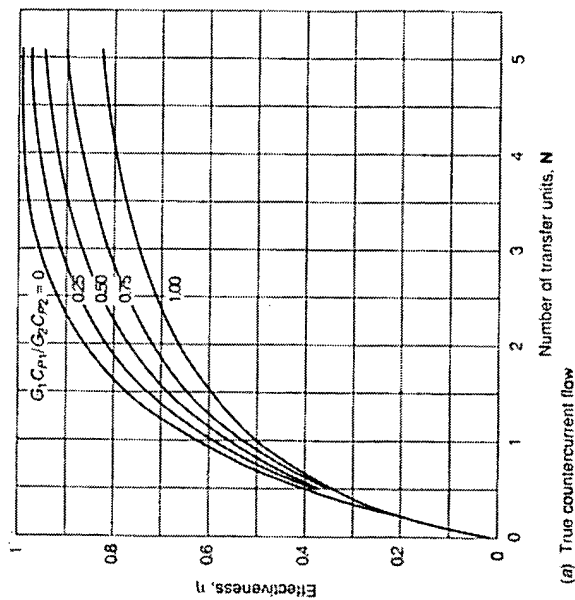
$$\eta = 1 - \exp(-N) \quad (9.245)$$

Effectiveness factors η are plotted against number of transfer units N with $(G_1 C_{p1}/G_2 C_{p2})$ as parameter for a number of different configurations by KAYS and LONDON⁽¹²⁵⁾. Examples for countercurrent flow (based on equation 9.235) and an exchanger with one shell pass and two tube passes are plotted in Figures 9.85a and b respectively.

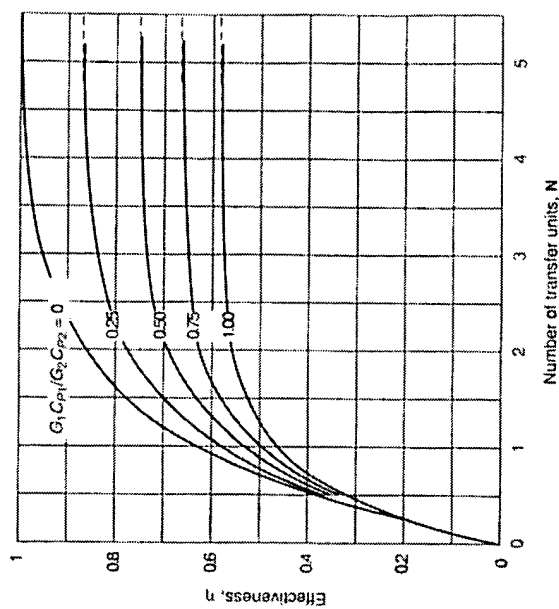
Example 9.30

A process requires a flow of 4 kg/s of purified water at 340 K to be heated from 320 K by 8 kg/s of untreated water which can be available at 380, 370, 360 or 350 K. Estimate the heat transfer surfaces of one shell pass two tube pass heat exchangers suitable for these duties. In all cases, the mean heat capacity of the water streams is 4.18 kJ/kg K and the overall coefficient of heat transfer is 1.5 kW/m² K.

HEAT TRANSFER



(a) True countercurrent flow



(b) One shell pass, two-tube pass exchanger

Figure 9.85. Effectiveness of heat exchangers as a function of number of transfer units⁽¹²⁵⁾

Solution

For the untreated water: $GC_p = (8.0 \times 4.18) = 33.44 \text{ kW/K}$

For the purified water: $GC_p = (4.0 \times 4.18) = 16.72 \text{ kW/K}$

Thus:

$$(GC_p)_{\min} = 16.72 \text{ kW/K} = G_1 C_{p1}$$

$$\text{and: } \frac{G_1 C_{p1}}{G_2 C_{p2}} = \frac{16.72}{33.44} = 0.5$$

From equation 9.235:

$$\eta = \frac{4.0 \times 4.18(340 - 320)}{4.0 \times 4.18(311 - 320)}$$

$$= \frac{20}{(311 - 320)}$$

Thus η may be calculated from this equation using values of $T_{11} = 380, 370, 360$ or 350 K and then N obtained from Figure 9.85b. The area required is then calculated from:

$$A = \frac{N(GC_p)_{\min}}{U} \quad (\text{equation 9.236})$$

to give the following results:

$T_{11} \text{ (K)}$	$\eta \text{ (-)}$	$N \text{ (-)}$	$A \text{ (m}^2\text{)}$
380	0.33	0.45	5.0
370	0.4	0.6	6.6
360	0.5	0.9	10.0
350	0.67	1.7	18.9

Obviously, the use of a higher untreated water temperature is attractive in minimising the area required, although in practice any advantages would be offset by increased water costs, and an optimisation procedure would be necessary in obtaining the most effective design.

9.10. OTHER FORMS OF EQUIPMENT

9.10.1. Finned-tube units

Film coefficients

When viscous liquids are heated in a concentric tube or standard tubular exchanger by condensing steam or hot liquid of low viscosity, the film coefficient for the viscous liquid is much smaller than that on the hot side and it therefore controls the rate of heat transfer. This condition also arises with air or gas heaters where the coefficient on the gas side will be very low compared with that for the liquid or condensing vapour on the other side. It is often possible to obtain a much better performance by increasing the area of surface on the side with the limiting coefficient. This may be done conveniently by using a finned tube as in Figure 9.86 which shows one typical form of such equipment which may have either longitudinal or transverse fins.

The calculation of the film coefficients on the fin side is complex because each unit of surface on the fin is less effective than a unit of surface on the tube wall. This arises because there will be a temperature gradient along the fin so that the temperature difference

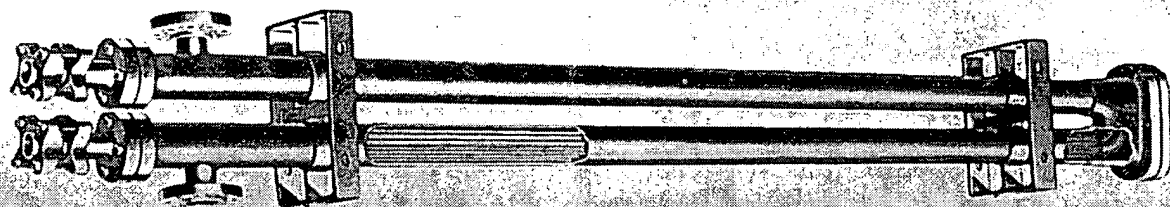


Figure 9.86a. Heat exchanger showing tubes with longitudinal fins

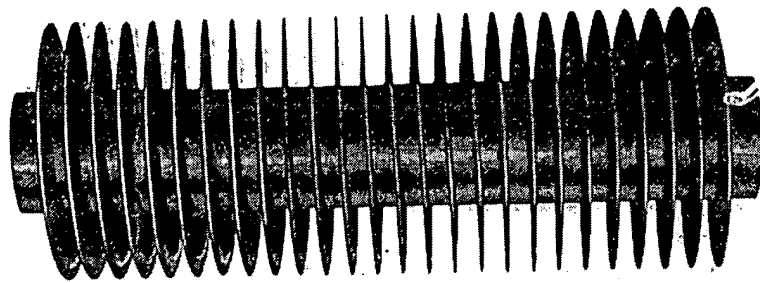


Figure 9.86b. Tube with radial fins

between the fin surface and the fluid will vary along the fin. To calculate the film coefficients it is convenient to consider firstly the extended surface as shown in Figure 9.87. A cylindrical rod of length L and cross-sectional area A and perimeter b is heated at one end by a surface at temperature T_1 and cooled throughout its length by a medium at temperature T_G so that the cold end is at a temperature T_2 .

A heat balance over a length dx at distance x from the hot end gives:

heat in = heat out along rod + heat lost to surroundings

$$\text{or: } -kA \frac{dT}{dx} = \left[-kA \frac{dT}{dx} + \frac{d}{dx} \left(-kA \frac{dT}{dx} \right) dx \right] + hb dx (T - T_G)$$

where h is the film coefficient from fin to surroundings.

Writing the temperature difference $T - T_G$ equal to θ :

$$kA \frac{d^2\theta}{dx^2} = hb \theta$$

Since T_G is constant, $d^2T/dx^2 = d^2\theta/dx^2$.

$$\text{Thus: } \frac{d^2\theta}{dx^2} = \frac{hb}{kA} \theta = m^2 \theta \quad \left(\text{where } m^2 = \frac{hb}{kA} \right)$$

and:

$$\theta = C_1 e^{mx} + C_2 e^{-mx}$$

In solving this equation, three important cases may be considered:

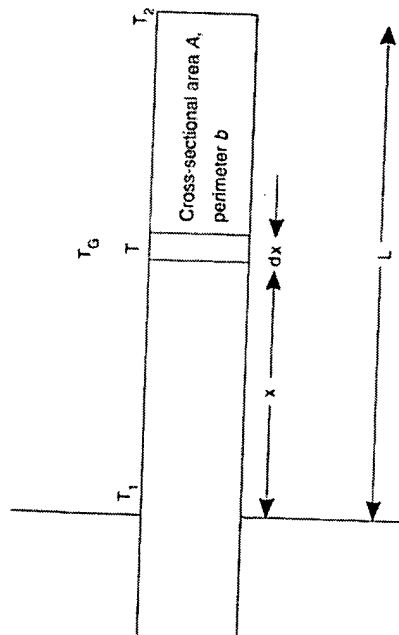


Figure 9.87. Heat flow in rod with heat loss to surroundings

(a) A long rod with temperature falling to that of surroundings, that is $\theta = 0$ when $x = \infty$:

In this case:

$$\theta = \theta_1 e^{-mx} \quad (9.248)$$

(b) A short rod from which heat loss from its end is neglected.

At the hot end: $x = 0$, $\theta = \theta_1 = C_1 + C_2$

At the cold end: $x = L$, $\frac{d\theta}{dx} = 0$

$$0 = C_1 m e^{mL} - C_2 m e^{-mL}$$

$$\theta_1 = C_1 + C_2 e^{2mL}$$

$$C_1 = \frac{\theta_1}{1 + e^{2mL}}, \quad C_2 = \frac{\theta_1}{1 + e^{-2mL}}$$

$$\theta = \frac{\theta_1 e^{mx}}{1 + e^{2mL}} + \frac{\theta_1 e^{2mx}}{1 + e^{-2mL}}$$

$$= \frac{\theta_1}{1 + e^{2mL}} [e^{mx} + e^{2mx} e^{-mx}] \quad (9.249)$$

$$\frac{\theta}{\theta_1} = \frac{e^{-mx} e^{mx} + e^{2mx} e^{-mx}}{e^{-mx} + e^{mx}}$$

$$\frac{\theta}{\theta_1} = \frac{\cosh m(L-x)}{\cosh mL} \quad (9.250)$$

This may be written:

(c) More accurately, allowing for heat loss from the end:

At the hot end: $x = 0$, $\theta = \theta_1 = C_1 + C_2$

At the cold end: $x = L$, $Q = hA\theta_{x=L} = -kA \left(\frac{d\theta}{dx} \right)_{x=L}$

The determination of C_1 and C_2 in equation 9.247 then gives:

$$\theta = \frac{\theta_1}{1 + J e^{-2mL}} (J e^{-2mL} e^{mx} + e^{-mx}) \quad (9.251)$$

$$J = \frac{km - h}{km + h}$$

where:

or, again, noting that $\cosh x = \frac{1}{2}(e^x + e^{-x})$ and $\sinh x = \frac{1}{2}(e^x - e^{-x})$:

$$\frac{\theta}{\theta_1} = \frac{\cosh m(L-x) + (h/mk) \sinh m(L-x)}{\cosh mL + (h/mk) \sinh mL} \quad (9.252)$$

The heat loss from a finned tube is obtained initially by determining the heat flow into the base of the fin from the tube surface. Thus the heat flow to the root of the fin is:

$$Q_f = -kA \left(\frac{dT}{dx} \right)_{x=0} = -kA \left(\frac{d\theta}{dx} \right)_{x=0}$$

For case (a):

$$Q_f = -kA(-m\theta_1) = kA\sqrt{\frac{hb}{kA}}\theta_1 = \sqrt{hb kA}\theta_1 \quad (9.253)$$

For case (b):

$$Q_f = -kAm\theta_1 \frac{1 - e^{-2ml}}{1 + e^{-2ml}} = \sqrt{hb kA}\theta_1 \tanh mL \quad (9.254)$$

For case (c):

$$Q_f = \sqrt{hb kA}\theta_1 \left(\frac{1 - e^{-2ml}}{1 + e^{-2ml}} \right) \quad (9.255)$$

These expressions are valid provided that the cross-section for heat flow remains constant. When it is not constant, as with a radial or tapered fin, for example, the temperature distribution is in the form of a *Bessel function* (26).

If the fin were such that there was no drop in temperature along its length, then the maximum rate of heat loss from the fin would be:

$$Q_{f \max} = bLh\theta_1$$

The fin effectiveness is then given by $Q_f/Q_{f \max}$ and, for case (b), this becomes:

$$\frac{kAm\theta_1 \tanh mL}{bLh\theta_1} = \frac{\tanh mL}{mL} \quad (9.256)$$

Example 9.31

In order to measure the temperature of a gas flowing through a copper pipe, a thermometer pocket is fixed perpendicularly through the pipe wall, the open end making very good contact with the pipe wall. The pocket is made of copper tube, 10 mm o.d. and 0.9 mm wall, and it projects 75 mm into the pipe. A thermocouple is welded to the bottom of the tube and this gives a reading of 475 K when the wall temperature is at 365 K. If the coefficient of heat transfer between the gas and the copper tube is $140 \text{ W/m}^2 \text{ K}$, calculate the gas temperature. The thermal conductivity of copper may be taken as 350 W/m K . This arrangement is shown in Figure 9.88.

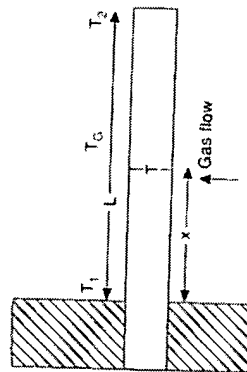


Figure 9.88. Heat transfer to thermometer pocket

Solution

If θ is the temperature difference ($T - T_2$), then:

$$\theta = \theta_1 \frac{\cosh m(L-x)}{\cosh mL}$$

$$\theta = \frac{\theta_1}{\cosh mL} \frac{hb}{kA}$$

$$m^2 = \frac{hb}{kA}$$

where the perimeter: $b = \pi \times 0.010 \text{ m}$ tube i.d. = 8.2 mm or 0.0082 m

cross sectional area of metal: $A = \frac{\pi}{4}(10.0^2 - 8.2^2) = 8.19 \pi \text{ mm}^2$ or $8.19 \pi \times 10^{-6} \text{ m}^2$

$$m^2 = \frac{(140 \times 0.010\pi)}{(350 \times 8.19\pi \times 10^{-6})} = 488 \text{ m}^{-2}$$

$$m = 22.1 \text{ m}^{-1}$$

$$\theta_1 = T_G - 365, \quad \theta_2 = T_G - 475$$

$$\frac{\theta_1}{\theta_2} = \cosh mL$$

$$\frac{T_G - 365}{T_G - 475} = \cosh(22.1 \times 0.075) = 2.72$$

$$T_G = 539 \text{ K}$$

Example 9.32

A steel tube fitted with transverse circular steel fins of constant cross-section has the following specification:

tube o.d.: $d_2 = 54.0 \text{ mm}$ fin diameter $d_1 = 70.0 \text{ mm}$
fin thickness: $w = 2.0 \text{ mm}$ number of fins/metre run = 230

Determine the heat loss per metre run of the tube when the surface temperature is 370 K and the temperature of the surroundings 280 K. The heat transfer coefficient between gas and fin is $30 \text{ W/m}^2 \text{ K}$ and the thermal conductivity of steel is 43 W/m K .

Solution

Assuming that the height of the fin is small compared with its circumference and that it may be treated as a straight fin of length $(\pi/2)(d_1 + d_2)$, then:

The perimeter: $b = \frac{2\pi(d_1 + d_2)}{2} = \pi(d_1 + d_2)$

The area: $A = \frac{\pi(d_1 + d_2)w}{2}$, i.e. the average area at right-angles to the heat flow

Then: $m = \left(\frac{hb}{kA} \right)^{0.5} = \left\{ \frac{h\pi(d_1 + d_2)}{k\pi(d_1 + d_2)w/2} \right\}^{0.5}$

$$= \left(\frac{2h}{kw} \right)^{0.5}$$

$$= \left(\frac{2 \times 30}{43 \times 0.002} \right)^{0.5}$$

$$= 26.42 \text{ m}^{-1}$$

From equation 9.254, the heat flow is given for case (b) as:

$$Q_f = mkA\theta_1 \frac{e^{2mL} - 1}{1 + e^{2mL}}$$

In this equation:

$$A = \frac{\pi(70.0 + 54.0) \times 2.0}{2} = 390 \text{ mm}^2 \text{ or } 0.00039 \text{ m}^2$$

$$L = \frac{d_1 - d_2}{2} = 8.0 \text{ mm or } 0.008 \text{ m}$$

$$mL = 26.42 \times 0.008 = 0.211$$

$$\theta_1 = 370 - 280 = 90 \text{ deg K}$$

$$Q_f = \frac{26.42 \times 43 \times 3.9 \times 10^{-4} \times 90(e^{0.422} - 1)}{1 + e^{0.422}}$$

$$= \frac{39.9 \times 0.525}{2.525} = 8.29 \text{ W per fin}$$

The heat loss per metre run of tube = $8.29 \times 230 = 1907 \text{ W/m}$
or:
 1.91 kW/m

In this case, the low value of mL indicates a fin efficiency of almost 1.0, though where mL tends to 10, efficiency falls to about 0.8.

Practical data

A neat form of construction has been designed by the Brown Finetube Company of America. On both prongs of a hairpin tube are fitted horizontal fins which fit inside concentric tubes, joined at the base of the hairpin. Units of this form can be conveniently arranged in banks to give large heat transfer surfaces. It is usual for the extended surface to be at least five times greater than the inside surface, so that the low coefficient on the fin side is balanced by the increase in surface. An indication of the surface obtained is given in Table 9.20.

Table 9.20. Data on surface of finned tube units^(a)

Pipe size outside diameter	mm	(in)	Outside surface of pipe		Number of fins	Height of fin		Surface of finned pipe (m ² /ft)		Height of fin (ft)
			(m ² /ft)	(ft ² /ft length)		12.7 mm	25.4 mm	0.5 in	1 in	
25.4	1	0.08	0.262		12	0.385	0.689	1.262	2.262	
					16	0.486	0.893	1.595	2.979	
48.3	1.9	0.15	0.497		20	0.587	1.096	1.927	3.593	
					24	0.660	1.167	2.164	3.830	
					28	0.761	1.371	2.497	4.497	
					36	0.863	1.574	2.830	5.164	
						1.066	1.980	3.498	6.497	

^(a) Brown Finetube Company.

A typical hairpin unit with an effective surface on the fin side of 9.4 m^2 has an overall length of 6.6 m, height of 0.34 m, and width of 0.2 m. The free area for flow on the fin side is 2.645 mm^2 against 1.320 mm^2 on the inside; the ratio of the transfer surface on the fin side to that inside the tubes is 5.93:1.

The fin film coefficient h_f has been expressed by plotting:

$$\frac{h_f}{C_p G'} \left(\frac{C_p \mu}{k} \right)^{2/3} \left(\frac{\mu}{\mu_s} \right)^{-0.14} \text{ against } \frac{d_e G'}{\mu}$$

where h_f is based on the total fin inside surface area (fin and tube), G' is the mass rate of flow per unit area, and d_e is the equivalent diameter, or:

$$d_e = \frac{4 \times \text{cross-sectional area for flow on fin side}}{\text{total wetted perimeter for flow (fin + outside of tube + inner surface of shell tube)}}$$

Experimental work has been carried out with exchangers in which the inside tube was 48 mm outside diameter and was fitted with 24, 28, or 36 fins (12.5 mm by 0.9 mm) in a 6.1 m length: the finned tubes were inserted inside tubes 90 mm inside diameter. With steam on the tube side, and tube oils and kerosene on the fin side, the experimental data were well correlated by plotting:

$$\frac{h_f}{C_p G'} \left(\frac{C_p \mu}{k} \right)^{2/3} \left(\frac{\mu}{\mu_s} \right)^{-0.14} \text{ against } \frac{d_e G'}{\mu}$$

Typical values were:

$$\frac{h_f}{C_p G'} \left(\frac{C_p \mu}{k} \right)^{2/3} \left(\frac{\mu}{\mu_s} \right)^{-0.14} = 0.25 \quad 0.055 \quad 0.012 \quad 0.004$$

$$\frac{d_e G'}{\mu} = 1 \quad 10 \quad 100 \quad 1000$$

Some indication of the performance obtained with *transverse finned tubes* is given in Table 9.21. The figures show the heat transferred per unit length of pipe when heating air on the fin side with steam or hot water on the tube side, using a temperature difference of 100 deg K. The results are given for three different spacings of the fins.

Table 9.21. Data on finned tubes

Inside diam. of tube	Outside diam. of fin	No. of fins/m run	Heat transferred (kW/m)						Inside diam. of tube	Outside diam. of fin	No. of fins/ft run	Heat transferred (Btu/h ft)		
			19 mm	25 mm	38 mm	50 mm	75 mm	140 mm				20	24	30
65	80	100	0.47	0.63	0.37	1.07	1.38							
			0.49	0.64	1.02	1.12	1.44							
			0.54	0.69	1.14	1.24	1.59							
Heat transferred (Btu/h ft)														
3 in	2 1/2 in	2 1/2 in	1 in	1 1/8 in	3/8 in	4 1/8 in	5 1/2 in							
20	24	30	485	650	1010	1115	1440							
			505	665	1060	1170	1495							
			565	720	1190	1295	1655							

(Data taken from catalogue of G. A. Harvey and Co. Ltd. of London.)

9.10.2. Plate-type exchangers

A series of plate type heat exchangers which present some special features was developed by the APV Company. The general construction is shown in Figure 9.89, which shows an Alfa-Laval exchanger and from which it is seen that the equipment consists of a series of parallel plates held firmly together between substantial head frames. The plates are one-piece pressings, frequently of stainless steel, and are spaced by rubber seals, gaskets cemented into a channel around the edge of each plate. Each plate has a number of troughs pressed out at right angles to the direction of flow and arranged so that they interlink with each other to form a channel of constantly changing direction and section. With normal construction the gap between the plates is 1.3–1.5 mm. Each liquid flows in alternate spaces and a large surface can be obtained in a small volume.

Because of the shape of the plates, the developed area of surface is appreciably greater than the projected area. This is shown in Table 9.22 for the four common sizes of plate

Table 9.22. Plate areas

Plate type	Projected area		Developed area	
	m ²	ft ²	m ²	ft ²
HT	0.09	1.00	0.13	1.35
HX	0.13	1.45	0.17	1.81
HM	0.27	2.88	0.35	3.73
HF	0.36	3.85	0.43	4.60

A high degree of turbulence is obtained even at low flowrates and the high heat transfer coefficients obtained are illustrated by the data in Table 9.23. These refer to the heating of cold water by the equal flow of hot water in an HF type exchanger (aluminium or copper), at an average temperature of 310 K.

Table 9.23. Performance of plate-type exchanger type HF

Heat transferred per plate		Water flow		U based on developed area	
W/K	Btu/h °F	lit/s	gal/h	kW/m ² K	Btu/h ft ² °F
1580	3000	0.700	550	3.70	650
2110	4000	1.075	850	4.94	870
2640	5000	1.580	1250	6.13	1080

(Courtesy of the APV Company.)

Using a stainless steel plate with a flow of 0.00114 m³/s, the heat transferred is 1760 W/K for each plate.

The high transfer coefficient enables these exchangers to be operated with very small temperature differences, so that a high heat recovery is obtained. These units have been particularly successful in the dairy and brewing industries, where the low liquid capacity and the close control of temperature have been valuable features. A further advantage is that they are easily dismantled for inspection of the whole plate. The necessity for the long gasket is an inherent weakness, but the exchangers have been worked successfully

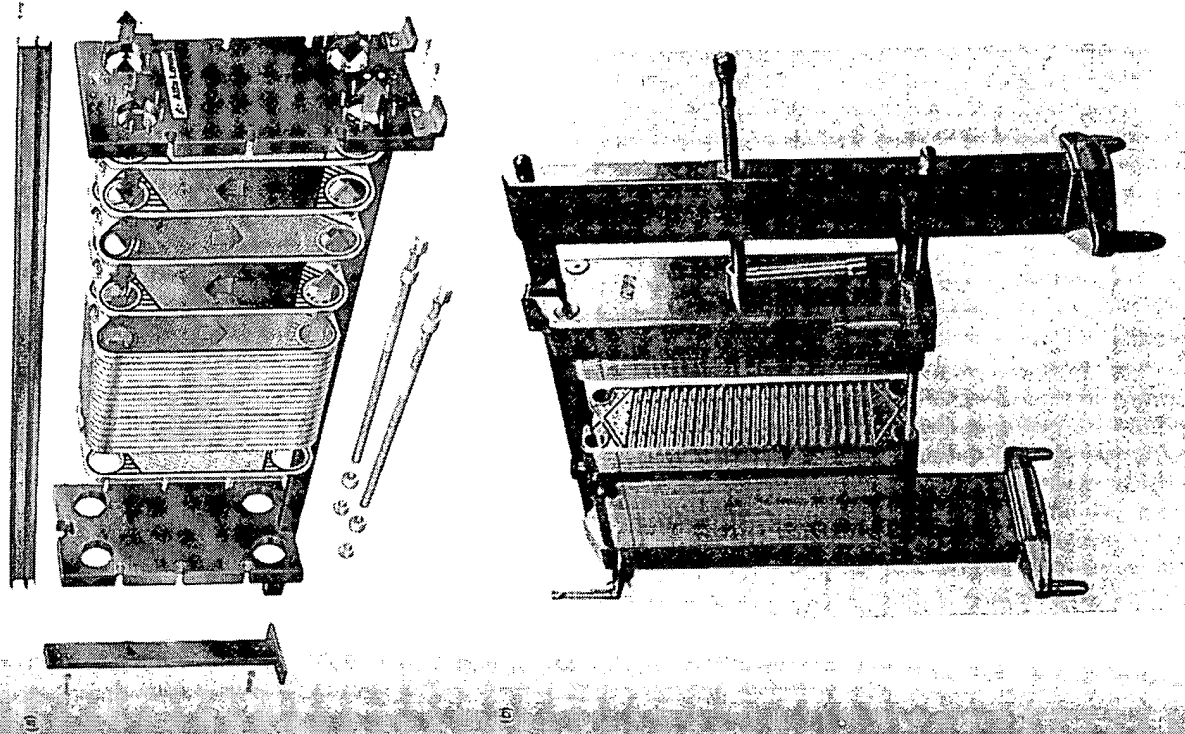


Figure 9.89. (a) Alfa-Laval plate heat exchanger (b) APV plate heat exchanger

up to 423 K and at pressures of 930 kN/m². They are now being used in the processing of gas industries with solvents, sugar, acetic acid, ammoniacal liquor, and so on.

9.10.3. Spiral heat exchangers

A spiral plate exchanger is illustrated in Figure 9.90 in which two fluids flow through the channels formed between the spiral plates. With this form of construction the velocity may be as high as 2.1 m/s and overall transfer coefficients of 2.8 kW/m² K are frequently obtained. The size can therefore be kept relatively small and the cost becomes comparable or even less than that of shell and tube units, particularly when they are fabricated from alloy steels.

A further design of spiral heat exchanger, described by NEIL⁽¹²⁷⁾, is essentially a single pass counterflow heat exchanger with fixed tube plates distinguished by the spiral winding of the tubes, each consisting, typically of a 10 mm o.d. tube wound on to a 38 mm o.d. coil such that the inner heat transfer coefficient is 1.92 times greater than for a straight tube. The construction overcomes problems of differential expansion rates of the tubes and the shell and the characteristics of the design enable the unit to perform well with superheated steam where the combination of counterflow, high surface area per unit volume of shell and the high inside coefficient of heat transfer enables the superheat to be removed effectively in a unit of reasonable size and cost.

9.10.4. Compact heat exchangers

Advantages of compact units

In general, heat exchanger equipment accounts for some 10 per cent of the cost of a plant at a level at which there is no great incentive for innovation. Trends such as the growth in energy conservation schemes, the general move from bulk chemicals to value-added products and plant problems associated with drilling rigs have, however, all prompted the development and increased application of compact heat exchangers. Here compactness is a matter of degree, maximising the heat transfer area per unit volume of exchanger and this leads to narrow channels. Making shell and tube exchangers more compact presents construction problems and a more realistic approach is to use plate or plate-fin heat exchangers. The relation between various types of exchanger, in terms of the heat transfer area per unit volume of exchanger is shown in Figure 9.91, taken from REDMAN⁽¹²⁸⁾. In order to obtain a thermal effectiveness in excess of 90 per cent, countercurrent flow is highly desirable and this is not easily achieved in shell and tube units which often have a number of tube-side passes in order to maintain reasonable velocities. Because of the baffle design on the shell-side, the flow at the best may be described as cross-flow, and the situation is only partly redeemed by having a train of exchangers which is an expensive solution. Again in dealing with high value added products, which could well be heat sensitive, a more controllable heat exchanger than a shell and tube unit, in which not all the fluid is heated to the same extent, might be desirable. One important application of compact heat exchangers is the cooling of natural gas on offshore rigs where space (costing as much as £120,000/m²) is of paramount importance.

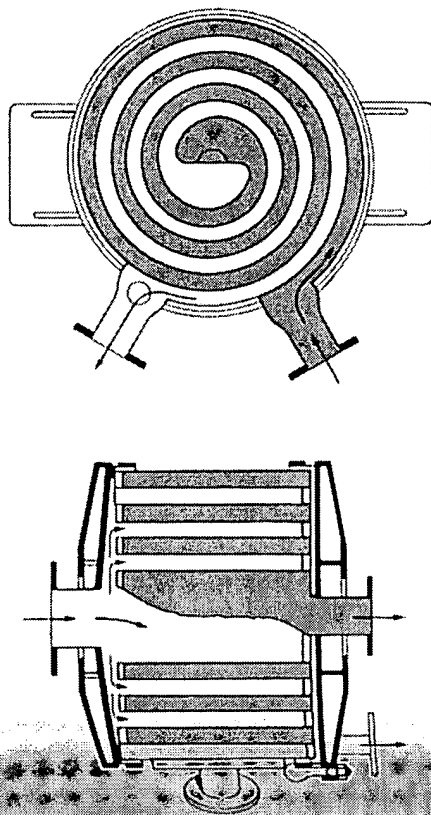


Figure 9.90. Spiral heat exchanger (a) Flow paths

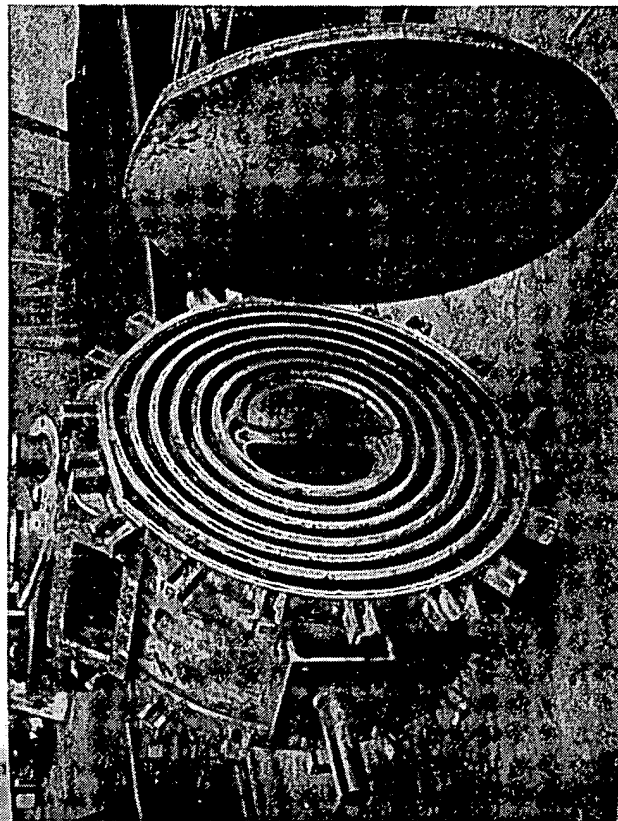


Figure 9.90. Spiral plate exchanger (b) with cover removed

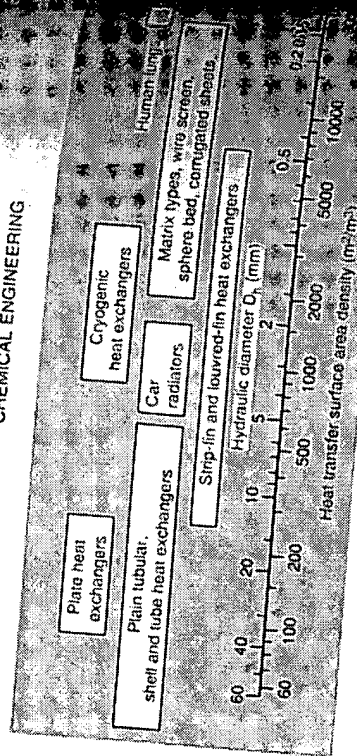


Figure 9.91. Surface area as a function of volume of exchanger for different types

Plate and fin exchangers

Plate and fin heat exchangers, used in the motor, aircraft and transport industries for many years, are finding increased application in the processing industries and in particular natural gas liquefaction, cryogenic air separation, the production of olefins and in production of hydrogen and carbon monoxide. Potential applications include ammonia production, offshore processing, nuclear engineering and syngas production. As described by GREGORY⁽¹²⁹⁾, the concept is that of flat plates of metal, usually aluminium, corrugated metal, which not only holds the plates together but also acts as a surface for heat transfer. Bars at the edges of the plates retain each fluid between the plates, and the space between each pair of plates, apportioned to each fluid according to the heat transfer and pressure drop requirements, is known as a layer. The heights of bars and corrugations are standardised in the UK at 3.8, 6.35, and 8.9 mm and in the USA at 3.18, 6.35, and 8.9 mm and in

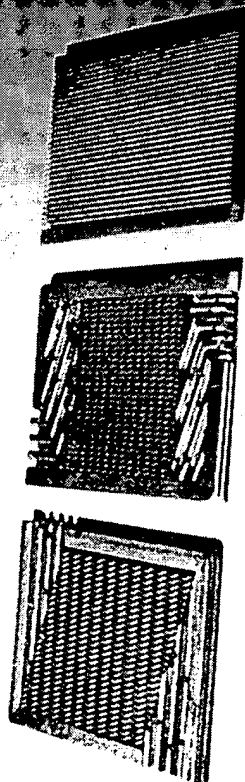


Figure 9.92. Plate and fin exchangers

There are four basic forms of corrugation: plain in which a sheet of metal is corrugated in the simplest way with fins at right angles to the plates; serrated where each set of fins sideways every 9.5 mm to give a zig-zag path; and perforated corrugation, which is used for a plain corrugation made from perforated material. Each stream to be heated

cooled can have different corrugation heights, different corrugation types, different numbers of layers and different entry and exit points including part length entry and exit. Because the surface in the hot fluid (or fluids) can vary widely from that in the cold fluid (or fluids) it is unrealistic to quote surface areas for either side, as in shell and tube units, though the overall surface area available to all the fluids is $1000 \text{ m}^2/\text{m}^3$ of exchanger.

In design, the general approach is to obtain the term (hA) for each stream, sum these together for all the cold and all the hot streams and determine an overall value of (hA) given by:

$$\frac{1}{(hA)_{ov}} = \frac{1}{(hA)_{hw}} + \frac{1}{(hA)_{cw}} \quad (9.257)$$

where ov , hw and cw refer, respectively, to overall, hot-side and cold-side values.

Printed-circuit exchangers

Various devices such as small diameter tubes, fins, tube inserts and porous boiling surfaces may be used to improve the surface density and heat transfer coefficients in shell and tube heat exchangers and yet these are not universally applicable and, in general, such units remain essentially bulky. Plate and fin exchangers have either limited fluid compatibility or limited inefficiency, problems which are overcome by using printed-circuit exchangers as described by JOHNSTON⁽¹³⁰⁾. These are constructed from flat metal plates which have fluid flow passages chemically milled into them by means of much the same techniques as are used to produce electrical printed circuits. These plates are diffusion-bonded together to form blocks riddled with precisely sized, shaped, routed and positioned passages, and these blocks are in turn welded together to form heat exchange cores of the required capacity. Fluid headers are attached to the core faces and sometimes the assembly is encapsulated. Passages are typically $0.3\text{--}1.5 \text{ mm}$ deep giving surface areas of $1000\text{--}5000 \text{ m}^2/\text{m}^3$, an order of magnitude higher than surface densities in shell and tube designs; and in addition the fine passages tend to sustain relatively high heat transfer coefficients, undiminished by fin inefficiencies, and so less surface is required.

In designing a unit, each side of the exchanger is independently tailored to the duty required, and the exchanger effectiveness (discussed in Section 9.9.4) can range from 2–5 per cent to values in excess of 98 per cent without fundamental design or construction problems arising. Countercurrent, co-current and cross-flow contacting can be employed individually or in combination.

A note of caution on the use of photo-etched channels has been offered by RAMSHAW⁽¹³¹⁾ who points out that the system is attractive in principle provided that severe practical problems such as fouling are not encountered. With laminar flow in matrices with a mean plate spacing of $0.3\text{--}1 \text{ mm}$, volumetric heat transfer coefficients of $7 \text{ MW/m}^3 \text{ K}$ have been obtained with modest pressure drops. Such values compare with $0.2 \text{ MW/m}^3 \text{ K}$ for shell and tube exchangers and $1.2 \text{ MW/m}^3 \text{ K}$ for plate heat exchangers.

9.10.5. Scraped-surface heat exchangers

In cases where a process fluid is likely to crystallise on cooling or the degree of fouling is very high or indeed the fluid is of very high viscosity, use is often made of scraped-surface heat exchangers in which a rotating element has spring-loaded scraper blades which wipe

the inside surface of a tube which may typically be 0.15 m in diameter. Double-pipe construction is often employed with a jacket, say 0.20 m in diameter, and one coming arrangement is to connect several sections in series or to install several pipes within a common shell. Scraped-surface units of this type are used in paraffin-wax plants and for evaporating viscous or heat-sensitive materials under high vacuum. This is an application to which the *thin-film device* is especially suited because of the very short residence time involved. In such a device the clearance between the agitator and the wall may be either fixed or variable since both rigid and hinged blades may be used. The process liquid continuously spread in a thin layer over the vessel wall and it moves through the device either by the action of gravity or that of the agitator or of both. A tapered or helical agitator produces longitudinal forces on the liquid.

In describing chillers for the production of wax distillates, NELSON⁽¹³²⁾ points out that the rate of cooling depends very much on the effectiveness of the scrapers, and quotes overall coefficients of heat transfer ranging from 15 W/m² K with a poorly fitting scraper to 90 W/m² K where close fitting scrapers remove the wax effectively from the chilled surface.

The *Votator* design has two or more floating scraper-agitators which are forced against the cylinder wall by the hydrodynamic action of the fluid on the agitator and by centrifugal action; the blades are loosely attached to a central shaft called the mutator. The votator is used extensively in the food processing industries and also in the manufacture of greases and detergents. As the blades are free to move, the clearance between the blades and the wall varies with operating conditions and a typical installation may be 75–100 mm in diameter and 0.6–1.2 m long. In the *spring-loaded* type of scraped-surface heat exchanger the scrapers are held against the wall by leaf springs, and again there is a variable clearance between the agitator and the cylinder wall since the spring force is balanced by the radial hydrodynamic force of the liquid on the scraper. Typical applications of this device are the processing of heavy waxes and oils and crystallising solutions. Generally the units are 0.15–0.3 m in diameter and up to 1.2 m long. Some of the more specialised heat exchangers and chemical reactors employ helical ribbons, augers or twisted tapes as agitators and, in general, these are fixed clearance devices used for high viscous materials. There is no general rule as to maximum or minimum dimensions since each application is a special case.

One of the earliest investigations into the effectiveness of scrapers for improving heat transfer was that of HUGGINS⁽¹³³⁾ who found that although the improvement with water was negligible, cooling times for more viscous materials could be considerably reduced. This was confirmed by LAUGHLIN⁽¹³⁴⁾ who has presented operating data on a system where the process fluid changes from a thin liquid to a paste and finally to a powder. HOULTON⁽¹³⁵⁾, making tests on the votator, found that back-mixing was negligible and some useful data on a number of food products have been obtained by BOLANOWSKI and LINEBERRY⁽¹³⁶⁾ who, in addition to discussing the operation and uses of the votator, quote overall heat transfer coefficients for each food tested. Using a *liquid-full* system, SKELLAND *et al.*^(137–139) have proposed the following general design correlation for the votator:

$$\frac{hd_v}{k} = c_1 \left(\frac{C_p \mu}{k} \right)^{c_2} \left(\frac{(d_v - d_r) \rho}{\mu} \right) \left(\frac{d_v N}{u} \right)^{0.82} \left(\frac{d_r}{d_e} \right)^{0.53} (n_B)^{0.53} \quad (9.258)$$

where for cooling viscous liquids $c_1 = 0.014$ and $c_2 = 0.96$, and for thin mobile liquids $c_1 = 0.039$ and $c_2 = 0.70$. In this correlation d_v is the diameter of the vessel, d_r is the diameter of the rotor and u is the average axial velocity of the liquid. This correlation may only be applied to the range of experimental data upon which it is based, since h will not approach zero as n_B , d_r , $(d_v - d_r)$, N and u approach zero. Reference to the use of the votator for crystallisation is made in Volume 2, Chapter 15.

The majority of work on heat transfer in *thin-film* systems has been directed towards obtaining data on specific systems rather than developing general design methods, although BOFFI *et al.*^(140–142) have developed the following correlations for heating without change of phase:

$$\frac{hd_v}{k} = Nu = 0.018 Re^{0.6} Re_c^{0.46} Pr^{0.57} \left(\frac{d_v}{l} \right)^{0.48} (n_B)^{0.24} \quad (9.259)$$

and for evaporation:

$$\frac{hd_v}{k} = Nu = 0.65 Re_c^{0.43} Re_c^{0.25} Pr^{0.33} (n_B)^{0.33} \quad (9.260)$$

From both of these equations, it will be noted that the heat transfer coefficient is *not* a function of the temperature difference. Here $Re_c'' = (d_v^2 N \rho / \mu)$ and $Re_c = (u d_v \rho / \mu)$, where d_v is the tube diameter and u is the average velocity of the liquid in the film in the axial direction.

It is also of significance that the agitation suppresses nucleation in a fluid which might otherwise deposit crystals.

9.11. THERMAL INSULATION

9.11.1. Heat losses through lagging

A hot reaction or storage vessel or a steam pipe will lose heat to the atmosphere by radiation, conduction, and convection. The loss by radiation is a function of the fourth power of the absolute temperatures of the body and surroundings, and will be small for low temperature differences but will increase rapidly as the temperature difference increases. Air is a very poor conductor, and the heat loss by conduction will therefore be small except possibly through the supporting structure. On the other hand, since convection currents form very easily, the heat loss from an unlagged surface is considerable. The conservation of heat, and hence usually of total energy, is an economic necessity, and some form of lagging should normally be applied to hot surfaces. Lagging of plant operating at high temperatures is also necessary in order to achieve acceptable working conditions in the vicinity. In furnaces, as has already been seen, the surface temperature is reduced substantially by using a series of insulating bricks which are poor conductors.

The two main requirements of a good lagging material are that it should have a low thermal conductivity and that it should suppress convection currents. The materials that are frequently used are cork, 85 per cent magnesite, glass wool, and vermiculite. Cork is a very good insulator though it becomes charred at moderate temperatures and is used mainly in refrigerating plants. Eighty-five per cent magnesite is widely used for lagging steam pipes and may be applied either as a hot plastic material or in preformed sections. The preformed sections are quickly fitted and can frequently be dismantled

and re-used whereas the plastic material must be applied to a hot surface and cannot be re-used. Thin metal sheeting is often used to protect the lagging.

The rate of heat loss per unit area is given by:

$$\frac{\text{total temperature difference}}{\text{total thermal resistance}}$$

For the case of heat loss to the atmosphere from a lagged steam pipe, the thermal resistance is due to that of the condensate film and dirt on the inside of the pipe, the pipe wall, that of the lagging, and that of the air film outside the lagging. Thus the unit length of a lagged pipe:

$$\frac{Q}{l} = \frac{\Sigma \Delta T}{\left[\frac{1}{h_i \pi d} + \frac{x_w}{k_w \pi d_w} + \frac{x_l}{k_l \pi d_m} + \frac{1}{(h_r + h_c) \pi d_o} \right]} \quad (9.26)$$

where d is the inside diameter of pipe, d_w the mean diameter of pipe wall, d_o the logarithmic mean diameter of lagging, d_s the outside diameter of lagging, x_w , x_l are the pipe wall and lagging thickness respectively, k_w , k_l the thermal conductivity of the pipe wall and lagging, and h_i , h_r , h_c the inside film, radiation, and convection coefficients.

Example 9.33

A steam pipe, 150 mm i.d. and 168 mm o.d., is carrying steam at 444 K and is lagged with 50 mm of 85 per cent magnesia. What is the heat loss to air at 294 K?

Solution

In this case:

$$\begin{aligned} d &= 150 \text{ mm} & \text{or} & 0.150 \text{ m} \\ d_o &= 168 \text{ mm} & \text{or} & 0.168 \text{ m} \\ d_w &= 159 \text{ mm} & \text{or} & 0.159 \text{ m} \\ d_s &= 268 \text{ mm} & \text{or} & 0.268 \text{ m} \\ d_m, \text{ the log mean of } d_o & \text{ and } d_s &= & 215 \text{ mm} \quad \text{or} \quad 0.215 \text{ m} \end{aligned}$$

The coefficient for condensing steam together with that for any scale will be taken as 8500 W/m² K, 45 W/m K, and k_l as 0.073 W/m K.

The temperature on the outside of the lagging is estimated at 314 K and $(h_r + h_c)$ will be taken as 10 W/m² K.

The thermal resistances are therefore:

$$\begin{aligned} \frac{1}{h_i \pi d} &= \frac{1}{8500 \times \pi \times 0.150} = 0.00025 \\ \frac{x_w}{k_w \pi d_w} &= \frac{0.009}{45 \times \pi \times 0.159} = 0.00040 \\ \frac{x_l}{k_l \pi d_m} &= \frac{0.050}{0.073 \times \pi \times 0.215} = 1.013 \\ \frac{1}{(h_r + h_c) \pi d_o} &= \frac{1}{10 \times \pi \times 0.268} = 0.119 \end{aligned}$$

The first two terms may be neglected and hence the total thermal resistance is 1.132 m K/W

The heat loss per metre length = $(444 - 294)/1.132 = 132.5 \text{ W/m}$ (from equation 9.26).

The temperature on the outside of the lagging may now be checked as follows:

$$\frac{\Delta T(\text{lagging})}{\Sigma \Delta T} = \frac{1.013}{1.132} = 0.895$$

$$\Delta T(\text{lagging}) = 0.895(444 - 294) = 134 \text{ deg K}$$

Thus the temperature on the outside of the lagging is $(444 - 134) = 310 \text{ K}$, which approximates to the assumed value.

Taking an emissivity of 0.9, from equation 9.119:

$$h_r = \frac{[0.9 \times 5.67 \times 10^{-8} (310^4 - 294^4)]}{(310 - 294)} = 7.40 \text{ W/m}^2 \text{ K}$$

From Table 9.5 for air ($Gr \cdot Pr = 10^4 - 10^9$), $n = 0.25$ and $C'' = 1.32$.

Substituting in equation 9.105 (putting l = diameter = 0.268 m):

$$h_c = C'' (\Delta T)^{0.25} l^{0.75} = 1.32 \left[\frac{310 - 294}{0.268} \right]^{0.25} = 3.67 \text{ W/m}^2 \text{ K}$$

and

Thus $(h_r + h_c) = 11.1 \text{ W/m}^2 \text{ K}$, which is close to the assumed value. In practice it is rare for forced convection currents to be absent, and the heat loss is probably higher than this value.

If the pipe were unlagged, $(h_r + h_c)$ for $\Delta T = 150 \text{ K}$ would be about $20 \text{ W/m}^2 \text{ K}$ and the heat loss would then be:

$$\begin{aligned} \frac{Q}{l} &= (h_r + h_c) \pi d_o \Delta T \\ &= (20 \times \pi \times 0.168 \times 150) = 1584 \text{ W/m} \\ &= 1.58 \text{ kW/m} \end{aligned}$$

or

Under these conditions it is seen that the heat loss has been reduced by more than 90 per cent by the addition of a 50 mm thickness of lagging.

9.11.2. Economic thickness of lagging

Increasing the thickness of the lagging will reduce the loss of heat and thus give a saving in the operating costs. The cost of the lagging will increase with thickness and there will be an optimum thickness when further increase does not save sufficient heat to justify the cost. In general the smaller the pipe the smaller the thickness used, though it cannot be too strongly stressed that some lagging everywhere is better than excellent lagging in some places and none in others. For temperatures of 373–423 K, and for pipes up to 150 mm diameter, LYLE⁽¹⁴³⁾ recommends a 25 mm thickness of 85 per cent magnesia lagging and 50 mm for pipes over 230 mm diameter. With temperatures of 470–520 K 38 mm is suggested for pipes less than 75 mm diameter and 50 mm for pipes up to 230 mm diameter.

9.11.3. Critical thickness of lagging

As the thickness of the lagging is increased, resistance to heat transfer by thermal conduction increases. Although the outside area from which heat is lost to the surroundings also increases, giving rise to the possibility of increased heat loss. It is perhaps easiest to think of the lagging as acting as a fin of very low thermal conductivity. For a cylindrical

pipe, there is the possibility of heat losses being increased by the application of lagging only if $hr/k < 1$, where k is the thermal conductivity of the lagging, h is the outside film coefficient, and r is the outside diameter of the pipe. In practice, this situation is likely to arise only for pipes of small diameters.

The heat loss from a pipe at a temperature T_S to surroundings at temperature T_A is considered. Heat flows through lagging of thickness x across which the temperature falls from a constant value T_S at its inner radius r , to an outside temperature T_L which is a function of x , as shown in Figure 9.93. The rate of heat loss Q from a length l of pipe is given by equation 9.262, by considering the heat loss from the outside of the lagging, and by equations 9.263 and 9.264, which give the transfer rate by thermal conduction through the lagging of logarithmic mean radius r_m :

$$Q = 2\pi l(r+x)(T_L - T_A)h \quad (9.262)$$

$$Q = \frac{2\pi l r_m}{x} k(T_S - T_L) \quad (9.263)$$

$$= \frac{2\pi l k}{\ln \frac{r+x}{r}} (T_S - T_L) \quad (9.264)$$

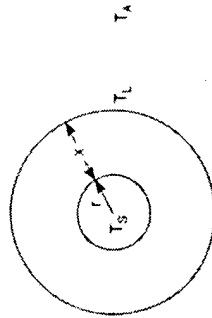


Figure 9.93. Critical lagging thickness

Equating the values given in equations 9.262 and 9.264:

$$(r+x)h(T_L - T_A) = \frac{k}{\ln \frac{r+x}{r}} (T_S - T_L)$$

Then:

$$a = (r+x) \frac{h}{k} \ln \frac{r+x}{r} = \frac{T_S - T_L}{T_L - T_A}$$

$$aT_L - aT_A = T_S - T_L$$

$$T_L = \frac{T_S + aT_A}{a+1}$$

Substituting in equation 9.262:

$$Q = 2\pi l(r+x) \left\{ \left(\frac{T_S + aT_A}{a+1} - T_A \right) \right\} h$$

$$= \frac{2\pi l h(r+x)}{a+1} (T_S - T_A)$$

$$= 2\pi l h(T_S - T_A) \left\{ (r+x) \frac{1}{1 + (r+x) \frac{h}{k} \ln \left(\frac{r+x}{r} \right)} \right\} \quad (9.265)$$

Differentiating with respect to x :

$$\frac{dQ}{dx} = \frac{2\pi l h(T_S - T_A)}{1 + (r+x) \frac{h}{k} \ln \frac{r+x}{r} - (r+x) \left[\frac{h}{k} \ln \frac{r+x}{r} + (r+x) \frac{h}{k} \frac{1}{(r+x)} \right]} \left[1 + (r+x) \frac{h}{k} \ln \left(\frac{r+x}{r} \right) \right]^2$$

The maximum value of $Q(Q_{\max})$ occurs when $dQ/dx = 0$.

that is, when: $1 - (r+x) \frac{h}{k} = 0$

$$x = \frac{k}{h} - r$$

(9.266)

or

When the relation between heat loss and lagging thickness exhibits a maximum for the unlagged pipe ($x = 0$), then:

$$\frac{hr}{k} = 1 \quad (9.267)$$

When $hr/k > 1$, the addition of lagging always reduces the heat loss.

When $hr/k < 1$, thin layers of lagging increase the heat loss and it is necessary to exceed the critical thickness given by equation 9.266 before any benefit is obtained from the lagging.

Substituting in equation 9.265 gives the maximum heat loss as:

$$Q_{\max} = 2\pi l h(T_S - T_A) \left\{ \frac{k}{h} \frac{1}{1 + \frac{h}{k} \ln \frac{k}{hr}} \right\}$$

$$= 2\pi l (T_S - T_A) k \frac{1}{1 + \ln \frac{k}{hr}} \quad (9.268)$$

For an unlagged pipe, $x = 0$ and $T_L = T_S$. Substitution in equation 9.262 gives the rate of heat loss Q_o as:

$$Q_o = 2\pi l r(T_S - T_A)h \quad (9.269)$$

$$\frac{Q_{\max}}{Q_o} = \frac{k}{rh} \left/ \left(1 + \ln \frac{k}{rh} \right) \right. \quad (9.270)$$

Thus:

The ratio Q/Q_o is plotted as a function of thickness of lagging (x) in Figure 9.94.

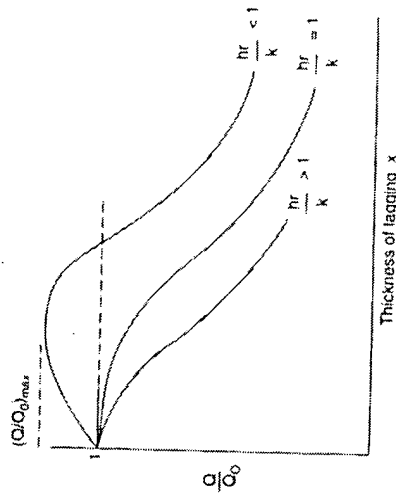


Figure 9.34. Critical thickness of lagging

Example 9.34

A pipeline of 100 mm outside diameter, carrying steam at 420 K, is to be insulated with a lagging material which costs £10/m³ and which has a thermal conductivity of 0.1 W/m K. The ambient temperature may be taken as 285 K, and the coefficient of heat transfer from the outside of the lagging to the surroundings as 10 W/m² K. If the value of heat energy is 7.5×10^{-4} £/MJ and the capital cost of the lagging is to be depreciated over 5 years with an effective simple interest rate of 10 per cent per annum based on the initial investment, what is the economic thickness of the lagging?

Is there any possibility that the heat loss could actually be increased by the application of too thin a layer of lagging?

Solution

For a thick-walled cylinder, the rate of conduction of heat through lagging is given by equation 9.21:

$$Q = \frac{2\pi k(T_i - T_o)}{\ln(d_o/d_i)} \quad \text{W}$$

where d_o and d_i are the external and internal diameters of the lagging and T_o and T_i the corresponding temperatures.

Substituting $k = 0.1$ W/mK, $T_o = 420$ K (neglecting temperature drop across pipe wall), and $d_i = 0.1$ m, then

$$\frac{Q}{l} = \frac{2\pi \times 0.1(420 - T_o)}{\ln(d_o/0.1)} \quad \text{W/m}$$

The term Q/l must also equal the heat loss from the outside of the lagging,

$$\text{or,} \quad \frac{Q}{l} = h_o(T_o - 285)\pi d_o = 10(T_o - 285)\pi d_o \quad \text{W/m}$$

Thus:

$$T_o = \left\{ \frac{Q}{l} \frac{1}{10\pi d_o} + 285 \right\} \quad \text{K}$$

Substituting:

$$\frac{Q}{l} = \frac{2\pi \times 0.1 \left[135 - \frac{Q}{l} \frac{1}{10\pi d_o} \right]}{\ln(d_o/0.1)}$$

$$\text{or} \quad \frac{Q}{l} = \frac{2\pi \times 0.1 \times 135}{\ln(d_o/0.1) + 2\pi \times 0.1 \times \frac{1}{10\pi d_o}} = \frac{84.82}{\ln(d_o/0.1) + (0.02/d_o)} \quad \text{W/m}$$

Value of heat lost = 7.5×10^{-4} £/MJ

$$\text{or} \quad \frac{84.82}{\ln(d_o/0.1) + (0.02/d_o)} \times 7.5 \times 10^{-4} \times 10^{-6} = \frac{6.36 \times 10^{-3}}{\ln(d_o/2.1) + (0.02/d_o)} \quad \text{£/ms}$$

Volume of lagging per unit pipe length = $\frac{\pi}{4}(d_o^2 - (0.1)^2)$ m³/m

Capital cost of lagging = £10/m³ or $\frac{\pi}{4}(d_o^2 - 0.01)10 = 7.85(d_o^2 - 0.01)$ £/m

Young that 1 year = 31.5 Ms, then:

Depreciation = $7.85(d_o^2 - 0.01)/(5 \times 31.5 \times 10^6) = 4.98 \times 10^{-8}(d_o^2 - 0.01)$ £/Ms

Interest charges = $(0.1 \times 7.85)(d_o^2 - 0.01)/(31.5 \times 10^6) = 2.49 \times 10^{-8}(d_o^2 - 0.01)$ £/Ms

Total capital charges = $7.47 \times 10^{-8}(d_o^2 - 0.01)$ £/Ms

Total cost (capital charges + value of heat lost) is given by:

$$C = \left\{ \frac{6.36}{\ln(d_o/0.1) + (0.02/d_o)} + 7.47(d_o^2 - 0.01) \right\} 10^{-8} \quad \text{£/Ms}$$

Differentiating with respect to d_o :

$$10^8 \frac{dC}{dd_o} = 6.36 \left[\frac{-1}{[\ln(d_o/0.1) + (0.02/d_o)]^2} \right] \left[\frac{1}{d_o} - \frac{0.02}{d_o^2} \right] + 7.47(2d_o)$$

In order to obtain the minimum value of C , dC/dd_o must be put equal to zero.

$$\text{Then} \quad \frac{1}{[\ln(d_o/0.1) + (0.02/d_o)]^2} = \frac{(7.47 \times 2)}{6.36} \left[\frac{d_o}{(1/d_o) - (0.02/d_o^2)} \right]$$

that is:

$$\frac{1}{[\ln(d_o/0.1) + (0.02/d_o)]^2} = \frac{2.35}{(d_o - 0.02)}$$

A trial and error solution gives $d_o = 0.426$ m or 426 mm

Thus, the economic thickness of lagging = $(426 - 100)/2 = 163$ mm

For this pipeline:

$$\frac{hr}{k} = \frac{10 \times (50 \times 10^{-3})}{0.1} = 5$$

From equation 9.267, the critical value of hr/k , below which the heat loss may be increased by a thin layer of lagging, is 1. For $hr/k > 1$, as in this problem, the situation will not arise.

9.12. FURTHER READING

- ANDERSON, E. E.: *Solar Energy Fundamentals for Designers and Engineers* (Addison-Wesley, Reading, Mass., 1982).
- AZIZI, D.: *Heat Transfer Applications in Process Engineering* (Noyes, New York, 1984).
- BACCHUS, J. R. and HARKER, J. H.: *Process Plant Design* (Heinemann, London, 1973).
- BIRD, R. B., STEWART, W. E. and LIGHTFOOT, E. N.: *Transport Phenomena* (Wiley, New York, 1960).
- CHAPMAN, A. J.: *Heat Transfer*, 2nd edn (Macmillan, New York, 1967).
- CHEREMISINOFF, N. P. (ed.): *Handbook of Heat and Mass Transfer*, Vol. 1, *Heat Transfer Operations*. (Gulf Publications, 1986).
- COLLIER, J. G.: *Convective Boiling and Condensation* (McGraw-Hill, New York, 1972).
- FOERT, E. R. G. and DRAKE, R. M., Jr.: *Analysis of Heat and Mass Transfer* (McGraw-Hill, New York, 1972).

**This Page is Inserted by IFW Indexing and Scanning
Operations and is not part of the Official Record**

BEST AVAILABLE IMAGES

Defective images within this document are accurate representations of the original documents submitted by the applicant.

Defects in the images include but are not limited to the items checked:

- ☐ BLACK BORDERS
- ☐ IMAGE CUT OFF AT TOP, BOTTOM OR SIDES
- ☒ FADED TEXT OR DRAWING
- ☐ BLURRED OR ILLEGIBLE TEXT OR DRAWING
- ☐ SKEWED/SLANTED IMAGES
- ☐ COLOR OR BLACK AND WHITE PHOTOGRAPHS
- ☐ GRAY SCALE DOCUMENTS
- ☐ LINES OR MARKS ON ORIGINAL DOCUMENT
- ☐ REFERENCE(S) OR EXHIBIT(S) SUBMITTED ARE POOR QUALITY
- ☐ OTHER: _____

IMAGES ARE BEST AVAILABLE COPY.

As rescanning these documents will not correct the image problems checked, please do not report these problems to the IFW Image Problem Mailbox.